Technical University of Denmark

DTU

Chemical Design of Functional Nanomaterials

Egeblad, Kresten; Christensen, Claus H.

Publication date:
2008

Document Version
Publisher's PDF, also known as Version of record

Link back to DTU Orbit

DTU Library
Technical Information Center of Denmark

Danish National Research Foundation´s
Center for Sustainable and Green Chemistry

Chemical Design of Functional Nanomaterials

200 nm

Kresten Egeblad

DTU

Abstract

This thesis deals with a very specific class of functional nanomaterials known as mesoporous zeolites. Zeolites are a class of crystalline aluminosilicate minerals characterized by featuring pores or cavities of molecular dimensions as part of their crystal structure. Mesoporous zeolites are zeolites which in addition to these channels and cavities, *i.e.* the micropores (less than 2 nm), also feature porosity in the mesopore size region (2-50 nm). The presence and ordered structure of the micropores is of profound influence for different applications of zeolites since they effectively make zeolites behave like molecular sieves capable of separating molecules by their size. This property in combination with acidic properties resulting from hydroxyl groups bridging silicon and aluminum ions in the zeolite framework make zeolites interesting as shape-selective solid acid catalysts. Unfortunately, diffusion in the micropores is inherently slow resulting in poor effective usage of zeolites in catalysis. To the end of improving diffusion in zeolites, several strategies have been pursued including developing wider-pore zeolite structures, preparing zeolites in nanocrystalline form, supporting zeolites on carriers, and introducing auxiliary pore systems in each individual zeolite crystal resulting in mesoporous zeolite single crystals. With the exception of the wide-pore zeolites, these materials are termed hierarchically porous zeolites since they feature two (or more) distinct pore systems; the micropores and the meso-/macropores. The main methods for preparing mesoporous zeolite single crystals are by crystallization of the zeolite in the presence of carbon which is subsequently removed by combustion or by subjecting normal purely microporous zeolites to alkaline treatments resulting in mesopore formation by selective extraction of silicon from the framework. It is described how various carbon templates allow for tuning the porosity of mesoporous zeolites and that cheap mesopore templates may be prepared by carbonization of sucrose. It is also described how the two main methods for preparing mesoporous zeolites can be combined so that the porosity of a mesoporous zeolite may be enhanced by subjecting it to alkaline treatment. Finally, it is described how crystallization of synthesis gels containing fluoride lead to new mesoporous zeolite-like materials, namely mesoporous aluminophosphate zeotypes.

iv

Dansk resumé

Denne afhandling omhandler en specifik klasse af funktionelle nanomaterials der går under betegnelsen mesoporøse zeolitter. Zeolitter er en klasse af krystallinske aluminosilikatmineraler kendetegnet ved at deres krystalstrukturer indeholder kanaler og kaviteter i samme størrelsesorden som små molekyler. Mesoporøse zeolitter er zeolitter som udover disse kanaler og kaviteter, dvs. mikroporerne (under 2 nm), også besidder porer i mesopore området (2-50 nm). Mikroporerernes tilstedeværelse og ikke mindst deres ordnede struktur er af stor betydning for zeolitters anvendelse eftersom de får zeolitter til at virke som molekyle-sier der er i stand til at separere molekyler fra hinanden baseret på deres størrelse. Denne egenskab sammenholdt med at zeolitter der indeholder hydroxybroer mellem silicium og aluminum ioner også virker som fastformige syrer har gjort at zeolitter har vakt stor interesse som form-selektive katalysatorer. Desværre foregår diffusion af molekyler uhyre langsomt i zeolitternes mikroporer hvilket resulterer i at zeolitkatalysatorer ikke er nær så effektivt udnyttet som de kunne være. Diffusionsproblemet er blevet tacklet på forskellige måder heriblandt ved udvikling af nye zeolitstrukturer med bredere pore-åbninger, fremstilling af nano-størrelse zeolitkrystaller, ved at supportere zeolitter på et porøst bærermateriale og ved at indføre yderligere pore systemer i de enkelte zeolitkrystaller (mesoporøse zeolit enkeltkrystaller). Med undtagelse af de såkaldte bred-porede zeolitter betegnes disse som materialer med hierarkisk porøsitet eftersom de indholder mere end et poresystem, nemlig mikroporerne og meso-/makroporerne. De mest studerede metoder til fremstilling af mesoporøse zeolit enkeltkrystaller på er ved krystallisation af zeolitfasen i tilstedeværelse af kulpartikler som så efterfølgende fjernes ved forbrænding eller ved at behandle almindelige zeolitkrystaller med base således at der selektivt opløses siliciumioner fra zeolitgitteret. Det beskrives hvorledes forskellige kulskabeloner kan anvendes til at tune mesoporøse zeolitters porøsitet og at disse kan fremstilles billigt ved at forkulle sukker. Det beskrives også hvorledes de to procedurer for fremstilling af mesoporøse zeolitter kan kombineres således at en mesoporøs zeolits porøsitet alstå kan forøges ved at behandle denne med base. Endelig beskrives det at krystallisation af syntesegeler der indeholder fluoridioner i tilstedeværelse af kul fører til nye mesoporøse materialer nært beslægtede med zeoliter, nemlig mesoporøse aluminophosphat zeotyper.

Preface

This thesis is submitted in partial fulfillment of the requirements for obtaining the Ph.D. degree from the Technical University of Denmark (DTU). It is based on work carried out from June 2005 to May 2008 at the Center for Sustainable and Green Chemistry (CSG), Department of Chemistry, under the supervision of Professor Claus Hviid Christensen. The Ph.D. project was funded by an internal scholarship from DTU. The thesis is based on some of the research projects I have contributed to and the publications resulting from these projects. These are listed below and reproduced in the appendix.

1. Javier Perez-Ramirez, Claus H. Christensen, Kresten Egeblad, Christina H. Christensen, Johan C. Groen, **Hierarchical Zeolites: Enhanced Utilisation of Microporous Crystals by Advances in Materials Design**, *Chem. Soc. Rev.* **2008**, *37*, 2530.
2. Kresten Egeblad, Christina H. Christensen, Marina Kustova, Claus H. Christensen, **Mesoporous Zeolite Crystals** in *Zeolites: From model materials to industrial catalysts*, J. Cejka, J. Perez-Pariente, W. J. Roth; Eds., Research Signpost, 2008, p. 391.
3. Kresten Egeblad, Christina H. Christensen, Marina Kustova, Claus H. Christensen, **Templating Mesoporous Zeolites**, *Chem. Mater.* **2008**, *20*, 946.
4. Kake Zhu, Kresten Egeblad, Claus H. Christensen, **Tailoring the Porosity of Hierarchical Zeolites by Carbon-templating**, *Stud. Surf. Sci. Catal.* **2008**, *174*, 285.
5. Kake Zhu, Kresten Egeblad, Claus H. Christensen, **Mesoporous carbons prepared from carbohydrate as hard template for hierarchical zeolites**, *Eur. J. Inorg. Chem.* **2007**, 3955.
6. Marina Kustova, Kresten Egeblad, Kake Zhu, Claus H. Christensen, **Versatile Route to Zeolite Single Crystals with Controlled Mesoporosity: in-situ Sugar Decomposition for Templating of Hierarchical Zeolites**, *Chem. Mater.* **2007**, *19*, 2915.
7. Martin S. Holm, Kresten Egeblad, Peter N. R. Vennestrøm, Christian G. Hartmann, Marina Kustova, Claus H. Christensen, **Enhancing the Porosity of Carbon-templated ZSM-5 by Desilication**, *Eur. J. Inorg. Chem.* **2008**, 5185.
8. Kresten Egeblad, Marina Kustova, Søren K. Klitgaard, Kake Zhu, Claus H. Christensen, **Mesoporous Zeolite and Zeotype Single Crystals Synthesized in Fluoride Media**, *Microporous Mesoporous Mater.* **2007**, *101*, 214.

In addition to the above I have also contributed to the following scientific publications which are not described in this thesis.

9. Claus H. Christensen, Betina Jørgensen, Jeppe Rass-Hansen, Kresten Egeblad, Robert Madsen, Søren K. Klitgaard, Stine M. Hansen, Mike R. Hansen, M. R., Hans C. Andersen, Anders Riisager, **Acetic Acid by aqueous-phase Oxidation of Ethanol with Air Using Heterogeneous Gold Catalysts**, *Angew. Chem. Int. Ed.* **2006**, *45*, 4648.

10. Arkady L. Kustov, Kresten Egeblad, Marina Kustova, Thomas W. Hansen, Claus H. Christensen, **Mesoporous Fe-Containing ZSM-5 Zeolite Single Crystal Catalysts for Selective Catalytic Reduction of Nitric Oxide by Ammonia**, *Top. Catal.* **2006**, *45*, 159.

11. Marina Kustova, Kresten Egeblad, K., Christina H. Christensen, Arkady L. Kustov, Claus H. Christensen, **Hierarchical zeolites: Progress on synthesis and characterization of mesoporous zeolite single crystal catalysts**, *Stud. Surf. Sci. Catal.* **2007**, *170*, 267.

12. Inger S. Nielsen, Esben Taarning, Kresten Egeblad, Robert Madsen, Claus H. Christensen, **Direct Aerobic Oxidation of Primary Alcohols to Methyl Esters Catalyzed by a Heterogeneous Gold Catalyst**, *Catal. Lett.* **2007**, *116*, 35.

13. Søren K. Klitgaard, Kresten Egeblad, Lærke T. Haahr, Martin K. Hansen, David Hansen, Jakob Svagin, Claus H. Christensen, **Self-assembly of C$_{60}$ into highly ordered chain-like structures on HOPG observed at ambient conditions**, *Surface Science* **2007**, *601*, L35.

14. Esben Taarning, Inger S. Nielsen, Kresten Egeblad, Robert Madsen, Claus H. Christensen, **Renewable Chemicals from Biomass by Gold-Catalyzed Aerobic Oxidation**, *ChemSusChem* **2008**, *1*, 75.

15. Søren K. Klitgaard, Kresten Egeblad, Michael Brorson, Konrad Herbst, Claus H. Christensen, **Turbostratic boron nitride coated on high surface area metal oxide templates**, *Eur. J. Inorg. Chem.* **2007**, *31*, 4873.

16. Charlotte C. Marsden, Esben Taarning, David Hansen, Lars Johansen, Søren K. Klitgaard, Kresten Egeblad, Claus H. Christensen, **Aerobic Oxidation of Aldehydes under Ambient Conditions Using Supported Gold Nanoparticle Catalysts**, *Green Chem.* **2008**, *10*, 168.

17. Esben Taarning, Anders T. Madsen, Jorge M. Marchetti, Kresten Egeblad, Claus H. Christensen, **Oxidation of Glycerol and Propanediols in Methanol over Heterogeneous Gold Catalysts**, *Green Chem.* **2008**, *10*, 408.

18. Søren K. Klitgaard, Kresten Egeblad, Uffe V. Mentzel, Andrey G. Popov, Thomas Jensen, Esben Taarning, Inger S. Nielsen, Claus H. Christensen, **Oxidations of amines with molecular oxygen using bifunctional gold-titania catalysts**, *Green Chem.* **2008**, *10*, 419.

19. Claus H. Christensen, Jeppe Rass-Hansen, Charlotte C. Marsden, Esben Taarning, Kresten Egeblad, **The Renewable Chemicals Industry**, *ChemSusChem* **2008**, *1*, 283.

20. Kresten Egeblad, Jeppe Rass-Hansen, Charlotte C. Marsden, Esben Taarning, Claus H. Christensen, **Heterogeneous Catalysis for Production of Value-added Chemicals from Biomass**, in *Catalysis*, J. J. Spivey; Ed., Royal Society of Chemistry, 2008, *accepted*.

Moreover, I have contributed to the following non-technical magazine articles and book chapters.

1. Kresten Egeblad, Claus H. Christensen, **Nanoteknologi – på vej mod en ny industriel revolution** in *Kemiske Horisonter*, DTU, 2006. (*in Danish*)
2. Kresten Egeblad, Søren K. Klitgaard, **Nanobolde og nanorør** in *Isis Kemi B*, Systime, 2006. (*in Danish*)
3. Søren K. Klitgaard, Kresten Egeblad, Hanne Falsig, Anne M. Frey, Betina Jørgensen, David Hansen, Lars Johansen, Claus H. Christensen, **Guld og flyvende grise – en opdagelsesrejse ind i nanokemiens verden**, *LMFK-bladet*, nr. 3, 2007 (*in Danish*)
4. Peter Vennestrøm, Kresten Egeblad, Claus H. Christensen, **Kolloider – på bølgelængde med lys og nanoteknologi**, *LMFK-bladet*, nr. 1, 2008 (*in Danish*)
5. Sofie E. Christiansen, Karen T. Leth, Kresten Egeblad, Claus H. Christensen, **Molekylsier – de vises sten** in *Nye Kemiske Horisonter*, DTU, 2007. (*in Danish*)
6. Søren K. Klitgaard, Kresten Egeblad, Claus H. Christensen, **Solceller – et strålende svar på den indlysende udfordring** in *Nye Kemiske Horisonter*, DTU, 2007. (*in Danish*)
7. Søren K. Klitgaard, Kresten Egeblad, Hanne Falsig, Jens K. Nørskov, Claus H. Christensen, **Jo mindre jo bedre – ultrasmå guldklumper sætter fart på kemien**, *Aktuel Naturvidenskab*, 2008 (*in Danish*)
8. Uffe V. Mentzel, Kresten Egeblad, Claus H. Christensen, **Bioraffinaderiet** in *Nanoteknologiske Horisonter*, DTU, 2008. (*in Danish*)

Finally, I thank Peter Kjelgaard Andersen for lending me his hermitage for parts of my writing period and my wife and children, Cathrine, Mads and Smilla, for their patience, love and understanding.

_____

Kresten Egeblad

Table of Contents

Introduction

The present thesis deals with chemical design of a very specific class of functional nanomaterials known as mesoporous zeolites. Mesoporous zeolites are zeolites featuring an auxiliary system of mesopores in addition to the intrinsic crystallographic micropore system of zeolites. Since mesoporous zeolites contain pores in two different size ranges, *i.e.* micropores (less than 2 nm in diameter) and mesopores (2-50 nm in diameter), they are considered to be hierarchically porous materials and are therefore also termed hierarchical zeolites. Due to the larger pores molecular transport proceed faster in mesoporous zeolites than in "conventional" zeolites. In consequence, a larger part of the zeolite crystal is utilized as catalyst in chemical reactions.

The thesis is divided into six chapters. In Chapter 1, the field of zeolites is introduced and the main problem associated with purely microporous zeolites is discussed. On a conceptual level, the solutions for solving this problem by materials design are discussed.

In Chapter 2, a literature overview on the field of hierarchical zeolites is provided. In this chapter the different types of hierarchical zeolite materials are briefly described and the methods for preparing them are categorized.

In Chapter 3, a more detailed and in-depth discussion of the properties of mesoporous zeolite single crystal materials is provided. The auxiliary porosity of these materials differs from that of the other hierarchical zeolites since it is incorporated into each individual zeolite crystals. Hence, the mesoporous zeolite single crystals are also known as hierarchical zeolite crystals.

In Chapter 4 are described three different templating approaches for tuning the properties of hierarchical zeolite crystals. It is shown that the amounts and sizes of the non-micropore porosity of these crystals can be varied and how larger zeolite crystals than normally obtained by carbon-templating can be prepared.

In Chapter 5 is described how the two main methods for preparing hierarchical zeolite crystals can be combined resulting in highly mesoporous zeolite single crystals. These are achieved by preparing mesoporous ZSM-5 by carbon-templating and subjecting this material to various post-synthetic alkaline treatments.

In Chapter 6 the preparation of mesoporous zeolites and mesoporous aluminophosphate zeotypes is described. The materials presented in this chapter are all prepared from synthesis gels containing fluoride anions crystallized in the presence of carbon.

1. On Zeolites and their Micropores

1.1. Introduction

Zeolites are a class of aluminosilicate minerals characterized by featuring pores or cavities of molecular dimensions as an integral part of their crystal structure. With pore diameters in the range 3-12 Å, the pores of zeolites are classified as micropores according to the IUPAC classification of porous materials.[1] Structurally, zeolites are built from tetrahedral TO_4 units which are organized into 3-dimensional networks by sharing of the oxygen corner-atoms in the TO_4 units. Including zeotypes, which are similar to zeolites but not necessarily of aluminosilicate composition, about 180 different structural assemblies are known whereof 48 are naturally occurring.[2]

Typically, the tetrahedrally coordinated T atoms in zeolites are silicon and aluminum, with the majority being silicon. They are normally found to obey what is known as Löwenstein's rule, which states that Al—O—Al linkages are forbidden, implying that the Si/Al ratio in the zeolite framework can not be smaller than unity. To put it in other words: zeolites can be conceived of as silicates with a certain portion of the silicon atoms being substituted with aluminum atoms – not the other way around. Since aluminum has a lower charge than silicon, substitution of aluminum for silicon leads to an overall negatively charged zeolite framework which entails two things: The environment inside the channels and cavities becomes increasingly polar and the need for charge-compensating cations arises to balance

the overall negative charge of the aluminosiliacate framework. If the charge-compensating cation is monovalent, there is obviously a one-to-one equivalency between the number of monovalent cations needed and the number of aluminum atoms substituted into the structure. In principle, all cations which are small enough to physically fit in the zeolite channels can function as charge-compensating cations, however, when the framework is balanced by protons hydrogen-bonded to the oxygen atoms bridging between aluminum and silicon atoms the zeolite becomes acidic. Such sites, *i.e.* Al—O(H)—Si linkages (see Figure 1.1), are known as Brønsted acid sites, and the number of these in the zeolite naturally correlates with the framework aluminum content of the zeolite as long as the zeolite obeys Löwenstein's rule. Thus, aluminosilicate zeolites comprising hydrogen as the charge-compensating cation are solid acid materials with the number of Brønsted acid sites determined by the degree of aluminum substitution.
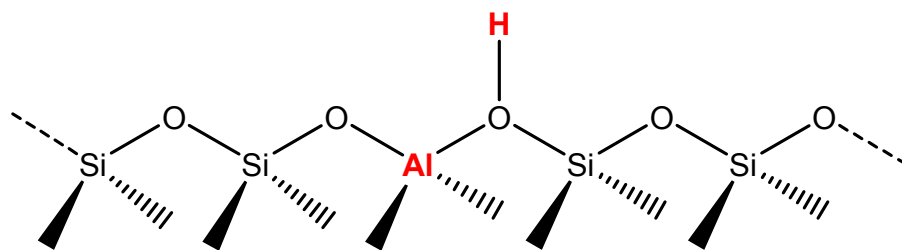
Figure 1.1 Illustration of a Brønsted acid site in a zeolite.

The inherent micropore system of zeolites which obviously extends throughout the entire crystal (because it is a crystal) has the effect of making zeolites capable of separating molecules by their size alone, since some molecules are small enough to be able penetrate into the zeolite whereas some are too big, see Figure 1.2. This molecular size exclusion principle is known as the molecular sieve effect and it is one of the most important intrinsic properties of zeolites. However, zeolites are not only capable of separating molecules by their molecular size but also by their polarity. Aluminum-rich zeolites have a polar interior which makes them hydrophilic and therefore capable of adsorbing polar molecules such as water. Conversely, zeolites with a low aluminum-content are less polar and therefore more

hydrophobic. In fact, the water adsorption capacity of aluminum-rich zeolites is so high that they are commonly used as desiccants and it is such a characteristic feature of zeolites that it is also the origin for their name: The term "zeolite" (which stems from greek and translates to "boiling stone"), was coined by the Swedish mineralogist A.F. Cronstedt when he observed that vast amounts of water evaporated from certain minerals when they were heated.
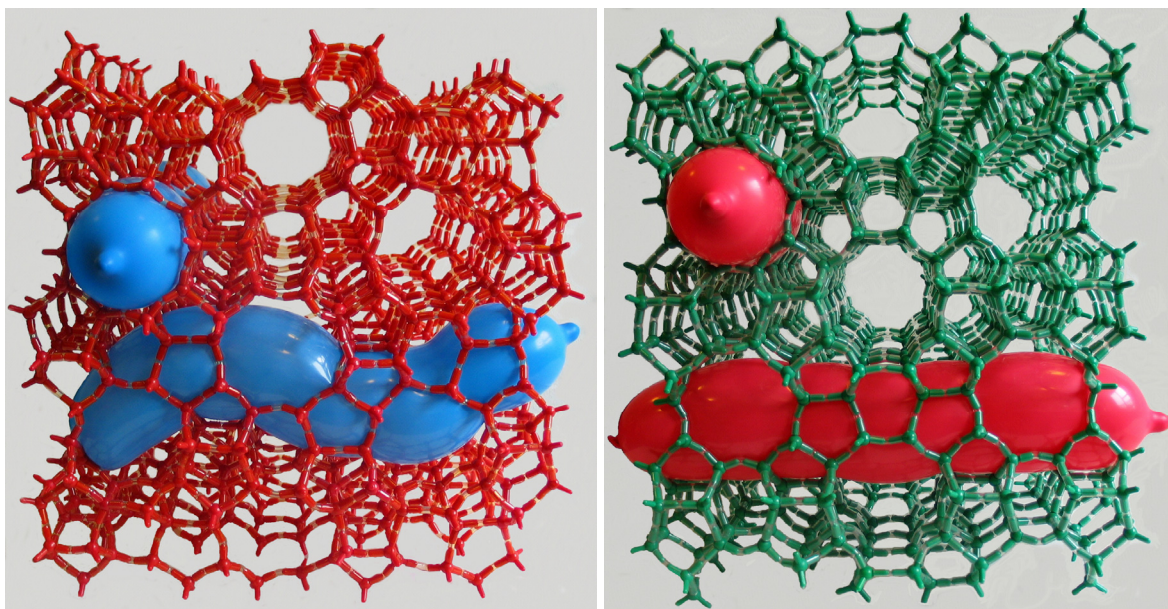
Figure 1.2 Models of two zeolite framework types with balloons in the channels. To the left is shown a model of the MFI structure type which features straight channels in one direction and sinusoidal channels in a direction orthogonal to it. To the right is shown a model of the MEL structure type which features straight only straight channels in two directions. In both cases, the diameters of the balloons are *ca.* 6.3 Å illustrating that it is impossible for molecules with a larger diameter than this to enter the pores of these zeolites.

As mentioned above, the molecular sieve effect is such an important feature of zeolites that several industrial applications are directly related to it. This is particularly true for the catalytic application of zeolites. Oversimplified perhaps, some catalytic applications of zeolites can be conceived of as reactive separation processes in the sense that some molecules are permitted to enter the reactive interior of the zeolite crystals whereas some are excluded due to their size. In that way, only certain reactant molecules in a reactant mixture are given the opportunity to penetrate into the catalytically active micropore system

of the zeolite. Thus, the molecular sieve effect induces a phenomenon known as reactant selectivity, which is visualized schematically using two heptane isomers in Figure 1.3 (top). Zeolites can also exhibit what is known as product selectivity which can be observed from a reaction in which several products are possible but only one is detected. An example of this (shown in Figure 1.3 middle) is the alkylation of toluene with methanol. In this reaction there is no intrinsic selectivity towards either xylene isomer so they are all formed in equilibrium amounts in the pores of the zeolite catalyst. However, *p*-xylene is smaller than the other isomers which means that its motion through the pores is faster. In fact, *p*-xylene moves so much faster than the other isomers that it is the only isomer removed from the equilibrium product mixture and hence it is effectively the only product of the reaction. The third kind of selectivity exhibited by zeolites is known as "restricted transition-state selectivity" and refers to the situation illustrated in Figure 1.3 (bottom) where certain possible transition states are too bulky to fit in the channels or cavities of the zeolite and thus cannot be formed during the course of a reaction.

Reactant selectivity

Product selectivity

Restricted transition-state selectivity
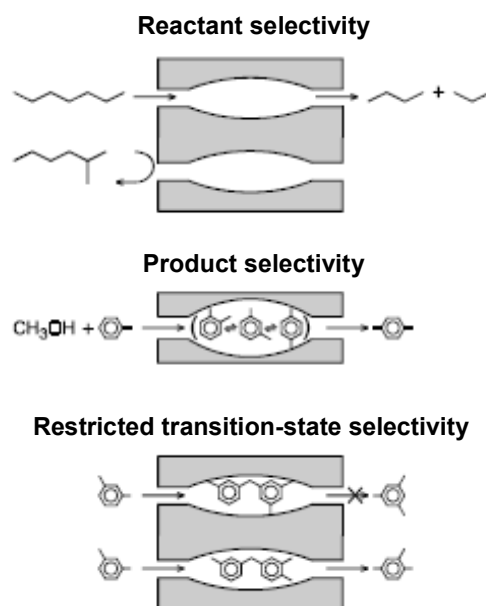
Figure 1.3 Three possible types of shape selectivity observed in zeolite catalysis due to their microporous structure.[3]

The molecular sieve effect and acid properties in a solid and relatively high-temperature stable class of materials are a powerful combination which has made zeolites the material

of choice for many catalytic applications. These include cracking reactions such as fluidized catalytic cracking (FCC) and hydrocracking, in which zeolites facilitate the break-down of larger molecules into smaller ones, but isomerization and alkylation are also typical reactions for which zeolites find use as catalysts. The FCC process is one of the best examples illustrating the impact zeolites have had on chemical industry. It is one of the most important catalytic processes at all with more than five million barrels of crude oil being converted into gasoline and other fuels per day in US refineries alone (2007).[4] Prior to the 1960s amorphous silica alumina gel type catalysts and clays were used as catalysts in the process. However, pioneering discoveries made in synthesizing highly acidic zeolite Y at Union Carbide in the 1950s subsequently lead to the introduction of these materials as catalysts for the FCC process in the 1960s. Zeolite Y proved to be a much more effective catalyst for the FCC process increasing the yield of gasoline by 54-60%.[5] Over the years, the impact of switching from amorphous catalysts to zeolites has thus been enormous in terms of profits as well as in terms of reduction in fossil resource requirements. The net added-value of switching has been conservatively estimated to be approximately US$ 1 trillion representing a reduction in FCC feedstocks for gasoline production of 12.6 billion barrels. This amount of FCC feedstocks correspond to 75 billion barrels of petroleum crude oil – the equivalent of 6% of the worlds known oil reserves today (1.238 billion barrels in 2007).[6]

1.2. Diffusion in zeolite micropores

Ironically, the micropore system is not only one of the main reasons for the success of zeolites in catalysis it is also their Achilles' heel in these applications. The reason for this is that molecular transport in spaces of about the same size as molecules is inherently slow since the molecules are almost always in physical contact with the pore walls which inevitably slow them down. Thus, the larger the molecules in comparison with the pore diameter, the slower are the motion of the molecules through the pores. Moreover, the similar sizes of the pores and the molecules entail that a single molecule in a channel will hinder the passage of other molecules through that channel. Or, to put it more severely, that all molecules in the channels effectively block each others passage. In effect, mass transfer

of reactants, intermediates and products to and from the reactive sites in the zeolite micropores can be severely hindered.

One of the main mechanisms of mass transfer in general is diffusion. As mentioned above, diffusion in microporous materials such as zeolites is much slower than in materials with larger pores due to size of the pores relative to the molecules. The mechanism of diffusion in these systems is termed intracrystalline or configurational diffusion and it is characterized by diffusivities in the range 10^{-8} to 10^{-20} m^2/s, see Figure 1.4. In comparison, diffusivities in the Knudsen regime which is the dominant mechanism for mesoporous materials are in the range 10^{-5} to 10^{-8} m^2/s. For many chemical reactions which take place at active sites in zeolite micropores the diffusivities are so low that the overall rate-limiting factor is in fact intracrystalline diffusion. When this is the case, the reaction is said to be in a diffusion-controlled or -limited regime.
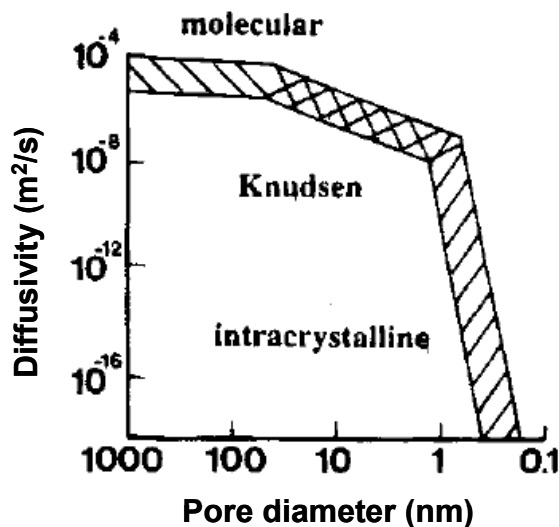
Figure 1.4 Relation between pore diameter and typical diffusivites illustrating three types of diffusion regimes: Molecular, Knudsen and intracrystalline.[7]

There are two consequences of diffusion limitations in zeolite catalysis. One is obviously that the observed rate of a given chemical reaction is lower than the intrinsic reaction rate implying kinetically that the reaction is not operated at its full potential. Another is that the concentration of molecules in the bulk of the zeolite crystal rapidly drops as the distance to

the exterior surface increases. The result of this concentration drop off is that only the outer-most part of the zeolite crystals are utilized in the chemical reaction. This is visualized in Figure 1.5.
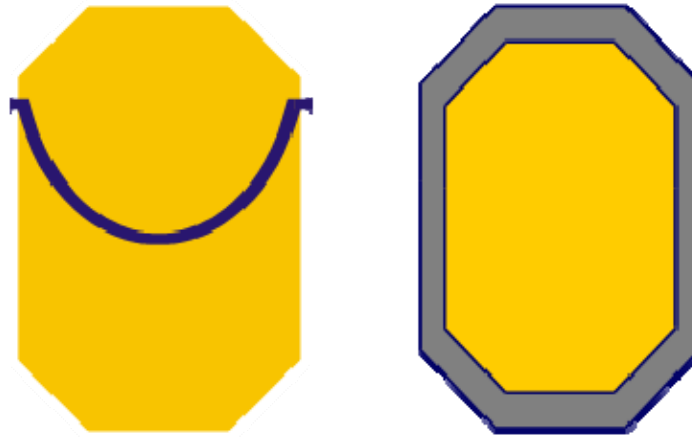
Figure 2.5 Schematic illustration of the concentration profile cross-Section of a zeolite crystal (left) and the corresponding utilized reaction zone shaded in grey (right).

The degree of catalyst utilization is usually described by chemical engineers as the ratio between the observed and the intrinsic rate of a chemical reaction and it is known as the effectiveness factor, $\eta = r_{\text{observed}} / r_{\text{intrinsic}}$. Thus, an effectiveness factor of $\eta = 1$ indicates that the reaction is running at full potential since the observed reaction rate is the same as the intrinsic reaction rate. Conversely, a very low effectiveness factor indicates that the observed rate is lower than the intrinsic rate. Low effectiveness factors are attained at high values of Thiele modulus, which is another dimensionless quantity used by chemical engineers. The Thiele modulus is used to describe intraparticle transport and for a first order reaction it can be expressed as

$$\phi = L\sqrt{\frac{k}{D}}$$

where L is the diffusion path length, k is the intrinsic rate constant and D is the effective diffusivity. Since the dimensions of k and D/L^2 are both s^{-1}, the Thiele modulus actually relates the intrinsic reaction rate to the rate of diffusion, *i.e.*

$$\phi = \sqrt{\frac{k}{D/L^2}} = \sqrt{r_{\text{intrinsic}}/r_{\text{diffusion}}}$$

1.3. Strategies for increasing catalyst effectiveness

From the expressions of the Thiele modulus shown above it can be seen that there are two conceptual ways of lessening the impact diffusion limitations has on the rate of a chemical reaction. One is to increase diffusivity (D); the other is to reduce the mean diffusion path length (L). However, increasing the diffusivity by increasing the pore diameter necessarily compromises the molecular sieve effect and the shape-selective properties of the zeolite – at least to some extent. Nevertheless, the preparation and study of so-called wide-pore zeolites has been an active field of research for some years now.

The second conceptual way of decreasing the impact of diffusion limitations in zeolite catalysis is reducing the mean diffusion path length. Reducing the mean diffusion path length can be done in two different ways: By decreasing the crystal size or by introducing an auxiliary pore system consisting of larger pores that intersect the micropores. However, introduction of an auxiliary pore system might also result in occluded mesopores which do not improve accessibility to the micropores. These three types of hierarchical pore systems are visualized in Figure 1.6.
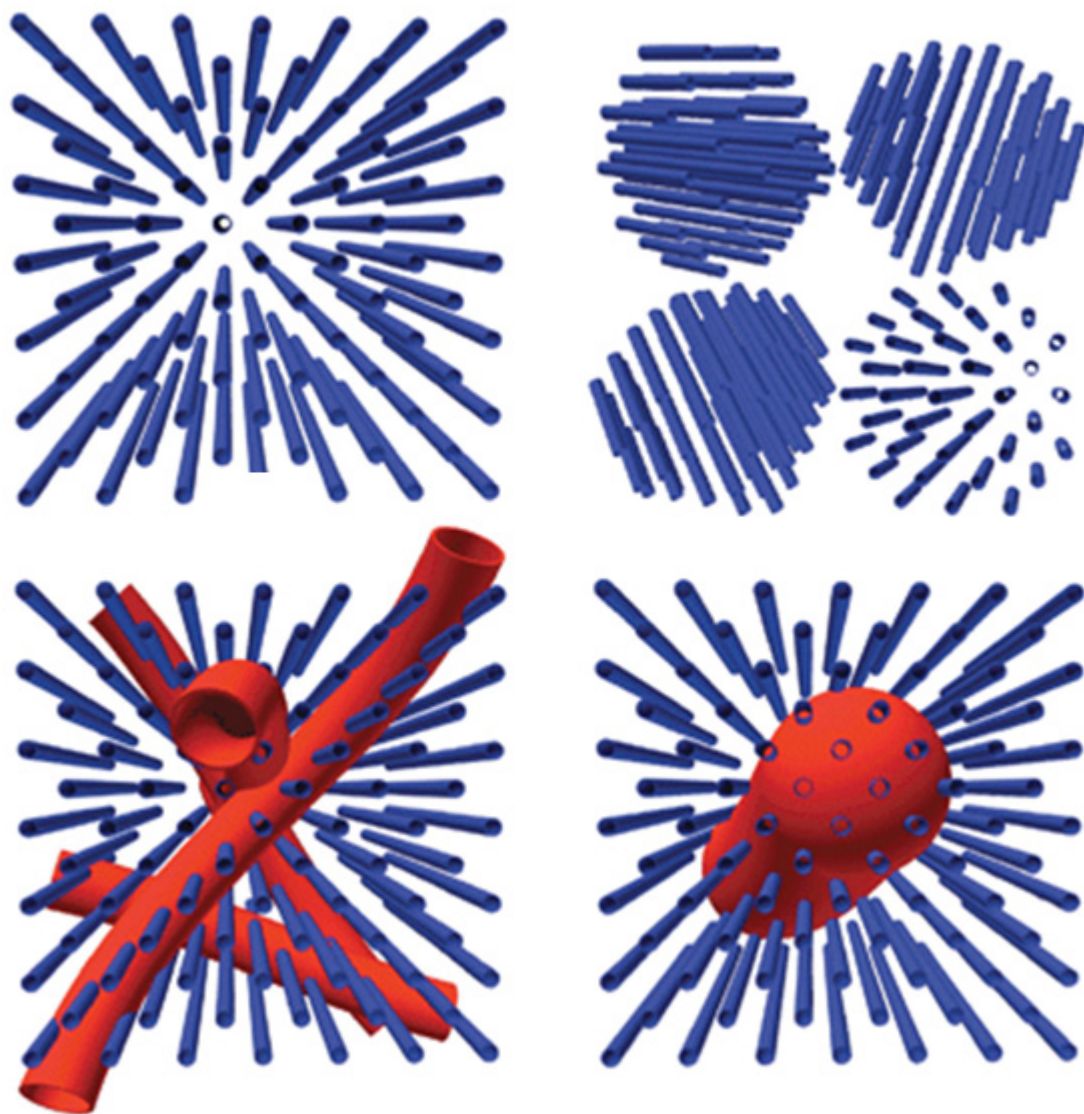
Figure 1.6 Schematic illustration of the two conceptual ways of reducing the diffusion path length through zeolite micropores. In the top left corner is shown an artistic view of a conventional zeolite micropore system. The top right image shows how the length of the micropores can be shortened by reducing the crystal size. The bottom left image shows how the micropores can be cut shorter by introduction of non-crystallographic mesopores. In the bottom right image is shown that the introduction of an auxiliary mesopore system can also result in occluded mesopores which are not accessible from the exterior.[8]

Thus, improving access to the interior of the zeolite crystals by reducing the mean diffusion path length is effectively the same as enhancing the exterior surface area by introducing additional porosity which can be either intercrystalline or intracrystalline. When the additional porosity is considerably larger than the micropores (pore diameter less than 2

nm), *i.e.* it is either in the mesopore region (pore diameter in the range 2-50 nm) or the macropore region (pore diameter larger than 50 nm), the resulting materials have two or more distinct level of porosity which will serve different functions in catalytic applications; the additional meso/macropore system is used for molecular transport to and from the active sites in the micropores. These materials are often termed hierarchically porous zeolites or simply hierarchical zeolites because they feature one or more levels of porosity than the microporosity.

However, there is of course also the possibility of designing completely new materials which have many of the same properties of zeolites but in which molecular transport is inherently faster. That is, materials which are thermally stable, acidic and in which the active sites are more accessible from the exterior. The search for materials trying to satisfy these needs has also been a flourishing research fields for the past 15 years, however, as they are not zeolites, they will not be discussed in the following chapters of this thesis.

1.4. Summary

Zeolites are aluminosilicate minerals which contain crystallographic micropore systems. These micropores make zeolites behave like molecular sieves finding application in adsorption, separation and catalysis. However, molecular diffusion in the micropore system is very slow, even compared to Knudsen diffusion, and the catalytic application of zeolites is therefore often found to be hindered by diffusion limitations. Conceptually, there are two methods for alleviating this problem: One is to increase the pore width; another is to decrease the mean diffusion path length. Both of these approaches have been pursued with the aim of preparing zeolites with improved accessibility to the active sites. However, as the strategy of decreasing the diffusion path length by introducing auxiliary pore systems in zeolite materials appears to be more general and more studied this approach is focused on presently.

2. Hierarchical Zeolite Materials

2.1. Introduction and overview

In this chapter is presented a highlight of hierarchical zeolite materials with improved accessibility to the active sites in the micropores. Several more detailed and comprehensive accounts covering these materials and their preparation are available in the literature.[8,9,10,11,12,13]

Overall, there are four different types of zeolite materials which offer improved accessibility to the active sites in the micropores. As illustrated in Figure 2.1, these are wide-pore zeolites, nanosized zeolites, zeolite composite materials and mesoporous zeolite crystals. Wide-pore zeolites are zeolites which are specifically designed to have larger micropores than zeolite structures commonly have. These are prepared as zeolites are normally prepared, *i.e.* by hydrothermal crystallization, only with rather exotic structure-directing agents in the synthesis gels compared to traditional zeolite syntheses. Over the years, several wide-pore zeolites have been reported and some of them have been compared to normal zeolites such as zeolite Y and zeolite Beta in various test reactions.[14,15,16,17] They typically compare very well to the normal zeolites in terms of activity as well as selectivity, however, from a scientific perspective the comparison is perhaps somewhat sought after since it is (obviously) different framework structures that are being compared. Obviously, wide-pore zeolites being purely microporous systems are different from the other materials described presently which all feature additional meso- or macropores, *i.e.* pores of diameter

2-50 nm and pores with diameters larger than 50 nm, respectively. Thus, in terms of the pore systems, the wide-pore zeolites are classified as having a unimodal pore size distribution whereas it for the materials in focus is hierarchical.
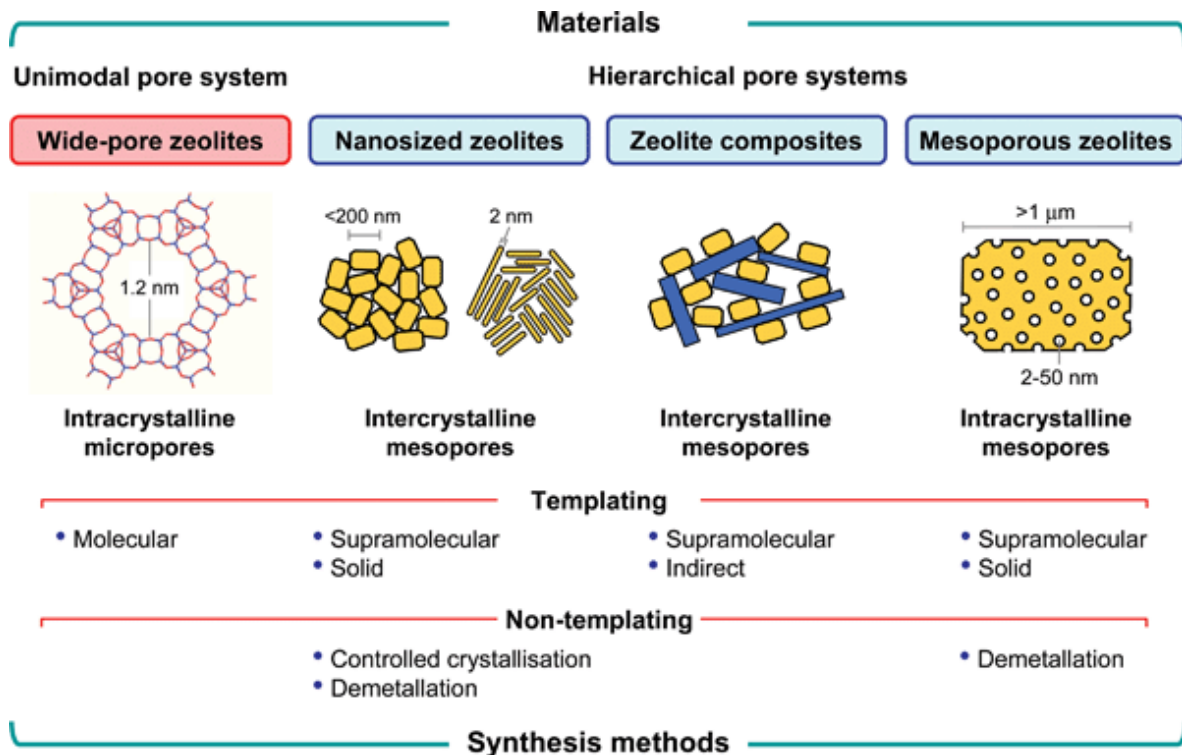
Figure 2.1 Classification of zeolite materials offering improved access to the active sites in the micropores with respect to their pore systems and the overall methods by which they are produced.

As mentioned above and visualized in Figure 2.1, the nanosized zeolites, zeolite composites and mesoporous zeolite crystals all have hiearachical pore systems in the sense that they feature an auxiliary pore system in addition to the crystallographic micropore system. In the case of the nanosized crystals the additional porosity originates from the packing of the nanocrystals and it is therefore termed intercrystalline. This is also the case for the composite zeolites which are materials consisting of small zeolite crystals supported on or incorporated into a porous mesostructured carrier material. Oppositely, the mesoporous crystals contain intracrystalline mesopores, *i.e.* the auxiliary pore system in these materials is incorporated into each individual crystal.

A classification of the methods available for preparing hierarchical zeolites is also provided in Figure 2.1. Overall, the different preparative strategies can be sorted with respect to whether or not the auxiliary mesopore system is generated by the aid of template or not. As such the methods are categorized as templating and non-templating approaches, and they are explained more fully in Section 2.2 and Section 2.3, respectively.

2.2. Templating approaches

Several types of templates have been applied for the preparation of hierarchical zeolites. These can be grouped into three different groups according to the nature of the interface between the zeolite crystal and the template exactly when the mesopore forms: Solid templating involving the application of a solid material as template for the auxiliary pore system; supramolecular templating which covers the use of surfactants to aid the mesopore formation; and indirect templating which cover methods in which the mesopore is formed in a separate step than zeolite crystallization.

2.2.1. Solid templating

Several solids have found application as templates for the synthesis of zeolites with hierarchical pore systems. In fact, this approach has proved to be a highly effective and versatile approach. The solid materials that have been applied as templates can be classified into the following subgroups.

1. Carbon nanoparticles, nanofibers and nanotubes
2. *Ad hoc* prepared carbon templates
3. Organic aerogels, polymers and resins
4. Biological materials

Aside from the above classes of templates there is also a few examples of the application of purely inorganic compounds such as $Mg(OH)_2$ and $CaCO_3$ as mesopore templates which was reported several years ago in the patent literature and recently also in the open literature.[18,19]

Carbon nanoparticles, nanofibers and nanotubes

Templating with carbon nanoparticles have resulted in all three classes of hierarchical zeolite materials: Nanosized zeolite crystals, carbon-supported zeolite nanocrystals and mesoporous zeolite crystals. Nanosized zeolite crystals can be synthesized by crystallization of the zeolite synthesis gel inside the porous voids of a mesoporous carbon and subsequently calcining the carbon-supported zeolite nanocrystalline material to produce a zeolite material consisting of nanocrystals. This approach, which has become known as confined space synthesis, is illustrated in Figure 2.2.[20]
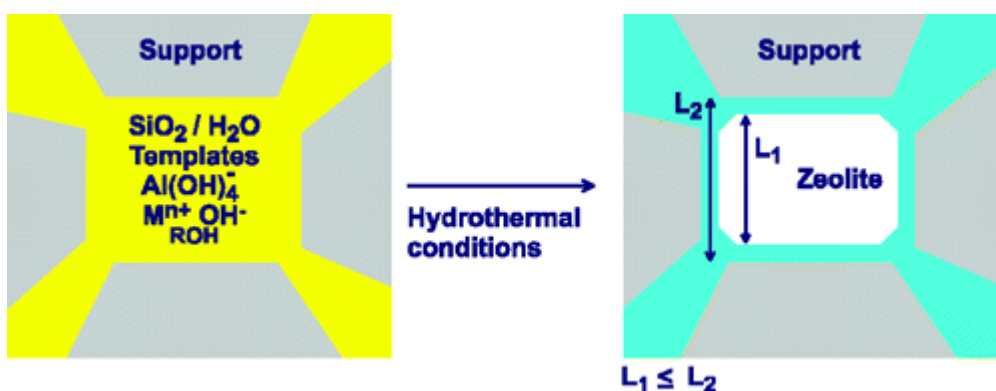
Figure 2.2 Confined space synthesis. Zeolite crystallization takes place inside the void space of a porous (carbon) matrix which hinders the crystals in growing larger than the void space.

The confined space synthesis approach has proved to be a relatively simple method by which several different zeolite structures can be produced with tunable crystal sizes dependent on the choice of carbon template.[20,21] A very systematic way of tuning the crystal size was reported in 2003 by Kim *et al.*, who showed that so-called colloid-imprinted carbons (CIC) can be produced with different pore sizes by carbonization of pitch in the presence of differently sized silica spheres, and allowed for the formation of differently, yet uniformly, sized zeolite nanocrystals.[22]

Crystallization of a zeolite gel adsorbed in the voids of a porous carbon can also lead to the encapsulation of the carbon particles by the growing zeolite resulting in zeolite crystals

embedded with carbon particles. Typically, encapsulation of carbon particles during growth as opposed to confined space synthesis results at higher ratios of synthesis gel relative to carbon template since more gel allows for the zeolite crystals to continue growth after nucleation in the voids of the carbon.[23] Combustion of the carbon particles embedded in the zeolite crystals lead to the formation of mesopores in the individual zeolite crystals as illustrated in Figure 2.3. These materials are known as mesoporous zeolite single crystals.[24]
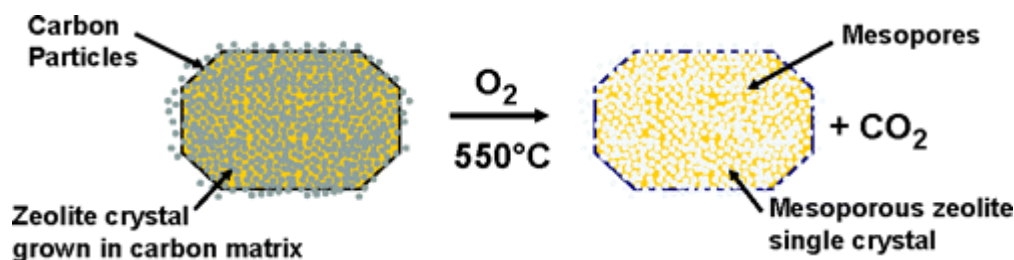
Figure 2.3 Mesoporous zeolite crystals can be prepared by combustion of carbon particles encapsulated in zeolite crystals during crystallization.

Carbon-templating has been extensively applied to produce several zeolite structure types in mesoporous single crystalline from, including MFI, MEL,[25] MTW[26] and BEA.[27,28] Recently, the family of mesoporous zeolites have been extended to also encompass aluminophosphate zeotypes with the availability of mesoporous CHA and AFI structures. Moreover, several different types of carbons have found application as mesopore templates, including different types of carbon nanoparticles,[29,30,31] nanotubes[32] and nanofibers. Thus, carbon-templating applying commercially available carbon materials is clearly a proven method for introduction of an auxiliary mesopore system in individual zeolite crystals.

Ad hoc prepared carbon templates

Aside from the application of commercially available carbons as mesopore templates several types of *ad hoc* prepared carbons have also been applied as mesopore templates. These carbons are prepared by carbonization of various precursors and can be classified into two groups:

1. Carbons prepared by carbonization in the presence of solid inorganic materials
2. Carbons prepared by carbonization in the absence of solid inorganic materials

To the first group belong the CICs mentioned above as well as a family of materials known as CMKs which are carbons prepared by decomposition of various precursors in the pores of ordered mesoporous materials such as MCM-41. Interestingly, the application of CMKs were reported at the same time by three groups independent of each other.[33,34,35] One group reported the application of CMK-3 which was prepared by carbonization of sucrose in the pores of SBA-15 followed by dissolution of the silica by hydrofluoric acid treatment. The CMK-3 carbons were then impregnated with zeolite synthesis gel components and the mixtures were subjected to hydrothermal crystallization conditions after which the zeolite/carbon mixtures were collected and calcined to produce highly crystalline mesoporous ZSM-5. Another group reported the preparation of a class of materials denoted RMMs (replicated mesoporous aluminosilicate molecular sieves) by use of CMK-3 and CMK-1 (the carbon replica of MCM-48) as mesopore templates. These materials were prepared by partial crystallization of aged aluminosilicate gels adsorbed onto the CMKs, to produce RMMs with ultra-small zeolite crystals in the pore walls. In these materials, the zeolite crystals are so small that they are undetectable by XRD, however, a weak band at 540 cm^{-1} in the FT-IR spectrum reveals their identity as zeolite secondary building units. Thus, these RMM materials belong to the group of zeolite composite materials according to the classification shown in Figure 2.1. The procedure reported by the third group differs from the others primarily in the sense that the silica used as the template for carbonization is in fact used as silica source rather than being dissolved away to produce a pure carbon template. Thus, the carbon/silica composites obtained by carbonization of mixtures of phenol and formaldehyde adsorbed on SBA-15, MCM-41 or MCM-48 were impregnated with TPA-OH and subjected to hydrothermal crystallization followed by calcination to produce different mesoporous zeolite materials depending on the type and morphology of the silica used in the preparation of the carbon. A procedure similar to this applying crystallization of a carbon/silica material, prepared by carbonization of sucrose adsorbed onto silica gel, into a mesoporous zeolite single crystalline material was reported in 2007.[36]

The second group of *ad hoc* prepared carbons applied in the synthesis of mesoporous zeolites are carbons which are prepared in the absence of solid inorganic materials. The prime examples of this approach are the preparations of mesoporous nanocrystalline ZSM-5 and NaY zeolites prepared using carbon aerogels made by carbonization of resorcinol-formaldehyde (RF) gels.[37,38] Both of the reported materials had mesopores with an average diameter of 10-11 nm, however, with a mesopore volume of 1.37 ml/g the NaY material was remarkably more mesoporous than the ZSM-5 material which had a mesopore volume of 0.2 ml/g. The mesoporosity of carbon aerogel templated ZSM-5 was later improved significantly by changing the molar ratio of resorcinol to formaldehyde in the precursor from 1:1 to 2:1 which resulted in a mesoporous ZSM-5 material with a mesopore volume of 0.98 ml/g.[39] Also mesoporous zeolite single crystalline materials have been prepared using pre-fabricated mesoporous carbons as the mesopore template. An example of this is the preparation and subsequent application in zeolite synthesis of a mesoporous carbon prepared by carbonization of a hydrothermally treated sucrose-ammonia mixture.[40]

Organic aerogels, polymers and resins

Also non-carbonized resorcinol-formaldehyde aerogels have been applied as mesopore templates as exemplified by the syntheses of mesoporous nanocrystalline ZSM-5 and NaA materials with mesopore volumes of 0.10 ml/g and 0.43 ml/g, respectively.[41,42] In comparison, the mesopore volume of the nanocrystalline ZSM-5 material obtained using a carbonized analogue of the same RF aerogel was 0.15 ml/g suggesting that there also could be ample room for improving the mesoporosity using pure organic aerogels as was reported using the carbonized RF aerogels mentioned above. Perhaps the main advantage of the aerogels is the fact that they can easily be prepared in macroscopic shapes which are not destroyed under hydrothermal conditions. Thus, it is possible to produce self-supporting zeolite monoliths in different shapes composed of closely packed zeolite nanocrystals. This was in fact reported in 2005 with the preparation of a mesoporous silicalite-1 monolith and its successful application in Beckmann rearrangement of cyclohexanone oxime.[43] The

authors used a second impregnation/crystallization step after carbonization of the aerogel as illustrated in Figure 2.4 in order to produce a more mechanically stable monolith.
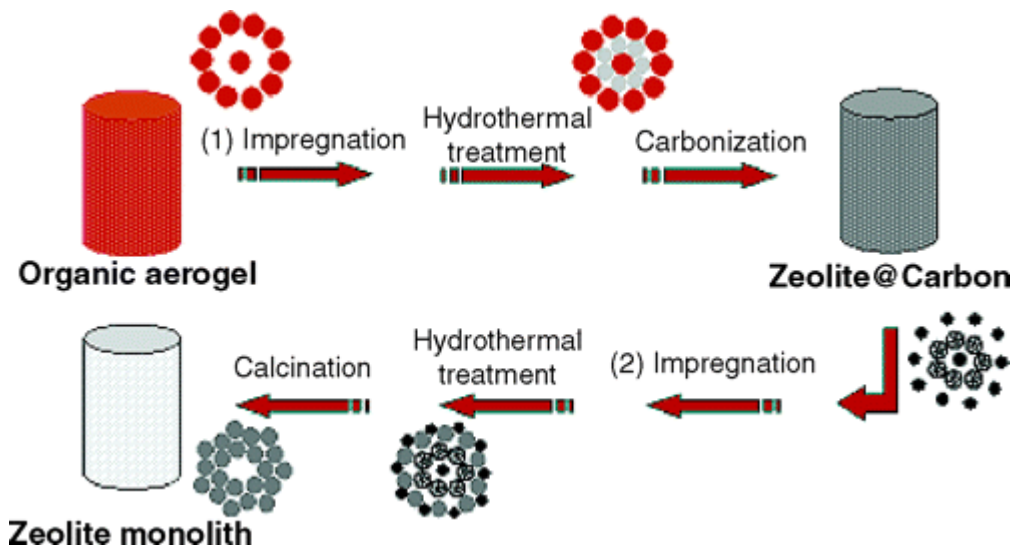
Figure 2.4 Schematic illustration of the synthetic pathway to monolithic silicalite-1. An organic aerogel is impregnated with zeolite synthesis gel and subsequently subjected to hydrothermal treatment and carbonization in Ar. The zeolite-carbon composite is then impregnated and subjected to crystallization again followed by calcination in air to produce a pure silicalite-1 monolith.

There are also examples of the application of different types of polymers and resins to produce hierarchical zeolites. In fact, one of the first methods for preparing hierarchial zeolites was reported in 1999 using close-packed polysterene beads as the template.[44] The silicalite-1 material obtained after calcination was a macroporous assembly of nanocrystals. Also hierarchical mesoporous silicalite-1 has been reported by use of a close-packed assembly of anionic ion-exchange resin beads as the template.[45] The reported material featured mesopores ranging from *ca.* 20 to *ca.* 50 nm in diameter. An example of the use of polymers is the application of mesoscale cationic polymers for the preparation of hierarchical mesporous zeolite *β* and ZSM-5 materials with mesopores in the same size range as the polymer template, *i.e.* 5-40 nm.[46] Another is the application of a silane-functionalized polymer which allows for the formation of very small and uniformly sized mesopores of 2.0-3.0 nm diameters depending on the initial molecular weight of the polymer.[47] In Figure 2.5 is shown the synthesis scheme applied by the authors.
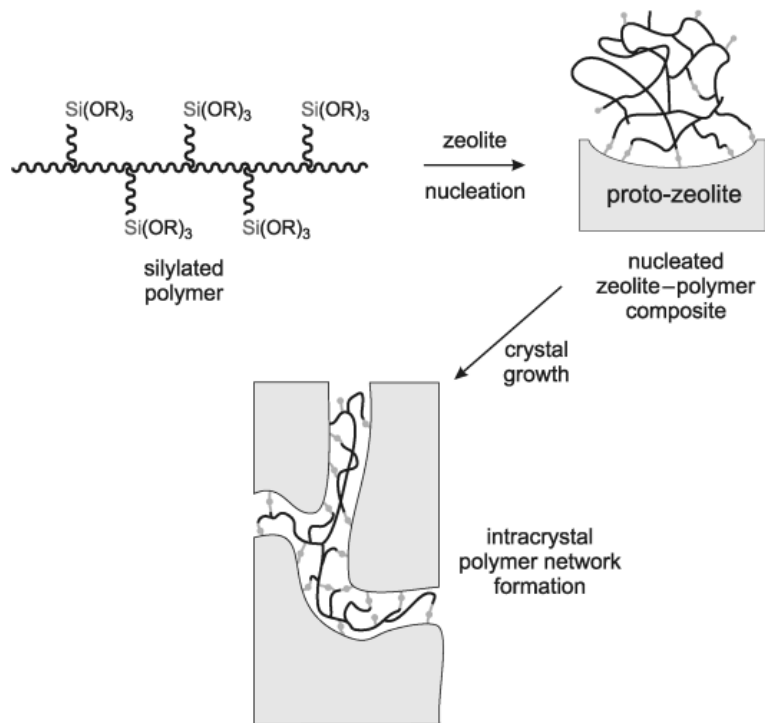
Figure 2.5 Conceptional approach to the synthesis of a zeolite with intracrystal mesopores using a silylated polymer as the mesoporogen.

Biological materials

There are also a few examples of biological materials being applied as solid templates for hierarchical porosity in zeolites. These include such diverse biological materials as bacteria, plants and starch. For instance, very long and wide (about 40 μm width) macroporous silicalite-1 fibers replicating the overall structure of bacterial supercellular threads were prepared by dispersing silicalite-1 nanocrystals on the macroscopic bacterial superstructure followed by calcination.[48] Another example of the preparation of macroporous zeolite fibers using biological material as macrotemplate is the preparation of 10 to 20 μm wide hollow zeolite fibers sing cedar or bamboo wood tissue as the template.[49] The procedure is illustrated schematically in Figure 2.6.
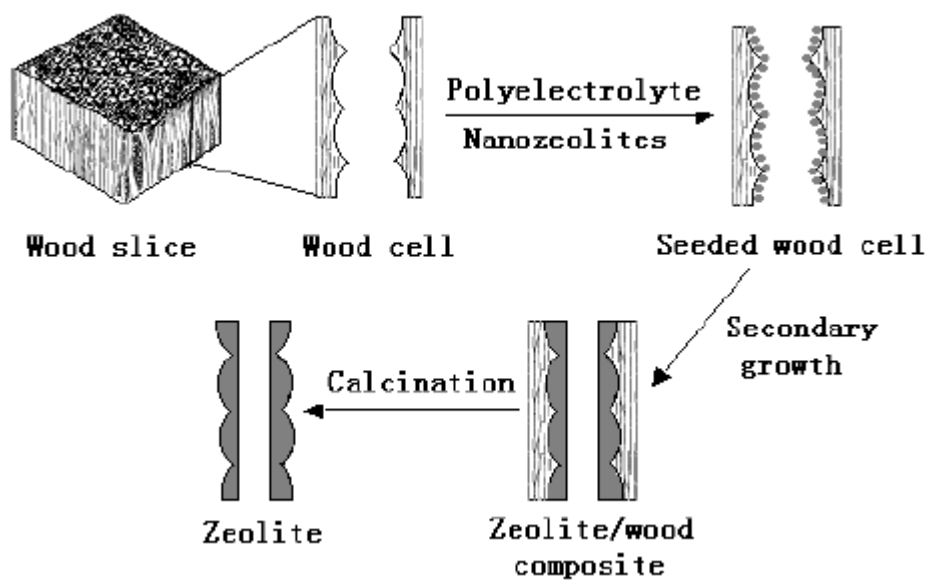
Figure 2.6 Preparation of hollow hierarchical zeolite structures using wood tissue as template. The wood cells are seeded with zeolite nanocrystals subjected to crystallization conditions and eventually calcined in air to produce hollow zeolite structures.

There are also examples of the application of leaves of *Equisetum arvense* as template for the preparation of hierarchical MFI and BEA zeolites.[50,51] The MFI material was prepared by one or two hydrothermal treatments of dry *Equisetum arvense* containing about 13 wt% amorphous silica with zeolite synthesis gel mixtures followed by subsequent calcination. After two hydrothermal treatments, no presence of amorphous silica was present indicating that the biogenic silica was used as silica source along with the silica in the precursor solution. The procedure afforded a hierarchical mesoporous silicalite-1 material replicating the morphological features of the biotemplate.

Also starch has been employed to produce zeolites with hierarchical porosity both by the use of starch gels and by the use of preformed starch sponges as the templates.[52] From mixtures of viscous starch gels with colloidal silica suspensions monoliths and films composed of agglomerated zeolite nanocrystals were prepared. In the case of the monolith, a mesoporous zeolite material was obtained featuring a narrow pore size distribution with an average diameter of 40 nm. The application of preformed starch sponges as template resulted in macroporous zeolite materials.

22

2.2.2. Supramolecular templating

There are also several reports concerning the application of supramolecular templating to prepare hierarchical zeolites. These approaches have been classified as either primary or secondary depending on the type of species being assembled by the surfactant: Primary supramolecular templating involving surfactant-mediated assembly of purely molecular species and secondary supramolecular templating involving surfactant-mediated assembly of partly crystalline species.

Primary supramolecular templating

Primary supramolecular templating methods can be divided into two subcategories depending on whether zeolite crystallization takes place on the external or internal surface of the surfactant assembly.

The first example of the preparation of mesoporous zeolites by crystallization on the external surface of a supramolecular assembly was reported in 2006.[53] With the preparation of mesoporous MFI and LTA zeolites, the authors showed that similar molecules containing long-chain alkylammonium moities in close proximity to hydrolysable methoxysilyl groups can function as mesopore template and structure-directing agent at the same time, and also partially as silica source. Later, also AFI and AEL aluminophosphate zeotypes were prepared using the same methodology, which is illustrated in Figure 2.7.[54]
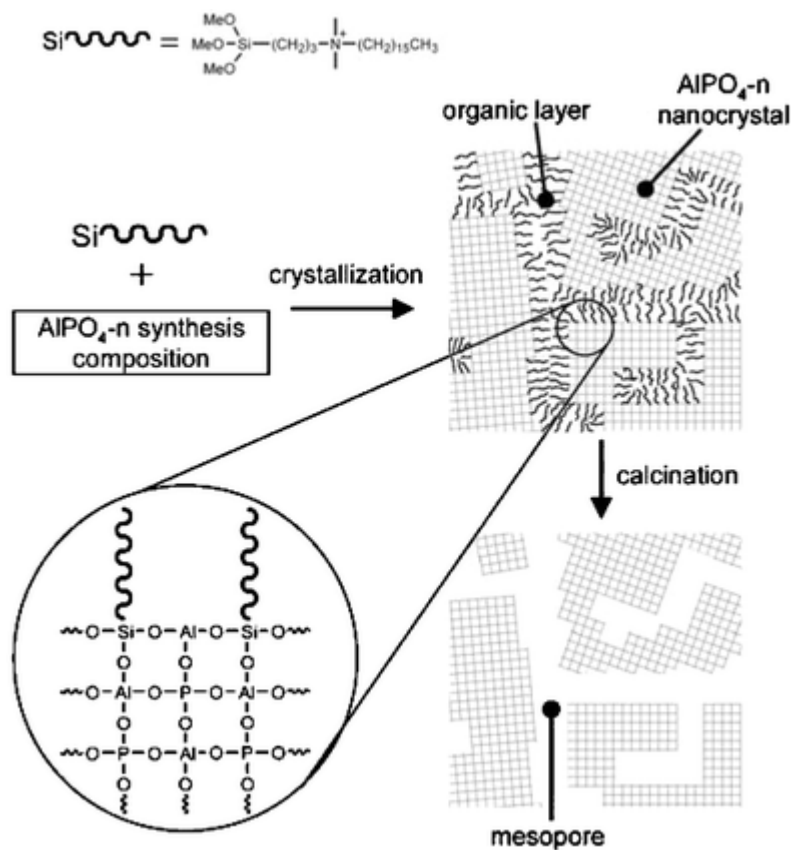
Figure 2.7 Proposed mechanism of mesopore formation using long-chain alkylammonium ions.

The other subcategory of primary supramolecular templating comprises approaches based on the crystallization of zeolites on the inside of surfactant assemblies. As such these approaches are in fact the supramolecular analogues to the confined space synthesis of nanocrystalline zeolites in porous carbon templates mentioned under solid templating above. Microemulsions prepared from a three-phase system composed of an aqueous phase containing the zeolite gel, an oil phase containing toluene and a surfactant phase containing cetyl trimethylammonium bromide (CTAB) and *n*-butanol were subjected to hydrothermal crystallization conditions.[55] The silicalite-1 crystals prepared using microemulsions were smaller in size than those prepared in the absence of the microemulsions and their morphology was shown to be dependent on the composition of the microemulsion being applied.

Secondary supramolecular templating

Secondary supramolecular templating methods can be divided into three subcategories depending on the specific function of the surfactant: One group of methods involves the use of surfactant in the assembly of protozeolitic nanoclusters into mesostructured materials; another group involves the use of surfactants to assemble a mesostructured coating on zeolite crystals; the third group involves methods in which the role of the surfactant is to swell or exfoliate the layers of a lamellar zeolite precursor material.

In the first group of methods involving surfactant-mediated assembly of zeolite embryos or nanocrystals into mesoporous materials are the synthesis of a class of materials known as MSU-materials (Michigan State University). These are materials prepared by adding a surfactant, typically cetyl trimethylammonium bromide, to a pre-formed zeolite synthesis gel mixture in order to facilitate the assembly of a mesostructured phase from the zeolite seed solution. By this method, hexagonal mesostructured phases resembling MCM-41 but containing zeolite nanocrystals are obtained. MSU-materials have been prepared from seeds of different structure types including FAU, MFI and BEA, and they are in general much more steam-stable than MCM-41 materials.[56,57,58] In some cases this can be attributed to the presence of structure-stabilizing carbon particles still present in the samples after calcination, however, there are also examples of steam-stable carbon-free MSU materials.[59] A highly related family of materials is the MAS-materials (mesoporous aluminosilicates) which are also prepared by surfactant-mediated assembly of zeolite seed solutions. MAS-materials comprising MFI, BEA and LTL structured nanocrystals as well as MTS-materials (mesoporous titanosilicates) composed of TS-1 nanocrystals have been prepared.[60,61,62,63,64] It is also possible to assemble cubic mesostructured phases resembling MCM-48 but containing MFI and BEA structured zeolite nanocrystals by a very similar approach.[65,66]

In the second group of methods is the surfactant-mediated coating of zeolite crystals with mesoporous phases. This procedure which involves subjecting pre-formed zeolite crystals impregnated with surfactants to MCM-41 synthesis conditions was first reported in 1996

with the preparation of a material composed of zeolite Y crystals overgrown with thin layers of MCM-41 structured material.[67] Also MOR/MCM-41 and BEA/MCM-41 type materials have been prepared using this methodology.[68,69]

The third group of methods is in principle much more limited than the first two since it requires a lamellar precursor which can be exfoliated into a nanocrystalline zeolite material by aid of a surfactant. There are not that many suitable precursors and in consequence, not many different materials have been prepared using this strategy. However, those materials that have been reported have very large surface areas and exhibit improved properties in catalytic applications.[70,71,72] A schematic illustration of the delamination of MCM-22 (P) to produce ITQ-2 is shown in Figure 2.8.
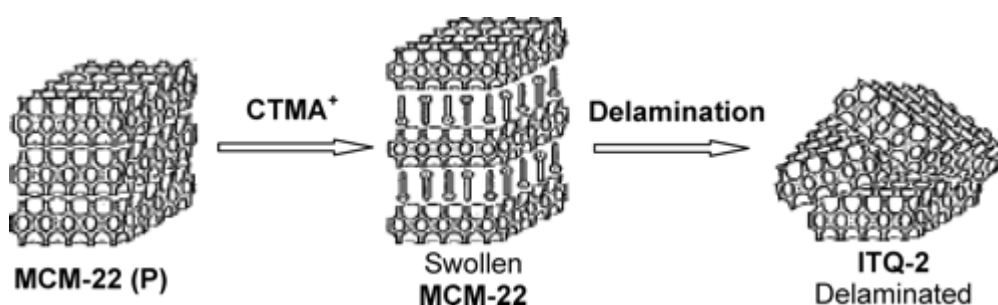
Figure 2.8 Scheme for the preparation of delaminated ITQ-2 from a lamellar zeolite precursor (MCM-22 (P)).[73]

2.2.3. Indirect templating

The third class of templating approaches is categorized as indirect templating since it involves methods for partially transforming mesostructured materials into mesoporous zeolite materials. Thus, the additional porosity of the final material largely stems from an already existing phase as opposed to being generated specifically by a mesopore template. Obviously, these approaches are borderline to non-templating approaches, however, the clear distinction is that a specific mesostructured material can be identified as a template.

Partial crystallization of preformed mesoporous materials

The first example of partial (or secondary) crystallization of an ordered mesoporous silicate to a mesoporous zeolite material was reported in 1997 when it was shown that tetrapropyl ammonium cations (TPA) adsorbed on the amorphous walls of a hexagonally ordered mesoporous silica can be partially crystallized to ultra-small zeolite secondary building units.[74] A few years later it was shown that it is also possible to produce mesoporous materials comprising XRD-visible zeolite nanocrystals in the pore walls.[75] To obtain this, the authors prepared a mesoporous material from a gel containing a surfactant as well as a structure directing agent and subsequently subjected the material to crystallization conditions. This resulted in the partial transformation of the mesoporous material to a mesoporous material comprising ZSM-5 nanocrystals in the pore walls. Essentially, the same type of material can be prepared by simply crystallizing MCM-41 impregnated with TPA in the presence of additional surfactant to prevent the collapse of the mesostructure during crystallization – however, only with limited success as hydrothermal treatment for more than 2 h caused the mesostructure to collapse even in the presence of surfactant.[76] The approach is illustrated in Figure 2.9.
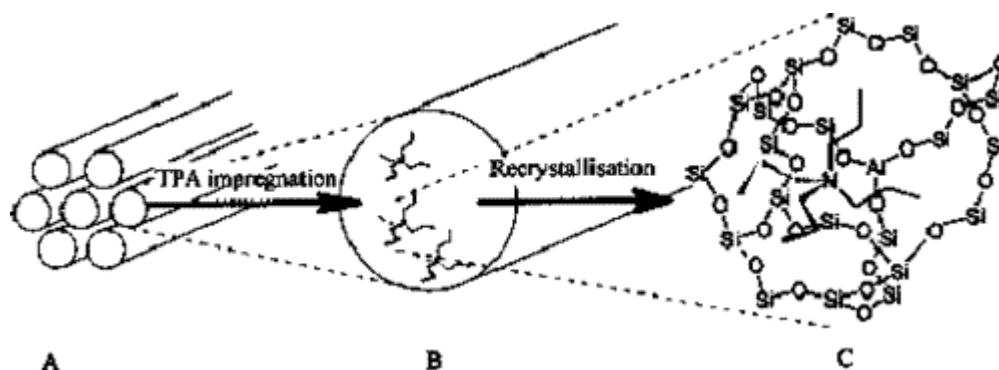
Figure 2.9 Schematic illustration of the pore wall crystallization approach. An ordered mesoporous material is impregnated with a zeolite structure-directing agent and subjected to hydrothermal crystallization conditions resulting in partial crystallization of the mesoporous silica into zeolite structural units.

Much more success has been achieved when thick-walled large-pore SBA-15 materials are applied as starting material for secondary crystallization. In this case, it was reported that as long crystallization time as 5 days of SBA-15 impregnated with TPA-OH resulted in a ZSM-5/SBA-15 type composite material retaining very high mesoporosity (mesopore volume of 1.25 ml/g) as well as a high degree of crystallinity (42%).[77] Also TS-1/SBA-15 type composite materials with high degrees of TS-1 crystallinities and high mesopore volumes can be prepared by secondary crystallization of pre-formed mesoporous titanosilicates.[78]

Deposition of zeolite seeds onto templated mesoporous materials

It is also possible to prepare nanocrystalline zeolite composite materials by crystallization of zeolite synthesis gels adsorbed onto mesoporous materials. Using this approach, an SBA-15 type material with narrow mesopores *ca.* 5.4 nm in diameter containing ZSM-5 embryos was prepared.[79] The authors have also reported that mesostructured cellular silica foams (MCF) can be used to prepare mesoporous MCF composites from ZSM-5 and NaY synthesis gels with much larger mesopores *ca.* 17.5 nm and 15.5 nm in diameters, respectively.[80] Furthermore, it is possible to prepare mesoporous zeolite beta/MCM-41 composite materials by simply impregnating colloidal suspensions of zeolite beta onto MCM-41 followed by calcination.[81]

Zeolitization of diatomaceous earth

Diatomaceous earth, *i.e.* fossil remnants of silica-rich diatoms (a class of algae), has also been used to prepare zeolites with hierarchical porosity serving both as silica source and mesopore template. The diatoms were seeded with a colloidal suspension of zeolite nanoparticles which attached to the surface and then immersed in a zeolite synthesis gel mixture and subjected to crystallization conditions.[82] This procedure afforded materials replicating the macroscale morphology of the diatoms but consisting of small zeolite crystals up to 300 nm in length. Thus, this approach is somewhat similar to the application of silica-rich plants as solid biological templates. However, as the majority of the silica (90%) was provided by the seeded diatoms these procedures are considered a

28

transformation of a siliceous material rather than an application of a solid template. Thus, zeolitization of diatomaceous earth is categorized as indirect templating.

2.3. Non-templated approaches

Zeolite materials with all kinds of hierarchical pore systems can also be synthesized in the complete absence of mesopore templates. Nanosized zeolite crystals, for instance, are prepared by tuning the crystallization conditions to favor nucleation over growth. Also, zeolite composites can be prepared by non-templated approaches. In fact, the vast majority of zeolite composite materials are prepared by extrusion of a zeolite-support composite paste or by spray-drying a slurry containing the zeolite, the support and the required binders, as these methods are applied on industrial scale for the preparation of supported zeolite catalysts. Finally, mesoporous zeolite crystals can be prepared by a non-templated approach termed demetallation because it involves extracting metal ions from the framework.

2.3.1. Demetallation

Demetallation involves the, more or less, selective dissolution of some part of a conventionally prepared zeolite by use of a chemical reagent. The conditions are typically quite harsh involving the use of strong acids, bases or complexing agents as zeolites are actually quite stable materials. There are many examples of dealumination[83] and desilication[84] found in the literature but also detitanation[85] has proved possible. The overall process is schematically illustrated in Figure 2.10.

29
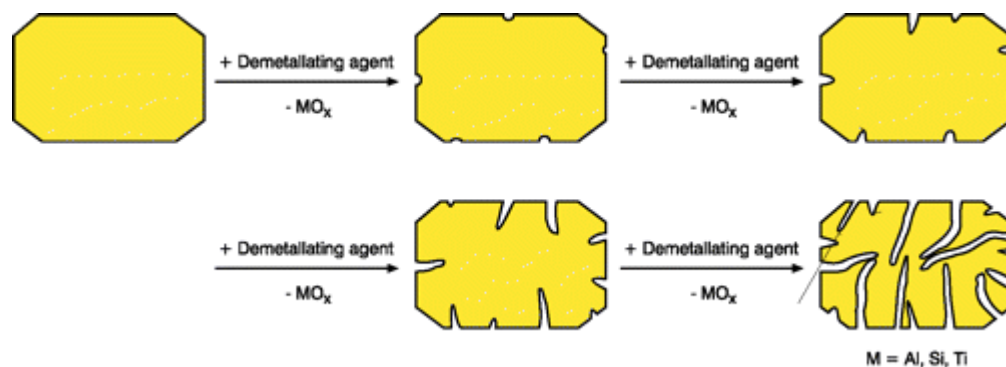
Figure 2.10 Schematic illustration of the demetallation approach. Metals such as Al, Si and Ti can be selectively dissolved from the zeolite framework by use of appropriate chemical treatment.

Dealumination of zeolite Y is the prototypical example of demetallation and it can be achieved by high-temperature steaming or by dissolution using strong acids. The purpose of these treatments is not as much to improve the transport properties of zeolites but rather improving the hydrothermal stability of these. Indeed, transmission electron microscopy reveals that the mesoporosity introduced by dealumination does not improve accessibility to the active sites significantly.[86] Another problem associated with dealumination of zeolites for catalytic purposes is the inevitability that dealumination decreases the acidity of the catalyst (since Brønsted acid sites in zeolites result from Al—O(H)—Si linkages as discussed in Chapter 1).

Desilication is another example of demetallation. The methodology was first reported in the open literature in 1992 when it was shown that alkaline treatment of conventional zeolite crystals resulted in the selective extraction of silicon from the framework yielding highly fragmented crystals.[87] The desilication method has since been refined and is now a very powerful method for preparing mesoporous zeolite crystals of several different framework structures. There are many factors that affect the outcome of subjecting zeolite crystals to alkaline treatment. Obviously, the concentration of OH^- in the treatment medium as well as the volume of this are important factors, but so is the distribution of aluminum in the framework. This has to do with the observation that extraction of framework silicon atoms in close proximity to aluminum atoms proceeds slower than dissolution of silicon atoms which are far away from aluminum atoms.[88] In consequence, the framework aluminum concentration largely determines the type of mesopores being formed by the etching process as illustrated schematically in Figure 2.11.[89]
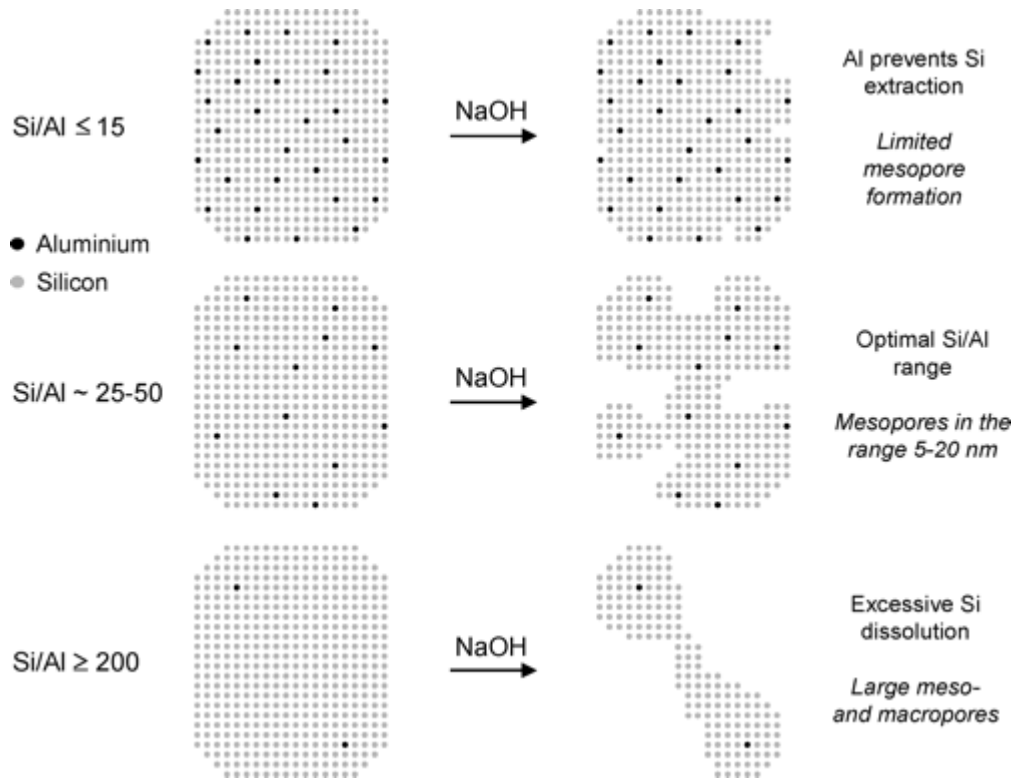
Figure 2.11 Effect of aluminum concentration on the type of mesopores generated in zeolite crystals by alkaline treatment.

As is evident from Figure 2.11 one of the drawbacks of the desilication approach is that it can only be used effectively to produce mesoporous zeolite crystals when the Si/Al ratio of the starting material is in a certain range. However, in this range, it is an easy and relatively straight-forward approach to upgrade the transport properties of existing zeolite materials. Obviously, desilication changes the Si/Al ratio of the treated material, however, in a good way one could argue, as it increases the aluminum concentration and thus also the acidity of the material. For instance, the Si/Al contents (measured by ICP-OES) of MFI zeolites treated with 0.2 M NaOH for 30 min at 65 °C changed from 26, 37 and 42 to 18, 24 and 29, respectively, and resulted in materials exhibiting mesopore surface areas of 195, 235 and 225 m^2/g as opposed to 35, 40 and 45 m^2/g in the starting materials. Thus, two properties, acidity and porosity were improved by the same treatment. Also the desilication time and temperature are influential to the properties of alkaline treated ZSM-5 and in a screening of several temperatures and reaction times it was shown that a temperature of 65 °C and a

treatment time of 30 min was optimal – at least in the case of an MFI zeolite with an Si/Al ratio of 37.[90] Also mesoporous MOR and MTW zeolites have been prepared by alkaline treatment of conventional zeolite powders.[91,92]

2.3.2. Controlled crystallization

As mentioned above, nanosized zeolite crystals can be prepared by tuning the crystallization to favor nucleation over growth. Naturally, this has to be specifically determined experimentally for any given zeolite recipe. Thus, there is no generic approach available to prepare zeolite nanocrystals in the absence of a specific template. On the positive side is, however, that it is fairly straight-forward to experimentally determine a method for preparation of a specific zeolite structure in nanocrystalline form. Thus, when a particular zeolite structure has shown promise in a specific catalytic application the task of improving the transport properties of this particular zeolite by preparing it in nanocrystalline form simply involves screening of a range of experimental conditions. A more detailed overview of the field can be found in the literature.[93]

2.4. Summary

In this chapter was presented an overview of the field of hierarchical zeolites with emphasis on categorization of the methods for preparing these materials. Hierarchical zeolites are zeolites which feature one or more levels of porosity in addition to the inherent micropore system characteristic of zeolites. There are three kinds of hierarchical zeolite materials: Nanosized zeolite crystals, composite materials containing zeolite nanocrystals and mesoporous zeolite crystals. The auxiliary porosity of the zeolite nanocrystal materials is classified as intercrystalline since it results from the packing of nanocrystals or can be attributed to the supporting phase of the composite. On the other hand, the auxiliary porosity of the mesoporous zeolite crystal is intracrystalline since it results from larger non-crystallographic pores interconnected with the micropores in each individual zeolite crystal.

The methods for preparing hierarchical zeolites can be divided into two main groups according to whether or not a template is used in their preparation. On the next level, the

templating approaches are divided into three subgroups, which are termed solid templating approaches, supramolecular templating approaches and indirect templating approaches. Solid templating approaches cover approaches in which templating is facilitated by solid materials such as commercially available or *ad hoc* prepared carbons, aerogels, polymers, resins and biological materials. Supramolecular templating can be divided into two subgroups which are termed primary and secondary and cover methods by which purely molecular or (partly) crystalline species are assembled by aid of surfactants. Primary supramolecular templating methods is divided into two subcategories depending on whether zeolite crystallization takes place on the external or internal surface of the surfactant assembly. Secondary supramolecular templating is divided into three subcategories depending on the function of the surfactant: Methods involving the assembly of protozeolitic nanoclusters (or seeds) into mesostructured materials; methods involving assembly of a mesostructured coating on the external surface of zeolite crystals; and methods involving exfoliation of lamellar zeolite precursor materials into nanocrystalline zeolite sheets. Indirect templating approaches are approaches involving partially transforming mesostructured materials into mesoporous zeolite materials. In this category belong methods for partial crystallization of (amorphous) mesostructured materials, incorporation of zeolite nanocrystals into an existing mesostructured phase or zeolitization of diatomaceous earth. Finally, the non-templated approaches are divided into two subgroups which are termed demetallation and controlled crystallization. Demetallation involves preferential extraction of a (semi-)metal from the zeolite framework whereas controlled crystallization refer to methods by which crystallization conditions are tuned to produce nanocrystals rather than micron-sized crystals.

3. Properties of Mesoporous Zeolite Crystals

3.1. Introduction

As evident from the preceding Chapter, the porosity of hierarchical zeolites can be classified as being either intercrystalline or intracrystalline. Intercrystalline porosity originates from the packing of (nano)crystals and is thus always present in particulate materials. Contrarily, intracrystalline auxiliary porosity is a distinct feature of hierarchical mesoporous zeolite crystals. This is visualized in Figure 3.1.
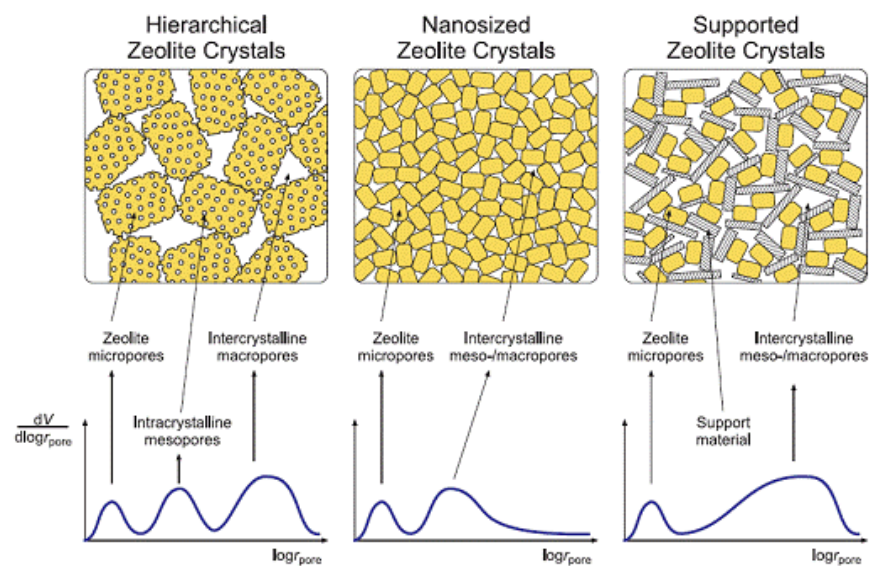
Figure 3.1 Schematic illustrations of the three types of hierarchical zeolite materials highlighting the origin of the different types of pores they feature.

From Chapter 2 it is clear that the most studied methods for preparing mesoporous zeolite crystals featuring intracrystalline auxiliary porosity are carbon-templating and desilication. In the present chapter, a more in-depth discussion of the properties of mesoporous zeolite crystals obtained by these approaches is presented.

3.2. Characterization techniques

In Table 3.1 is listed the most common methods applied for characterization of mesoporous zeolite crystals.

Table 3.1 Techniques commonly applied for characterization of mesoporous zeolite crystals.

Technique	Information
N_2 and Ar physisorption measurements	Porosity (micro- and mesopores), surface area
Hg intrusion porosimetry (MIP)	Porosity (meso- and macropores)
X-ray diffraction (XRD) on powdered samples	Framework structure type, phase purity, crystallinity
Scanning electron microscopy (SEM)	Morphology, material crystallinity and homogeneity, nature of porosity
Transmission electron microscopy (TEM)	Morphology, crystallinity of individual crystals, nature of porosity
Temperature programmed desorption of chemisorbed ammonia	Framework aluminum content
FTIR spectroscopy of chemisorbed pyridine	Brønsted and Lewis acidity
^{27}Al MAS NMR spectroscopy	Framework aluminum content

Physisorption measurements, typically using N_2 or Ar as the adsorbate, reveal information about the textural properties of microporous and mesoporous materials, *e.g.* surface areas and pore volumes. These, typically using N_2 or Ar as the adsorbate, are often used to probe the pore characteristics of porous materials. For materials with combined micro- and mesoporosity, characterization of the porosity using N_2 or Ar physisorption is often accompanied by other types of investigations as well, in order to get a more detailed picture. Mercury intrusion porosimetry (MIP) is used to investigate the nature of the porosity that is not in the micropore region and to determine whether the auxiliary porosity

is occluded inside the crystals or accessible from the external surface of the zeolite crystal. Powder X-ray diffraction (XRD) is used to determine the framework structure type of the prepared material as well as the phase-purity of it. Scanning and transmission electron microscopy (SEM and TEM) are both frequently used for investigating the morphology, crystallinity and homogeneity of the mesoporous zeolite crystals and in particular to obtain direct visual information on the nature of the auxiliary porosity. As mentioned in Chapter 1, the acidic properties of zeolites in general are related to the framework aluminum concentration. Ideally, this is identical to the bulk aluminum concentration, however, this is obviously not necessarily true. Thus, aluminum concentration is usually determined using a combination of bulk elemental analysis techniques such as ICP in combination with more specific framework probing techniques such as temperature programmed desorption of ammonia (NH_3-TPD), FTIR of chemisorbed pyridine or ^{27}Al MAS NMR spectroscopy.

3.3. Textural properties

The most widely applied technique for characterization of the textural properties of zeolites is physisorption measurements using N_2 (or Ar). Most N_2 physisorption isotherms for solid materials in general can be classified as one of Types I-VI according to the IUPAC classification system. The isotherms in this classification system are shown in Figure 3.2
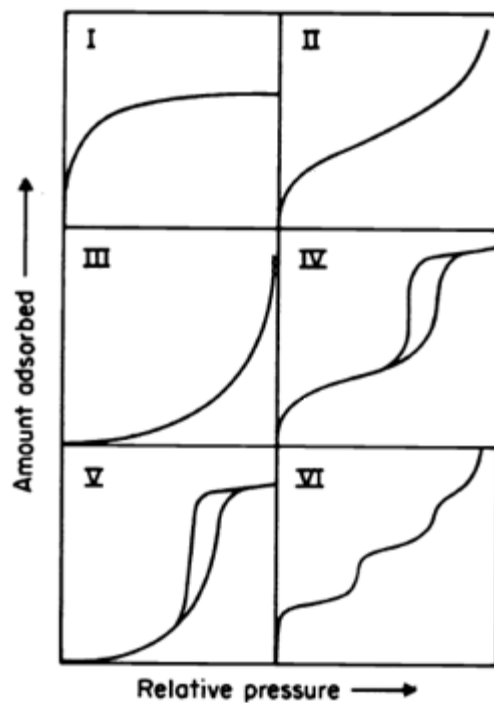
Figure 3.2 Types of physisorption isotherms in the IUPAC classification system.

In the IUPAC classification system, N_2 physisorption isotherms for conventional zeolites are classified as type I isotherms indicating that these are microporous solids with very limited mesoporosity, whereas the isotherms for zeolites with larger amounts of mesoporosity in addition to the micropores, *i.e.* mesoporous zeolite crystals, are classified as type IV isotherms. Due to the crystallographically well-defined micropore system all zeolite materials show gas uptake capacities at low relative pressures corresponding to the filling of the micropores. After complete filling, the gas uptake capacity of conventional zeolites is very limited, indicating that no additional porosity exist in the mesopore region (2-50 nm diameter). Type IV isotherms are characterized by exhibiting hysteresis between the adsorption and desorption branches of the isotherms due to capillary condensation of the adsorbate in mesopores of the adsorbent. Except for type II isotherms which may be given by macroporous zeolites, types III, V and VI isotherms are not commonly given by zeolite materials. The physisorption isotherms associated with mesoporous zeolite crystal materials prepared by either desilication or carbon-tempating are typical Type IV isotherms as exemplified in Figure 3.3 which illustrates the physisorption isotherms and pore-size

distribution calculated by the BJH method[94] of a ZSM-5 material before and after desilication.[90]
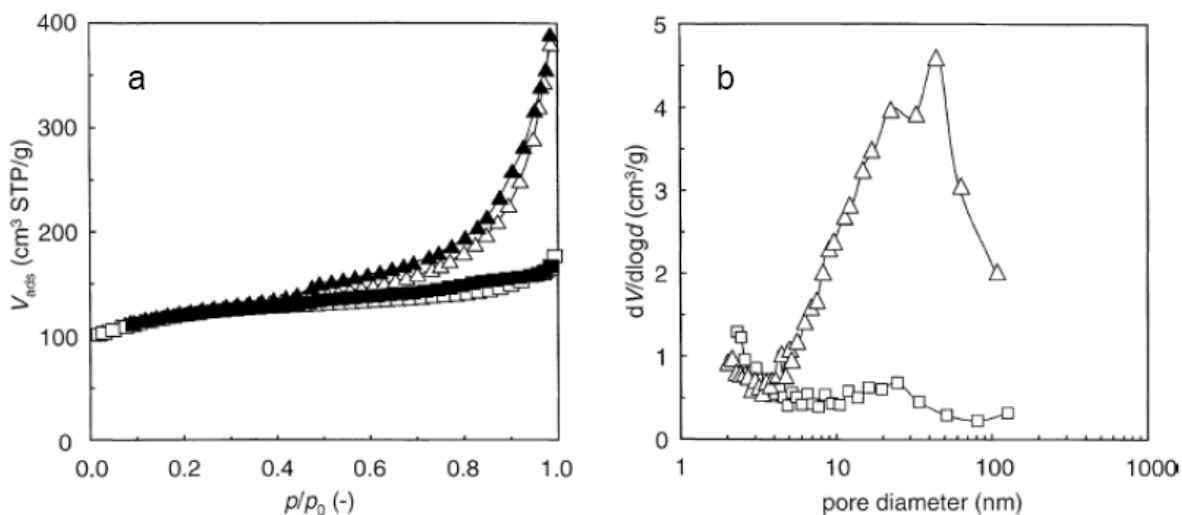
Figure 3.3 Physisorption isotherms (a) and BJH pore-size distributions (b) for conventional (squares) and mesoporous (triangles) ZSM-5 prepared by desilication.

As evident from Figure 3.3 the physisorption isotherm obtained for the non-treated ZSM-5 (squares) can be classified as a type I isotherm. However, after subjecting the sample to desilication, a material exhibiting a typical type IV physisorption isotherm is obtained (triangles) as determined by the hysteresis behavior observed between the adsorption and desorption branches. The BJH pore-size distributions of the same samples before and after alkaline treatment also shown in Figure 3.3 show that the parent material has only little porosity in the mesopore region, whereas the desilicated sample clearly contains mesopores centered around *ca.* 30 nm. As mentioned earlier, it is possible to calculate the pore volume and surface area of mesoporous zeolites from physisorption data. If a mesoporous zeolite sample contains no appreciable amount of macroporosity, the mesopore volume, *i.e.* the pore volume of a sample that results from mesopores, is determined by subtracting the micropore volume (calculated by the *t*-plot method[95] from the total pore volume (total volume of gas adsorbed at a relative pressure of 0.99)). Mesopore volumes of zeolite materials with intracrystalline porosity are typically in the range 0.2-1.0 ml/g. Surface areas of mesoporous zeolite materials are usually given as BET[96] surface areas although this method is not strictly applicable to microporous materials such as zeolites. Nevertheless,

BET surface areas provide a "fingerprint" of the given zeolite material. The porosity of mesoporous zeolites has also been investigated using Hg intrusion porosity measurements. In general, mesopore sizes and volumes determined by Hg intrusion are in excellent accordance with mesopore sizes and volumes determined by N_2 physisorption measurements.[36,97] Thus, Hg intrusion porosimetry measurements confirm that the mesopores of mesoporous zeolite crystals are fully accessible and distributed throughout the individual crystals but it clearly does not provide information about the micropores.

3.4. Structural chemistry

The most prominent and straight-forward method of investigating the structure and crystallinity of mesoporous zeolite single crystal materials is by X-ray diffraction of powdered samples. Representative XRD patterns of mesoporous ZSM-5 samples obtained by both techniques are shown in Figure 4.4 along with the XRD pattern of a conventional micron-sized ZSM-5 sample.
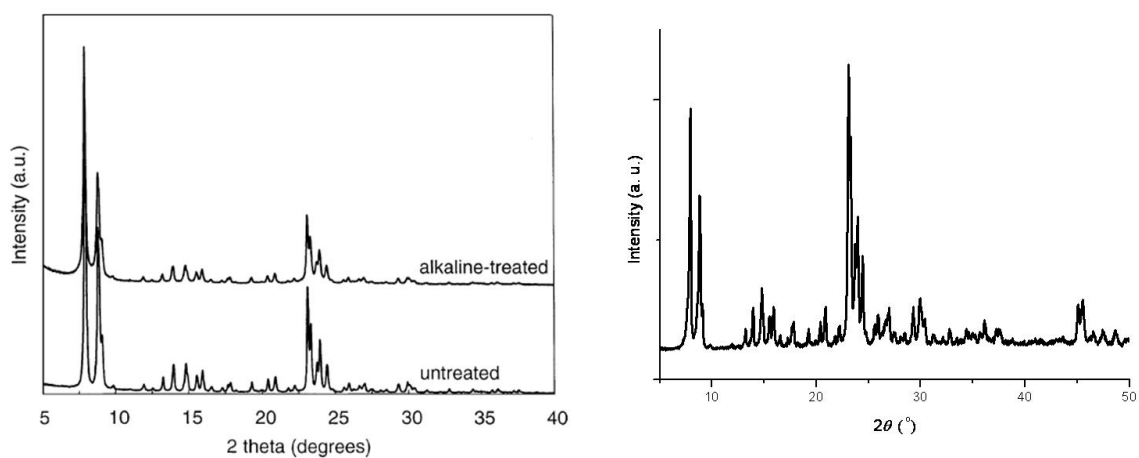
Figure 3.4 Representative XRD patterns of mesoporous and conventional ZSM-5 single crystal materials before and after desilication (left) and prepared by carbon-templating (right).

As seen in the XRD patterns of the ZSM-5 samples, all materials consist exclusively of highly crystalline and phase-pure MFI-structured material. Further analyses of the XRD patterns of the mesoporous samples reveal that the peaks are broader than in the

conventional micron-sized zeolite sample. In fact, they are as broad as the peaks in the pattern obtained from a nanosized zeolite sample, as illustrated in Figure 3.5.
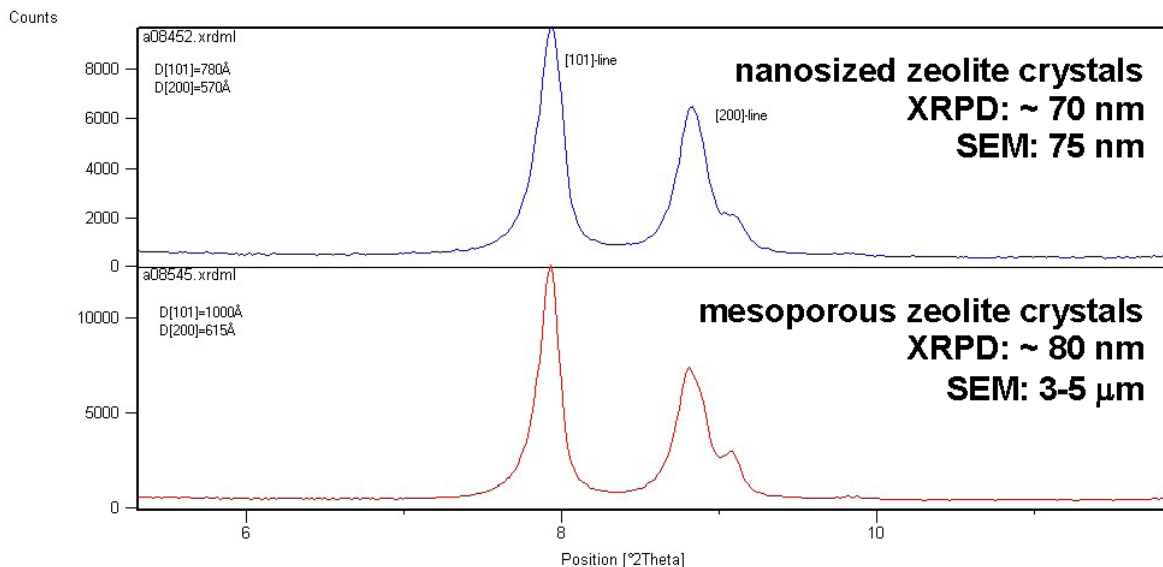
Figure 3.5 Close-up on the [101] and [200]-reflections in XRD patterns of nanosized zeolite crystals and carbon-templated mesoporous zeolite single crystals.

Thus, crystal size determination by use of the Scherrer equation would falsely suggest the crystal size of the mesoporous zeolites to be in the nanosized range. However, the Scherrer equation merely provides information about the mean size of the coherently diffracting entities in the crystal, *i.e.* the mean crystal size. For most crystals, this crystal size is in reasonable agreement with the true crystal size, however, in mesoporous zeolite crystals the longer-range ordering is disturbed by the presence of non-crystallographic voids, *i.e.* the mesopores. Thus, XRD cannot be applied to determine whether the mesopores in mesoporous zeolite materials are intercrystalline or intracrystalline, *i.e.* whether the individual crystals are nanosized or mesoporous. To determine the size of the individual crystals of mesoporous zeolite materials, more direct imaging techniques such as scanning electron microscopy and transmission electron microscopy must be used. Scanning electron microscopy in particular is frequently used to determine the size and morphology of the individual crystals of a particular zeolite sample as it is often directly visible whether the sample consists of agglomerates of nanosized crystals or contains larger porous crystal.

Typical low and high magnification scanning electron microscopy images of a mesoporous ZSM-5 sample synthesized by carbon-templating are shown in Figure 3.6.
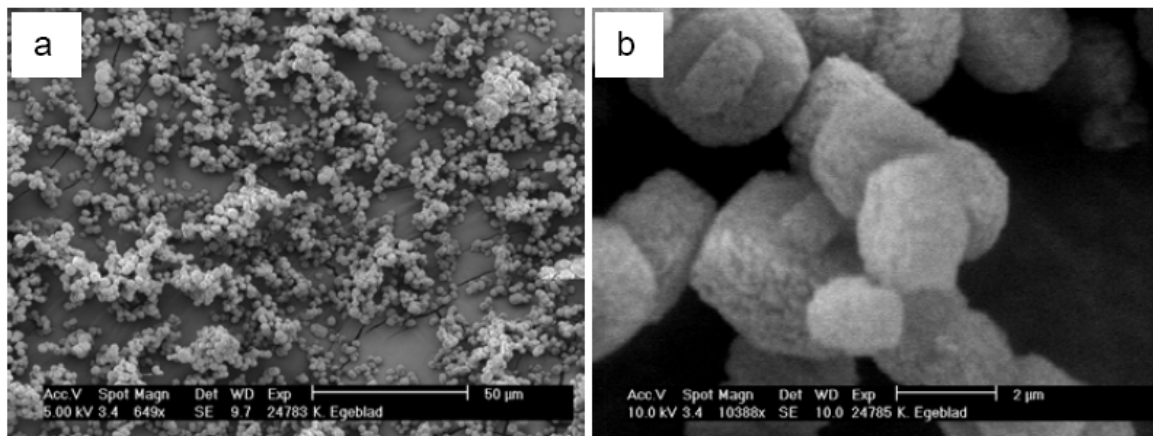
Figure 3.6 Scanning electron microscopy images of a mesoporous ZSM-5 sample produced by carbon-templating recorded at (a) low magnification and (b) high magnification.

As seen in Figure 3.6 mesoporous zeolite crystals prepared by carbon-templating exhibit a sponge-like morphology but at the same time, they retain the coffin-like shape characteristic of MFI-structured zeolites. As also evident from the SEM images shown in Figure 3.6 it is possible with the carbon-templating methodology to obtain mesoporous zeolite samples with a very homogeneous crystal size distribution. In general, the crystal sizes of mesoporous zeolite crystals prepared by carbon-templating are in the range of 1-5 μm but nanosized mesoporous zeolite crystals have indeed also been reported. Since mesopore generation by desilication is a post-synthesis chemical treatment, the crystal size distribution of the mesoporous zeolite crystals produced by desilication should directly reflect that of the parent material – at least if the desilication treatment has resulted in mesopores as opposed to merely peeling layers off of the treated crystals. Thus, by the alkaline treatment procedure it is as easy to produce mesoporous zeolite materials consisting of large crystals as it is to produce the parent zeolite with desired framework Si/Al ratios. In general, as shown in Figure 3.7, mesoporous ZSM-5 crystals produced by desilication of conventional zeolite samples with framework Si/Al ratios in the range 20-50 retain the morphology of the parent sample. However, as also evident from the SEM image

shown in Figure 3.7, excessive alkaline treatment of zeolite samples even with an optimal framework Si/Al is destructive for the crystals.[98]
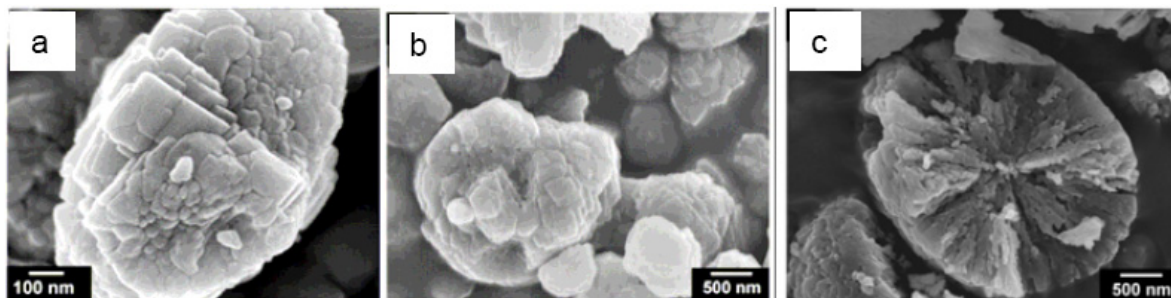
Figure 3.7 SEM images of (a) non-treated ZSM-5 crystals (Zeolyst, CBV8020, NH$_4$) with framework Si/Al=37, (b) same sample after optimal alkaline treatment (10 cm^3 of 0.2 M NaOH and 330 mg of zeolite, 338 K, 30 min) and (c) sample after excessive alkaline treatment (50 cm^3 of 0.2 M NaOH and 330 mg of zeolite, 338 K, 30 min).

Transmission electron microscopy is also frequently used to study mesoporous zeolite materials. Comparison of transmission electron microscopy images of conventional zeolites with mesoporous zeolites prepared by either carbon-templating or desilication very visibly reveals the porosities of the individual crystals; conventional zeolite crystals appear to be dense exhibiting no distinct contrast difference throughout the crystals whereas mesoporous zeolite crystals show pronounced contrast differences and therefore appear to be sponge-like rather than dense. Typical TEM images of mesoporous zeolite crystals prepared by either of the two methods are shown in Figure 3.8 along with a TEM image of conventional zeolite crystals.
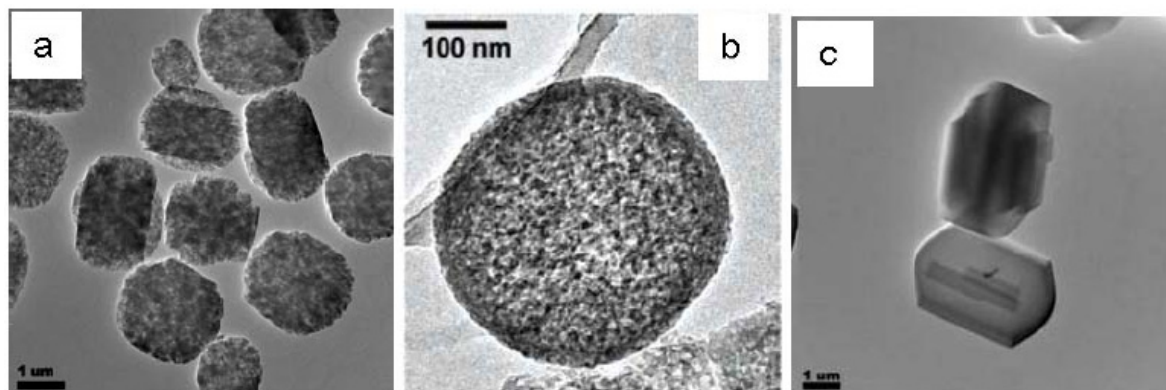
Figure 3.8 TEM images of (a) mesoporous silicalite-1 prepared by carbon-templating, (b) mesoporous ZSM-5 prepared by alkaline treatment[99] and (c) conventional silicalite-1 crystals.

The contrast difference seen in the TEM images in Figure 3.8 is due to less absorption of the electron beam by passage through a mesoporous crystal than through a conventional crystal. Thus, an electron beam transmitted through a mesoporous zeolite crystal encounters fewer atoms than an electron beam transmitted through a conventional zeolite crystal of equal thickness. As mesoporous zeolite crystals are composed of crystalline domains and void domains distributed more or less randomly throughout the crystals, these crystals appear to be white-spotted particles in TEM images, indicating that mesoporous zeolite crystals prepared by either carbon-templating or desilication contain intracrystalline porosity. Cross-sectional (3D-)TEM images of mesoporous zeolite crystals prepared by carbon-templating clearly show that the mesopore system extends throughout the entire crystals starting at the external surface. Final proof of the single-crystalline nature of mesoporous zeolite crystals has also been provided by careful TEM studies using the selected area electron diffraction (SAD) technique on individual crystals in the powdered samples. As shown in Figure 3.9 the electron diffraction pattern obtained from an isolated mesoporous ZSM-5 particle is an array of reflections rather than concentric circles which would result from a polycrystalline agglomerate.
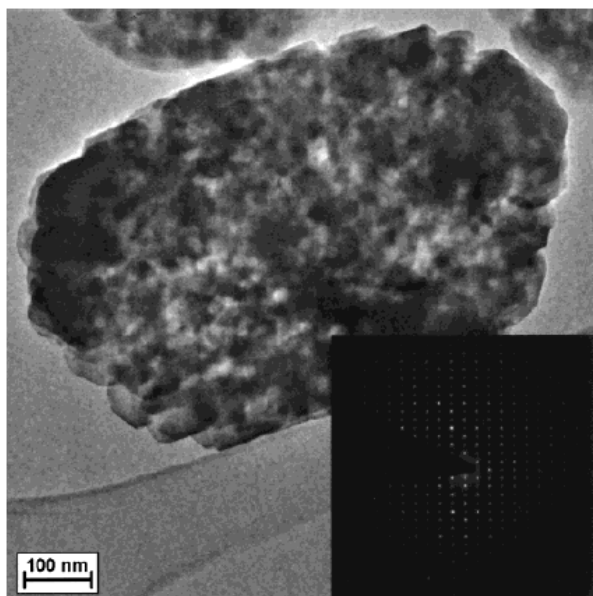
Figure 3.9 TEM image and SAD pattern of a mesoporous ZSM-5 crystal prepared by carbon-templating.

This diffraction pattern that can be completely ascribed to a twinned MFI crystal unambiguously proving that mesoporous zeolite crystals prepared by carbon-templating are indeed single crystals rather than agglomerates of nanosized crystals.

3.5. Acidic properties

As mentioned earlier, the acidic properties of zeolites are closely related to the framework aluminum concentration which is usually determined by techniques such as NH_3-TPD which method gives a measure of both the number and strength of the acid sites of the zeolite. By the carbon-templating procedure it is possible to produce zeolites with varying amounts of acidities by using different aluminum sources in the synthesis gels. In Table 3.2 is listed NH_3 desorption capacities and results of elemental analyses of mesoporous zeolite crystal materials prepared from different aluminum sources.[100]

Table 3.2 Aluminum content determined by NH_3-TPD, IR of chemisorbed pyridine and ^{27}Al MAS NMR of conventional and mesoporous ZSM-5 prepared by carbon-templating.

Sample	Aluminum Source	Si/Al ratio[a]	Al content, µmol/g	Amount of NH_3 desorbed, µmol/g	Si/Al ratio[b]
ZSM-5	aluminum isopropoxide	14.4	870	740	16.6
ZSM-5	aluminum isopropoxide	31.2	529	464	32.3
ZSM-5	sodium aluminate	16.8	825	350	43.9
ZSM-5	sodium aluminate	34.3	451	336	46.9

[a] Elemental analysis results
[b] NH_3-TPD results

As seen in Table 3.2, when sodium aluminate is used as aluminum source, a discrepancy between Si/Al ratios determined by NH_3-TPD and Si/Al ratios determined by elemental analysis is observed, indicating that not all of the aluminum in the mesoporous zeolite crystals is present in the framework, as only framework aluminum contributes significantly to the acidity. However, when aluminum isopropoxide is used instead, much more

aluminum appears to be incorporated into the framework, resulting in an overall higher total acidity as measured by NH_3-TPD. Thus, Table 3.2 shows that zeolite crystals with substantial amount of acid sites (> 700 μmol/g) may be prepared by carbon-templating and that the framework Si/Al content should not exclusively be determined by bulk elemental analysis techniques. The acidity range possible to achieve for mesoporous zeolite crystal materials prepared by desilication is more limited due to the fact that mesopore generation by this procedure is very much dependent on the Si/Al ratio of the parent zeolite. As pointed out previously, the framework Si/Al content of the parent zeolite before alkaline treatment, should be in the approximate range 20-50 in order to achieve reasonable mesopore content. However, since desilication results in preferential extraction of silicon from the framework, the aluminum concentration relative to silicon gradually increases during the alkaline treatment. This is shown in Figure 3.10 for mesoporous MFI and MOR prepared by alkaline treatment.[101] Clearly, the NH_3-TPD method does not provide information on the relative amounts of Brønsted and Lewis acid sites, and such studies have not yet been reported for mesoporous zeolite crystals.
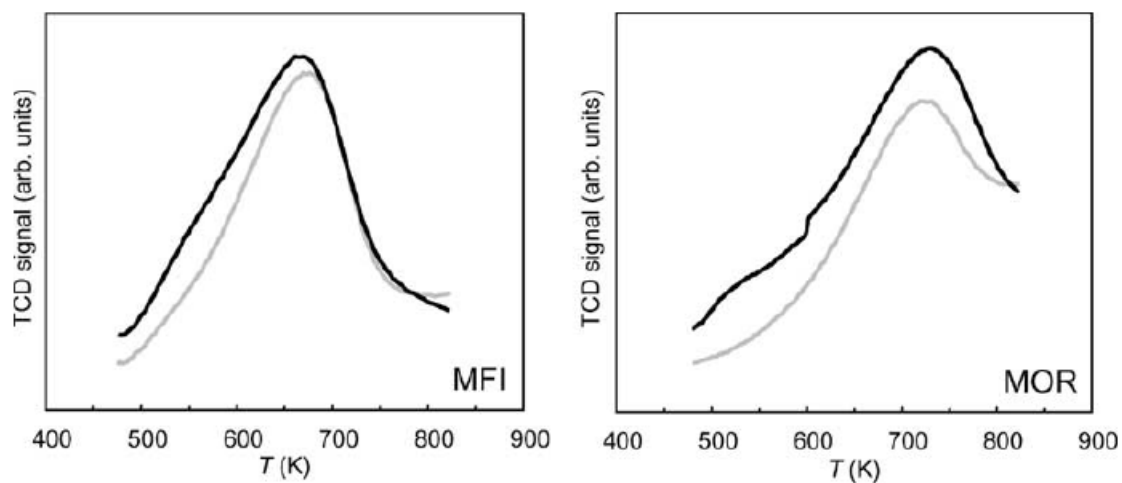
Figure 3.10 NH_3-TPD curves for mesoporous (black line) and conventional (grey line) zeolite crystals of MFI and MOR structure type.

The framework aluminum concentration of mesoporous zeolites have also been investigated using FTIR spectroscopy of pyridine chemisorbed onto acid sites and by ^{27}Al

MAS NMR spectroscopy. In general, good agreement is found for aluminum concentrations determined by these methods in comparison with NH_3-TPD results as shown in Table 3.3.

Table 3.3 Aluminum content determined by NH_3-TPD, IR of chemisorbed pyridine and ^{27}Al MAS NMR of conventional and mesoporous ZSM-5 prepared by carbon-templating.

Sample	NH$_3$-TPD	pyridine-IR	^{27}Al NMR
Conventional	71	70	70
Mesoporous	116	110	120

3.6. Diffusional properties

The main purpose of introducing mesoporosity into individual zeolite crystals is to enhance the rate of diffusion of reactants, intermediates and products within the individual zeolite crystals during catalytic reactions. The diffusional properties of mesoporous zeolite crystal materials compared to conventional zeolites have been investigated by gas adsorption and desorption experiments and by diffusion of liquids in zeolite crystals. In Figure 3.11 is shown the results of gas diffusion experiments for mesoporous and conventional ZSM-5 crystals as a function of time.
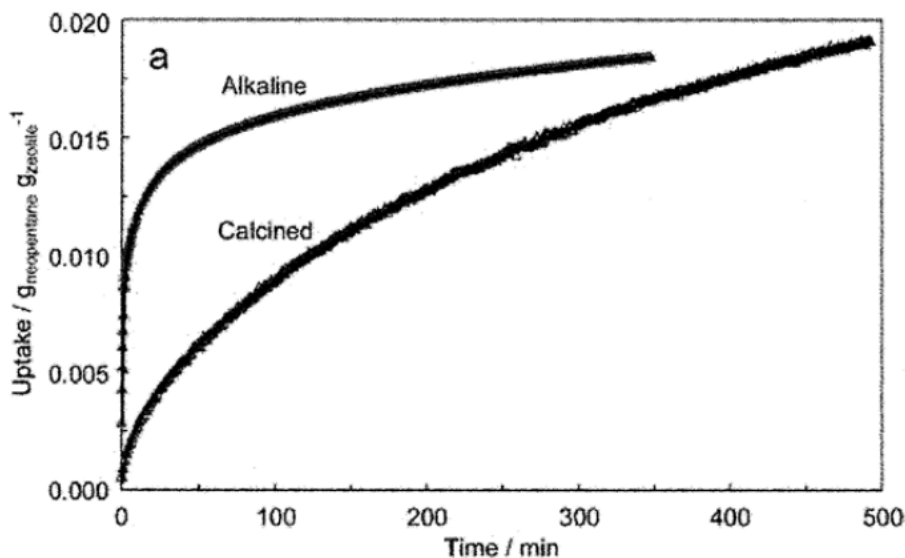
Figure 3.11 Adsorption of neopentane in alkaline treated ZSM-5.[102]

As seen in Figure 3.11, mesoporous ZSM-5 prepared by desilication shows much faster neo-pentane adsorption capabilities than conventional, non-treated ZSM-5: 50% of the maximum neopentane uptake is achieved after only 2 min for the mesoporous sample and after approximately 120 min for the conventional sample. From these data, the average characteristic diffusion time was determined to be more than 2 orders of magnitude shorter in the mesoporous sample than in the conventional sample. Figure 3.12 shows that also desorption of *i*-butane out of saturated ZSM-5 crystals is much faster for carbon-templated mesoporous zeolite crystals than for conventional zeolite crystals.[103]
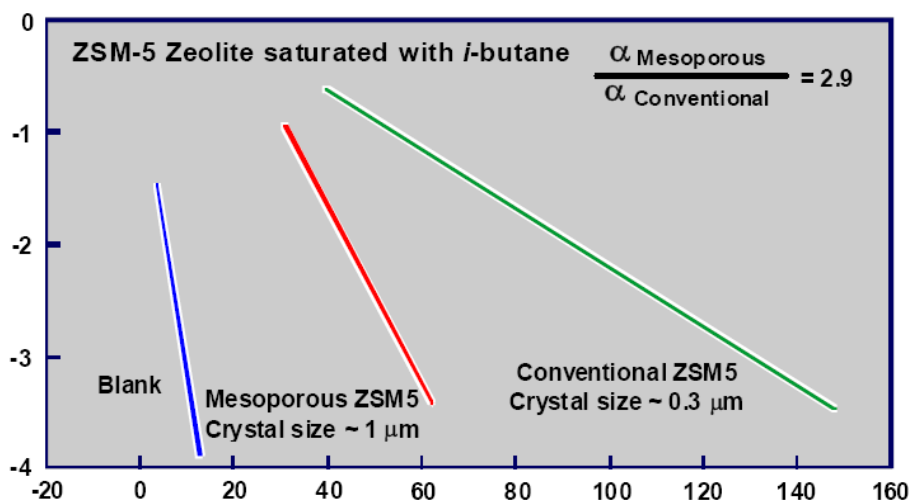
Figure 3.12 Desorption of *i*-butane in carbon-templated ZSM-5 as compared to conventional ZSM-5.

Likewise, comparative experiments with diffusion of liquids adsorbed onto mesoporous and conventional silicalite-1 materials have been conducted.[104] These experiments clearly show that also diffusion of molecules out of mesoporous zeolite crystals into a liquid is much faster than out of conventional crystals. In Figure 3.13 is shown the results of diffusion experiments with *n*-hexadecane (at different loadings) and mesitylene out of mesoporous and conventional silicalite-1 crystals.

48
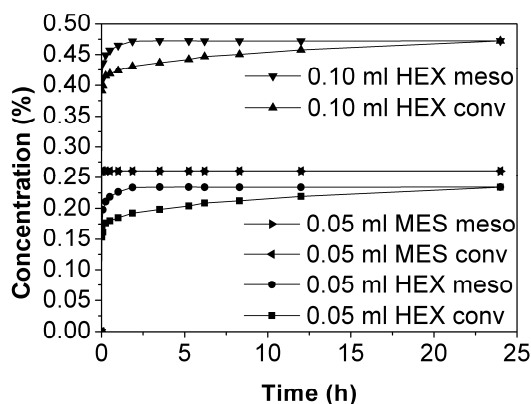
Figure 3.13 Diffusion of *n*-hexadecane and mesitylene in mesoporous and conventional silicalite-1 crystals.

It can be seen from Figure 3.13 that diffusion of *n*-hexadecane is much faster out of mesoporous than out of conventional silicalite-1, as the concentration of *n*-hexadecane in *n*-hexane increases much more rapidly for the mesoporous sample regardless of the amount of *n*-hexadecane adsorbed in the zeolite micropores prior to the diffusion experiment. It is also seen that mesitylene is too bulky a molecule to penetrate to the micropore system of silicalite-1, since no change in concentration is observed over time demonstrating that the mesitylene is only adsorbed on the external surface of the zeolite materials.

3.7. Summary

In this chapter was described the most commonly methods for characterization of mesoporous zeolite crystals as well as the typical results obtained using these techniques. The framework structure type(s) as well as the phase-purity of mesoporous zeolite crystals are determined by powder XRD diffraction which also reveals information of the size of the crystals. However, care must be taken in determining the crystal size using XRD alone since mesoporous crystals exhibit similar line-broadening as nanosized crystals. This observation is in fact easily explained since mesoporous zeolite crystals are composed of crystalline domains and void domains. Importantly, the crystalline domains are interconnected and thus appear as a single crystal which is also evident from SAD patterns

obtained from individual zeolite particles. Physisorption measurements using N_2 and Ar as the adsorbate are commonly used to investigate the textural properties of mesoporous zeolite crystals. A characteristic feature of these isotherms is that they exhibit hysteresis between the adsorption and desorption branches. Thus, the isotherms given by these materials are type IV isotherms according to the IUPAC classification system indicating that they are mesoporous. SEM and TEM techniques are used to investigate the morphology of the crystals as well as for obtaining direct visual images of the porosity of the materials. Typically, the auxiliary intracrystalline porosity of the mesoporous zeolite crystal is clearly visible from the TEM images since these reveal highly contrasted crystals as opposed to non-contrasted images obtained by TEM of conventional crystals. The acidity of zeolites in general is correlated to the framework aluminum concentration, thus bulk techniques for determining the Al content are normally used in combination with more specific framework probing techniques such as NH_3-TPD or FT-IR of chemisorbed species. The diffusional properties of mesoporous zeolites have been investigated using gases as well as liquids. These experiments reveal that diffusion of both gases and liquids proceed faster in mesoporous zeolites than in conventional analogues.

4. Tuning the Properties of Hierarchical Zeolites by Templating Methods

4.1. Introduction

As evident from Chapter 2 the application of templates for the introduction of additional porosity in zeolites has been widely reported. Numerous templates have been applied and many different materials have been prepared with great success. Thus, templating methods constitute a highly versatile group of methods for the achievement of mesoporosity in zeolites. In the present chapter is described how templating approaches can be applied to tune the porosity properties of hierarchical zeolites.

The first reported example of mesoporous zeolite single crystals obtained by carbon-templating involved the use of 12 nm diameter carbon particles with the trade name Black Pearls 2000 (BP2000) as the mesopore template. This highly porous carbon material is by far the most widely applied mesopore template since it has been used to produce a range of different mesoporous zeolites.[24,25,28,104] Materials prepared using BP2000 as the carbon template are usually very homogeneous in crystals size averaging 1-2 μm on the longest axis and they typically feature mesopores with diameters ranging from 20 to 50 nm. Other carbons have been applied as mesopore templates as well including Mogul L and Monarch carbons, however, systematic studies on the application of a family of differently sized carbon particle templates have only been published recently using four different Raven carbons (RV) as templates. Another method for tuning the hierarchical porosity of zeolites

which was also reported recently is the application of porous carbons specifically designed for the purpose of templating additional porosity in zeolites. A third method for tuning the porosity of hierarchical zeolites which was published recently is the application of *in situ* prepared carbon-silica gel composites with different carbon contents serving as silica source and mesopore template simultaneously.

4.2. Experimental

4.2.1. Preparation of mesoporous silicalite-1 using Raven carbons

A series of silicalite-1 zeolites were prepared by sequential impregnation of zeolite synthesis gel components onto different Raven carbons as follows: Mixtures of tetrapropyl ammonium hydroxide (TPAOH, 3.44 g, 40 wt%), water (0.5 g) and ethanol (3.03 g) were impregnated onto different amounts of dry Raven carbons, as listed in Table 4.1., and left to dry overnight. Then, the dry carbon samples were impregnated with tetraethyl orthosilicate (TEOS, 3.87 g) and left overnight before being transferred to Teflon-beakers which were placed in Teflon-lined autoclaves with 10-15 ml water outside the beaker. The autoclaves were then heated to 180 °C for 3 days after which the solid materials were collected by filtration and washed with *ca.* 1 l water. The washed materials were dried at 120 °C and then calcined in air at 550 °C for 24 h to produce white zeolite powders.

Table 4.1 Particle sizes, pore volumes and amounts of Raven carbons applied.

	RV500	RV1200	RV7000	RV5000
Particle size (nm)[a]	53	20	11	8
V_{total} (ml/g)	0.07	0.19	0.89	-
Amount of carbon in gel (g)	11.2	16.0	8.0	3.0

[a] Carbon particle sizes were taken from the data sheets provided by the suppliers.

The calcined zeolite samples were characterized by powder X-ray diffraction, nitrogen physisorption and scanning electron microscopy techniques. The XRD measurements were conducted on a Philips PW 3710 X-ray Diffractometer. Nitrogen adsorption and desorption isotherms were measured at liquid nitrogen temperature on an Micromeritics ASAP 2020 apparatus. Prior to physisorption measurements, all samples were outgassed under vacuum at 200 °C overnight. Total surface areas were calculated according to the BET method.

Micropore volumes were calculated by the *t*-plot method. Total pore volumes were estimated from the amount of N_2 adsorbed at $p/p_0 = 0.99$. Meso-/macropore volumes were calculated by subtracting micropore volumes from total pore volumes. SEM analyses were performed on a Philips XL20 FEG. The calcined samples were placed on a carbon film and Pt was evaporated on the samples for approximately 20 min in order to achieve sufficient conductivity.

4.2.2. Preparation of mesoporous silicalite-1 using pre-treated carbons

A series of silicalite-1 materials were prepared by sequential impregnation of zeolite synthesis gel components onto pre-treated carbon templates. Prior to their application in synthesis RV5000 and BP2000 were heated at 600 °C for 5 h in N_2 atmosphere. These samples are denoted RV5000H and BP2000H, respectively. Furthermore, another BP2000 sample (4 g) was suspended in a solution of sodium citrate (1.5 g) in water (200 ml) and stirred until the water had evaporated. The BP2000 impregnated with sodium citrate was dried at 110 °C overnight and then applied in zeolite synthesis. This carbon is denoted BP2000C. Using BP2000H and BP2000C 2.0 g of template were applied in synthesis using the amounts and the procedure described above (Section 4.2.1.), whereas the amounts in the case of RV5000H were 3.0 g template, 1.7 g TPAOH, 0.3 g H_2O, 1.5 g ethanol and 2.0 g TEOS. The prepared materials were characterized as described above (Section 4.2.1.)

4.2.3. Preparation of mesoporous carbon template

A porous carbon template was prepared by dissolving sucrose (13.1 g, 98%) in a mixture of ethanol (9.6 ml, absolute), water (7.5 ml) and ammonia (1.0 ml, 25 wt%) while stirring at 50 °C for 1.5 h. Then, the mixture was transferred to a Teflon beaker which was placed in a Teflon-lined autoclave. The autoclave was then heated to 180 °C for 2 days after which the brown solid material which retained the shape of the beaker was removed. The brown solid was then crushed in a mortar and transferred to a horizontal tube furnace and heated to 850 °C for 5 h in a flow of N_2 to produce a black carbonaceous solid. The black solid was characterized by thermal gravimetry (TG), differential scanning calorimetry (DSC), N_2 physisorption measurements and CHN elemental analysis. The TG measurements were

conducted with NETZSCH STA 409 PC/PG equipment with a ramp of 20 °C under a 20 ml/min N_2 flow. The DSC measurements were conducted using a TA-2620 DSC equipped with cryostat cooling. The N_2 physisorption measurements were conducted as described above (Section 4.2.1.). CHN elemental analysis was performed with a CE Instruments FLASH 1112 Series EA.

4.2.4. Preparation of mesoporous silicalite-1 using pre-formed mesoporous carbon

A mesoporous silicalite-1 material was prepared by sequential impregnation of zeolite synthesis gel components onto 2.5 of the porous carbon template prepared as described above (Section 4.2.3.): TPAOH (3.4 g) was mixed with ethanol (2.0 ml) and impregnated onto the carbon template. After being dried in air overnight, TEOS (3.0 ml) was impregnated onto the material which was left for 1 d before being transferred to a Teflon beaker placed in a Teflon-lined autoclave with 10 ml water outside the beaker. The autoclave was heated to 180 °C for 3 d before the solid material was collected by filtration, washed, dried and calcined in air to produce a white zeolite powder. The zeolite powder was characterized by powder XRD, SEM, transmission electron microscopy, selected area electron diffraction, N_2 physisorption measurements and Hg intrusion porosimetry. XRD, SEM and N_2 physisorption measurements were performed as described above (Section 4.2.1.). Mercury porosimetry was measured by intrusion using Quantachrome equipment. TEM was performed with a JEM 2000FX using an accelerating voltage of 300 kV. SAD was used to obtain electron diffraction patterns from individual grains of powder. A few mg of the powdered samples were suspended in 2 ml ethanol and the suspension was sonicated for 1 h. Then, the suspension was allowed to settle for 15 min, before a drop was taken and dispersed on a 300 mesh copper grid coated with holey carbon film.

4.2.5. Preparation of carbon-silica composites

Carbon-silica composites were prepared by one or more impregnations of heated aqueous solutions of sucrose onto silica gel and calcining the sucrose-silica mixture in Ar or N_2 at 500 °C for 15-16 h to produce black carbon-silica composites. The most concentrated impregnation liquids can be produced by heating a mixture of sucrose (40 g) and water (10

54

g) to *ca.* 90 °C resulting in a hot syrupy liquid and then impregnating it directly onto hot (110 °C) silica gel.

4.2.6. Preparation of mesoporous zeolites using carbon-silica composites

Mesoporous ZSM-5 and ZSM-11 were prepared by adding the carbon-silica composites described above (Section 4.2.5.) to mixtures containing the remaining zeolite synthesis gel components. For the preparation of ZSM-5, carbon-silica composites were added to mixtures of TPAOH (33.83 g, 20 wt%), water (8.5 g), NaOH (0.53 g) and $NaAlO_2$ (0.08 g) resulting in synthesis gels with molar compositions 1 Al_2O_3 : 181 SiO_2 : 36 TPA_2O : 15 Na_2O : 1029 H_2O. For the preparation of ZSM-11, the carbon-silica composite was added to a mixture of tetrabutyl ammonium hydroxide (TBAOH, 21.58 g, 40 wt%), water (30 g), NaOH (0.53 g) and $NaAlO_2$ (0.08 g). The zeolite synthesis gels were stirred for 1 h before being transferred to Teflon-beakers which were placed in Teflon-lined autoclaves. The autoclaves were then heated to 180 °C for 3 days after which the solid materials were collected by filtration, washed, dried and calcined in air at 550 °C for 20 h to produce white zeolite powders.

4.3. Results and discussion

4.3.1. Characterization of the mesoporous carbon template

The results of the TG and DSC measurements performed on the brown solid obtained by hydrothermal treatment of a sucrose-ammonia mixture as described above (Section 4.2.3.) are shown in Figure 4.1.
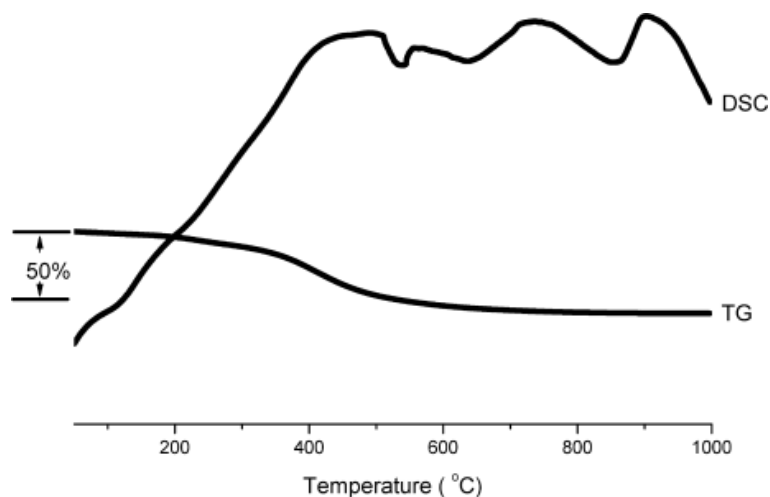
Figure 4.1 TG and DSC profiles of the solid obtained after hydrothermal treatment of a mixture of sucrose and ammonia.

The TG measurements show that there is a *ca.* 50% weight-loss from the brown solid upon heating it, predominantly in the temperature range 400 to 500 °C. This weight-loss is due to dehydration of the sucrose. From the DSC profile, also shown in Figure 4.1, it is seen that several endothermic peaks appear at temperatures above 500 °C. These are most likely due to carbonization of the decomposed sucrose since carbonization is an endothermic process. Thus, the TG and DSC measurements suggest that the brown solid is transformed into a carbonaceous solid upon heating in the absence of air.

The porous black solid obtained as described above (Section 4.3.2) is a carbonaceous material containing carbon (86.5 wt%), nitrogen (1.17 wt%) and hydrogen (1.25 wt%) as determined by CHN elemental analysis with the remaining content most likely being oxygen present in the form of hydroxy groups. Nitrogen physisorption isotherms of the black solid and the pore size distribution plot associated therewith are shown in Figure 4.2.
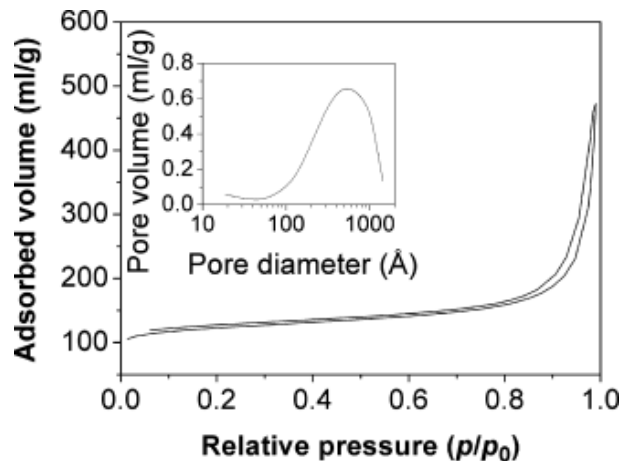
Figure 4.2 Nitrogen adsorption/desorption isotherms of the porous carbon obtained by carbonizing sucrose. The inset shows the pore size distribution obtained from the desorption branch of the isotherm using the BJH method.

As shown in Figure 4.2 the physisorption isotherm obtained from the black solid exhibits a type IV hysteresis loop indicating that the material contains pores in the mesopore size range. This is also evident from the pore size distribution plot shown in the inset, where it is seen that the pore size distribution of the carbon is very broad and extends from the mesopore to the macropore region.

4.3.2. Characterization of the zeolites by XRD

Using the Raven carbons as received it was possible to prepare phase-pure silicalite-1 samples except in the case of RV5000 where all attempts were unsuccessful. It was, however, possible to produce phase-pure silicalite-1 using the pre-heated RV5000H carbon as template as well as from BP2000H. Also BP2000C and the pre-formed mesoporous carbon described above (Section 4.2.3.) were successfully applied as templates resulting in phase-pure silicalite-1 samples. Finally, the preparations of ZSM-5 and ZSM-11 materials from the carbon-silica composites were also successful since phase-pure powders were obtained. A representative XRD diagram obtained from mesoporous silicalite-1 prepared from the pre-formed carbon template is shown in Figure 4.3.
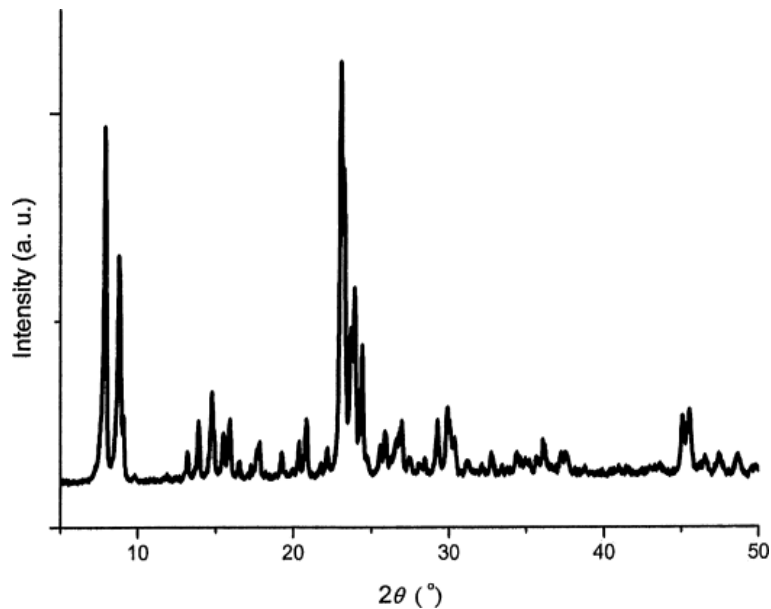
Figure 4.3 Powder XRD diagram of the silicalite-1 material prepared from the pre-formed carbon template.

4.3.2. Characterization of the zeolites by nitrogen physisorption and mercury intrusion

In Table 4.2 are listed the pore volumes and BET surface areas of the zeolite samples prepared using the procudures described above.

Table 5.2 BET surface areas and pore volumes of the prepared samples.

Zeolite	Template	S_{BET} (m^2/g)	V_{micro}[a] (ml/g)	$V_{meso/macro}$[b] (ml/g)
Silicalite-1	RV500	405	0.14	0.11
Silicalite-1	RV1200	360	0.11	0.44
Silicalite-1	RV7000	357	0.11	0.48
Silicalite-1	RV5000H	391	0.079	0.33
Silicalite-1	BP2000H	395	0.10	0.27
Silicalite-1	BP2000C	388	0.068	0.35
Silicalite-1	Carbon preformed from sucrose and ammonia	403	0.09	0.37
ZSM-5	Carbon-silica composite with C/Si = 0.58	359	0.14	0.04
ZSM-5	Carbon-silica composite with C/Si = 0.87	361	0.14	0.05
ZSM-5	Carbon-silica composite with C/Si = 1.75	356	0.15	0.08
ZSM-11	Carbon-silica composite with C/Si = 0.58	372	0.14	0.04

[a] Micropore volumes are calculated using the t-plot method
[b] Meso/macropore volumes are calculated as total pore volumes minus micropore volumes.

Table 4.2 reveals that all zeolite materials are microporous materials with surface areas typical for zeolites. It is also seen that there is a rather large variation in meso-/macropore

volume of the materials. This difference is attributed to the different templates being applied in the synthesis. The highest pore volumes are obtained using RV1200 and RV7000 carbons as templates whereas the lowest are obtained using the carbon-silica composites with low carbon contents (C/Si = 0.58). It is, however, seen that by successive impregnations of sucrose onto the carbon-silica composites it is possible to increase the mesopore volume by a factor of two, cf. ZSM-5 prepared using carbon-silica composites with C/Si = 0.58 and 1.75. Moreover, Table 4.2 reveals that pre-treatment of BP2000 with sodium citrate is more effective than preheating since the BP2000C templated silicalite-1 has a substantially higher mesopore volume than the BP2000H templated material.

In Figure 4.4 is shown the physisorption isotherm and pore size distribution plot associated with the silicalite-1 material prepared using the carbon template prepared from sucrose and ammonia as the template.
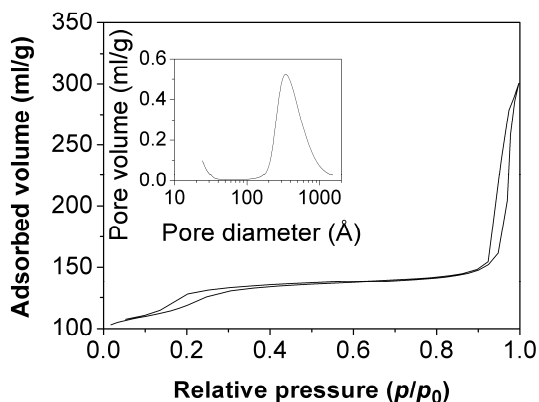
Figure 4.4 Nitrogen adsorption-desorption isotherms of the mesoporous silicalite-1 material prepared form the pore-formed carbon template after combustion of the carbon and organic templates. The inset shows the pore size distribution obtained from the desorption branch of the isotherm using BJH method.

The physisorption isotherm shown in Figure 4.4 is typical for mesoporous silicalite-1 materials prepared by carbon templating and is shown here as a representative example. As seen, the isotherm exhibits hysteresis in two regions of relative pressure, above $p/p_0 = 0.9$ and in the p/p_0 range of 0.1 to 0.3. The hysteresis loop at higher relative pressures indicate

that the isotherm is a type IV isotherm according to the IUPAC classification, whereas the hysteresis loop in the lower relative pressure range is not associated with mesoporosity but is the result of a phase-transformation of N_2 in the micropores of pure silica MFI zeolites. In Figure 4.4 is also shown the pore size distribution plot derived from the desorption isotherm. This shows that the material has pores in the meso- and macropore size range, centered at *ca.* 31 nm. These observations are backed by Hg intrusion porosimetry measurements which also show that the material contains larger macropores which are not efficiently measured using physisorption.

In Figure 4.5 are shown the pore size distribution plots obtained from the desorption branches of the physisorption isotherms of the zeolite samples prepared using Raven carbons and pre-treated RV5000 and BP2000 carbons.
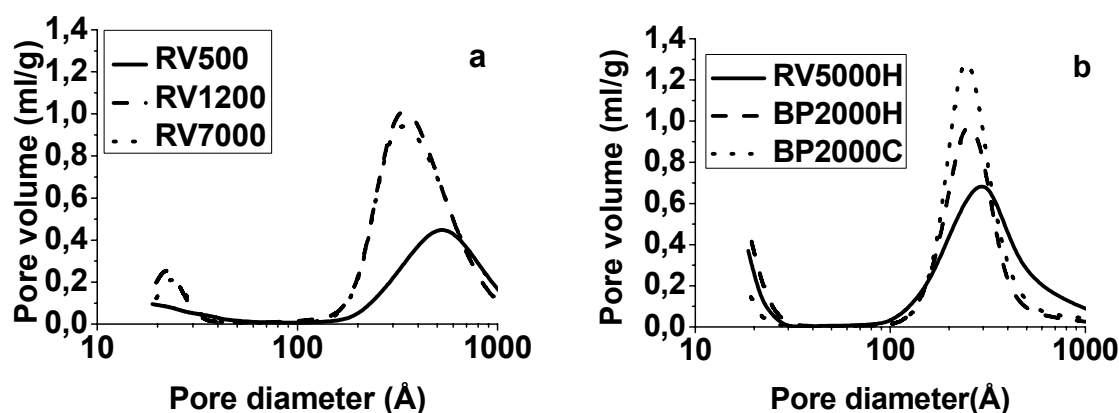
Figure 4.5 Pore size distributions of hierarchical silicalite-1 samples synthesized from RV carbons and pre-treated RV5000 and BP2000 carbons.

As seen in Figure 4.5 the size distribution of pores in the RV1200 and RV7000 templated materials centered at 35 nm appear almost identical even though the diameter of the 20 nm RV1200 carbon particles is almost twice that of the 11 nm RV7000. These observations suggest that in the case of these smaller particulate carbons it is aggregates of carbon particles that are encapsulated during zeolite crystallization as opposed to individual carbon particles. In Figure 4.5 it is also seen that templating with the 53 nm particle sized RV500

60

carbon results in a meso-/macroporous zeolite material with a broad pore size distribution centered at about 55 nm suggesting that in the case of this (relatively) large-sized particle carbon material, it is perhaps individual carbon particles or at least very small aggregates that are encapsulated. Moreover, it is seen from Figure 4.5 that the silicalite-1 materials obtained using the pre-heated RV5000H and BP2000H carbons are also porous with pore size distributions centered at *ca.* 30 and 25 nm, respectively, and that silicalite-1 produced using BP2000C as template is also a porous material with a pore size distribution centered at *ca.* 25 nm. The pores of the BP2000H and BP2000C templated materials are in a relatively narrow size range in the mesopore region, whereas the pore size distribution of the RV5000H templated material is broader and extends from the mesopore to the macropore region.

In Figure 4.6 are shown the pore size distrubtion plots of the ZSM-5 materials prepared using carbon-silica composites containing different amounts of carbon.
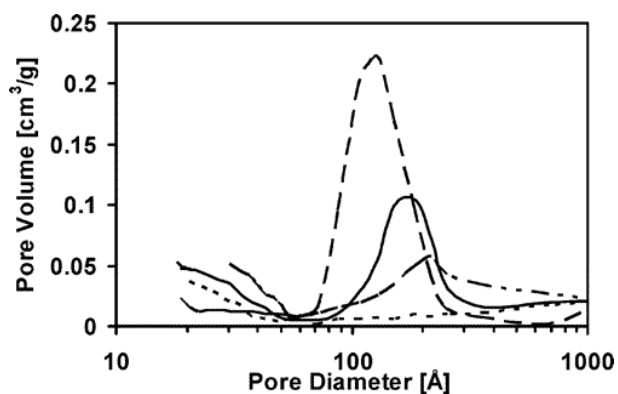
Figure 4.6 Controlled mesoporosity of zeolites prepared from carbon-silica composites simply by varying the amount of sugar decomposed in the silica (from top C/Si = 1.75; 0.87; 0.58; 0.0).

It is seen in Figure 4.6 that the size of the pores in ZSM-5 prepared using different amounts of carbon in the composites are somewhat different: Using a low amount of carbon (C/Si = 0.58) results in a very broad pore size distribution whereas a relatively high amount of carbon results in a zeolite material with a more narrow pore size distribution centered at *ca.* 11 nm. Thus, of all the materials described here, the ZSM-5 materials prepared using the

carbon-silica composites with C/Si = 1.75 and C/Si = 0.87 have the smallest mesopores. This can probably be attributed to the carbon particle aggregates encapsulated during crystallization being smaller than in the composites than in the case of the other templates. One explanation for why for smaller carbon aggregates are encapsulated using the composites is that the formation of the carbon aggregates takes in the limited spaces of the voids in the silica gel. Another is that the carbon particles are much more intimately mixed with the silica prior to crystallization of the latter into a zeolite phase resulting in much better dispersed and probably also smaller carbon particles being encapsulated. Thus, the formation of carbon particles by *in situ* decomposition of sucrose onto silica gel produces intimately mixed carbon-silica composites which can be transformed into mesoporous zeolites featuring relatively small and narrow mesopore size distribution by crystallization and subsequent combustion.

4.3.4. Characterization of the zeolites by electron microscopy

All the zeolites prepared as described above were studied using scanning and transmission electron microscopy techniques. In Figure 4.7 are shown a series of SEM images recorded from the silicalite-1 material prepared using the pre-formed carbon template.
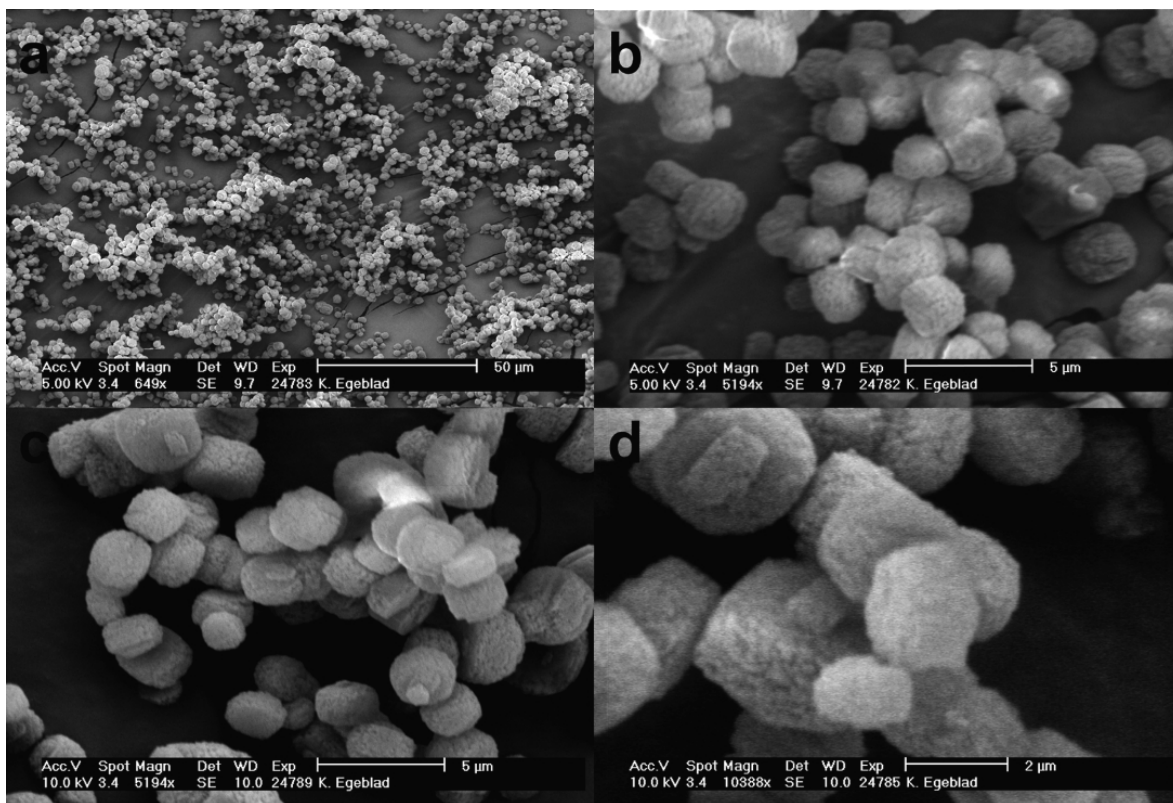
Figure 4.7 SEM images of the mesoporous silicalite-1 single crystals prepared using the pre-formed carbon template at different magnifications.

The images shown in Figure 4.7 show that the silicalite-1 material prepared from the pre-formed carbon template consists of very uniformly sized crystals. It is also seen that these crystals are very uniform in size and appearance. The crystals look like very typical mesoporous zeolite crystals since they feature the characteristic sponge-like morphology. Moreover, they have the typical coffin-shape morphology commonly observed for MFI structured zeolites. Thus, the images shown in Figure 4.7 support the evidence from XRD and N_2 physisorption that the material produced using the pre-formed carbon template is a mesoporous silicalite-1 material containing intracrystalline mesopores.

The SEM images recorded from the Raven carbon templated zeolites as well as those prepared using pre-treated carbons were in general very similar to those shown in Figure 4.7. However, the material prepared using pre-heated RV5000H looks quite different from the others since it appears to consist of heavily intergrown crystals, as shown in Figure 4.8.
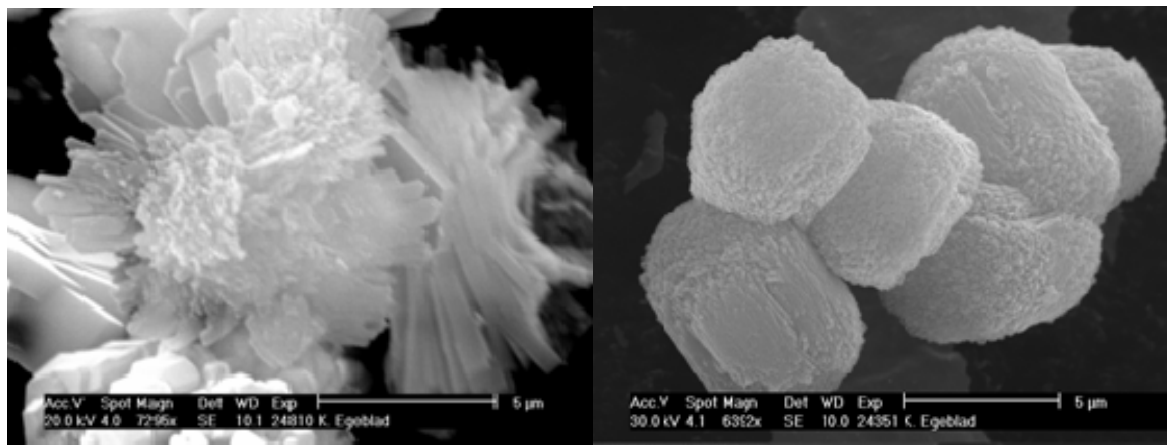
Figure 4.8 SEM images of RV5000H and BP2000C templated mesoporous zeolite samples.

In Figure 4.8 is also shown an SEM image of mesoporous silicalite-1 prepared using BP2000C as the template. It is evident from the image that this material is very similar to that visualized in Figure 4.7 although the crystals appear to be bigger. The larger size of these crystals can only be explained by the citrate pretreatment method since mesoporous silicalite-1 crystals prepared using BP2000 and BP2000H are typically *ca.* 2 μm on the longest axis.

Figure 4.9 shows representative SEM and TEM images of mesoporous ZSM-5 prepared from the carbon-silica composite.
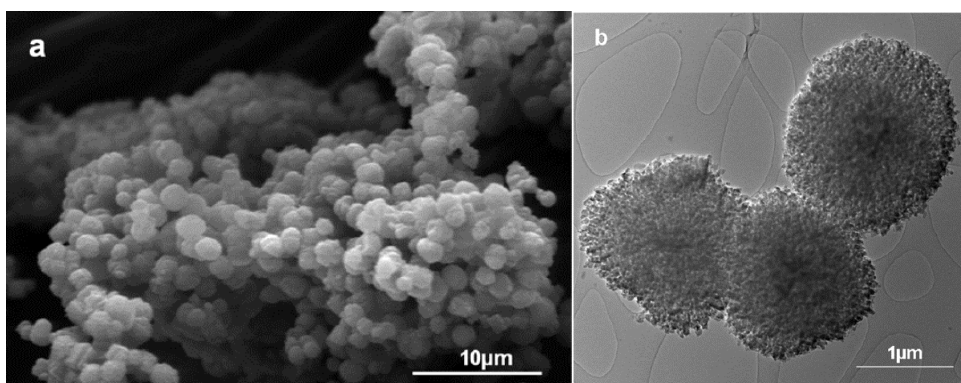
Figure 4.9 Representative (a) SEM and (b) TEM images of mesoporous ZSM-5 zeolite single crystals prepared by *in situ* carbon templating using carbon-silica composites.

The SEM image shown in Figure 4.9 illustrates that the zeolites prepared using the carbon-silica composites are very similar in appearance to those prepared using the carbon templates. Thus, they are also mesoporous MFI zeolites. The mesoporosity of these crystals is very visual from the TEM image which is also shown in Figure 4.9. It is seen as the brighter spots which appear all over the crystals. For comparison, TEM images of the silicalite-1 material prepared using the pre-formed carbon template as well as silicalite-1 crystals prepared in the absence of an auxiliary template are shown in Figure 4.10.
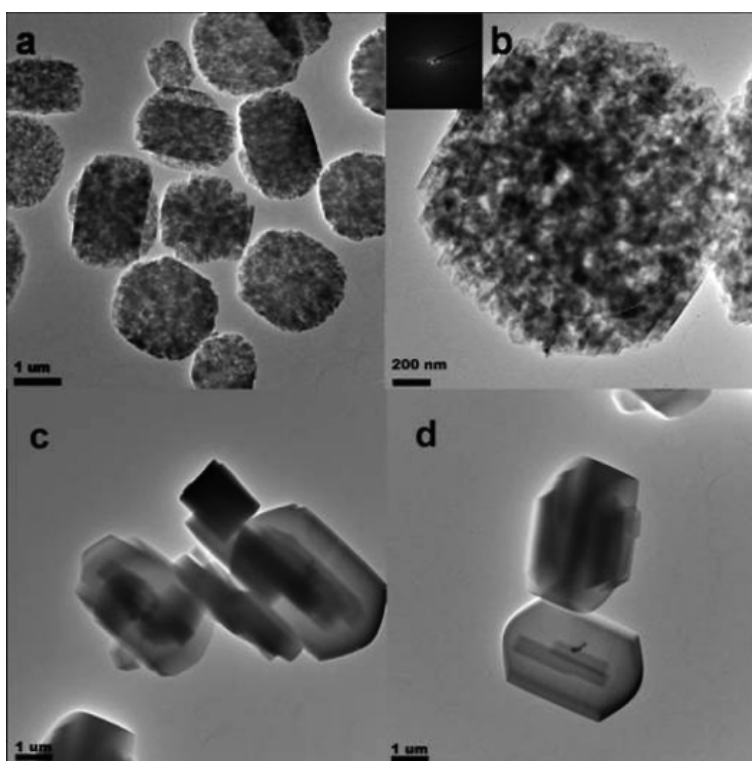
Figure 4.10 TEM images of the mesoporous silicalite-1 single crystals prepared using the pre-formed carbon precursor. The inset in (b) shows the SAD pattern of a circular area centered in the middle of the zeolite crystal, c) and d) shows images of analogously prepared zeolite without the carbon template.

The TEM images shown in Figure 4.9 and Figure 4.10 clearly reveal that the appearances of conventional and mesoporous zeolite crystals are quite different: Conventional crystals have very straight edges and they show no changes in contrast in the TEM, aside of course

from the twinning, whereas mesoporous crystals are very rugged in the edges and show clear differences in contrast. The selected area electron diffraction pattern shown in Figure 4.10 provides unequivocal proof to the often-disputed notion that these crystals are in fact single crystals with intracrystalline porosity. As mentioned earlier, this point was in fact proved in the very first report on mesoporous zeolite crystals.

4.4. Summary

Mesoporous zeolites were prepared using different templating approaches. It was shown that mesoporous zeolites can be prepared using Raven carbons and that the porosities of the Raven templated carbons are very broad extending from the mesopore region to the macropore region. However, using RV5000 as received, a zeolite phase could only be obtained by pre-heating the carbon in N_2. Pre-heated BP2000 as well as BP2000 impregnated with sodium citrate were also applied as templates and in the case of the citrate-impregnated BP2000 very large mesoporous crystals were obtained. In the present chapter it was also shown that carbonization of a sucrose-ammonia mixture leads to a porous carbon which can be effectively used for preparation of mesoporous zeolite crystals. Thus, mesoporous zeolites can be prepared from cheap mesopore templates and variation in these will most likely lead to mesoporous zeolite with different porosity properties. A third method described in the present chapter was the *in situ* decomposition of sucrose on silica gel resulting in carbon-silica composites which can be applied as mesopore templates and silica source simultaneously. By this method it is very easy to tune the mesoporosity of the zeolites simply by varying the amount of sucrose impregnated onto the silica. The sizes of the pores produced using this method are smaller than the pore sizes usually obtained using carbon-templating which is probably due to smaller carbon aggregates being encapsulated during crystallization.

5. Increasing the Porosity of Mesoporous Zeolites by Alkaline Treatment

5.1. Introduction

For the preparation of mesoporous zeolite crystals, *i.e.* zeolites featuring intracrystalline mesoporosity, two approaches have received significant attention. As evident from Chapter 2 and Chapter 3 these are the carbon-templating and alkaline treatment methods. Briefly, carbon-templating involves crystallization of a zeolite phase in the presence of carbon resulting in zeolite crystals embedded with carbon. Subsequent post-combustion of the carbon produces zeolite crystals featuring intracrystalline mesopores. Desilication, on the other hand, is a post-synthetic alkaline treatment method by which intracrystalline mesopores are produced in zeolite crystals by preferential extraction of silicon over aluminum. In the present chapter it is exploited how these methods can complement each other so as to increase the mesoporosity of mesoporous zeolites prepared by carbon-templating by alkaline post-treatment. This was in fact attempted earlier, however, with limited success.

5.2. Experimental

5.2.1. Preparation of mesoporous H-ZSM-5 by templating with BP2000

A mesoporous ZSM-5 sample was prepared by sequential impregnations of a zeolite synthesis gel with a Si/Al ratio of 45 as follows: A freshly prepared solution of aluminum isopropoxide (0.084 g) dissolved in tetrahydrofuran (6 ml) was quickly impregnated onto

BP2000 (2 g) and the carbon was left to dry overnight. Then, the dry carbonaceous material was impregnated with a mixture of tetrapropylammonium hydroxide (3.44 g, 40 wt%), sodium hydroxide (0.1 g), water (0.5 g) and ethanol (3.03 g), and left to dry overnight. The next day, the carbonaceous material was impregnated with tetraethyl orthosilicate (3.87 g) and left to dry overnight before being transferred to a Teflon-beaker which was placed in a Teflon-lined autoclave with 10-15 ml water outside the beaker. The autoclave was then heated to 180 °C for 5 days after which the solid material was collected by filtration, washed, dried and calcined in air at 550 °C for 20 h to produce a white zeolite powder. The zeolite powder was then transformed from the Na-form to the H-form by ion-exchanging it three times with 1 M NH_4NO_3 and calcining it at 550 °C for 4 h.

The H-ZSM-5 material was characterized by powder X-ray diffraction, N_2 physisorption, temperature programmed desorption of NH_3, scanning electron microscopy, transmission electron microscopy and selected area electron diffraction. Powder XRD patterns were obtained using a Bruker AXS powder diffractometer. Nitrogen physisorption measurements were with a Micromeritics ASAP 2020 apparatus as described in Section 4.2.1. NH_3-TPD measurements were performed with a Micromeritics Autochem II equipped with a TCD detector. Dry weight of the sample was found after evacuation at 300 °C for 1 h. Weakly bound NH_3 was desorbed prior to measurement at 100 °C in a He flow of 25 ml/min for 1 h or at 175 °C in a He flow of 50 ml/min for 2 h, respectively. SEM images were recorded with a JEOL JSM 5900 equipped with a LaB_6 filament. Prior to measurements, the samples were sputter-coated with Au for 40 s using a Polaron SC 7620. TEM images and SAD patterns were recorded with a JEM 2000 FX electron microscope as described in Section 4.2.4.

5.2.2. Alkaline treatment of mesoporous H-ZSM-5 prepared by carbon-templating
The mesoporous H-ZSM-5 sample prepared as described above (Section 5.2.1.) was subjected to different alkaline treatment protocols by immersion of the sample in aqueous solutions of sodium hydroxide at 65 °C for various periods of time. After reaction, the desilicated samples were collected by filtration and washed thoroughly with water. The

obtained desilicated samples were characterized using the methods described above (Section 5.2.1.). Prior to the NH_3-TPD measurements, the samples were transformed into the proton-form by a similar procedure as described in Section 5.2.1. Two series of desilication experiments were conducted and the experimental details of these are listed in Table 5.1 along with data obtained from the N_2 physisorption, XRD and NH_3-TPD analyses. One series involved treating the parent mesoporous H-ZSM-5 sample for a fixed period of time (30 min) with different volumes of 0.1 M NaOH (samples 1-5 in Table 5.1). The other series involved treating the parent sample with fixed volumes of 0.2 M NaOH for different periods of time (samples 6-11).

Table 5.1 Textural data from N_2 adsorption/desorption experiments on the parent and desilicated samples.[a]

Sample	Base amount (mmol/g)	Time (min)	S_{BET} (m²/g)	S_{meso} (m²/g)	V_{meso}[a] (ml/g)	V_{micro} (ml/g)	$D[101]$[a] (Å)	Acidity[b] (mmol/g)
Parent	-	-	408	117	0.30	0.11	677	0.164
1	3	30	408	162	0.37	0.11	595	0.180
2	5	30	422	195	0.47	0.10	513	0.206
3	7.5	30	478	222	0.63	0.11	494	0.235
4	10	30	478	232	0.72	0.10	460	0.272
5	15	30	503	234	0.75	0.11	386	0.293
6	8	5	295	142	0.33	0.06	-	-
7	8	10	466	241	0.64	0.10	-	-
8	8	15	443	210	0.66	0.10	-	-
9	8	20	456	208	0.70	0.11	-	-
10	8	30	450	201	0.73	0.11	-	-
11	8	70	445	181	0.65	0.11	-	-

[a] $V_{meso} = V_{ads,P/P0 = 0.99}$ - V_{micro}. V_{micro} from t-plot. S_{meso} from BJH. Surface area of pores 17-3000 Å.
[b] Scherrer equation.
[c] NH_3-TPD. NH_3 desorbed at 175 °C for 2 h.

5.3. Results and discussion

5.3.1. Characterization of the zeolites using XRD

The parent mesoporous H-ZSM-5 as well as all the desilicated samples are phase-pure MFI structured materials as determined by powder XRD. In Figure 5.1 are shown the powder XRD patterns obtained from the parent sample and the samples obtained using various volumes of sodium hydroxide solution (samples 1-5).
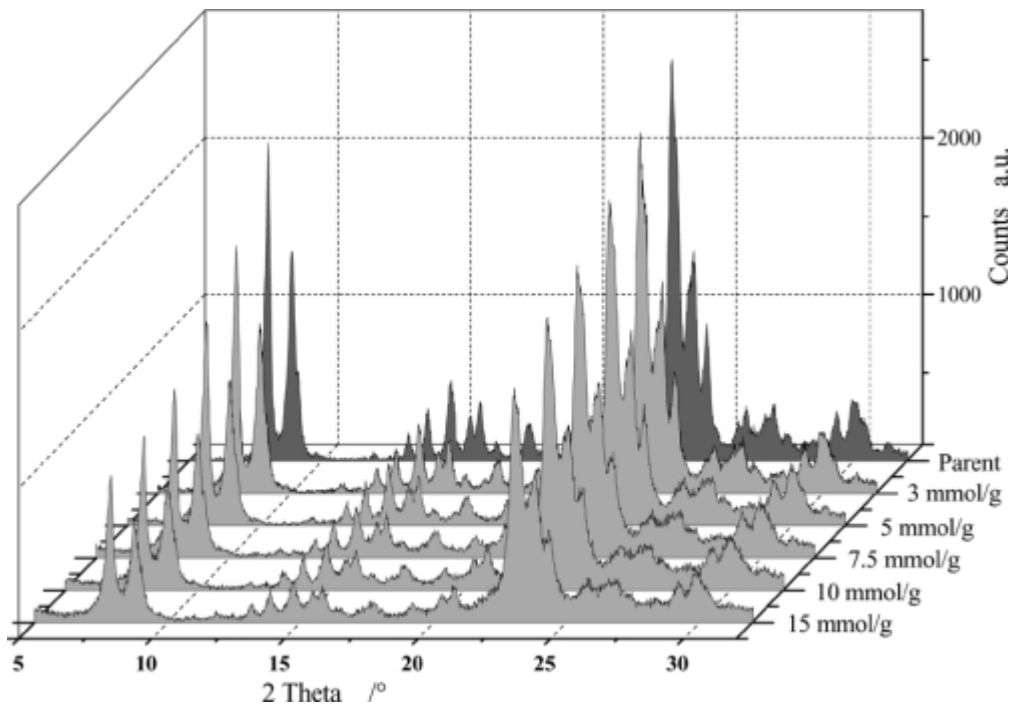
Figure 5.1 Powder XRD patterns of the parent sample and samples 1-5 desilicated for 30 min with increasing desilication strength.

It is seen in Figure 5.1 that the samples are all crystalline and contain exclusively MFI structured material. It is also seen that the intensity of the reflections gradually decrease as the amount of base applied for the desilication is increased. This observation is in excellent agreement with results obtained after desilication of conventional zeolite samples.[105,106] Another thing to note in the XRD patterns is that reflections are relatively broad, which is commonly observed for mesoporous zeolite crystals despite the fact the crystals are actually quite big as is clearly visualized by electron microscopy techniques (see Section 5.3.3.) The reason for this, as was also commented on in Section 3.4, is that mesoporous zeolite crystals are comprised of interconnected domains of crystalline material which are in registry and interconnected domains of void space. In other words, (macroscopic) mesoporous zeolite crystals (as imaged in electron microscopes) are composed of smaller crystalline domains (as determined using the Scherrer equation). Thus, the effective average crystal diameters calculated using the Scherrer equation should be associated with the crystalline domains rather than with the entire macroscopic crystal. This implies, that the decrease in effective average crystal diameter upon increasing the desilication strength

70

which is apparent from Table 5.1 can be attributed to increased mesoporosity in the samples.

5.3.2. Characterization of the zeolites using N_2 physisorption

The pore volumes as well as BET and mesopore surface areas of the parent and desilicated samples are listed in Table 5.1. It is seen that the samples are all microporous indicating that it is possible to increase the mesoporosity without destroying the micropores. It is also seen that the carbon-templated parent sample is in fact quite mesoporous to begin with (V_{meso} = 0.30 ml/g), and that the mesopore volume can be increased by more than a factor of two by desilication, up to 0.75 ml/g for sample 5. A similar increase in mesopore surface area, from 117 m^2/g to up to 241 m^2/g, for the parent and sample 7, respectively, is also observed. Thus, there is no doubt from Table 6.1. that desilication can be applied as an effective tool for increasing the porosity of carbon-templated mesoporous zeolites. Moreover, it is evident from Table 5.1 that the desilication of mesoporous ZSM-5 proceeds relatively fast, since the mesopore volume as well as mesopore surface of sample 7 (treated with 0.2 M NaOH for 10 min) have doubled to 0.64 ml/g and 241 m^2/g, respectively. Futher extension of the alkaline treatment (up to 30 min) only has a marginal effect on the mesopore volume and prolonged treatment times (70 min) has a detrimental effect on the mesopore surface area which is due to the size of the pores increasing into the macropore region.

In Figure 5.2 are shown physisorption isotherms of the parent sample as well as samples 1-4. It is seen that isotherms are all type IV isotherms which are given by mesoporous materials. Moreover, it is seen that the mesopore volume increases with increasing desilication strength and that the adsorption and desorption isotherms exhibits hysteresis starting at relative pressures of *ca.* 0.45 for low treatment strengths (samples 1 and 2). This is attributed to the formation of new smaller mesopores which is also evident from the pore size distribution plots shown in Figure 5.2. The formation of new smaller pores in a zeolite which already has mesopores is interesting because it indicates that it is possible to prepare zeolites with multi-level mesoporosity by coupling of the carbon-templating and

desilication methods. However, as is apparent from Figure 5.2 these small mesopores are gradually increased in size as indicated by the disappearance of small mesopores and a corresponding increase in larger mesopores with increasing desilication strengths (samples 3 and 4).
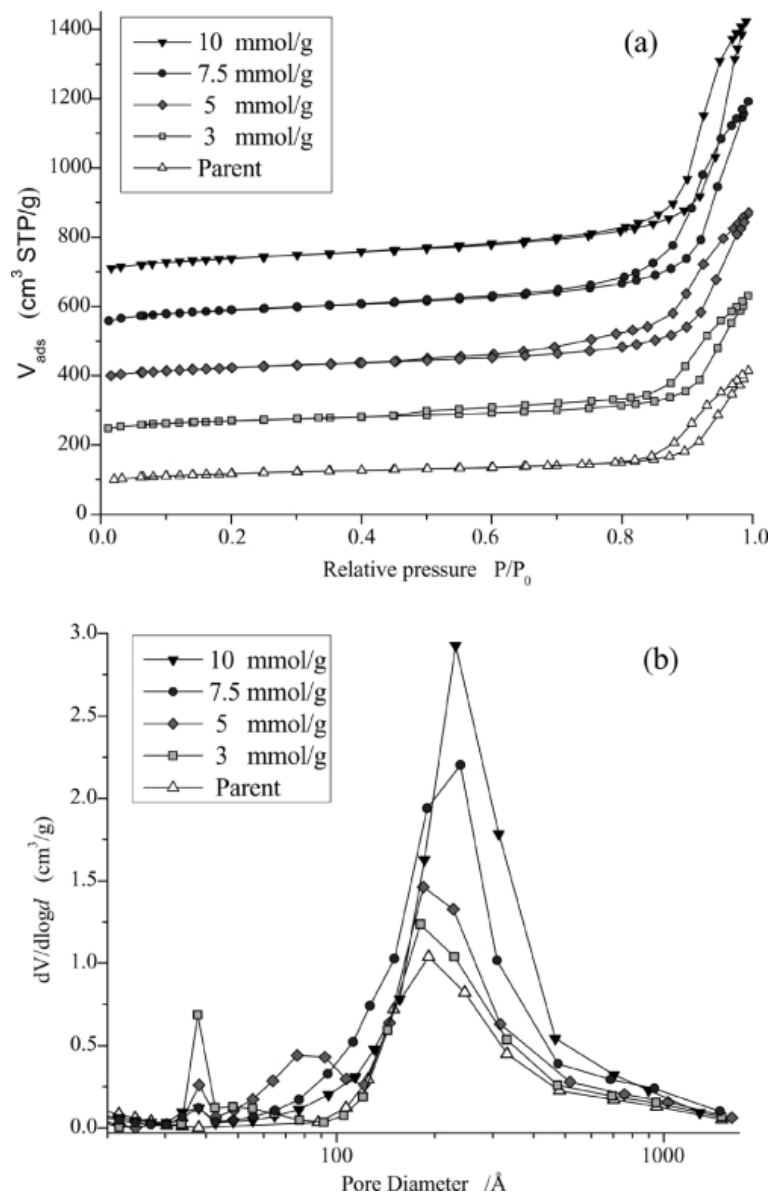
Figure 5.2 N$_2$ adsorption/desorption isotherms of the parent along with samples 1-4. Isotherms of samples 1-4 are offset by 150 for illustrative reasons. (b) BJH-derived pore-size distributions.

5.3.3. Characterization of the zeolites using NH_3-TPD

In Figure 5.3 are shown the NH_3-TPD plots obtained from the parent sample and samples 1-5 pre-heated to two different temperatures.
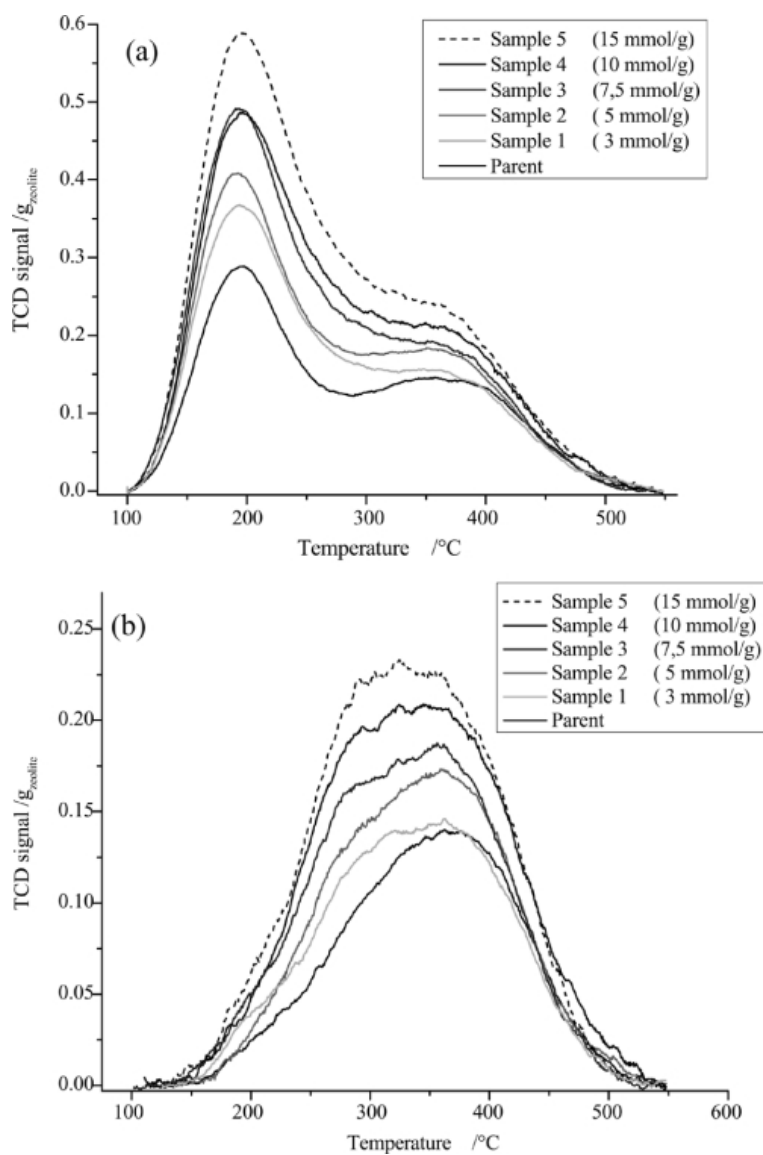
Figure 5.3 NH_3 desorption curves of parent sample and samples 1-5. Weakly bound NH_3 desorbed in He at (a) 100 °C for 1 h and (b) at 175 °C desorbing for 2 h.

The plots obtained after desorbing weakly bound NH_3 at 100 °C all show two distinct desorption peaks. The higher-temperature desorption peak is attributed to Brønsted framework aluminum sites whereas the lower-temperature desorption peak is associated

with weaker acid sites. It is also seen that increasing the desilication treatment strength increases the acidity of the samples. From the plots obtained after desorbing weakly bound at 175 °C, also shown in Figure 5.3, it is seen that an increasing part of the overall acidity result from a shoulder on the low-tempeature side of the desorption maximum at *ca.* 365 °C which more significantly contributes as the treatment strength is increased. This appearance of this shoulder in the TPD profiles is most likely due to ammonia desorption from partial (extra) framework aluminum sites resulting from the desilication treatment.

The acidities of the parent sample and samples 1-5 derived from the NH$_3$-TPD profiles obtained after desorbing weakly bound ammonia at 175 °C are listed in Table 5.1. Comparison between the acidity of the parent sample with acidities of known reference samples indicates that the Si/Al ratio of this sample is close to 45. This implies that all the aluminum in the synthesis gel is incorporated in the zeolite structure since the Si/Al ratio in the synthesis gel is also 45. As was also evident from Figure 5.3 the results listed in Table 5.1 clearly show that the desilication treatment effectively increases the framework aluminum concentration since the desilicated samples become increasingly acidic.

5.3.4. *Characterization of the zeolites using electron microscopy*

The prepared parent sample as well as the desilicated samples were investigated with scanning and transmission electron microscopy techniques in order to obtain direct visual images of how the desilication treatments affected the already mesoporous materials. From the SEM analyses it is clear that the crystals become increasingly sponge-like but retain their original size. This is clearly seen in Figure 5.4 in which SEM images of the parent sample and desilicated samples 7 and 10 are shown along with a TEM image of sample 10. Judged from the SEM images the crystals are all about 2-3 μm on the longest axis which is significantly larger than effective average crystal diameter determined using the Scherrer equation on the D[101] reflection as discussed above (Section 5.3.1.). From the SEM images it also appears that the crystals become increasingly fragmented in appearance which support the same conclusion as the XRD data suggested, namely that the interconnected crystalline domains decrease in size with increasingly harsh desilication

74

treatment. The sponge-like morphology is also clearly seen in the TEM image. Unfortunately, these highly mesoporous crystals are significantly less stable in the electron beam of the TEM than the mesoporous silicalite-1 crystals described in the previous chapter. In fact they are so less stable that it was not possible to record a good SAD image.
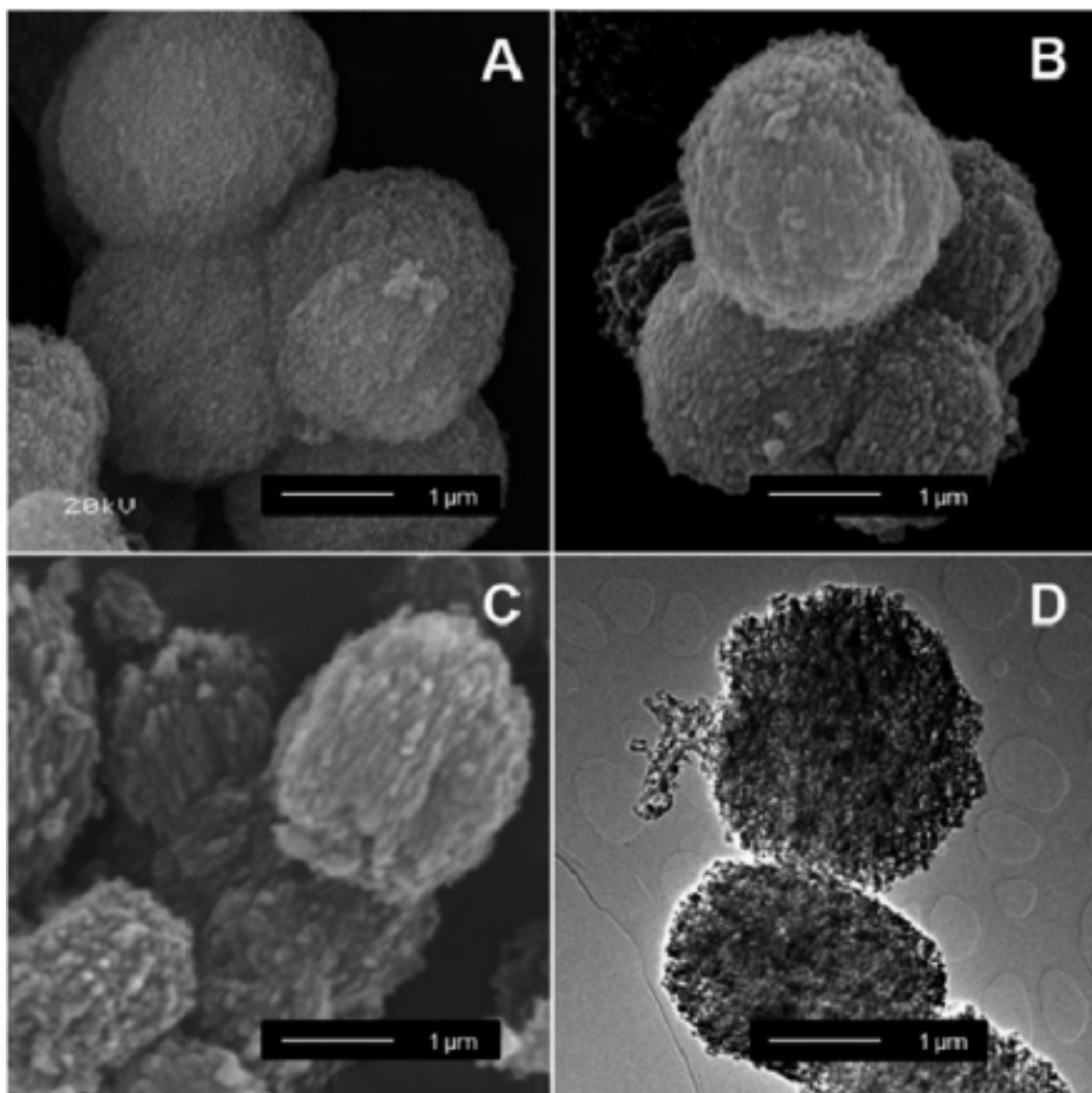
Figure 5.4 (a)-(c) SEM images of the parent sample, sample 7 (desilicated 10 min) and sample 10 (desilicated 30 min), respectively. (d) TEM image of sample 10 (desilicated 30 min).

5.4. Conclusions

In the present chapter it was shown that the two main methods for preparing mesoporous zeolite crystals can be effectively combined. Thus, desilication of already mesoporous zeolite crystals enhanced the mesopore volume as well as mesopore surface area of this material, despite the fact that it contained appreciable mesoporosity to begin with. Two desilication procedures were applied in the present study, one involving variation in the amount of hydroxide being applied and one involving variation in the reaction time. Physisorption data revealed that both methods were effective for the generation of additional mesoporosity in the sample, and that newly generated smaller mesopores contribute to the overall mesopore volume at milder desilication treatments. As the desilication strength is increased these pores grow larger eventually extending into the macropore region. It can easily be envisaged that the porosity of other mesoporous carbon-templated zeolites can be enhanced as well.

6. The Fluoride Route to New Mesoporous Materials

6.1. Introduction

Zeolites are typically prepared by hydrothermal crystallization of alkaline synthesis gels. [107] In these alkaline gels, the OH^- ions serve as mineralizing agents in the sense that they solubilize silicon and aluminum species in the form of hydroxy anions which are then able to partake in the crystallization of the zeolite phase. However, the concentration of hydroxide ions has to be very high in order to solubilize silicon and aluminum since more or less hydrated silica and alumina precipitates will form in more neutral solutions. Solubilization of silicon and aluminum ions is also possible using F^- ions as it is also possible to form fluorocomplexes of both silicon and aluminum. The advantage of these complexes relative to the hydroxy complexes is that they are stable in acidic, neutral and even alkaline solutions. The use of fluoride as the mineralizing agent in zeolite synthesis gels has thus made it possible to prepare zeolites from neutral and acidic gels as well as from alkaline ones. [108] In this chapter is described how fluoride containing synthesis gels can be crystallized in the presence of carbon leading to mesoporous zeolites and that fluoride containing aluminophosphate gels allow the formation of mesoporous aluminophosphate zeotype materials.

6.2. Experimental

6.2.1. Preparation of conventional and mesoporous zeolites from fluoride media

Mesoporous MFI, MEL and BEA structured zeolites were prepared by impregnation of the synthesis gel components onto BP2000 followed by hydrothermal crystallization and combustion of the carbon. Analogous conventional samples were prepared from similar gels in the absence of carbon.[109,110] The gel used in the preparation of the ZSM-5 samples was prepared by stirring a mixture of tetraethyl orthosilicate (TEOS, 3.47 g, 98 wt%) with tetraethyl ammonium hydroxide (TEAOH, 4.92 g, 35 wt%) for 10 min before adding a clear solution of $Al(NO_3)_3 \cdot 9H_2O$ (0.075 g) in water (0.55 g) and then, in the case of the mesoporous sample, BP2000 (2 g). After 6 h, HF (0.585 g, 40 wt%) was added to the gels which were then transferred to Teflon beakers placed in a Teflon-lined autoclaves and crystallized at 170 °C for 3 days (the conventional sample) or 5 days (the mesoporous sample), before the solid materials were collected, washed with water, dried and then calcined in air to produce white zeolite powders. The ZSM-11 samples were prepared by a similar procedure from gels containing TEOS (3.47 g), tetrabutyl ammonium hydroxide (TBAOH, 7.58 g, 40 wt%), $Al(NO_3)_3 \cdot 9H_2O$ (0.075 g), water (0.55 g) and HF (0.585 g), which were crystallized at 170 °C for 3 or 6 days for the conventional and mesoporous samples, respectively. The BEA materials were prepared from gels containing TEOS (3.47 g), TEAOH (8.00 g), water (0.55 g) and HF (0.95 g) which were crystallized at 140 °C for 5 days in both cases.

The materials were characterized by powder XRD, N_2 physisorption measurements, scanning electron microscopy, transmission electron microscopy and selected area electron diffraction techniques. All of these methods were used as described previously (Chapter 4).

6.2.2. Preparation of mesoporous zeotypes from fluoride media

Mesoporous AFI and CHA structured zeotypes were prepared by sequential impregnations of required synthesis gel components onto BP2000 carbon followed by hydrothermal crystallization and combustion of the carbon. For reference, conventional samples were prepared from similar gels in the absence of carbon.[111,112] The conventional AFI material

was prepared as follows: To a cool (0 °C) solution of H_3PO_4 (1.5 g, 85 wt%), water (1ml) and triethyl amine (TEA, 1.62 g) was added aluminum isopropoxide (AIPO, 2.04 g) and, after 2 h, HF (0.27 g, 48 wt%). The mixture was stirred for 2 h before being transferred to a Teflon-beaker placed in a Teflon-lined autoclave with *ca.* 20 ml water outside the beaker. The autoclave was then heated to 175 °C for 2 days before the solid material was collected by filtratation, washed with water, dried and calcined to obtain a fine white powder. The synthesis of conventional CHA was based on the procedure published by Tuel et al. AIPO (2.04 g) was suspended in water (8.7 g) and H_3PO_4 (1.15 g, 85 wt%), HF (0.21 g, 48 wt%) and piperidine (PIP, 0.85 g, 99%) was added. The gel was then transferred to a Teflon-beaker placed in a Teflon-lined autoclave with *ca.* 20 ml water outside the beaker. The autoclave was then heated to 190 °C for 5 days.

Two mesoporous AFI aluminophosphates were prepared as follows: Solutions of AIPO (2.04 g) dissolved in tetrahydrofuran (THF, 7 ml) were impregnated onto BP2000 (2 g) and the carbons were left to dry overnight. Then, they were impregnated with aqueous solutions of H_3PO_4 (1.5 g, 85 wt%), TEA (1.62 g for sample "AlPO-5 (s1)" and 2.53 g for sample "AlPO-5 (s2)") and HF (0.27 g, 48 wt%) and transferred to Teflon-beakers in which they were crystallized at 175 °C for 3 days as described above. The mesoporous CHA material was prepared by a similar procedure from a synthesis gel containing PIP (0.85 g) in stead of TEA. This gel was crystallized at 190 °C for 5 days. After crystallization, the synthesis products were recovered by filtration, washed, dried and calcined to produce fine white powders.

6.3. Results and discussion

6.3.1. Characterization of samples using XRD

In Figure 6.1 are shown the powder XRD patterns obtained from the calcined conventional and mesoporous zeolite and zeotype samples. It is seen that all samples appear to be highly crystalline materials, however, the diagram of AlPO-5 (s1) also shows the presence of amorphous material in this sample. Because of this, AlPO-5 (s2) was synthesized with 50%

structure-directing agent in the gel. As evident from the powder XRD diagram of this sample, this procedure resulted in a phase-pure AFI structured sample.
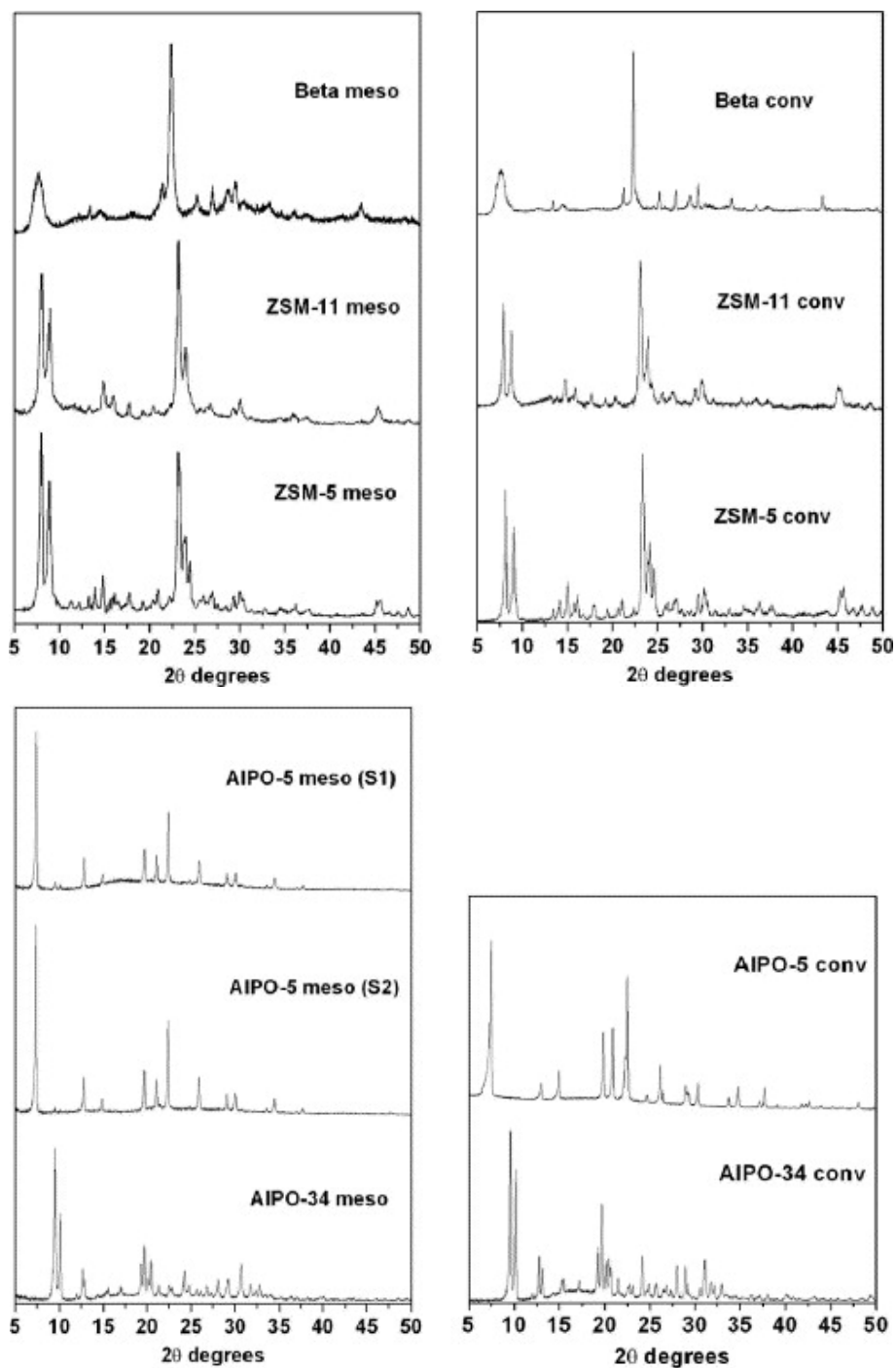
Figure 6.1 Powder XRD patterns of the conventional and mesoporous zeolite and zeotype samples prepared in fluoride media.

6.3.2. Characterization of samples using physisorption

In Figure 6.2 are presented the physisorption isotherms given by the mesoporous zeolites and zeotype materials and the pore-size distributions derived therefrom. The pore volumes and BET surface areas calculated from these data are listed in Table 6.1.
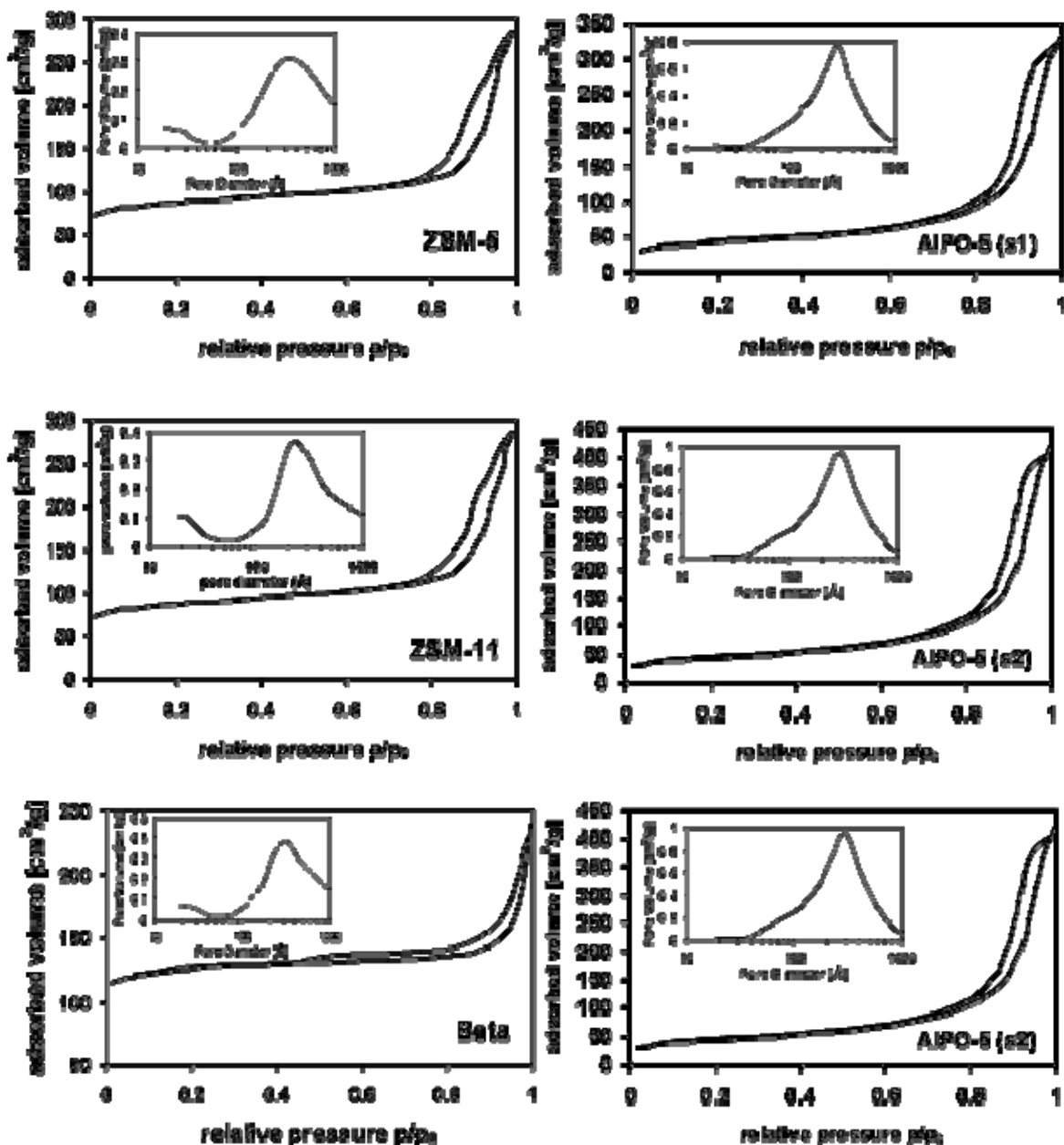
Figure 6.2 Nitrogen adsorption and desorption isotherms of the mesoporous zeolite and zeotype samples synthesized in fluoride media.

Table 6.1 Nitrogen physisorption data of the samples after combustion of the organic template and the carbon matrix.

Zeolite/zeotype	Conventional/mesoporous	V_{micro} $(cm^3/g)^a$	V_{meso} $(cm^3/g)^b$	S_{BET} $(m^2/g)^c$
ZSM-5	conv.	0.12	0.01	399
ZSM-5	meso.	0.11	0.31	346
ZSM-11	conv.	0.12	0.02	364
ZSM-11	meso.	0.10	0.29	342
BEA	conv.	0.20	0.03	499
BEA	meso.	0.18	0.36	507
AlPO-5	conv.	0.001	0.003	5
AlPO-5 (s1)	meso.	0.02	0.37	150
AlPO-5 (s2)	meso.	0.01	0.45	154
AlPO-34	conv.	0.26	0.007	563
AlPO-34	meso.	0.18	0.47	494

[a] Calculated by t-plot method.
[b] Calculated by BJH method (desorption).
[c] Calculated by BET method.

From Figure 6.2 it is seen that all the isotherms exhibit typical hysteresis behavior between the adsorption and desorption branches and can therefore be classified as type IV isotherms. Moreover, they are very similar in appearance suggesting that the materials from which they were measured are most likely very similar. From the insets showing the pore-size distributions it is evident that the sizes of the pores extend from the mesopore range into the macropore range. Inspection of Table 6.1 reveals that, with the exception of the AlPO-5 samples, all samples have large BET surface areas. It is also seen that the samples crystallized from gels adsorbed on carbon have much higher mesopore volumes than the samples synthesized conventionally which all have very small mesopore volumes. For the AlPO-34 samples the increase in mesopore volume upon crystallization in the presence of carbon is most evident: The conventional AlPO-34 sample has a mesopore volume of 0.007 ml/g whereas the carbon-templated sample has a mesopore volume of 0.47 ml/g.

6.3.3. Characterization of samples using electron microscopy

The prepared samples were investigated using scanning and transmission electron microscopy. Unfortunately, the mesoporous aluminophosphate zeotypes were too unstable in the electron beam to get images of sufficient quality. The SEM images of the conventional and mesoporous zeolite and zeotype samples are shown in Figure 6.3 and

Figure 6.4, respectively. The images of the ZSM-5 and ZSM-11 sample show the typical sponge-like coffin-shape morphology characteristic of mesoporous MFI and MEL type crystals. As evident, these crystals look very different from the conventional analogues which are more regular in shape. The SEM images of the Beta zeolites show that the mesoporous crystals are smaller than the conventional crystals and that they are also much more sponge-like in appearance. From alkaline gels, only nanocrystalline mesoporous Beta has been obtained, however, these images show that mesoporous Beta crystals were indeed crystallized using F^- as the mineralizing agent.
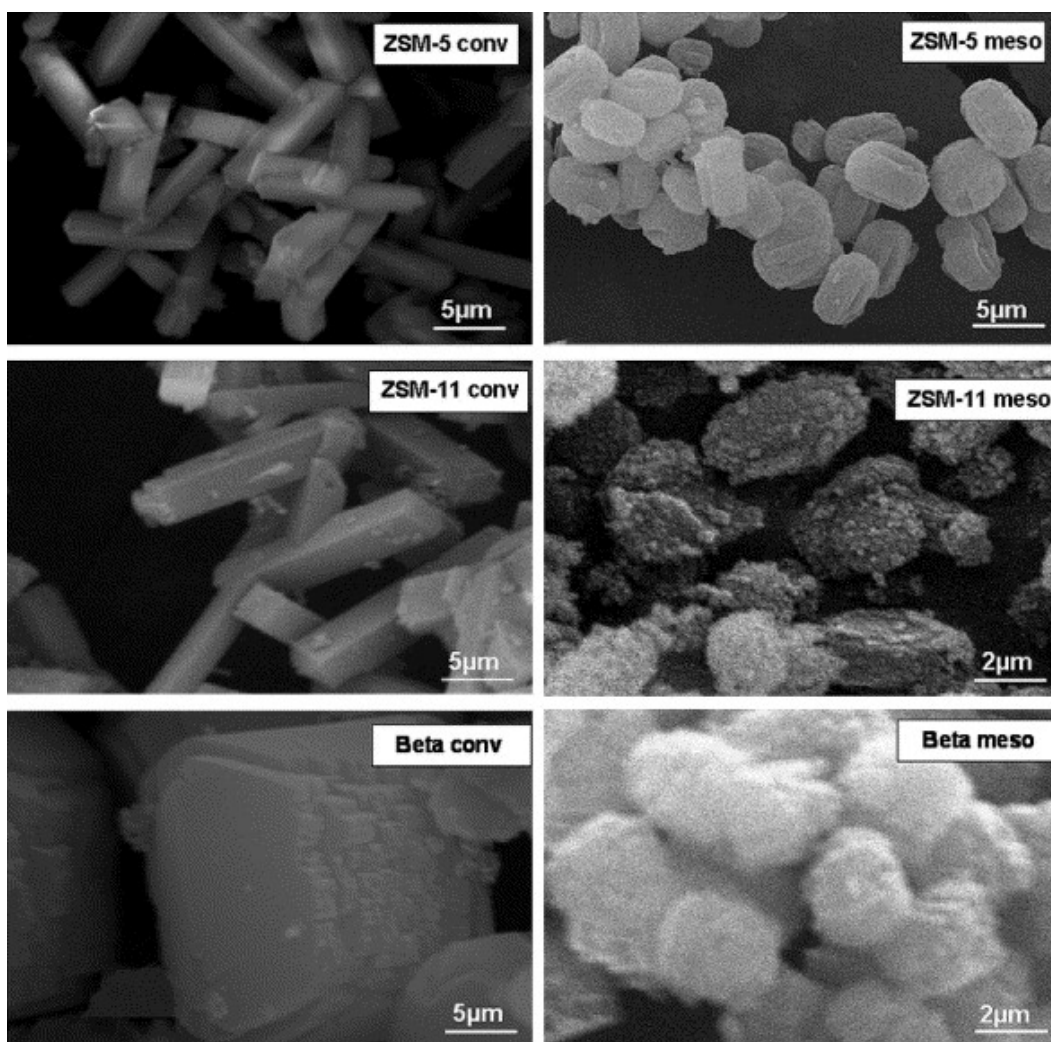
Figure 6.3 SEM images of conventional and meosporous ZSM-5, ZSM-11 and Beta zeolites synthesized in fluoride media.

The SEM image of the conventional AlPO-5 material show that this material consists of very long needle-shaped crystals. This needle-shaped morphology is also evident in the images of the mesoporous samples, however, crystals with plate-like morphology are also seen in the images of the mesoporous AlPO-5 (s2) which was crystallized with 50% more structure-directing agent in the gel than the AlPO-5 (s1) sample. This suggests that mesoporous AFI materials can be synthesized with different crystals morphologies simply by changing the amount of structure-directing agent in the gel. Since no nanosized crystals were found during the SEM analyses of the mesoporous AlPO-5 the mesoporosity of these materials is probably intracrystalline even though they do not exhibit the characteristic sponge-like appearance commonly observed for mesoporous zeolite crystals. Contrarily, the sponge-like appearance of the mesoporous AlPO-34 sample is clearly visible in the SEM image shown in Figure 6.4. From this SEM image it appears that the mesoporosity of this sample stems from agglomerates of nanocrystals, however, it might also result from intracrystalline mesoporosity as in the case of the other samples presented here. To shed light on the matter, the materials were studied using TEM with the hope of recording selected area electron diffraction patterns from sponges like the one shown in the SEM image. Unfortunately, the mesoporous AlPO materials were too unstable to obtain TEM images of sufficient quality. It was, however, possible to obtain good-quality TEM images of the mesoporous Beta zeolite sample. From the representative TEM image shown in Figure 6.5 it is clear that crystals are relatively large and porous single crystals.
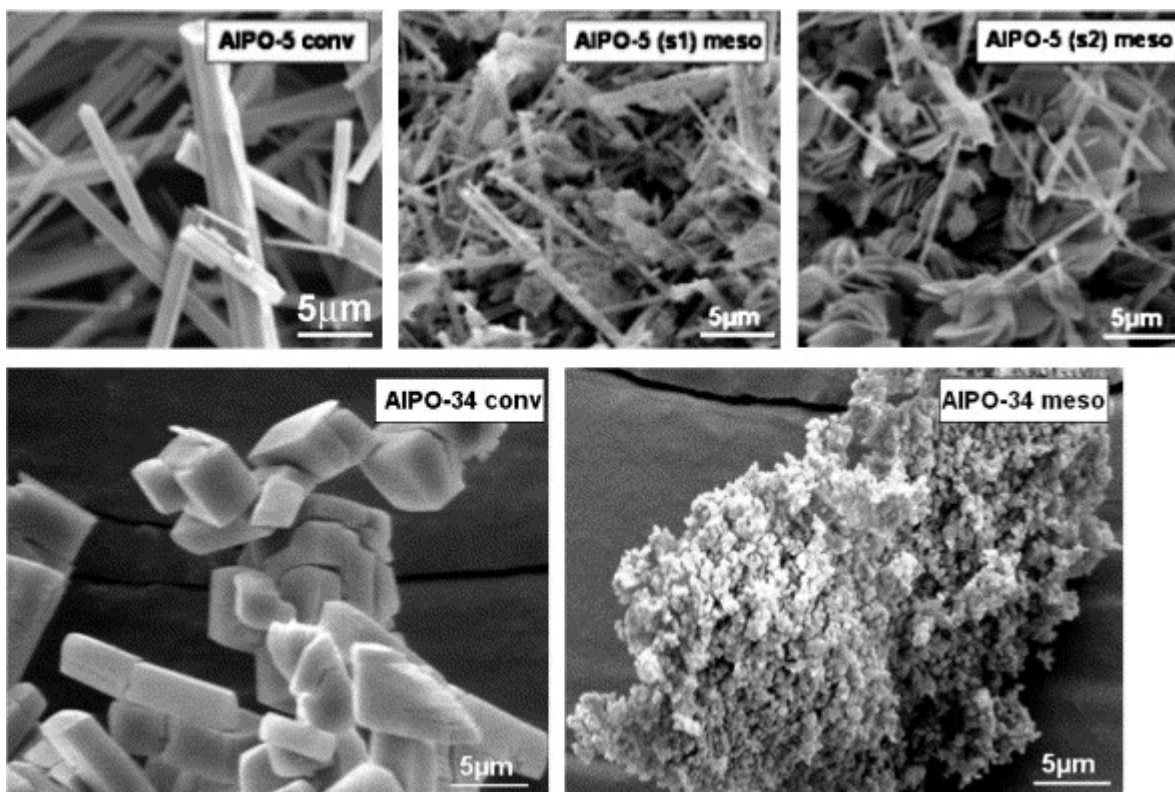
Figure 6.4 SEM images of conventional and mesoporous AlPO-5 and AlPO-34 materials synthesized in fluoride media.
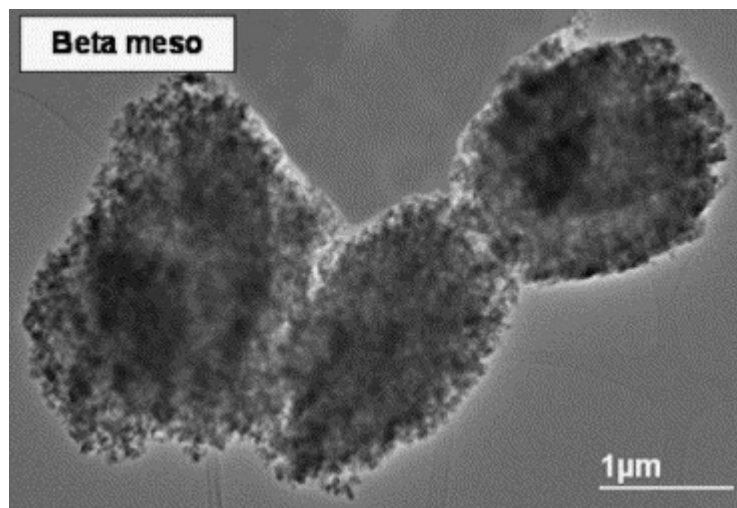
Figure 6.5 TEM image of mesoporous zeolite Beta synthesized in fluoride media.

6.4. Summary

In the present chapter it was shown that mesoporous zeolite materials can be crystallized in the presence of carbon from synthesis gels containing fluoride as the mineralizing agents. Using this method it was possible to prepare mesoporous ZSM-5 and ZSM-11 from neutral gels and moreover, it was possible to prepare zeolite beta as mesoporous crystals. Additionally, the preparation of mesoporous aluminophosphate zeotypes is possible from crystallization of fluoride containing synthesis gels in the presence of carbon. Thus, the preparation and characterization of mesoporous AlPO-5 and AlPO-34 materials was also presented in the present chapter. Electron microscopy studies of these materials reveal that the origin of the porosity of the AlPO-34 is not easily recognized as with the other samples and, unfortunately, TEM and SAD investigations of this material proved ineffective in shedding light on the matter since the material was unstable in the electron beam.

Conclusions

In this thesis the subject of mesoporosity in zeolites was discussed. Initially, in Chapter 1, an introduction to field of zeolites and the importance of their micropores were given. It was explained that much of the success of zeolites results from their inherent micropore systems which make them useful for adsorption, separation and catalysis, however, it was also explained that molecular diffusion is very slow in these micropores which hinder their effectiveness for catalytic applications. As was also discussed, there are two conceptual methods for improving the effectiveness of zeolites in catalysis, one is to create larger micropores and the other is to shorten the length of the micropores so the diffusion path length is reduced.

In Chapter 2, an overview of the field of zeolite materials with improved diffusional properties was given with special emphasis to materials featuring hierarchical pore systems. There are three types of hierarchically porous zeolite materials: nanosized crystals, supported zeolites and mesoporous zeolite crystals and these may be prepared by several methods which are categorized in Chapter 2. Overall, the methods can be divided into two groups: Templating approaches and non-templated approaches. Templating approaches cover methods involving the application of a specific template for templating the auxiliary (non-micropore) porosity and these are classified into solid, supramolecular or indirect

templating approaches. The non-templated approaches are termed demetallation and controlled crystallization.

In Chapter 3, a more in-depth discussion of the properties of materials composed of mesoporous zeolite crystals was presented. These materials differ from the two other types of hierarchical zeolite materials since the auxiliary pore system of these materials is incorporated into each individual zeolite crystal. The commonly applied methods for investigation of mesoporous zeolite materials are described and the typical results obtained using these methods are explained. From this chapter it is evident that mesoporous zeolite crystals are indeed single-crystalline materials with improved diffusional properties.

In Chapter 4 were presented three strategies for tuning the properties of mesoporous zeolite single crystals by templating approaches. It is described that the crystal sizes of mesoporous silicalite-1 prepared from BP2000 impregnated with sodium citrate prior to its application in zeolite synthesis are larger than normally afforded using BP2000 as template. A method for preparing a cheap carbon template by carbonization of a sucrose-ammonia mixture and applying this as mesopore template is also described in Chapter 4. As is the application of this as mesopore template for the preparation of hierarchical silicalite-1. Thus, cheap porous carbons are easily prepared and applied as templates for mesoporosity in zeolites. Additionally, the application of carbon-silica composites as mesopore templates and silica source was described in Chapter 4. Composites with varying C/Si ratios are easily prepared by *in situ* decomposition of sucrose impregnated on silica gel thus provide a simple method for tuning the mesoporosity of hierarchical zeolites.

In Chapter 5 it was described how the porosity of mesoporous ZSM-5 prepared by carbon-templating can be enhancing by subjecting the material to a desilication treatment, *i.e.* immersing it in an alkaline solution for a short period of time. Thus, in Chapter 6 is described how the two main methods for preparing mesoporous zeolite crystals can be combined to produce highly mesoporous zeolite single crystals.

In Chapter 6 was described that also synthesis gels containing F⁻ can be crystallized in the presence of carbon resulting in mesoporous zeolites and aluminophosphate zeotype materials. In the Chapter it was shown that the presence of fluoride as opposed to hydroxide in zeolite synthesis gels opens the possibility of synthesizing several new mesoporous materials which are not available by crystallization of alkaline gels. Thus, the preparation of mesoporous zeolite Beta crystals and mesoporous AlPO-5 and AlPO-34 materials were described.

References

[1] K.S.W. Sing, D.H. Everett, R.A.W. Haul, L. Moscou, R.A. Pierotti, J. Rouquerol, T. Siemieniewska, *Pure Appl. Chem.* **1985**, *57*, 603

[2] Website of the International Zeolite Association. Available at http://www.iza-structure.org/databases/

[3] Adapted from C.J.H. Jacobsen, I. Schmidt, A. Boisen, K. Johannsen, *Katalytisk Kemi*. Holte Bogtrykkeri A/S, 2002

[4] Website of the Energy Information Administration under the US Department of Energy. Available at http://tonto.eia.doe.gov/dnav/pet/pet_pnp_dwns_dc_nus_mbblpd_m.htm

[5] J.A. Rabo, M.W. Schoonover, *Appl. Catal. A* **2001**, *222*, 261.

[6] BP Statistical Review of World Energy, June 2008. Available at www.bp.com/statisticalreview.

[7] Adapted from A. Corma, *Chem. Rev.* **1995**, *95*, 559

[8] J. Perez-Ramirez, C.H. Christensen, K. Egeblad, C.H. Christensen, J.C. Groen, *Chem. Soc. Rev.* **2008**, *37*, 2530

[9] K. Egeblad, C.H. Christensen, M. Kustova, C.H. Christensen, *Chem. Mater.* **2008**, *20*, 946

[10] K. Egeblad, C.H. Christensen, M. Kustova, C.H. Christensen, *Mesoporous Zeoilite Crystals* in *Zeolites: From Model Materials to Industrial Catalysts*, Eds: J. Cejka, J. Perez-Pariente, W.J. Roth. Research Signpost, 2008, p. 391

[11] Y. Tao, H. Kanoh, L. Abrams, K. Kaneko, *Chem. Rev.* **2006**, *106*, 896

[12] J. Cejka, S. Mintova, *Catal. Rev.-Sci. Eng.* **2007**, *49*, 457

[13] M. Hartmann, *Angew. Chem. Int. Ed.* **2004**, *43*, 5880

[14] C.C. Freyhardt, M. Tsapatsis, R.F. Lobo, K.J. Balkus, Jr., M.E. Davis, *Nature* **1996**, *381*, 295

[15] M.E. Davis, C. Saldarriaga, C. Montes, J. Garces, C. Crowder, *Nature* **1988**, *331*, 698

[16] A. Corma, M.J. Diaz-Cabanas, J. Martinez-Triguero, F. Rey, J. Rius, *Nature* **2002**, *418*, 514

[17] A. Corma, M.J. Diaz-Cabanas, F. Rey, S. Nicolopoulos, K. Boulahya, *Chem. Commun.* **2004**, *1356*

[18] C.J.H. Jacobsen, J. Houzvicka, I. Schmidt, C. Madsen, A. Carlsson, *U.S. Patent* no. 6,565,826, **2003**

[19] H. Zhu, Z. Liu, Y. Wang, D. Kong, X. Yuan, Z. Xue, *Chem. Mater.* **2008**, *20*, 1134

[20] C. Madsen, C.J.H. Jacobsen, *Chem. Commun.* **1999**, 673

[21] I. Schmidt, C. Madsen, C.J.H. Jacobsen, *Inorg. Chem.* **2000**, *39*, 2279

[22] S.-S. Kim, J. Shah, T.J. Pinnavaia, *Chem. Mater.* **2003**, 1664

[23] C.J.H. Jacobsen, J. Houzvicka, A. Carlsson, I. Schmidt, *Stud. Surf. Sci. Catal.* **2001**, *135*, 167

[24] C.J.H. Jacobsen, C. Madsen, J. Houzvicka, I. Schmidt, A. Carlsson, *J. Am. Chem. Soc.* **2000**, *122*, 7116

[25] M.Yu. Kustova, P. Hasselriis, C.H. Christensen, *Catal. Lett.* **2004**, *96*, 205

[26] X. Wei, P.G. Smirniotis, *Microporous Mesoporous Mater.* **2006**, *89*, 170

[27] Z. Pavlackova, G. Kosova, N. Zilkova, A. Zukal, I. Cejka, *Stud. Surf. Sci. Catal.* **2006**, *162*, 905

[28] K. Egeblad, M. Kusotva, S.K. Klitgaard, K. Zhu, C.H. Christensen, *Microporous Mesoporous Mater.* **2007**, *101*, 214

[29] A.H. Janssen, I. Schmidt, C.J.H. Jacobsen, A.J. Koster, K.P. de Jong, *Microporous Mesoporous Mater.* **2003**, *65*, 59

[30] Y.H. Chou, C.S. Cundy, A.A. Garforth, V.L. Zholobenko, *Microporous Mesoporous Mater.* **2006**, *89*, 78

[31] K. Zhu, K. Egeblad, C.H. Christensen, *Stud. Surf. Sci. Catal.* **2008**, *172*, 285

[32] I. Schmidt, A. Boisen, E. Gustavsson, K. Ståhl, S. Pehrson, S. Dahl, A. Carlsson, C.J.H. Jacobsen, *Chem. Mater.* **2001**, *13*, 4416

[33] C.S. Cho, S.D. Choi, J.-H. Kim, G.-J. Kim, *Adv. Funct. Mater.* **2004**, *14*, 49

[34] Z. Yang, Y. Xia, R. Mokaya, *Adv. Funct. Mater.* **2004**, *16*, 727

[35] A. Sakhtivel, S.-J. Huang, W.-H. Chen, Z.-H. Lan, K.-H. Chen, T.-W. Kim, R. Ryoo, A.S.T. Chiang, S.-B. Liu, *Chem. Mater.* **2004**, *16*, 3168

[36] M. Kustova, K. Egeblad, K. Zhu, C.H. Christensen, *Chem. Mater.* **2007**, *19*, 2915

[37] Y. Tao, H. Kanoh, K. Kaneko, *J. Am. Chem. Soc.* **2003**, *125*, 6044

[38] Y. Tao, H. Kanoh, K. Kaneko, *J. Phys. Chem. B* **2003**, *107*, 10974

[39] Y. Tao, H. Kanoh, Y. Hanzawa, K. Kaneko, *Colloids Surf., A* **2004**, *241*, 75

[40] K. Zhu, K. Egeblad, C.H. Christensen, *Eur. J. Inorg. Chem.* **2007**, *25*, 3955

[41] Y. Tao, Y. Hattori, A. Matumoto, H. Kanoh, K. Kaneko, *J. Phys. Chem. B* **2005**, *109*, 194

[42] Y. Tao, H. Kanoh, K. Kaneko, *Langmuir* **2005**, *21*, 504

[43] W.-C. Li, A.-H. Lu, R. Palkovits, W. Schmidt, B. Spliethoff, F. Schüth, *J. Am. Chem. Soc.* **2005**, *127*, 12595

[44] B.T. Holland, L. Abrams, A. Stein, *J. Am. Chem. Soc.* **1999**, *121*, 4308

[45] L. Tosheva, V. Valtchev, J. Sterte, *Microporous Mesoporous Mater.* **2000**, *35-36*, 621

[46] F.-S. Xiao, L. Wang, C. Yin, K. Lin, Y. Di, J. Li, R. Xu, D.S. Su, R. Schlögl, T. Yokoi, T. Tatsumi, *Angew. Chem. Int. Ed.* **2006**, *45*, 3090

[47] H. Wang, T.J. Pinnavaia, *Angew. Chem. Int. Ed.* **2006**, *45*, 7603

[48] B. Zhang, S.A. Davis, N.H. Mendelson, S. Mann, *Chem. Commun.* **2000**, 781

[49] A. Dong, Y. Wang, Y. Tang, N. Ren, Y. Zhang, Y. Yue, Z. Gao, *Adv. Mater.* **2002**, *14*, 926

[50] V. Valtchev, M. Smaihi, A.-C. Faust, L. Vidal, *Angew. Chem. Int. Ed.* **2003**, *42*, 2782

[51] V. Valtchev, M. Smaihi, A.-C. Faust, L. Vidal, *Chem. Mater.* **2004**, *16*, 1350

[52] B. Zhang, S.A. Davis, S. Mann, *Chem. Mater.* **2002**, *14*, 1369

[53] M. Choi, H.S. Cho, R. Srivastava, C. Venkatesan, D.-H. Choi, R. Ryoo, *Nat. Mater.* **2006**, *5*, 718

[54] M. Choi, R. Srivastava, R. Ryoo, *Chem. Commun.* **2006**, 4380

[55] J.-C. Lin, M.Z. Yates, *Langmuir* **2006**, *21*, 2117

[56] Y. Liu, W. Zhang, T.J. Pinnavaia, *J. Am. Chem. Soc.* **2000**, *122*, 8791

[57] Y. Liu, W. Zhang, T.J. Pinnavaia, *Angew. Chem. Int. Ed.* **2001**, *40*, 1255

[58] P. Prokesova, S. Mintova, J. Cejka, T. Bein, *Mater. Sci. Eng. C* **2003**, *23*, 1001

[59] Y. Liu, T.J. Pinnavaia, *J. Mater. Chem.* **2002**, *12*, 3179

[60] Z. Zhang, Y. Han, L. Zhu, R. Wang, Y. Yu, S. Qiu, D. Zhao, F.S. Xiao, *Angew. Chem. Int. Ed.* **2001**, *40*, 1258

[61] Y. Han, F.S. Xiao, S. Wu, Y. Sun, X. Meng, D. Li, S. Lin, F. Deng, X. Ai, *J. Phys. Chem. B.* **2001**, *105*, 7953

[62] Y. Han, S. Wu, Y. Sun, D. Li, F.S. Xiao, J. Liu, X. Chang, *Chem. Mater.* **2002**, *14*, 1144

[63] F.S. Xiao, Y. Han, Y. Xu, X. Meng, M. Yang, S. Wu, *J. Am. Chem. Soc.* **2002**, *124*, 888

[64] Y. Di, Y. Yu, Y. Sun., X. Yang, S. Lin, M. Zhang, S. Li, F.S. Xiao, *Microporous Mesoporous Mater.* **2003**, *62*, 221

[65] P. Prokesova, S. Mintova, J. Cejka, T. Bein, *Microporous Mesoporous Mater.* **2003**, *64*, 165

[66] Y. Xia, R. Mokaya, *J. Mater. Chem.* **2004**, *14*, 863

[67] K.R. Kloetstra, H.W. Zandbergen, J.C. Jansen, H.V. van Bekkum, *Microporous Mesoporous Mater.* **1996**, *6*, 87

[68] S. Wang, T. Dou, Y. Li, Y. Zhang, X. Li, Z. Yan, *Catal. Commun.* **2005**, *6*, 87

[69] Y.-S. Ooi, R. Zakaria, A.R. Mohamed, S. Bhatia, *Appl. Catal., A* **2004**, *274*, 15

[70] A. Corma, V. Fornes, J. Martinez-Triguero, S.B. Pergher, *J. Catal.* **1999**, *186*, 57

[71] A. Corma, U. Diaz, M.E. Domine, V. Fornes, *Angew. Chem. Int. Ed.* **2000**, *39*, 1499

[72] A. Corma, V. Fornes, U. Diaz, *Chem. Commun.* **2001**, 2642

[73] Adapted from J. Cejka, *Stud. Surf. Sci. Catal.* **2005**, *157*, 111

[74] K.R. Kloetstra, H. van Bekkum, J.C. Jansen, *Chem. Commun.* **1997**, 2281

[75] L. Huang, W. Guo, P. Deng, Z. Xue, Q. Li, *J. Phys. Chem. B* **2000**, *104*, 2817

[76] M.J. Verhoef, P.J. Kooyman, J.C. van der Waal, M.S. Rigutto, J.A. Peters, H. van Bekkum, *Chem. Mater.* **2001**, *13*, 683

[77] D. Trong On, S. Kaliaguine, *Angew. Chem. Int. Ed.* **2001**, *40*, 3248

[78] D. Trong On, D. Lutic, S. Kaliaguine, *Microporous Mesoporous Mater.* **2001**, *44-45*, 435

[79] D. Trong On, S. Kaliaguine, *Angew. Chem. Int. Ed.* **2002**, *41*, 1036

[80] D. Trong On, S. Kaliaguine, *J. Am. Chem. Soc.* **2003**, *125*, 618

[81] V. Mavrodinova, M. Popova, V. Valchev, R. Nickolov, Ch. Minchev, *J. Colloid Interface Sci* **2005**, *286*, 286

[82] M.W. Anderson, S.M. Holmes, N. Hanif, C.S. Cundy, *Angew. Chem. Int. Ed.* **2000**, *39*, 2707

[83] S. van Donk, A.H. Janssen, J.H. Bitter, K.P. de Jong, *Catal. Rev.* **2003**, *45*, 297

[84] J.C. Groen, J.A. Moulijn, J. Perez-Ramirez, *J. Mater. Chem.* **2006**, *16*, 2121

[85] C.C. Pavel, S.H. Park, A. Dreier, B. Tesche, W. Schmidt, *Chem. Mater.* **2006**, *18*, 3813

[86] A.H. Janssen, A.J. Koster, K.P. de Jong, *Angew. Chem. Int. Ed.* **2001**, *40*, 1102

[87] R.M. Dessau, E.W. Valyocsik, N.H. Goeke, *Zeolites* **1992**, *12*, 776

[88] A. Cizmek, B. Subotic, I. Smit, A. Tonejc, R. Aiello, F. Crea, A. Nastro, *Microporous Mater.* **1997**, *8*, 159

[89] J.C. Groen, J.C. Jansen, J.A. Moulijn, J. Perez-Ramirez, *J. Phys. Chem. B* **2004**, *108*, 13062

[90] J.C. Groen, L.A.A. Peffer, J.A. Moulijn, J. Perez-Ramirez, *Colloids Surf., A* **2004**, *241*, 53

[91] J.C. Groen, T. Sano, J.A. Moulijn, J. Perez-Ramirez, *J. Catal.* **2007**, *251*, 21

[92] X. Wei, P.G. Smirniotis, *Microporous Mesoporous Mater.* **2006**, *97*, 97

[93] L. Tosheva, V.P Valtchev, *Chem. Mater.* **2005**, *17*, 2494

[94] P. Barret, L.G. Joyner, P.P. Halenda, *J. Am. Chem. Soc.* **1951**, *73*, 373

[95] B.C. Lippens, B.G. Linsen, J.H. de Boer, *J. Catal.* **1964**, *3*, 32

[96] S. Brunauer , P.H. Emmett , E. Teller , *J. Am. Chem. Soc.* **1938** , *60* , 309

[97] J.C. Groen, S. Brouwe, L.A.A. Peffer, J. Perez-Ramirez, *Part. Part. Syst. Charact.* **2006**, *23*, 101

[98] J.C. Groen, J.A. Moulijn, J. Perez-Ramirez, *Ind. Eng. Chem. Res.* **2007**, *46*, 4193

[99] J.C. Groen, T. Bach, U. Ziese, A.M. Paulaime-van Donk, K.P. de Jong, J.A. Moulijn, J. Perez-Ramirez, *J. Am. Chem. Soc.* **2005**, *127*, 10792

[100] M. Yu. Kustova, A.L. Kustov, C.H. Christensen, *Stud. Surf. Sci. Catal.* **2005**, *158B*, 255

[101] J.C. Groen, L.A.A. Peffer, J.A. Moulijn, J. Perez-Ramirez, *Microporous Mesoporous Mater.* **2004**, *69*, 29

[102] J.C. Groen, W. Zhu, S. Brouwer, S.J. Huynink, F. Kapteijn, J.A. Moulijn, J. Perez-Ramirez, *J. Am. Chem. Soc.* **2006**, *129*, 355

[103] C.H. Christensen,, K. Johannesen, E. Törnqvist, I. Schmidt, H. Topsøe, C.H. Christensen, *Catal. Today* **2007**, *128*, 117

[104] M. Kustova, K. Egeblad, C.H. Christensen, A.L. Kustov, C.H. Christensen, *Stud. Surf. Sci. Catal.* **2007**, *170A*, 267

[105] Y. Song, X. Zhu, T. Song, Q. Wang, L. Xu, *Appl. Catal. A* **2006**, *302*, 69

[106] J.S. Jung, J.W. Park, G. Seo, *Appl. Catal. A* **2005**, *288*, 149

[107] J.M. Chezeau, L. Delmotte, J.L. Guth, M. Soulard, *Zeolites* **1989**, *9*, 78

[108] E.M. Flanigen, R.L. Patton, *U.S. patent* no. 4,073,865, **1978**

[109] M.A. Camblor, A. Corma, S. Valencia, *Chem. Commun.* **1996**, 2365

[110] J.E. Hazm, P. Caullet, J.L. Paillaud, M. Soulard, L. Delmotte, *Microporous Mesoporous Mater.* **2001**, *43*, 11

[111] C.S. Cundy, *Stud. Surf. Sci. Catal.* **2005**, *157*, 65

[112] A. Tuel, S. Caldarelli, A. Meden, L.B. McCusker, C. Baerlocher, A. Ristic, N. Rajic, G. Mali, V. Kaucic, *J. Phys. Chem. B* **2000**, *104*, 5697

Appendix

Hierarchical zeolites: enhanced utilisation of microporous crystals in catalysis by advances in materials design

Javier Pérez-Ramírez,*[ab] Claus H. Christensen,[cd] Kresten Egeblad,[c] Christina H. Christensen[d] and Johan C. Groen[ef]

The introduction of synthetic zeolites has led to a paradigm shift in catalysis, separations, and adsorption processes, due to their unique properties such as crystallinity, high-surface area, acidity, ion-exchange capacity, and shape-selective character. However, the sole presence of micropores in these materials often imposes intracrystalline diffusion limitations, rendering low utilisation of the zeolite active volume in catalysed reactions. This *critical review* examines recent advances in the rapidly evolving area of zeolites with improved accessibility and molecular transport. Strategies to enhance catalyst effectiveness essentially comprise the synthesis of zeolites with wide pores and/or with short diffusion length. Available approaches are reviewed according to the principle, versatility, effectiveness, and degree of reality for practical implementation, establishing a firm link between the properties of the resulting materials and the catalytic function. We particularly dwell on the exciting field of hierarchical zeolites, which couple in a single material the catalytic power of micropores and the facilitated access and improved transport consequence of a complementary mesopore network. The carbon templating and desilication routes as examples of bottom-up and top-down methods, respectively, are reviewed in more detail to illustrate the benefits of hierarchical zeolites. Despite encircling the zeolite field, this review stimulates intuition into the design of related porous solids (116 references).

1. Evolution of porous materials: from disorder to hierarchy

1.1 Bright and dark sides of zeolites

Porous solids contribute to the welfare of society, mediating a multitude of applications in industry, environmental protection, and medicine, as well as in emerging areas such as nanotechnology, photonics, microelectronics, and bioengineering. The art, science, and engineering of making porous materials generally cover understanding and controlling the size, shape, and connectivity of the voids and channels built into solid frameworks, generally of inorganic nature. Over the last decade,

[a] *Institute of Chemical Research of Catalonia (ICIQ), Avinguda Països Catalans 16, 43007 Tarragona, Spain. E-mail: jperez@iciq.es; Fax: +34 977 920 224; Tel: +34 977 920 236*
[b] *Catalan Institution for Research and Advanced Studies (ICREA), Passeig Lluís Companys 16, 08020 Barcelona, Spain*
[c] *Center for Sustainable and Green Chemistry, Department of Chemistry, Technical University of Denmark, DK-2800 Lyngby, Denmark*
[d] *Haldor Topsøe A/S, Nymøllevej 55, DK-2800 Lyngby, Denmark*
[e] *DelftChemTech, Delft University of Technology, Julianalaan 136, 2628 BL Delft, the Netherlands*
[f] *Delft Solids Solutions B.V., Rotterdamseweg 183c, 2629 HD Delft, the Netherlands*

Javier Pérez-Ramírez (Benidorm, 1974) studied Chemical Engineering and obtained his PhD at TU Delft (2002). After a period in industry (2002–2005), he was appointed ICREA Professor at the Institute of Chemical Research of Catalonia, Tarragona, Spain. His research group develops nanostructured materials and reactor engineering concepts for application in heterogeneous catalysis.

Javier Pérez-Ramírez

Claus Hviid Christensen (born Jacobsen, Denmark, 1968) studied chemistry at the University of Copenhagen (1987–1992). After some years at Haldor Topsoe A/S (1990–2003), he became Professor of Chemistry at the Technical University of Denmark (2003–2008) and then moved back to Haldor Topsoe A/S (2008). His work focuses on the discovery of new catalysts and processes.

Johan C. Groen (Vlaardingen, The Netherlands, 1968) studied chemistry and received his PhD at the Delft University of Technology on the thesis entitled "Mesoporous Zeolites Obtained by Desilication" with Prof. J. A. Moulijn and Prof. J. Pérez-Ramírez as promotors. He is co-founder and scientific director of Delft Solids Solutions, a company devoted to contract research on porous materials.

we have witnessed great progress in the ability to fabricate new porous materials with defined structural, compositional, interfacial, and morphological properties.[1–6] This has created an impressive materials supermarket awaiting novel or improved applications.

Traditional porous solids used as catalysts, catalyst supports, and adsorbents, *e.g.* alumina, silica, and activated carbon, are mostly disordered in the sense of having random pore distributions covering indiscriminately the micro (<2 nm), meso (2–50 nm), and even macro (>50 nm) size ranges. The prime objective was, and in many cases still is, the attainment of several hundreds of square meters area per gram of solid without predefined pore geometry characteristics. The introduction of the first synthetic zeolites in the 1950s and the discovery of high-silica zeolites in the 1970s brought about a paradigm shift in the field of porous materials. Zeolites are a unique class of crystalline aluminosilicates with very high surface areas, being a consequence of ordered micropores of molecular dimensions (typically 0.25–1 nm) that enable shape-selective catalytic transformations. Fig. 1(a) illustrates a typical isotherm of the MFI-type ZSM-5 zeolite, containing a multi-dimensional network of micropores of 0.56 nm (Fig. 1(b)). Fundamental and practical interest of zeolites is largely a direct consequence of the fact that their bulk properties can be manipulated through variations in the atomic structure. Today, more than 170 different zeolite structures have been reported,[7] enabling the practice of *pore engineering* and offering seemingly endless possibilities to tailor these materials for chemical reactions.

However, zeolites and in general materials with active sites confined in micropores, are often victims of their own success,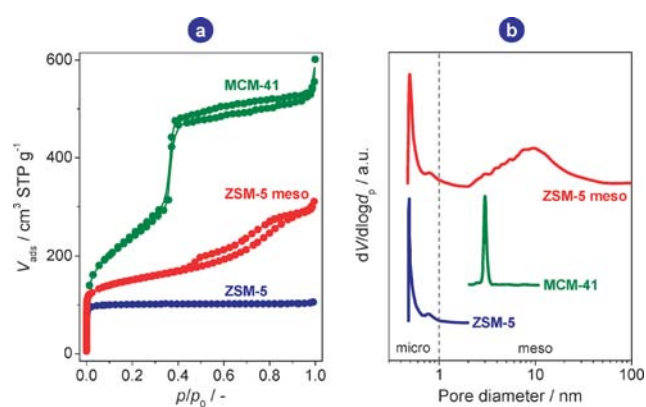 as the sole presence of micropores can impose severe mass-transfer constraints on the rate of catalysed reactions.[8–16] Diffusion, the main mechanism of mass transfer in micro- and mesoporous materials, is of crucial importance for their application in separation and catalysis, since the molecular mobility ultimately determines the rate of the overall processes.[8] Like the impeded human transit in crowded department stores and the dilatory traffic during rush hour in any metropolis, the intracrystalline motion of molecules in zeolite pores is intrinsically slow. The transport of a molecule in a pore of closely similar size is hindered, being further aggravated by the fact that reactants and products have different agendas: reactants enter while products abandon the pore system. Diffusion limitations due to restricted access and slow transport to/from the active site provoke low catalyst utilisation. This represents a major drawback in most industrial reactions catalysed by zeolites, *e.g.* cracking, oxidation, (hydro)isomerisation, alkylation, and esterification, as they do not operate at their full potential. In particular applications, *e.g.* the well-known methylation of toluene by methanol over H-ZSM-5, operation under strongly diffusion limited conditions is beneficial in order to enhance the fraction of *p*-xylene in the isomer distribution.[9,10] To this end, large zeolite crystals, *i.e.* long diffusion path lengths, and low acidity at the external surface are preferred. Bringing the accessibility problem to the extreme, the size exclusion principle of "to fit or not to fit" disables processing molecules larger than the pore entrance. According to industrial directives in terms of sharp conversions and intensified processes, future developments in zeolite catalysis should focus on more efficient catalyst utilisation for targeted reactions.

1.2 Strategies to increase catalyst effectiveness

In reaction engineering, the degree of catalyst utilisation is classically described by the effectiveness factor (Fig. 2). Full utilisation of the catalyst particle ($\eta \rightarrow 1$) represents a situation where the observed reaction rate equals the intrinsic reaction rate due to operation in the chemical regime, *i.e.* free of any diffusion constraints. In terms of intraparticle transport, this is attained at low values of the Thiele modulus ($\phi \rightarrow 0$). Contrarily, $\phi = 10$ renders $\eta = 0.1$, meaning that only 10% of the catalyst volume is effectively used in the reaction. Transport limitations negatively impact not only on activity, but occasionally also on selectivity and stability (lifetime), *i.e.* the three distinctive features of any catalyst. Since the intrinsic rate coefficient k_v is fixed for a given reaction and zeolite, keeping the Thiele modulus small implies the practise of two basic strategies: shortening the diffusion length L and/or enhancing the effective diffusivity D_{eff} in the zeolite pores. In the latter line of thinking, ordered mesoporous materials (OMMs) with regular pores in the typical range of 2–15 nm have intensively been developed since the 1990s.[11–15] MCM-41 is prototypical in this category, displaying one-dimensional ordered arrays of non-intersecting hexagonal channels with controlled size in the range of 2–10 nm (Fig. 1). The diffusion regime in mesopore catalysts is typically bulk or Knudsen diffusion and this leads to diffusivities several orders of magnitude higher than in micropores, which often display an activated (configurational) diffusion mechanism. However,

Fig. 1 Nitrogen isotherms at 77 K (a) and BJH pore size distributions (b) of characteristic porous solids. Purely microporous zeolites (*e.g.* ZSM-5) show N$_2$ uptake at low relative pressure followed by a plateau, the result of uniform micropores of 0.56 nm and the absence of larger pores. Ordered mesoporous materials (*e.g.* MCM-41) present N$_2$ uptake at intermediate relative pressure due to the presence of uniform mesopores of 3 nm, *ca.* 5 times larger than in typical zeolites. The isotherm of mesoporous ZSM-5, obtained by modification of the parent zeolite by desilication (details in text), shows N$_2$ uptake in various regions of the isotherm. The resulting material contains both micropores (0.56 nm) and mesopores (10 nm). The occurrence of a bimodal (or multimodal) pore distribution illustrates in broad terms what a hierarchical porous solid refers to.
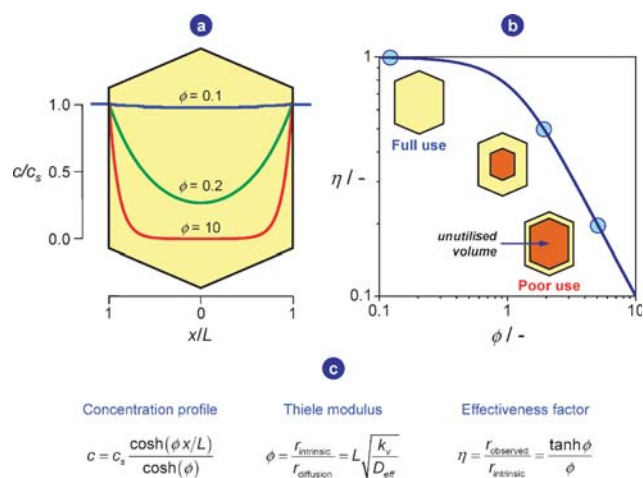
Fig. 2 Concentration profiles across a zeolite crystal (slab geometry) at different values of the Thiele modulus, ϕ (a). The reactant concentration across a zeolite crystal is extinguished ($c/c_s = 0$) near the surface at $\phi = 10$, while being practically uniform and very similar to the surface concentration ($c/c_s = 1$) at $\phi = 0.1$. The dependence of the effectiveness factor on the Thiele modulus is shown in (b). Low Thiele moduli lead to full catalyst utilisation ($\phi \to 0$, $\eta \to 1$) while high Thiele moduli render a poorly utilised catalyst ($\phi \to \infty$, $\eta \to 1/\phi$). Relevant equations to construct the graphs (a) and (b) are given in (c). They were derived assuming steady-state diffusion and reaction, slab model, first-order irreversible reaction, and isothermal conditions. Baur and Krishna[116] addressed the applicability of classical definitions of Thiele modulus and effectiveness factor for zeolites.

the *a priori* very optimistic hopes for moving the zeolite catalysis to the meso-scale by using OMMs have so far not crystallised in industrial applications due to the limited success in mimicking the unique functionalities of zeolites. Consequently, research has primarily aimed at effective chemical modification of the amorphous walls in OMMs by *e.g.* grafting[16] or crystallisation[17,18] to generate active sites equivalent to those in zeolites.

From this key learning, the scientific community started to look for alternative strategies leading to improved accessibility of the active sites confined in zeolites, which are elaborated in the next section. Two fundamentally different approaches can be adopted: (1) increasing the width of the micropores or (2) shortening the micropore diffusion path length. For several decades, researchers have pursued the preparation of *new* "large-cavity" and "wide-pore" zeolites (up to 1.25 nm), containing rings of 12 or more T-atoms. Most of these low-framework density structures, among many others VPI-5,[19] UTD-1,[20] and ECR-34,[21] suffer from similar problems as OMMs, *i.e.* low thermal stability, low acidity, and unidirectional pore systems. Recently, wide-pore zeolites with multidirectional channels have indeed been obtained, *e.g.* ITQ-15,[22] ITQ-21,[23] and ITQ-33[24] further realising the "promise of emptiness".[25]

For a given zeolite framework, the basic strategy to change the diffusion path length is altering crystal size and morphology using particular crystallisation conditions. Aiming at shorter diffusion path lengths in micropores of *existing* zeolites, "hierarchical" systems have been developed and have attracted rapidly growing attention. Broadly speaking,

materials with structural hierarchy exhibit structure on more than one length scale.[26] Hierarchical porous materials integrate multiple levels of porosity. In zeolites, this can be attained by decreasing the crystal size or by introducing an additional (meso)pore system within an individual zeolite crystal. Importantly, for a material to be denoted hierarchical, it is required that each level of porosity has a distinct function; the functionality is the differentiating feature with respect to a disordered porous material. The topics of wide-pore and hierarchical zeolites have been presented in various reviews, mini-reviews, and perspectives covering particular synthetic approaches.[11,17,18,25,27–31] However, there exists an urgent need to quantitatively compare the various methods for their preparation, and not least to describe in detail the properties of the materials as well as to establish a firm link to catalysis. We set ourselves this task in this review, pinpointing which methods are most useful for different types of studies and applications. Although focus is on the zeolite field, we attempted to synthesise concepts that are generally applicable for the design of other types of porous materials.

1.3 Hierarchical systems

Generally speaking, hierarchical porous solids can be characterised by the number of porosity levels in the material and their individual geometry. As exemplified by the mesoporous ZSM-5 in Fig. 1, the prime aim of hierarchical zeolites is coupling in a single material the catalytic features of micropores and the improved access and transport consequence of additional pores of larger size. However, the connectivity between the various levels of pores is vital to maximise the benefits of hierarchy in catalysed reactions. Interconnected hierarchy refers to the network of voids generated in the intercrystalline space by fragmentation of the microporous crystal (Fig. 3(a)) into nanocrystals (Fig. 3(b)). Intraconnected hierarchy makes reference to the occurrence of mesopores in the microporous crystal (Fig. 3(c) and (d)). The schematic representations in Fig. 3(b)–(d) shorten the length of the micropores in a similar way with respect to Fig. 3(a) as the result of smaller crystals or intracrystalline voids. Besides, the three configurations could result in qualitatively similar N_2 isotherms and pore size distributions as that of mesoporous ZSM-5 in Fig. 1. A shorter diffusion length is necessary to increase the catalyst effectiveness, but it is not a sufficient condition. For example, the system in Fig. 3(d), which could well represent a hollow zeolite crystal, is transport-wise ineffective. This is due to the fact that the mesovoids are entrapped in the microporous matrix and thus only accessible *via* the micropores. Oppositely, the mesopores in Fig. 3(c) are directly accessible from the outer surface of the zeolite crystal, similarly to the intercrystalline space in nanocrystals (Fig. 3(b)). In the latter two cases, the condition that mesopores enhance the molecular transport to/from the active sites in the micropores has been satisfied. Thus, introducing mesopores in zeolites could be ineffective for application if not properly located in the crystal. Consequently, engineering hierarchical materials in general, and zeolites in particular, requires a careful design aiming not only at extensively generating large pores, but principally at locating them in
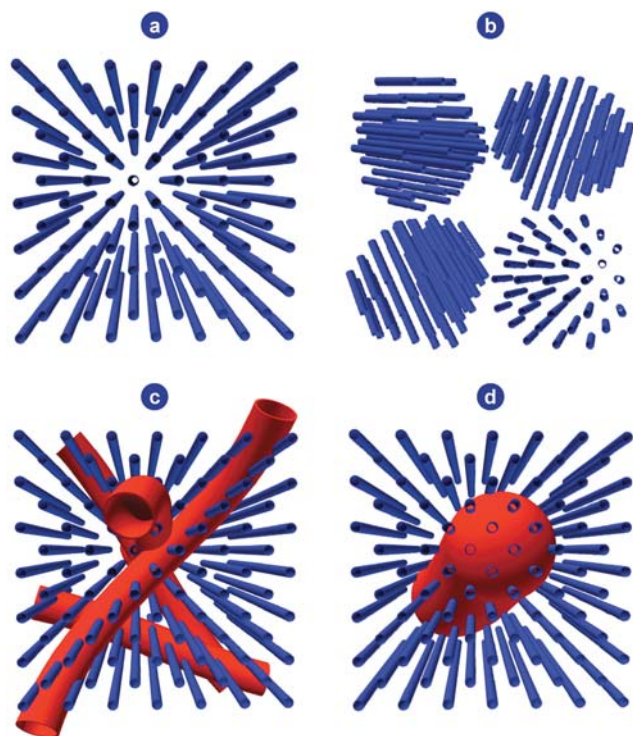
Fig. 3 Different degrees and types of hierarchy can be defined in porous materials. A purely microporous zeolite is considered as a non-hierarchical system according to the single dimension of the pores represented simplistically by the ordered blue sticks (a). The fragmentation of the zeolite into small nanocrystals engenders a network of mesopores constituting the intercrystalline space, leading to an interconnected hierarchical system (b). The term interconnected makes reference to the fact that the micropores in two crystals are bridged by interparticle voids. Intraconnected hierarchical systems are shown in (c) and (d). In these schemes, micropores are crossed by larger pores that are introduced within the zeolite crystal. Two extreme cases can be devised in this category: accessible mesopores that can be entered from the external surface of the zeolite crystals (c) and non-accessible mesovoids that are occluded in the microporous matrix (d). The systems (b), (c) and (d) could lead to similar N_2 isotherms and pore size distributions, resembling that of the mesoporous ZSM-5 in Fig. 1. However, the type and specific location of the mesoporosity largely determine whether the hierarchical system is a more efficient catalyst than the non-hierarchical (purely microporous) one.

harmony with the micropores. This is captured well by the quote by the French architect Robert Le Ricolais, which can be adapted to the topic of this review as "the art of making hierarchical materials is where to put the pore".

2. Zeolites with improved utilisation: materials and methods

As illustrated in Fig. 4, four different types of zeolite-based materials exist that offer improved accessibility to the catalytically active sites located in the microporous crystal:

1. *Wide-pore zeolites*, having substantially wider micropores than regular zeolite structures.

2. *Nanosized zeolites* having only intercrystalline pores or voids.

3. *Zeolite composites* featuring zeolite crystals supported on a material that is typically mesoporous or macroporous. In this case, the support material provides the pores required for improving mass transport to and from the zeolite crystals.

4. *Mesoporous zeolite crystals*, which exhibit intracrystalline mesopores. The introduction of mesopores into zeolite crystals can be conceived in two conceptually different ways. The mesopores are either introduced into the zeolite crystals directly during the crystallisation of the zeolite or they are introduced by a post-synthetic treatment step.

The materials in Fig. 4 can be categorised into two different groups according to the nature of their porosity. Thus, wide-pore zeolites are characterised by having a *unimodal* pore system, whereas nanosized zeolites, zeolite composites, and mesoporous zeolites are characterised by featuring *hierarchical* pore systems, since they combine the intracrystalline micropores having well-defined pore sizes and geometries determined by the crystal structure with larger pores that can be either intercrystalline (Fig. 3(b)) or intracrystalline (Fig. 3(c) and (d)).

Several synthesis strategies have been pursued to produce zeolite materials with improved accessibility. Most of the synthesis methods known today make use of templates in order to control the generation of mesopores. However, it is also possible to induce mesoporosity in zeolite materials without any template. Templating methods can be classified according to the nature of the interface between the zeolite crystal and the mesopore exactly when the mesopore starts to form.[28] In this categorisation, three classes of templating methodologies can be discerned: *solid templating*, *supramolecular templating*, and *indirect templating*. In solid and supramolecular templating, the zeolite crystal is in intimate contact with either a solid material or a supramolecular assembly of organised surfactant molecules that are subsequently removed to engender mesopores. Recently, the terms endo-templating and exo-templating have also been proposed to distinguish between these two approaches for introducing mesopores in materials.[32] In indirect templating, a preformed templated mesoporous material is either (partially) transformed into a mesoporous zeolite material or applied as a supporting material for controlled deposition of zeolite crystals. Both cases result in a composite material comprising zeolite crystals embedded in or deposited onto a mesoporous material. The non-templating methods fall under two general headings: *controlled crystallisation* and *demetallation*, and they entail either controlling the crystallisation conditions so that predominantly nanosized zeolite crystals are formed, or the preferential extraction of at least one of the constituent metallic elements of the zeolite framework, respectively.

2.1 Templating methods

Supramolecular and solid templates have been applied to control mesopore formation during zeolite crystallisation. Although a variety of solids have been used, it appears that the most general and versatile approach is to employ different types of porous carbons.[33–43] Carbon templating methods can be tuned to yield either nanosized zeolite crystals[34] or mesoporous zeolite crystals[35] and they will be dealt with in
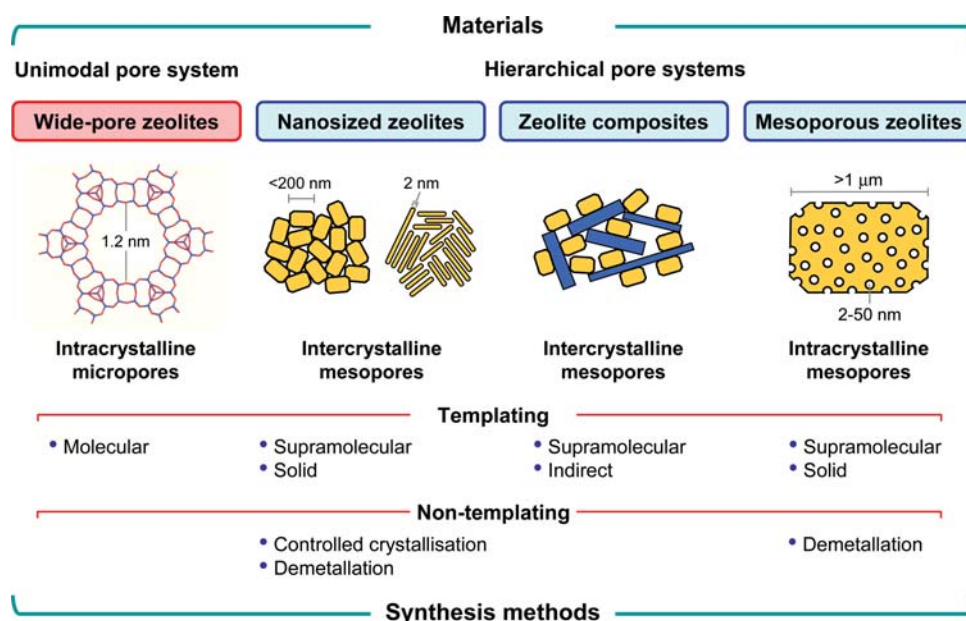
Fig. 4 Categorisation of zeolite materials with enhanced improved transport characteristics. Wide-pore zeolites increase the catalyst effectiveness by attaining higher intracrystalline diffusivity (D_{eff}), while the hierarchical pore systems reduce the characteristic diffusion length (L). Both approaches reduce the Thiele modulus defined in Fig. 2. The synthetic strategies leading to these architectures follow templating or non-templating routes, as detailed in the text.

detail in section 3.1. Other solid templates include resins,[44] organic aerogels,[45,46] and polymers,[47,48] biological templates such as bacteria,[49] plants,[50,51] and starch,[52] as well as purely inorganic compounds such as $Mg(OH)_2$[53] and $CaCO_3$.[53,54]

The supramolecular templating method involves the use of surfactant molecules to actively direct the synthesis of large micropores or mesopores. If we first consider the attempts to increase the pore size of the zeolite micropores, the only viable preparative strategy has proved to be the design of new molecular templates that lead to crystallisation of zeolite or zeotype framework structures with larger pore openings than those previously known. Over the last years, there have been numerous successful examples of wide-pore zeolites discovered with this approach,[20,22–24,55] and it has become possible to significantly accelerate this discovery process by applying high-throughput synthesis techniques.[24] However, it also appears clear that this approach has some severe limitations, since there are relatively few wide-pore zeolites. It is almost exclusively a trial-and-error approach and the operational window concerning chemical composition is relatively narrow.[25] As a consequence, parallel synthesis methodologies are of vital importance and there are still no real possibilities for predicting e.g., the acidity or the hydrothermal stability of the resulting zeolites. Thus, even when a new wide-pore zeolite is obtained, there is no way of knowing in advance whether it will prove useful in a given catalytic application before testing it explicitly. Therefore, it is difficult to directly link the zeolite discovery work with ongoing catalyst development efforts. Besides, routes to large-cavity and wide-pore zeolites are "exotic" in the sense of the required incorporation of germanium and the presence of fluoride in the synthesis composition. In addition, the cost of the structure-directing agent is usually very high compared to more standard zeolites.

Besides zeolites featuring wide micropores, supramolecular approaches can be used to synthesise hierarchical zeolites. They can be classified as either primary or secondary methods, depending on whether the surfactant assists in the assembly of purely molecular species (primary) or partly crystalline species (secondary). There are two distinct approaches to primary supramolecular templating. One is when zeolite crystallisation takes place on the external surface of a surfactant assembly, another is when it takes place inside. There are not many successful examples of the first approach. In fact, the only general route is to apply tuneable organosilanes such as $[(CH_3O)SiC_3H_6N(CH_3)_2C_nH_{2n+1}]Cl$ as both a silica source and supramolecular template.[56,57] By varying the alkyl chain length, it is possible to obtain mesoporous materials with controlled mesopore diameters, up to 20 nm. The other primary supramolecular templating approach is to prepare microemulsions, or reverse micelles, and then apply the confined space within these nanodroplets as a means for controlling the sizes of the zeolite crystals during synthesis.[58,59]

On the other hand, there are three types of secondary supramolecular templating methods that are based on assembly of partly crystalline species. One is the application of surfactants to mediate the assembly of so-called zeolite embryos or seeds into mesoporous structures. Several types of composite materials have been prepared in this way. A class of materials commonly referred to as MSU[60,61] and MAS/MTS[15,62,63] have received attention in recent years partly owing to the fact that they are highly stable in steam at temperatures up to 1073 K. MSU materials have been assembled from zeolite embryos of several different structure types. Another type of secondary supramolecular templating is coating zeolite crystals with a thin layer of mesoporous material by aid of surfactants. Using this procedure, FAU

coated with a 5–20 nm layer of MCM-41 structured materials have been produced, and this material exhibited higher conversion than ultra-stable Y in vacuum gas oil cracking of heavy molecules.[62] However, these materials have been shown to be less active and selective towards liquid gasoline products compared to similar mesoporous materials prepared by assembly of zeolite seeds in palm oil cracking using MCM-41/beta composites.[63] The third secondary supramolecular templating method is to apply surfactants to swell and ex-foliate layered zeolite precursors into so-called delaminated zeolites. The delamination procedure results in layered zeolite structures, which typically exhibit improved accessibility of the active sites due to their nanosheet-like morphology. These materials, e.g. ITQ-2[64] (delaminated MCM-22(P)), ITQ-6[65] (delaminated PREFER), and ITQ-18[66] (delaminated NU-6(2)) typically possess very large external surface areas (600–800 $m^2 \ g^{-1}$). Unfortunately, the versatility of this approach is restricted to the few available zeolite precursors with layered structure.

In the indirect templating method, the hierarchical zeolite material is produced in the absence of a distinct mesopore or macropore template but instead from a partial transformation of an ordered zeolite precursor material or by controlled deposition of zeolite crystals onto a mesoporous supporting material.[17,18,28] In either case, the overall morphology of the mesoporous zeolite composite is more or less maintained during the zeolite crystallisation or deposition step. Thus, in this method the templating is indirect, and it can in fact be considered a borderline case between templating and non-templating methods. Typically, the indirect templating method gives composite materials consisting of supported nanosized zeolite crystals. Most reports on indirect templating are concerned with the partial (or secondary) crystallisation of mesoporous materials into zeolite structures.[67–70] Using this methodology, highly mesoporous and relatively stable zeolite materials have been prepared, particularly when thick-walled SBA-15 have been used as the starting material.[67,68] However, also crystallisation of zeolite seeds adsorbed on mesoporous materials such as SBA-15[69] and mesostructured cellular foams,[70] as well as zeolitisation of diatomaceous earth[71,72] are examples of indirect templating. Recently, the partial transformation of a disordered amorphous aluminosilicate into ZSM-5 zeolite/mesophase composite in the presence of TPAOH has been reported as a simple route to synthesise hierarchical systems via solid-phase crystallisation.[73]

2.2 Non-templating methods

The last two synthesis methods listed in Fig. 4, i.e. demetallation and controlled crystallisation, are non-templating methods. In the demetallation method, one constituent is preferentially extracted from a preformed zeolite material to form mesoporous zeolite crystals. The traditional method for introducing intracrystalline pores in zeolites is by dealumination, which involves preferential extraction of framework aluminium by steaming or acid leaching treatment.[30,31] Steam treatment is the presently used method in industry to induce mesoporosity in zeolites. A more powerful strategy is the selective removal of framework silicon,[74] which will be dealt

with in detail in the following section. Recently, partial leaching of titanium and silicon in ETS-10, a titanosilicate material, by treatment in H_2O_2 under microwave irradiation, resulted in intracrystalline mesoporosity and improved catalytic performance in the Beckmann rearrangement of cyclohexanone oxime.[75]

In the controlled crystallisation method,[76,77] the crystallisation conditions are regulated to favour nucleation over crystal growth. In many ways, this is a very desirable way to improve the accessibility of the active sites in zeolite catalysts since it does not require discovery of an entirely new structure type but 'merely' the development of a modified synthesis procedure that favours nucleation over growth for the desired zeolite material. Thus, when it becomes clear that a particular zeolite shows promise in a given catalytic application, it is relatively straightforward to target modified synthesis methods that lead to decreased zeolite crystal sizes. This can be achieved by adding growth inhibitors, by increasing the supersaturation, or by quenched crystallisation. Despite the fact that considerable success has been achieved throughout the last decades in the synthesis of nanosized zeolite crystals,[76,77] unfortunately no generic approach to achieve nanosized crystals of the many available zeolite structures is known.[28] Accordingly, this approach typically also involves massive screening of zeolite synthesis schemes, similar to the approach to obtain large-cavity and wide-pore zeolites. Application of nanocrystals engenders issues related to separation in order to avoid contamination of the final product.[76] In addition, nanocrystals typically possess a relatively low internal surface area due to the decrease in microporosity with decreasing crystal size.[77]

3. Bottom-up vs. top-down approaches

In this section, hierarchical zeolites obtained by two particular routes, i.e. carbon templating and desilication are elaborated as selected examples of bottom-up and top-down synthetic approaches, respectively. Both routes are contrasted in terms of versatility, effectiveness in porosity generation, diffusion, and catalysis, and last but not least scalability. In fact, both methodologies are amenable to practical implementation.

3.1 Carbon templating

Originally, the carbon-templating approach was conceived in an attempt to develop a general method for synthesizing nanosized zeolite crystals with controlled size distributions.[34] The simple, underlying idea is that crystallisation of a zeolite inside the pores of an inert matrix would prevent the zeolite crystals from growing any larger than the size of the pores in the matrix material. Thus, the zeolite was synthesised in such a way that the entire synthesis gel was loaded exclusively into the pores of the matrix before the crystallisation was initiated. This proved to be a viable approach to give high-quality, nanosized zeolite crystals with MFI and BEA structures and with crystal size distributions controlled largely by the pore size distribution of the chosen matrix. By use of carbon, it was possible to recover the pure zeolite by simply combusting the auxiliary template.[78] This methodology was coined "confined space synthesis" to emphasise that the growth of the zeolite

This journal is © The Royal Society of Chemistry 2008

Chem. Soc. Rev., 2008, 37, 2530–2542 | 2535

crystals occurred inside the pores of carbon. Clearly, the nanosized zeolite crystals obtained by this method feature the intracrystalline micropores characteristic of ordinary zeolites plus an additional mesopore system resulting from the packing of the small zeolite crystals, *i.e.* intercrystalline pores or voids (Fig. 3(b)). However, attempts to further develop this methodology showed serendipitously that a completely different class of materials could be obtained by essentially applying the same approach. In fact, by only changing the crystallisation conditions slightly, it proved possible for zeolite crystals not only to nucleate inside the carbon matrix but also to continue their growth through the surrounding carbon pore system in such a way that the zeolite crystals encapsulate part of the carbon matrix. Thus, the zeolite crystals essentially become replicas of the carbon pore systems in which they are grown, and when the carbon matrix is removed by combustion relatively large zeolite crystals featuring an intracrystalline mesopore system result (Fig. 5(a)).

Zeolite materials produced by carbon templating are called mesoporous zeolite crystals. The materials are highly defected structures (see the scanning electron micrograph in Fig. 5(b)) that can have intracrystalline mesopore volumes exceeding 1 cm^3 g^{-1}. High-resolution transmission electron microscopy (TEM) coupled with selected area electron diffraction (SAED)[35,79] (Fig. 5(c)) proved that they can still be considered single crystals. Thus, it is noteworthy that the introduction of a zeolite gel into a porous carbon can lead to two fundamentally different types of materials. Whether the use of carbon as a template results in the formation of nanosized zeolite crystals or in mesoporous zeolite single crystals depends solely on the rate of nucleation relative to the rate of zeolite growth, and this must be determined experimentally for any given zeolite recipe. For the mesoporous zeolite single crystals, the pore size

of the intracrystalline mesopores directly reflect the size, shape, and connectivity of the carbon particles in the matrix, and accordingly it is appropriate to classify the carbon as a template. This was clearly demonstrated by using carbon templates with different sizes and different morphologies.[80] In particular, it was shown that by using carbon nanotubes, it was possible to obtain zeolite crystals with mesopore systems that exactly replicated the structure of the original carbon nanotube template.[81] By use of stereo-TEM[80] and TEM tomography,[82] the mesopore system of the treated zeolites can be mapped in great detail. The mesopores extend throughout the entire zeolite crystal and thereby provide improved access to the zeolite micropores. Fig. 5(d) shows the nitrogen isotherm and pore size distribution plot (inset) of mesoporous silicalite-1 prepared by carbon templating, whose morphology is presented in Fig. 5(b). The pore size distribution shows that the additional porosity induced by carbon-templating is typically in the mesopore range. The increased mesoporosity is also evident from comparative diffusion experiments conducted with mesoporous and conventional zeolites.[83] This is depicted in Fig. 5(e), which shows that desorption of isobutane proceeds significantly faster out of mesoporous ZSM-5 than it does out of conventional ZSM-5. Naturally, the increased rate of diffusion observed for mesoporous zeolite crystals also has implications on their performance as catalysts. Thus, mesoporous zeolite crystals are typically more active as catalysts than conventional crystals, as exemplified in Fig. 5(f) for the vapour-phase benzene alkylation with ethylene to ethylbenzene.[84] Due to the alleviated diffusion limitation, the apparent activation energy of the mesoporous zeolite (slope of the Arrhenius plot) was higher than that of the purely microporous zeolite (77 *vs.* 59 kJ mol^{-1}). What is perhaps less obvious is why these catalysts, and hierarchical zeolites in general, also offer a higher selectivity to the monoalkylated
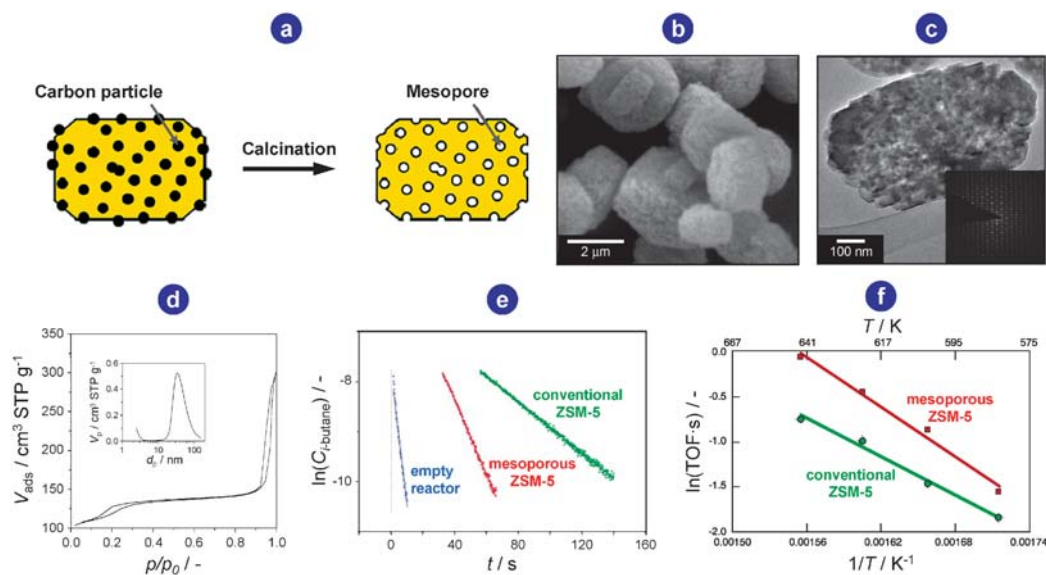
Fig. 5 Schematic illustration of zeolite crystallisation in the presence of an auxiliary carbon template resulting in hierarchical microporous–mesoporous zeolite crystals (a). Representative SEM (b) and TEM (c) images of the templated zeolites, including the electron diffraction pattern. The zeolite prepared by carbon templating evidences extensive mesoporosity as revealed by N$_2$ adsorption, with pores centered at 40 nm (d). The elution of isobutane (e) and the turnover frequency in the vapour-phase benzene alkylation (f) over the hierarchical zeolite (mesoporous ZSM-5) is largely improved compared to the microporous counterpart (conventional ZSM-5).

benzene in comparison with the purely microporous analogues. This can be explained by the shortened diffusion path length that decreases the average residence time of reacted molecules in the micropores. This suppresses successive alkylation steps of the desired ethylbenzene to polyalkylbenzenes.

Today, a wide range of zeolite structure types (MFI,[32] MEL,[85] BEA,[86] MTW,[87] CHA,[88] AFI[88]) has become available in the form of mesoporous single crystals, and it appears that other structures should be available analogously. Thus, the carbon-templating approach seems to be a versatile method for introducing mesopores into zeolites and it also provides some opportunities for tailoring the pore system to the desired application by choosing suitable carbon templates. Importantly, the method is applicable to all zeolites irrespective of their chemical composition, and therefore also to zeotype materials that do not necessarily contain silicon or aluminium. Furthermore, carbon-templating allows independent control of the mesoporosity and the acidity.

Industrial use of the method might be hampered by the fact that the suitable carbon templates (in terms of morphology, porosity, and purity) can be quite expensive, and because efficient introduction of the zeolite gel into the carbon can require more elaborate synthesis steps. Recently these hurdles were alleviated to some extent by the so-called *in situ* carbon templating method, in which the carbon template is generated by decomposing a carbohydrate, *e.g.* sugar, inside the pores of the silica source used for the zeolite crystallisation.[89] Compared to the original carbon-templating method, this approach provides less control of the pore size and geometry but instead it allows careful tailoring of the mesopore volume since this can be controlled simply by adjusting the amount of carbohydrate decomposed inside the silica. In any case, the removal of the template by combustion is a critical step to obtain high quality mesoporous zeolites. This aspect requires careful consideration, particularly in large-scale production.

3.2 Desilication

Despite numerous works available on (partial) dissolution of silicon from amorphous or even crystalline silica entities, the potential of this post-synthesis method for controlled porosity development has been unrecognised for a long time. In the early 1990s, Dessau *et al.*[90] reported an anisotropic and excessive dissolution of ZSM-5 crystals upon treatment in hot alkaline Na_2CO_3 solution, which has been speculatively attributed to the presence of an aluminium gradient in the zeolite crystals. In 1997, a distinctive role of aluminium on the kinetics of silicon dissolution upon treatment of silicalite-1 and ZSM-5 in concentrated NaOH solutions was identified by Čižmek *et al.*[91] The presence of aluminium in the zeolite framework dramatically slowed down the dissolution kinetics. In these works, however, no attention was paid to the structural, morphological, and textural changes of the treated materials. The first paper highlighting the presence of mesopores in ZSM-5 zeolites by framework silicon extraction in alkaline medium appeared in the year 2000 by the Matsukata group.[92] Although the newly obtained mesoporosity was initially attributed to intercrystalline pores by

dissolution of crystal boundaries, subsequent systematic studies by Groen *et al.*[93,94] over ZSM-5 confirmed that controlled desilication mainly induces intracrystalline mesoporosity whereas preserving most of the original microporosity. A combinatorial-type program was conducted to elucidate the role of both treatment variables such as time, temperature, and stirring speed and material related parameters like framework Si/Al ratio, crystal size, and different framework types.[95,96] These studies pointed towards a key role of framework aluminium that highly determines the alkaline treatment's chance of success (Fig. 6). The alkaline-assisted hydrolysis of the Si–O–Si bonds from the zeolite framework can be directed towards mesoporosity development when operating in an appropriate window of Si/Al ratios. Aluminium in framework positions suppresses the extraction of neighbouring silicon species. Besides aluminium, also other trivalent cations such as iron have proven to be as effective as aluminium in directing the silicon extraction towards mesoporosity development.[97] This knowledge has been used to fabricate hollow zeolite crystals upon desilication of Al-zoned ZSM-5 crystals, though the resulting system is a hierarchical system with occluded extra porosity (Fig. 7(a)).[98] Due to the presence of entrapped mesoporosity, hollow crystals are not optimal architectures to improve the catalytic activity of zeolites in diffusion-limited reactions, despite the shorter diffusion lengths by dissolution of the crystals' interior. Accordingly, the removal of framework species should desirably generate accessible mesopores from the external surface, such as those in Fig. 3(c). A uniform incorporation of accessible mesoporosity in the microporous matrix has been achieved by desilication of ZSM-5 with an isotropic distribution of aluminium in the crystal and analogous extraction of silicon (Fig. 7(b)).[99] The so-obtained materials present an accessible hierarchically architectured micro- and mesoporous system. An important feature of the alkaline-treated mesoporous zeolites is the preservation of the intrinsic Brønsted acidity of the zeolite framework, which is in contrast to zeolites modified by the traditional dealumination post-treatment (Fig. 7(c)). Besides, the mesoporosity achieved upon the latter treatment is frequently occluded in the microporous matrix[100,101] and thus less effective as compared to the hierarchical system in the uniformly desilicated zeolite crystals.[99] The presence of extra-framework aluminium species, *e.g.* obtained by a dealumination post-treatment, inhibits the extraction of framework silicon during alkaline treatment of ZSM-5. Accordingly, an independent tailoring of porous and acidic properties can only be successfully achieved by a successive combination of treatments in which the desilication treatment is performed first followed by dealumination.[102]

Successful extrapolation of the alkaline treatment to MOR[103] and MTW[104] topologies have confirmed the crucial role of framework aluminium and the generality of the desilication approach. For these zeolite types, similar ranges of framework Si/Al ratios were a prerequisite for achieving controlled mesoporosity development coupled to preserved acidity. However, operating in the optimal Si/Al ratio window of 25–50 is not the only intrinsic condition for treatment's success. Additionally, a high stability of framework aluminium is crucial to exert its pore-directing role. This has
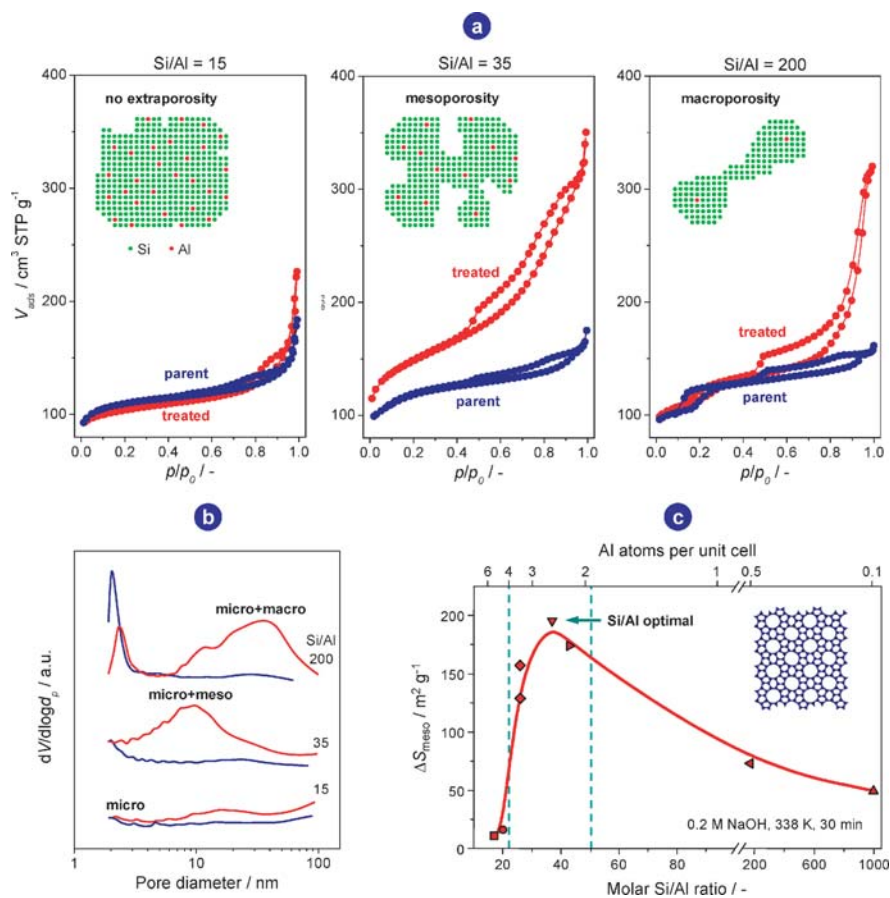
This journal is © The Royal Society of Chemistry 2008

Chem. Soc. Rev., 2008, **37**, 2530–2542 | 2537

Fig. 6 The nitrogen isotherms of parent and alkaline-treated ZSM-5 zeolites of different starting Si/Al ratios (a) show the impact of the alkali treatment on the porous properties of the resulting materials. At low Si/Al ratios, a minor change in porosity has been concluded whereas at higher Si/Al a remarkably increased uptake is achieved in the treated samples, indicative of enhanced porosity. The insets in (a) represent a simplified schematic representation of the influence of the Si/Al ratio on the porosity development. The BJH pore size distribution (b) obtained from the adsorption branch of the N_2 isotherms in (a) quantitatively describes the porosity development in the ZSM-5 zeolites. A negligible extraporosity generation in the zeolites of low Si/Al ratio is obtained, which thus remain a purely microporous system, a combined micro- and mesoporous architecture in the case of intermediate Si/Al ratios, and combined micro- and macroporosity in the high-silica ZSM-5 zeolites. The different extent of extraporosity development in the ZSM-5 zeolites by varying the Si/Al ratio impacts on the newly developed mesopore surface area (c). At low and high Si/Al ratios, the minor extraporosity and macroporosity, respectively, moderately increase the mesopore surface area. At Si/Al ratios in the range of 20–50, controlled desilication leads to an impressive increase in mesopore surface area up to 200 m^2 g^{-1}, which effectively contributes to the more efficient utilisation of the hierarchical porous architecture. In this optimal range of Si/Al ratios, the original micropore volume is decreased by only 25% maximally with a preserved micropore size.

been supported by systematic investigations of the alkaline treatment over beta zeolite crystals synthesised in fluoride-medium. The relatively low stability of aluminium in the four-membered rings of the BEA framework turned out to be incapable of directing the mesoporosity development coupled to a preservation of the Brønsted acidity.[105] Consequently, the characteristics of the starting zeolite in terms of amount (Si/Al ratio), nature (framework or extra-framework), and distribution of metal species in the crystal volume are important aspects to tailor mesoporous zeolites by desilication.

The newly introduced mesoporosity achieved by selective silicon removal leads to a greatly improved physical transport in the zeolite crystals as was revealed by transient uptake experiments of neopentane in ZSM-5 crystals[99] (Fig. 7(d)) and diffusion studies of *n*-heptane, 1,3-dimethylcyclohexane, *n*-undecane in mesoporous ZSM-12,[104] and diffusion and

adsorption studies of cumene in mesopore structured ZSM-5.[106] Up to three orders of magnitude enhanced rates of diffusion were concluded in the hierarchical systems as compared to their purely microporous precursors due to improved accessibility and a distinct shortening of the micropores. Catalytic testing of various mesoporous zeolites has proven the effectiveness of the desilication approach. A 20 times higher activity of alkaline-treated ZSM-5 has been concluded by Choi *et al.*[107] in the liquid-phase degradation of HDPE. Zhao *et al.*[106] reported doubled conversion in cumene cracking over desilicated ZSM-5 compared to the parent zeolite. A recent *in situ* microspectroscopic study on the oligomerisation of styrene derivatives revealed a greatly enhanced accessibility of the micropores in the hierarchical ZSM-5 zeolites obtained by desilication (Fig. 7(e)).[108] Application of mordenite[103] and ZSM-5[105] in the liquid-phase benzene alkylation evidenced a higher activity and selectivity
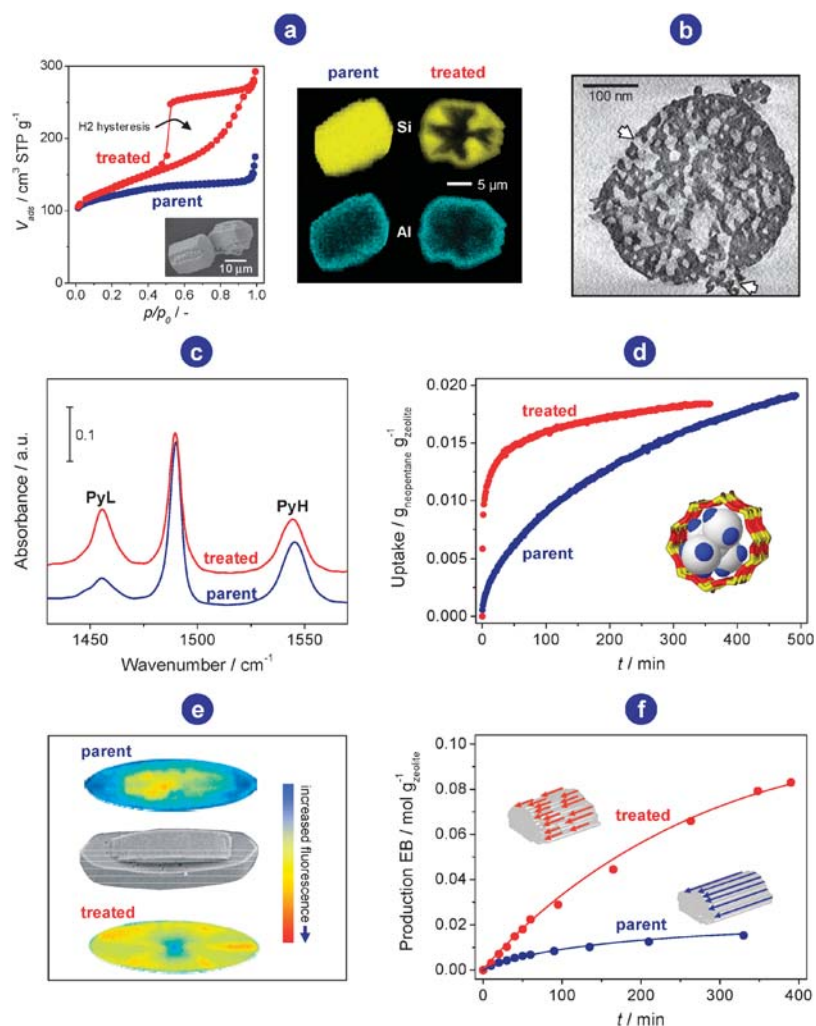
Fig. 7 SEM-EDX micrographs of large, in TPAOH-synthesised, ZSM-5 crystals evidence an anisotropic aluminium profile across the crystal volume, which shows an up to 30 times higher concentration of aluminium in the outer rim as compared to the interior of the crystals. Desilication of such zeolite crystals induces encapsulated porosity as shown by the IUPAC H2-type hysteresis loop of the N_2 adsorption isotherm (a). This observation emphasises the crucial role of the distribution of framework aluminium on the porosity development upon silicon extraction and points to the importance of the quality of the parent material. A 3-D TEM virtual cross section proves that desilication of ZSM-5 with a uniform incorporation of aluminium in the zeolite framework homogeneously generates extensive intracrystalline mesoporosity (b); arrows indicate access points to the mesopores from the external surface. Pyridine adsorption on the parent and desilicated ZSM-5 zeolites confirms preservation of the original Brønsted acidity (PyH) and generation of new Lewis acid sites (PyL) (c). The latter is the result of realumination of the zeolite framework during the alkaline treatment. Transient uptake experiments of neopentane at 393 K conclude a 2–3 orders of magnitude enhanced rate of diffusion in the desilicated hierarchical ZSM-5 crystals compared to the purely microporous parent crystals (d). *In situ* confocal fluorescence spectroscopy measured during oligomerisation of 4-methoxystyrene at 373 K reveals a more uniform yellow coloration in large-crystal mesoporous ZSM-5 zeolites due to the improved diffusion and accessibility of the treated zeolite crystals as compared to the microporous counterparts (e). Liquid-phase benzene alkylation with ethylene over mordenite greatly benefits from the introduced mesoporosity upon desilication, from 5 m^2 g^{-1} in the parent zeolite to 100 m^2 g^{-1} in the treated zeolite (f). An up to six times higher productivity of ethylbenzene coupled to minimised deactivation by coke is obtained in the mesoporous mordenite due the effectively shortened diffusion path length that greatly relieves the single file diffusion penalty in the one-dimensional zeolite structure.

to ethylbenzene of the mesoporous zeolites (Fig. 7(f)). Song *et al.*[109] reported a higher stability of desilicated ZSM-5 in butane aromatisation. The benefits of alkaline treatment on the activity, selectivity, and stability of ZSM-5 in the conversion of methanol to gasoline[110] and methanol to propylene[111] have also been demonstrated. The interplay between enhanced mass transport due the shorter diffusion path length and the preserved acidity has proven to be essential in achieving the greatly improved performance over these mesoporous zeolite

crystals. In addition, an enhanced ion-exchange capability by the higher aluminium concentration in desilicated zeolites with ameliorated access to the ion-exchange sites[112] or alteration of the active sites by the desilication treatment[113] results in more effective (redox) catalysts. The highly chemically controlled nature of the desilication treatment in alkaline medium makes scaling up rather straightforward and thus amenable to practical implementation. A first scaling up from the milligram to the kilogram scale has successfully been realised by means of a

6-liter stirred tank reactor with an increased solid–liquid ratio with no deterioration of the properties of the resulting materials.[96]

As noted above, desilication mostly creates intracrystalline porosity in channel-type zeolites such as ZSM-5, ZSM-12, mordenite, and beta. Recently, it has shown that silicon leaching can be also used to fabricate octadecasil nanocrystals (10–25 nm) with a high degree of intercrystalline porosity (*ca.* 200 m^2 g^{-1}) and a preserved structure.[114] Clathrasils, *i.e.* zeolite-related materials consisting of window-connected cages, are impenetrable to typical sorbate molecules such as N_2 or reactants such as hydrocarbons, and hence have no prospective for catalytic applications. The zero-dimensional character of these materials conditions the alkaline to operate in a different manner, as the cages cannot be accessed. Therefore, instead of attaining perforated crystals as in channel-type zeolites, clathrasil crystals are fragmented and peeled by the base, resulting in nanosized crystals. This widens the scope of these compounds, opening room for application as catalysts and/or catalyst supports.

4. Conclusions and outlook

During the last decade, hierarchical zeolites have emerged as an important class of materials in zeolite science and technology, and they attract continuously increasing interest. The optimal design of hierarchical zeolites requires the generation of multiple levels of porosity being appropriately connected in order to maximise the benefits of hierarchy in catalysed reactions. Ultimately, the art of making hierarchical materials is where to put the pore. Today, several different types of hierarchically organised zeolitic materials are available and a multitude of preparative methods have been developed to target the synthesis of specific materials. It has been shown conclusively, and in accordance with expectations, that in these materials, the micropores are indeed much more accessible due to significantly improved mass transport in the hierarchical zeolites compared with conventional zeolites featuring only micropores. The improved catalytic performance of hierarchical porous zeolite structures has been automatically attributed to enhanced transport, most of the times without direct evidence of the diffusion characteristics. Consequently, the diffusion studies should increasingly accompany papers dealing with the synthesis and catalytic application of hierarchical zeolites.

So far, the improved accessibility has been the main motivation for developing this class of materials. Herein, we tried to categorise these materials and the methods for their synthesis, and to highlight examples in which superior catalytic performance of the hierarchical zeolites appears to be directly related to the improved mass transport. To illustrate state-of-the-art achievements in the field, we have presented prominent examples of the various approaches available to prepare hierarchical zeolites. It should be clear that each method has its advantages and disadvantages, and more importantly, that there is ample room for extending and improving all the currently known methods. In fact, it appears likely that entirely new methods will emerge and contribute to the existing options for designing hierarchical zeolites. Besides

zeolite composites, substantial efforts have been devoted to the development of the carbon-templating method and the desilication method. For the latter two methods, quantitative studies related to the improved diffusion, detailed characterisation studies, and also several examples of improved catalytic performance have been reported. Therefore, we have focused on these methods to in-depth illustrate the opportunities with hierarchical zeolite materials and to clearly establish the link between materials design and catalytic performance. However, with the different materials available and the various preparative methods ready to hand, it is interesting to discuss which materials and which of the currently known methods are indeed the most promising, going beyond laboratory scale toward implementation. This is clearly a most difficult question, and the answer appears to depend on many factors in a quite complicated way. If we, for simplicity, limit our discussion to pure zeolite materials, it appears that there are no obvious advantages of any particular type of zeolite material, *i.e.* nanosized zeolite crystals and hierarchical zeolite crystals are expected to have quite similar properties thereby showing analogous catalytic performance. However, there could easily be some more subtle differences *e.g.* in the thermal and hydrothermal stability of the different materials or in the handling of the materials, but such studies have not yet crystallised. Thus, in selecting one particular method for synthesizing hierarchical zeolites, the most important thing is to consider the objective of the study. If it is imperative to achieve very accurate control over the pore size distribution *e.g.*, to tailor systems for fundamental studies, clearly the supramolecular templating methods appear most promising, and in particular the method by the group of Ryoo seems to allow the most precise control of the pore system.[27,56] A most recent work by the same group claims distinctive catalytic activity of the mesopores in hierarchical MFI zeolites,[115] implying a dual functionality of the mesoporosity in hierarchical systems as transport facilitator and active catalyst. This opens wide avenues for dedicated transformations of larger molecules. Still, a point of concern is the fact that the supramolecular templating methods are in general economically prohibitive for the vast majority of possible industrial applications of these hierarchical zeolites. In this case, desilication and *in situ* carbon templating methods appear much more viable. If the desilication method can be made to work with the desired zeolite structure and the relevant Si/Al ratio, this would be the obvious choice due to its simplicity, scalability, and low cost. In desilication, the flexibility to tailor the mesoporosity is so far basically limited to the Si/Al ratio, temperature, and time. Accordingly, research efforts should be directed toward increasing the tuning capabilities of the desilication treatment and to widen the applicability of this treatment to other frameworks. In other cases, the carbon-templating route would be the preferred alternative, since this method is versatile and allows more control over the pore size distribution though not nearly to the same degree as that reported with the supramolecular templating methods. Mei *et al.*[111] have for the first time compared in the same study mesoporous ZSM-5 obtained by templating with starch and by desilication for the methanol-to-propylene reaction. The template route led to enhanced mesoporosity in the zeolite

crystals compared with alkaline treatment. However the mesopores in the former sample were mainly located inside the zeolite body and played a limited role in the diffusion of gas molecules. In contrast, the open mesopores in the desilicated zeolite catalyst enhanced the diffusion of the primary olefin products (propylene and butylene), and inhibited undesirable secondary reactions. As a result, the propylene-to-ethylene ratio and propylene selectivity were most effectively enhanced in the alkaline-treated catalyst. Clearly, there can be many other factors to consider than those presented here. Moreover, it is anticipated that improved insight into the capabilities of the different synthetic methods will appear during the coming years and this can obviously refine these considerations. Accordingly, it is concluded that the field of hierarchical zeolites will continue to attract increasing attention during the years to come. These new efforts will lead to a substantial improvement in our understanding of zeolite catalysis and possibly also to significant technological developments through the implementation of hierarchical zeolites in industrial processes.

Acknowledgements

References

1 M. E. Davis, *Nature*, 2002, **417**, 813–821.
2 M. Tsapatsis, *AIChE J.*, 2002, **48**, 654–660.
3 A. Stein, *Adv. Mater.*, 2003, **15**, 763–775.
4 A. Corma and M. E. Davis, *ChemPhysChem*, 2004, **5**, 304–313.
5 H. C. Zheng, *J. Mater. Chem.*, 2006, **16**, 649–662.
6 H. K. Chae, D. Y. Siberio-Perez, J. Kim, Y. B. Go, M. Eddaoudi, A. J. Matzger, M. O'Keeffe and O. M. Yaghi, *Nature*, 2004, **427**, 523–527.
7 C. Baerlocher, W. M. Meier and D. H. Olson, *Atlas of Zeolite Framework Types*, Elsevier, Amsterdam, 5th edn, 2001.
8 J. Kärger and D. Freude, *Chem. Eng. Technol.*, 2002, **25**, 769–778.
9 K. Beschmann, L. Riekert and U. Müller, *J. Catal.*, 1994, **145**, 243–245.
10 J.-H. Kim, T. Kunieda and M. Niwa, *J. Catal.*, 1998, **173**, 433–439.
11 A. Corma, *Chem. Rev.*, 1997, **97**, 2373–2420.
12 A. Taguchi and F. Schüth, *Microporous Mesoporous Mater.*, 2005, **77**, 1–45.
13 C. T. Kresge, M. E. Leonowicz, W. J. Roth, J. C. Vartuli and J. S. Beck, *Nature*, 1992, **359**, 710–712.
14 D. Zhao, J. Feng, Q. Huo, N. Melosh, G. H. Fredrickson, B. F. Chmelka and G. D. Stucky, *Science*, 1998, **23**, 548–552.
15 Z. Zhang, Y. Han, L. Zhu, R. Wang, S. Qiu, D. Zhao and F.-S. Xiao, *Angew. Chem., Int. Ed.*, 2001, **40**, 1258–1262.
16 R. Mokaya, *ChemPhysChem*, 2002, **3**, 360–363.
17 V. Meynen, P. Cool and E. F. Vansant, *Microporous Mesoporous Mater.*, 2007, **104**, 26–38.
18 J. Čejka and S. Mintova, *Catal. Rev. Sci. Eng.*, 2007, **49**, 457–509.
19 M. E. Davis, C. Saldarriaga, C. Montes, J. Garces and C. Crowder, *Nature*, 1988, **331**, 698–699.
20 C. C. Freyhardt, M. Tsapatsis, R. F. Lobo, K. J. B. Jr and M. E. Davis, *Nature*, 1996, **381**, 295–298.
21 K. G. Strohmaier and D. E. W. Vaughan, *J. Am. Chem. Soc.*, 2003, **125**, 16035–16039.
22 A. Corma, M. J. Díaz-Cabañas, F. Rey, S. Nicolopoulus and K. Boulahyab, *Chem. Commun.*, 2004, 1356–1357.
23 A. Corma, M. J. Díaz-Cabañas, J. Martínez-Triguero, F. Rey and J. Rius, *Nature*, 2002, **418**, 514–517.
24 A. Corma, M. J. Díaz-Cabañas, J. L. Jordá, C. Martínez and M. Moliner, *Nature*, 2006, **443**, 842–845.
25 R. F. Lobo, *Nature*, 2006, **443**, 757–758.
26 R. Lakes, *Nature*, 1993, **361**, 511–515.
27 B. F. Chmelka, *Nat. Mater.*, 2006, **5**, 681–682.
28 K. Egeblad, C. H. Christensen, M. Kustova and C. H. Christensen, *Chem. Mater.*, 2008, **20**, 946–960.
29 M. Hartmann, *Angew. Chem., Int. Ed.*, 2004, **43**, 5880–5882.
30 Y. Tao, H. Kanoh, L. Abrams and K. Kaneko, *Chem. Rev.*, 2006, **106**, 896–910.
31 S. van Donk, A. H. Janssen, J. H. Bitter and K. P. de Jong, *Catal. Rev. Sci. Eng.*, 2003, **45**, 297–319.
32 F. Schüth, *Angew. Chem., Int. Ed.*, 2003, **42**, 3604–3622.
33 R. Ryoo, S. H. Joo and S. Jun, *J. Phys. Chem. B*, 1999, **103**, 7743–7446.
34 C. Madsen and C. J. H. Jacobsen, *Chem. Commun.*, 1999, 673–674.
35 C. J. H. Jacobsen, C. Madsen, J. Houzvicka, I. Schmidt and A. Carlsson, *J. Am. Chem. Soc.*, 2000, **122**, 7116–7117.
36 S.-S. Kim, J. Shah and T. J. Pinnavaia, *Chem. Mater.*, 2003, **15**, 1664–1668.
37 S. I. Cho, S. D. Choi, J.-H. Kim and G.-J. Kim, *Adv. Funct. Mater.*, 2004, **14**, 49–54.
38 A. Sakhtivel, S.-J. Huang, W.-H. Chen, Z.-H. Lan, K.-H. Chen, T.-W. Kim, R. Ryoo, A. S. T. Chiang and S.-B. Liu, *Chem. Mater.*, 2004, **16**, 3168–3175.
39 Z. Yang, Y. Xia and R. Mokya, *Adv. Mater.*, 2004, **16**, 727–732.
40 Y. Zhang, T. Okubo and M. Ogura, *Chem. Commun.*, 2005, 2719–2720.
41 Y. Fang and H. Hu, *J. Am. Chem. Soc.*, 2006, **128**, 10636–10637.
42 M. Ogura, Y. Zhang, S. P. Elangovan and T. Okubo, *Microporous Mesoporous Mater.*, 2007, **101**, 224–230.
43 H. Li, Y. Sakamoto, Z. Liu, T. Ohsuna, O. Terasaki, M. Thommes and S. Che, *Microporous Mesoporous Mater.*, 2007, **106**, 174–179.
44 L. Tosheva, V. Valtchev and J. Sterte, *Microporous Mesoporous Mater.*, 2000, **35–36**, 621–629.
45 Y. Tao, H. Kanoh and K. Kaneko, *Langmuir*, 2005, **21**, 504–507.
46 W.-C. Li, R. Palkovits, W. Schmidt, B. Spliethoff and F. Schüth, *J. Am. Chem. Soc.*, 2005, **127**, 12595–12600.
47 F.-S. Xiao, L. Wang, C. Yin, K. Lin, Y. Di, J. Li, R. Xu, D. S. Su, R. Schlögl, T. Yokoi and T. Tatsumi, *Angew. Chem., Int. Ed.*, 2006, **45**, 3090–3093.
48 H. Wang and T. J. Pinnavaia, *Angew. Chem., Int. Ed.*, 2006, **45**, 7603–7606.
49 S. A. Davis, S. L. Burkett, N. H. Mendelson and S. Mann, *Nature*, 1997, **385**, 420–423.
50 A. Dong, Y. Wang, Y. Tang, N. Ren, Y. Zhang, Y. Yue and Z. Gao, *Adv. Mater.*, 2002, **14**, 926–929.
51 V. Valtchev, M. Smaihi, A.-C. Faust and L. Vidal, *Angew. Chem., Int. Ed.*, 2003, **42**, 1369–1375.
52 B. Zhang, S. A. Davis and S. Mann, *Chem. Mater.*, 2002, **14**, 1369–1375.
53 C. J. H. Jacobsen, J. Houzvicka, I. Schmidt, C. Madsen and A. Carlsson, *US Pat.*, 6,565,826, 2003.
54 H. Zhu, Z. Liu, Y. Wang, D. Kong, X. Yuan and Z. Xue, *Chem. Mater.*, 2008, **20**, 1134–1139.
55 A. Corma, F. Rey, J. Rius, M. J. Sabater and S. Valencia, *Nature*, 2004, **431**, 287–290.
56 M. Choi, H. S. Cho, R. Srivastava, C. Venkatesan, D.-H. Choi and R. Ryoo, *Nat. Mater.*, 2006, **5**, 718–723.
57 M. Choi, R. Srivastava and R. Ryoo, *Chem. Commun.*, 2006, 4380–4382.
58 S. Schacht, Q. Huo, I. G. Voigt-Martin, G. D. Stucky and F. Schuth, *Science*, 1996, **273**, 768–771.
59 J. C. Lin and M. Z. Yates, *Langmuir*, 2005, **21**, 2117–2120.
60 Y. Liu, W. Zhang and T. J. Pinnavaia, *J. Am. Chem. Soc.*, 2000, **122**, 8791–8792.

This journal is © The Royal Society of Chemistry 2008

Chem. Soc. Rev., 2008, **37**, 2530–2542 | 2541

61 Y. Liu, W. Zhang and T. J. Pinnavaia, *Angew. Chem., Int. Ed.*, 2001, **40**, 1255–1258.
62 K. R. Kloetstra, H. W. Zandbergen, J. C. Jansen and H. van Bekkum, *Microporous Mater.*, 1996, **6**, 287–293.
63 Y.-S. Ooi, R. Zakaria, A. R. Rahman and S. Bhatia, *Appl. Catal., A*, 2004, **274**, 15–23.
64 A. Corma, V. Fornés, J. Martínez-Triguero and S. B. Pergher, *J. Catal.*, 1999, **186**, 57–63.
65 A. Corma, U. Diaz, M. E. Domine and V. Fornés, *Angew. Chem., Int. Ed.*, 2000, **39**, 1499–1501.
66 A. Corma, V. Fornés and U. Díaz, *Chem. Commun.*, 2001, 2642–2643.
67 D. Trong-On and S. Kaliaguine, *Angew. Chem., Int. Ed.*, 2001, **40**, 3248–3251.
68 D. Trong-On, D. Lutic and S. Kaliaguine, *Microporous Mesoporous Mater.*, 2001, **44–45**, 435–444.
69 D. Trong-On and S. Kaliaguine, *Angew. Chem., Int. Ed.*, 2002, **41**, 1036–1040.
70 D. Trong-On and S. Kaliaguine, *J. Am. Chem. Soc.*, 2003, **125**, 618–619.
71 M. W. Anderson, S. M. Holmes, N. Hanif and C. S. Cundy, *Angew. Chem., Int. Ed.*, 2000, **39**, 2707–2710.
72 Y. Wang, Y. Tang, A. Dong, X. Wang, N. Ren and Z. Gao, *J. Mater. Chem.*, 2002, **12**, 1812–1818.
73 J. Wang, J. C. Groen, W. Yue, W. Zhou and M.-O. Coppens, *Chem. Commun.*, 2007, 4653–4655.
74 J. C. Groen, J. A. Moulijn and J. Pérez-Ramírez, *J. Mater. Chem.*, 2006, **16**, 2121–2131.
75 C. C. Pavel, R. Palkovits, F. Schüth and W. Schmidt, *J. Catal.*, 2008, **254**, 84–90.
76 S. C. Larsen, *J. Phys. Chem. C*, 2007, **111**, 18464–18474.
77 M. A. Camblor, A. Corma and S. Valencia, *Microporous Mesoporous Mater.*, 1998, **25**, 59–74.
78 C. J. H. Jacobsen, C. Madsen, T. V. W. Janssens, H. J. Jakobsen and J. Skibsted, *Microporous Mesoporous Mater.*, 2000, **39**, 393–401.
79 K. Zhu, K. Egeblad and C. H. Christensen, *Eur. J. Inorg. Chem.*, 2007, 3955–3960.
80 A. H. Janssen, I. Schmidt, C. J. H. Jacobsen, A. J. Koster and K. P. de Jong, *Microporous Mesoporous Mater.*, 2003, **65**, 59–75.
81 I. Schmidt, A. Boisen, E. Gustavsson, K. Stahl, S. Pehrson, S. Dahl, A. Carlsson and C. J. H. Jacobsen, *Chem. Mater.*, 2001, **13**, 4416–4418.
82 A. Boisen, I. Schmidt, A. Carlsson, S. Dahl, M. Brorson and C. J. H. Jacobsen, *Chem. Commun.*, 2003, 958–959.
83 C. H. Christensen, K. Johannsen, E. Törnqvist, I. Schmidt, H. Tøpsoe and C. H. Christensen, *Catal. Today*, 2007, **128**, 117–122.
84 C. H. Christensen, K. Johannsen, I. Schmidt and C. H. Christensen, *J. Am. Chem. Soc.*, 2003, **125**, 13370–13771.
85 M. Y. Kustova, P. Hasselriis and C. H. Christensen, *Catal. Lett.*, 2004, **96**, 205–211.
86 Z. Pavlackova, G. Kosova, N. Zilkova, A. Zukal and J. Čejka, *Stud. Surf. Sci. Catal.*, 2006, **162**, 905–912.
87 X. Wei and P. G. Smirniotis, *Microporous Mesoporous Mater.*, 2006, **89**, 170–178.
88 K. Egeblad, M. Kustova, S. K. Klitgaard, K. Zhu and C. H. Christensen, *Microporous Mesoporous Mater.*, 2007, **101**, 214–223.
89 M. Kustova, K. Egeblad, K. Zhu and C. H. Christensen, *Chem. Mater.*, 2007, **19**, 2915–2917.
90 R. M. Dessau, E. W. Valyocsik and N. H. Goeke, *Zeolites*, 1992, **12**, 776–779.
91 A. Čižmek, B. Subotic, I. Smit, A. Tonejc, A. Rosario, F. Crea and A. Nastro, *Microporous Mater.*, 1997, **8**, 159–169.
92 M. Ogura, S. Y. Shinomiya, J. Tateno, Y. Nara, E. Kikuchi and H. Matsukata, *Chem. Lett.*, 2000, 82–83.
93 J. C. Groen, J. C. Jansen, J. A. Moulijn and J. Pérez-Ramírez, *J. Phys. Chem. B*, 2004, **108**, 13062–13065.
94 J. C. Groen, L. A. A. Peffer, J. A. Moulijn and J. Pérez-Ramírez, *Chem.–Eur. J.*, 2005, **11**, 4983–4994.
95 J. C. Groen, L. A. A. Peffer, J. A. Moulijn and J. Perez-Ramírez, *Colloids Surf., A*, 2004, **241**, 53–58.
96 J. C. Groen, J. A. Moulijn and J. Pérez-Ramírez, *Ind. Eng. Chem. Res.*, 2007, **14**, 4193–4201.
97 J. C. Groen, L. Maldonado, E. Berrier, A. Brückner, J. A. Moulijn and J. Pérez-Ramírez, *J. Phys. Chem. B*, 2006, **110**, 20369–20378.
98 J. C. Groen, T. Bach, U. Ziese, A. M. Paulaime-van Donk, K. P. de Jong, J. A. Moulijn and J. Pérez-Ramírez, *J. Am. Chem. Soc.*, 2005, **127**, 10792–10793.
99 J. C. Groen, W. Zhu, S. Brouwer, S. J. Huynink, F. Kapteijn, J. A. Moulijn and J. Pérez-Ramírez, *J. Am. Chem. Soc.*, 2007, **129**, 355–360.
100 P. Kortunov, S. Vasenkov, J. Kärger, R. Valiullin, P. Gottschalk, M. F. Elía, M. Perez, M. Stöcker, B. Drescher, G. McElhiney, C. Berger, R. Gläser and J. Weitkamp, *J. Am. Chem. Soc.*, 2005, **127**, 13055–13059.
101 A. H. Janssen, A. J. Koster and K. P. de Jong, *Angew. Chem., Int. Ed.*, 2001, **40**, 1102–1104.
102 J. C. Groen, J. A. Moulijn and J. Pérez-Ramírez, *Microporous Mesoporous Mater.*, 2005, **87**, 153–161.
103 J. C. Groen, T. Sano, J. A. Moulijn and J. Pérez-Ramírez, *J. Catal.*, 2007, **251**, 21–27.
104 X. Wei and P. G. Smirniotis, *Microporous Mesoporous Mater.*, 2006, **97**, 97–106.
105 J. C. Groen, S. Abelló, L. Villaescusa and J. Pérez-Ramírez, *Microporous Mesoporous Mater.*, 2008, **114**, 93–102.
106 L. Zhao, B. Shen, J. Gao and C. Xu, *J. Catal.*, 2008, **258**, 228–234.
107 D. H. Choi, J. W. Park, J.-H. Kim and Y. Sugi, *Polym. Degrad. Stab.*, 2006, **91**, 2860–2866.
108 M. H. F. Kox, E. Stavitski, J. C. Groen, J. Pérez-Ramírez, F. Kapteijn and B. M. Weckhuysen, *Chem.–Eur. J.*, 2008, **14**, 1718–1725.
109 Y. Song, X. Zhu, Y. Song and Q. Wang, *Appl. Catal., A*, 2006, **288**, 69–77.
110 M. Bjørgen, F. Joensen, M. Spangsberg Holm, U. Olsbye, K.-P. Lillerud and S. Svelle, *Appl. Catal., A*, 2008, **345**, 43–50.
111 C. Mei, P. Wen, Z. Liu, H. Liu, Y. Wang, W. Yang, Z. Xie, W. Hua and Z. Gao, *J. Catal.*, 2008, **258**, 243–249.
112 I. Melian-Cabrera, S. Espinoza, J. C. Groen, B. van der Linden, F. Kapteijn and J. A. Moulijn, *J. Catal.*, 2006, **238**, 250–259.
113 J. C. Groen, A. Bruckner, E. Berrier, L. Maldonado, J. A. Moulijn and J. Pérez-Ramírez, *J. Catal.*, 2006, **243**, 212–216.
114 J. Pérez-Ramírez, S. Abelló, L. A. Villaescusa and A. Bonilla, *Angew. Chem., Int. Ed.*, 2008, **47**, 7913–7917.
115 V. N. Shetti, J. Kim, R. Srivastava, M. Choi and R. Ryoo, *J. Catal.*, 2008, **254**, 296–303.
116 R. Baur and R. Krishna, *Catal. Today*, 2005, **105**, 173–179.

Templating Mesoporous Zeolites[†]

Kresten Egeblad,[‡] Christina H. Christensen,[§] Marina Kustova,[‡,§] and
Claus H. Christensen*[,‡]

*Center for Sustainable and Green Chemistry, Department of Chemistry, Technical University of Denmark,
Building 206, 2800 Lyngby, Denmark, and Haldor Topsøe A/S, Nymøllevej 55, 2800 Lyngby, Denmark*

Received August 7, 2007. Revised Manuscript Received November 6, 2007

The application of templating methods to produce zeolite materials with hierarchical bi- or trimodal pore size distributions is reviewed with emphasis on mesoporous materials. Hierarchical zeolite materials are categorized into three distinctly different types of materials: hierarchical zeolite crystals, nanosized zeolite crystals, and supported zeolite crystals. For the pure zeolite materials in the first two categories, the additional meso- or macroporosity can be classified as being either intracrystalline or intercrystalline, whereas for supported zeolite materials, the additional porosity originates almost exclusively from the support material. The methods for introducing mesopores into zeolite materials are discussed and categorized. In general, mesopores can be templated in zeolite materials by use of solid templating, supramolecular templating, or indirect templating. In this categorization of templating methods, the nature of the interface between the zeolite crystal and the mesopore exactly when the mesopore starts to form is emphasized. In solid templating, the zeolite crystal is in intimate contact with a solid material that is being removed to produce the mesoporosity. Similarly, in supramolecular templating, the zeolite crystal is in direct contact with a supramolecular assembly of organized surfactants, which is removed to generate the mesopores. On the other hand, in the indirect templating method, the interface is between the zeolite crystal and solvent molecules, or possibly a gas phase. It is shown that the available templating approaches are quite versatile, and accordingly, it is possible to produce a very wide range of hierarchical zeolite materials. The resulting zeolite materials, featuring noncrystallographic mesopores in addition to the crystallographic micropores, exhibit significantly enhanced diffusional properties in comparison with purely microporous zeolite materials. These enhanced mass transport properties have been shown in several cases to result in significantly improved catalytic properties in a range of important reactions.

Introduction

Zeolites are crystalline aluminosilicates build from TO_4 tetrahedra (T = Si, Al) that are arranged in such a manner that intracrystalline pores and cavities of molecular dimensions are present. Typically, these zeolite pores have diameters in the range of 4–12 Å and they are therefore called micropores according to the IUPAC classification of porous materials.[1] The sizes and shapes of the micropores, and the cavities, are determined exclusively by the crystal structure of the zeolite. Thus, the micropores can be categorized as crystallographic micropores. Currently, more than 170 different zeolite structure types have been characterized and several new types still appear every year. Each zeolite structure type features a unique micropore system. In chemical industry, zeolites are among the most important families of materials with a multitude of technical applications.[2,3] Accordingly, there are numerous reviews that cover some of the currently most important industrial uses such as in ion-exchange,[2–5] sorption,[2–5] and heterogeneous catalysis[2,3,6–8] but also possible new, emerging applications[9–13] attract considerable attention. At the same time, there are significant ongoing efforts to continuously improve our fundamental understanding of zeolite materials and recent reviews describe, for example, state-of-the-art of hydrothermal zeolite synthesis,[14,15] the use of in situ characterization techniques to zeolite catalysts,[16] diffusion in zeolites,[17] zeolite membrane materials,[18] and the application of theoretical modeling in zeolite science.[19]

Much of the success of zeolites in chemistry and chemical engineering can be attributed to the presence of the well-defined micropores, which are responsible for the well-known molecular sieve effect. Thus, in heterogeneous catalysis, the availability of a wide range of zeolite structures with different micropore architectures makes it possible to conduct shape-selective catalysis, which represents one of the most significant achievements in the history of catalysis.[20] With shape-selective catalysts, it is possible to conduct highly selective catalytic transformations on the basis of the complete exclusion, or on the strongly hindered diffusion, of certain reactants, intermediates, or products in the zeolite micropores. Alternatively, shape-selectivity can occur because of the sterically confined reaction space present in the vicinity of the active sites that are preferably located in the zeolite micropores. This can favor one reaction path (transition state) over another.

Generally, zeolites are very versatile catalysts that can be tailored to achieve optimum performance in a wide range

* Corresponding author. Tel: 45 45252402. Fax: 45 45883136. E-mail: chc@kemi.dtu.dk.
† Part of the "Templated Materials Special Issue".
‡ Technical University of Denmark.
§ Haldor Topsøe A/S.

Reviews

Chem. Mater., Vol. 20, No. 3, 2008 947

of catalytic reactions. Thus, the catalytically active sites in zeolite micropores can be acid sites that result from the charge compensation of the framework with protons, which is necessary when, for example, Al^{3+} substitutes Si^{4+} in the framework, or it can be redox-active sites resulting when the charge compensation is done by ion exchange with redox-active ions such as Fe(III), Cu(II), Co(II), or Ag(I) rather than with protons. Additionally, redox-active sites can be obtained by incorporating redox active metals ions, e.g., Ti, V, Mn, Fe, Co, Ga, Sn, etc., directly into the zeolite framework by isomorphous substitution of other T atoms. Therefore, zeolite catalysts attract significant attention in many areas of heterogeneous catalysis both for purely fundamental reasons because they can be tailored to allow careful and systematic studies of various structure–activity relationships and in numerous industrial applications where they can be active, selective, durable, and relatively inexpensive catalysts.

However, in numerous cases, the sole presence of micropores also imposes significant limitations on the range of reactions that are efficiently catalyzed by zeolite catalysts. This is clearly the case for reactions involving reactants or products that are so large that they are effectively excluded from the zeolite micropores. However, also for reactants and products that are smaller than the micropores, it is often not possible to explore the full potential of the zeolite catalysts. It is clear that if the zeolite catalyst could in principle transform the reactant(s) into the desirable product(s) at a rate higher than the rate of diffusion of reactants, intermediates, and products in the zeolite, then the overall reaction rate will be limited by the rate of diffusion. Thus, the reaction is in a diffusion-controlled regime and the effectiveness factor, which is the ratio of the actual rate of reaction to the rate that would have resulted for the reaction if no diffusion-limitation was present, can be significantly below 0.1. This would correspond to less than 10% of the zeolite actually being used for the catalytic reaction simply because mass transport to and from the active sites is hindered. Thus, several strategies have been pursued to increase the accessibility of the active sites in zeolite catalysts, and various aspects of these efforts have been reviewed and highlighted during the last years.[21–32]

Here, we review the possibilities for preparing mesoporous zeolites by templating approaches. Such mesoporous zeolites contain, in addition to the crystallographic micropore system characteristic of zeolites, also an independent mesopore system, i.e., a pore system with pore diameters in the range of 2−50 nm.[1] In all known cases today, the mesopore system in mesoporous zeolites can be considered a noncrystallographic pore system because the sizes and shapes of the mesopores are not related in any way to the crystal structure of the zeolite, and because the orientation of the individual pores is typically random. Certainly, this pore system is not ordered at the atomic level. Therefore, mesoporous zeolites can be considered hierarchical porous materials,[26] meaning they exhibit at least two types of pore systems that have sizes in distinctly different ranges, i.e., in the micropore range and the mesopore range. Such materials can be prepared by a range of different templated and nontemplated methods, as

outlined below. Generally, the templating approaches makes it possible a priori to tailor the pore size of the mesopores by use of a mesopore template with a characteristic size, which after removal leaves behind mesopores with essentially the same size and shape as that of the mesopore template. Fundamentally, templating approaches to mesoporous zeolites are interesting as they turn out to define state-of-the-art in the design of hierarchical porous materials and thus they provide a benchmark for new materials and a constant source of inspiration for the development of new and improved methodologies. Obviously, it is possible that templating approaches to mesoporous zeolites could be important in supplying improved zeolite catalysts in a range of existing catalytic processes, but they could also facilitate an extension of the current scope of industrial zeolite catalysis to include completely new reactions. Moreover, mesoporous zeolites with their improved mass-transport properties could also find applications in separations, specifically when transient phenomena are of key importance, i.e., in non-steady-state systems such as hydrocarbon traps in automotive emission systems or in certain pressure-swing adsorption technologies.

Mesoporosity in Zeolites

During the past decade, significant efforts have been devoted to developing methods that introduce mesoporosity in zeolite materials by different approaches. In practice, the resulting mesoporous zeolite materials can be categorized into three distinctly different types of materials. Figure 1 shows schematic illustrations of these different types of materials that can be termed hierarchical zeolite crystals, nanosized zeolite crystals, and supported zeolite crystals, respectively, and it shows typical pore size distributions for the various materials. The first category of materials, the hierarchical zeolite crystals, includes ordinary zeolite crystals having additional porosity present in each individual zeolite crystal. Depending on their size, these additional pores are either mesopores (diameter below 50 nm) or macropores (diameter above 50 nm).[1] Accordingly, the hierarchical zeolite crystals could be further categorized as either mesoporous or macroporous zeolite crystals, but in the present context, this distinction is somewhat arbitrary and will not be used to strictly differentiate between materials except that our focus will be on the mesoporous zeolite crystals. Thus, the mesoporous zeolite crystals feature the typical crystallographic micropores characteristic of the given zeolite structure and an additional intracrystalline mesopore system. Finally, yet another pore system will exist as a consequence of the packing of the zeolite crystals in the material. This pore system is an intercrystalline pore system. The pore sizes and geometries of these pores are determined by the size, shape, and packing of the zeolite crystals in the material, which can obviously be packed more or less loosely. Typically, these intercrystalline pores are relatively large macropores because zeolite crystals normally have dimensions in the micrometer-range, and we will not discuss them in any detail. However, in some cases when the hierarchical zeolite crystals are very small (average crystal size below about 50 nm), it should be noted that they can contribute significantly to the observed mesoporosity.
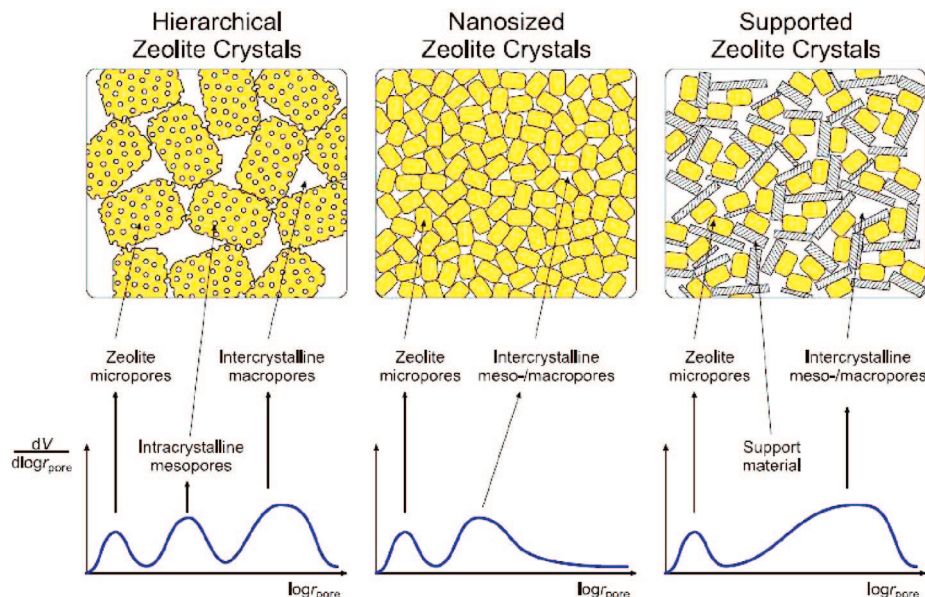
Figure 1. Categorization of hierarchical zeolite materials into hierarchical zeolite crystals, nanosized zeolite crystals, and supported zeolite crystals. The origin of the different types of pores in the materials is illustrated schematically.

The second category of materials, the nanosized zeolite crystals, includes ordinary zeolite crystals with typical crystal sizes below 100 nm, which is much smaller than what is usually seen for zeolites. Clearly, the nanosized zeolite crystals feature the conventional, intracrystalline, and crystallographically well-defined micropore system characteristic of zeolites. Moreover, it has an intercrystalline mesopore system, which results from the packing of the nanosized zeolite crystals in the material. This intercrystalline mesopore system is obviously analogous to the intercrystalline macropore system described above for the mesoporous zeolite crystals. However, because of the typically smaller sizes of the nanosized zeolite crystals compared to the hierarchical zeolite crystals, the resulting pores are also typically smaller. Thus, for the nanosized zeolite crystals, controlling the mesopore size and mesopore shape translates into controlling the size, shape, and packing of the nanosized zeolite crystals.

The third category of materials, the supported zeolite crystals, is characterized by the zeolite crystals being dispersed or supported in the pore system of another material. Thus, contrary to the mesoporous zeolite crystals and the nanosized zeolite crystals, the supported zeolite crystals are not a purely zeolitic material but instead a composite material, and the mesopores results mainly from the presence of the nonzeolitic material. Accordingly, supported zeolite crystals will feature an intracrystalline micropore system that is solely attributed to the zeolite crystals in the material. The pore sizes of the mesopores are largely determined by the support material, which can be a very disordered material such as a typical catalyst–support like amorphous silica, but it can also be a highly ordered material like a mesoporous molecular sieve. Thus, in principle, the mesopores could be categorized as either intercrystalline or intracrystalline mesopores depending on the nature of the support material. Moreover, it would be possible for the pore system to have micropores or macropores; for the present categorization, this is not important. Clearly, the presence of the zeolite crystals

on the support material will alter the pore size of the material relative to that of the pure support. Here, the relative sizes of the zeolite crystals and the primary particles comprising the support material are of key importance for the pore size distribution; the packing of the material will clearly also be a key parameter in defining the porosity.

The vast majority of mesoporous (hierarchical) zeolite materials reported so far can be easily categorized as one of the three types of materials outlined above. However, it is clear that mesoporous zeolite materials that are simple combinations of materials from the different categories can also be envisaged, such as hierarchical nanosized zeolite crystals or supported hierarchical zeolites, and some of these materials are in fact already known. Nevertheless, the three categories seem to represent a useful way to distinguish between various mesoporous zeolite materials, and most importantly, the origin of the mesoporosity in the three different categories is fundamentally different, which makes the categorization easy to apply in practice. However, even though the origin of mesoporosity in the materials is fundamentally different, it is interesting to note that some of the preparative methods available to synthesize these mesoporous zeolite materials can in fact be tuned to produce different types of materials in the categorization. Figure 2 illustrates the templating methods available to produce hierarchical zeolites and emphasizes that some of these methods can in fact be used to produce different types of hierarchical zeolite materials. Thus, Figure 2 categorizes the templating methods available for producing hierarchical zeolites and provides a link between the methods and the materials.

Here, the preparative methods available for synthesizing hierarchical zeolites are termed: solid templating, supramolecular templating, and indirect templating. In addition, a number of nontemplated methods are available that yield mesoporous zeolite materials. In the solid templating method, the zeolite is grown in the presence of a solid material, which
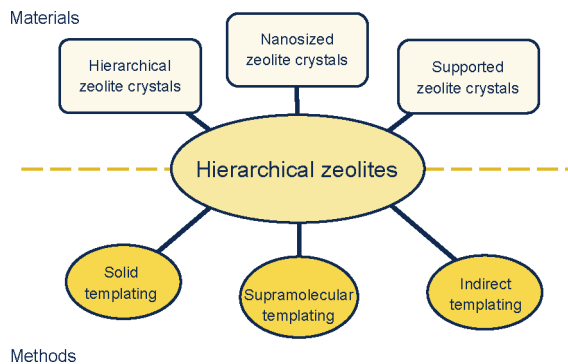
Reviews

Chem. Mater., Vol. 20, No. 3, 2008 949

Figure 2. Categorization of templating methods available to synthesize hierarchical zeolite materials.

Figure 3. Confined space synthesis of nanosized zeolite crystals inside a porous support resulting in supported zeolite crystals. The underlying idea is that the zeolite crystals will not grow larger than the pores, and the support will disperse the zeolite crystals. Some supports may be removed by proper chemical treatments, making it possible to isolate the nanosized zeolite crystals.

is eventually removed to generate porosity, and therefore,the solid acts as a pore template. Typically, the solid template is removed by combustion but in principle it might also be removed by dissolution or sublimation. In the supramolecular templating method, a supramolecular assembly of surfactants is used as the mesopore template. After crystallization, the template can typically be removed by combustion or extraction whereby porosity is generated. In the indirect templating method, a templated mesoporous nonzeolitic material is first formed,and in a separate step, the mesoporous nonzeolitic material is more or less completely transformed into the mesoporous zeolite, or the zeolite is deposited onto the templated mesoporous material. Thus, the templating effect is considered to be indirect, becausemplate is not present when the zeolite crystallizes. However, the resulting mesoporous zeolite material can still maintain some of the order or structure of the original template if only a limited reorganization of solid material occurs during zeolite crystallization or processing, for example, as in a pseudomorphic transformation. Thus, the approach can still be termed templating, albeit the templating is indirect. Thus, the present categorization emphasizes the nature of the interface between the zeolite crystal and the mesopore exactly when the mesopore forms. In solid templating, the zeolite crystal is in intimate contact with the solid material that is being removed to produce the mesoporosity. Similarly, in supramolecular templating, the zeolite crystal is in direct contact with the supramolecular assembly of organized surfactants that is removed to generate the pores. On the other hand, in the indirect templating method, the interface is between the zeolite crystal and solvent molecules, or possibly a gas phase.

Finally, there are a range of nontemplated methods that yield hierarchical zeolite materials. Here, the most prominent methods, such as dealumination,[21,22] desilication,[23] and detitanation[25] (jointly termed demetalation), are briefly introduced to enable a comparison of the templated and the most important nontemplated methods, but it is outside the scope of the present review to include all nontemplated methods available to prepare mesoporous zeolites.

Previously, the templating of solid, high-surface-area inorganic materials has been categorized as either endotemplating or exotemplating.[29] In that categorization, the solid templating method is clearly an example of exotemplating because the materials forms inside a rigid porous solid.

Contrary to this, the supramolecular templating is a perfect example of endotemplating, where the templating species are occluded in the forming solid.

In the following sections, we will present the preparative methods available for templating mesoporous zeolites and the resulting mesoporous zeolite materials in more detail. We will use the categorization of the preparative methods outlined in Figure 2 to organize the discussion. This should clearly illustrate the significant efforts that have already been devoted to this field and should indicate where new discoveries could be possible or desirable.

Solid Templating

Solid templating is a very versatile method for synthesizing mesoporous materials featuring all three types of porosities shown in Figure 1. As examples, solid templating has been applied to produce macroporous MFI zeolite crystals by applying polystyrene beads[33] or ion-exchange resins[34] as the macropore template and nanosized ZSM-5 crystals by carrying out the crystallization in the confined space of amorphous carbon black and then removing the carbon black by combustion.[35] Also, the third class of hierarchical porous materials, the supported zeolite crystals, are simply available by crystallizing zeolites on, for example, a porous carbon and not removing the carbon afterward, resulting in carbon-supported zeolite crystals.[35]

Templating with Carbon Nanoparticles, Nanofibers, and Nanotubes. Solid templating employing porous carbons as the mesopore template can be tuned to produce mesoporous zeolite crystals, nanosized zeolite crystals, or carbon-supported zeolite crystals. Nanosized crystals are produced when zeolite crystallization takes place in the confined space of a porous carbon with little or no encapsulation of the carbon particles during synthesis. By this approach, it is possible to control the size of the zeolite crystals by proper choice of carbon template, as shown schematically in Figure 3.

Using the confined space synthesis approach in the voids of carbon blacks or carbon aerogels (see next section), a variety of different zeolites including ZSM-5, zeolite β, zeolite X, zeolite A, and zeolite Y with controllable crystal sizes have been reported.[35–38]

Contrary to the nanosized zeolite crystals prepared in the confined space of porous carbons, the so-called mesoporous zeolite single crystals contain a network of mesopores within
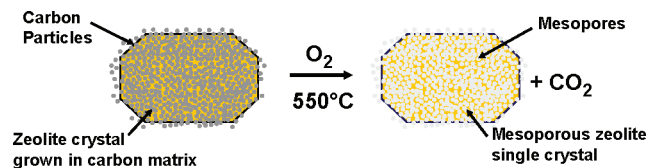
Figure 4. Growth of a zeolite crystal around carbon particles resulting in a zeolite crystal embedded with carbon particles. The carbon particles may subsequently be removed by combustion, yielding a porous spongelike zeolite single crystal.

each individual zeolite crystal.[39] These materials are produced when the porous carbon material is encapsulated by the growing zeolite crystals during synthesis, resulting in zeolite crystals embedded with carbon after zeolite crystallization. Removal of the embedded carbon matrix after synthesis results in porous zeolite single crystals, as shown schematically in Figure 4.

Whether nanosized crystals or mesoporous crystals are obtained by carbon-templating is determined by the experimental factors that influence nucleation rates relative to growth rates.[40] With relatively high nucleation rates, nanosized zeolites are favored, whereas relatively high growth rates favor mesoporous zeolite single crystals. In practice, it is even possible to obtain hybrid materials, nanosized hierarchical zeolite crystals.[40] So far, the carbon-templating methodology has been applied to produce mesoporous zeolite single crystals of MFI,[39,41,42] MEL,[43] MTW,[44] and BEA[41] framework structures as well as hierarchical aluminum phosphates of CHA[45] and AFI[45] framework structures. A thorough study on the application of different carbon templates as well as different synthesis conditions with the goal of finding a low-cost route to ZSM-5 was recently reported by Chou et al.[46] Also, carbon nanotubes have been applied as combustible carbon templates in the synthesis of mesoporous zeolites, resulting in mesoporous zeolite crystals containing relatively straight and uniformly sized mesopore channels that extend throughout the entire crystals.[47,48] The same can be obtained using carbon nanofibers that are much cheaper than nanotubes.[49]

Recent installments in the field of mesoporous single crystals prepared by carbon-templating are the application of microwave heating to facilitate crystal growth[50] and the successful adoption of the fluoride route for conventional zeolite synthesis to work for carbon-templating of mesoporous zeolite single crystals.[45] By the latter method, the synthesis of related aluminum phosphate materials in mesoporous modifications has proved possible.

Carbon Templates Formed Prior to Zeolite Synthesis. Preformed carbon templates made by carbonization of various materials have been applied in the synthesis of mesoporous zeolites. Pinnavaia et al. applied colloidal imprinted carbon (CIC), made by carbonizing at 900 °C pitch imprinted with colloidal silica and etching away the silica by hydrofluoric acid leaching, as a solid template for the synthesis of nanosized ZSM-5 in the confined space of the CIC.[51] By varying the size of the silica colloid used for imprinting the pitch, CICs of different pore size distributions can be obtained. Consequently, nanosized zeolite crystals of different size ranges can be obtained by tuning the CIC

template. Colloidal silica has also very recently been used to template a porous carbon prepared by partial carbonization of sucrose with sulfuric acid and subsequently removing the silica template by hydrofluoric acid leaching.[52] Application of this carbon as a mesopore template resulted in mesoporous silicalite-1 single crystals.

The preparation of carbon–silica composite materials by carbonization of various molecules in the pores of ordered mesoporous materials such as MCM-41 and SBA-15 is a field of its own.[53] These so-called CMK materials have been applied as starting materials for crystallization of zeolites as the carbon template is already intimately admixed with the silica source. Remarkably, this was reported almost simultaneously by three independent research groups.[54–56] Cho et al. described procedures for the preparation of mesoporous zeolite powders, monoliths and films, which involved carbonization of a phenol-formaldehyde resin in the pores of MCM-41, MCM-48, and SBA-15 and the subsequent application of these carbon–silicate mixtures as starting materials for zeolite crystallization.[54] The XRD patterns of the afforded materials revealed the presence of ZSM-5 crystals as well as disordered mesoporous phases, suggesting that the amorphous pore walls of the mesoporous templates are partly transformed into ZSM-5 crystals and encapsulate carbon during the course of the crystallization. After zeolite crystallization, the carbon embedded in the zeolite crystals is removed by combustion, resulting in mesoporous zeolite crystals. The powdered mesoporous zeolite sample as well as the monolith and the film all exhibited high mesopore surface areas and volumes. Yang et al. reported a similar procedure, applying a carbon replica of SBA-15, so-called CMK-3, as the mesopore template.[55] The prepared materials were highly crystalline mesoporous ZSM-5 samples having mesopore surface areas and mesopore volumes up to 382 m^2/g and 0.37 mL/g, respectively. The report by Sakthivel et al. describes the use of CMK-1 and CMK-3 mesoporous carbon molecular sieve replicas of MCM-48 and SBA-15, respectively, as the mesopore templates.[56] CMK-1 or CMK-3 were impregnated with ZSM-5 gel components and subjected to hydrothermal treatment for 1–5 days. This resulted, after calcination, in aluminosilicate replicas of the mesoporous carbon templates, denoted RMM-1 and RMM-3, featuring the characteristic cubic and hexagonal low-index reflections in the XRD patterns. No ZSM-5 reflections were observed in the XRD patterns of the materials subjected to hydrothermal treatment for 3 days or less; however, FTIR revealed the presence of zeolite secondary structural building units by featuring a broad absorption at ca. 540 cm^{-1}. Thus, RMM-1 and RMM-3 appears in fact to be composite materials consisting of mesoporous MCM-48-type and SBA-15-type with nanosized zeolite structural units embedded in the pore walls. Reports on the transformation of CMK-3 into ZSM-5 by vapor-phase transport of the structure-directing agent can also be found.[57,58] Recently, Fang and Hu reported the use of CMK-5, another carbon replica of SBA-15, to produce an ordered mesoporous aluminosilicate material with zeolite crystals embedded in the pore walls, as revealed by the XRD pattern.[56] The material, denoted as OMZ-1 by the

Reviews

Chem. Mater., Vol. 20, No. 3, 2008   951

authors, had a mesopore surface area and mesopore volume of 389 m^2/g and 0.50 mL/g, respectively.

Very recently, two different approaches involving the preparation and application of porous carbons prepared by carbonizing sucrose were reported.[60,61] The first report applied hydrothermal treatment of a sucrose−ammonia mixture followed by carbonization of the mixture at 850 °C.[60] The afforded porous carbon was the impregnated with silicalite-1 synthesis gel mixture and subjected to hydro-thermal treatment to allow for the zeolite phase to crystallize. The zeolite material resulting after combustion of the carbon consisted of homogeneously sized mesoporous silicalite-1 single crystals. The second report concerned the preparation of a carbon−silica composite material made simply by impregnating a solution of sucrose onto silica gel and carbonizing the material at elevated temperature.[61] The carbon−silica composite was then applied as silica source for the crystallization of mesoporous ZSM-5 single crystals. Also, silica−carbon composites made by carbonization of rice husks have been applied as starting materials for synthesis of mesoporous zeolites.[62]

Use of Aerogel, Polymer, and Resin Templates. The first report on the utilization of carbon aerogels for templating mesoporous zeolites appeared in 2003.[63] Tao et al. prepared a mesoporous ZSM-5 monolith with bimodal pore size distribution comprising very uniformly sized mesopores (average diameter of 11 nm) using a carbonized resorcinol−formaldehyde aerogel, i.e., a carbon aerogel, as the mesopore template. The carbon aerogel was impregnated with ZSM-5 synthesis gel components and subjected to hydrothermal treatment to allow for the crystallization of the zeolite phase. During the course of the crystallization, the zeolite crystals grew in the confined space of the carbon aerogel producing a phase-pure mesoporous ZSM-5 powder consisting of nanosized crystals. The same methodology was also applied for the synthesis of mesoporous NaY, resulting in a highly mesoporous NaY material (mesopore volume 1.37 cm^3/g) consisting of nanosized crystals.[38] Because the porosity of carbon aerogels are quite easy to tune by, for example, varying the molar ratios of the starting materials, resorcinol, and formaldehyde, the porosity of the resultant zeolite materials are also easily tuned. This was demonstrated for mesoporous ZSM-5 samples produced from two different carbon aerogels prepared by carbonization of resorcinol−formaldehyde aerogels.[64] The ZSM-5 sample produced from a carbonized 2:1 RFA had a mesopore volume of 0.98 cm^3/g, whereas a ZSM-5 sample produced from a 1:1 RFA had a mesopore volume of 0.34 cm^3/g.

Also, noncarbonized resorcinol−formaldehyde aerogels have been used to synthesize mesoporous zeolites, exemplified with the synthesis of nanosized zeolite A by crystallization in a resorcinol−formalde aerogel.[65] Thus, although resorcinol-formaldehyde aerogels are not as porous as their carbonized analogues, and therefore result in less mesoporous zeolites, as shown in a comparative study of mesoporous ZSM-5 samples,[66] they offer interesting possibilities for synthesizing other zeolite framework structures in mesoporous form. Another advantage of resorcinol−formaldehyde aerogels is that they are easily produced in monolithic form,

paving the way for monolithic self-supported mesoporous zeolite catalysts. The preparation of macroporous monolithic silicalite-1 foams was reported 2001 by Yoon et al. by growing zeolite crystals on polyurethane foam,[67] and recently, mesoporous monolithic silicalite-1 was prepared from resorcinol−formaldehyde aerogel templates were shown to exhibit high catalytic activity as well as excellent selectivity in the Beckmann rearrangement of cyclohexanone oxime.[68]

Very recently, Xiao et al. reported the use of a cationic polymer as mesopore template for the synthesis of mesoporous zeolite β.[69] The synthesis involved adding the polymer to a zeolite β synthesis gel and crystallization of the mixture under hydrothermal conditions. Subsequent calcination of the product afforded mesoporous zeolite β with a mesopore size distribution of 5–40 nm, which exhibited higher conversion and better selectivity than a conventional zeolite β sample in catalytic alkylation of benzene with 2-propanol. Also, mesoporous ZSM-5 could be prepared using this methodology. Another very recent strategy concerning the use of polymers for templating mesoporosity in zeolites was reported by the group of Pinnavaia.[70] A silane-functionalized polymer was impregnated with ZSM-5 gel components and subjected to hydrothermal treatment. During crystallization of the zeolite phase, the silyl groups were hydrolyzed and attached to the surface of the nucleating zeolite crystals, thereby incorporating the polymer in the zeolite crystal. After calcination of the polymer, mesoporous zeolite crystals are obtained. The main advantage of this templating method is that the intracrystalline mesopores of the resulting crystals are small and homogeneously sized (average pore size 2.0–3.0 nm).

Macrotemplating using polystyrene beads was one of the first types of solid templating of hierarchical zeolites to be reported.[33] Stein et al. impregnated zeolite synthesis gel components onto a close-packed array of polystyrene beads. After crystallization and removal of the latex spheres, a macroporous beehive structure with walls of silicalite-1 was obtained. Similarly, core−shell building blocks consisting of latex-beads coated with zeolites were used to prepare macroporous zeolite monoliths.[71] Using ion-exchange resin beads as the template, researchers obtained mesoporous silicalite-1 microspheres by crystallization of a silicalite-1 synthesis gel adsorbed onto anionic ion-exchange resin beads.[34] The calcined silicalite-1 microspheres exhibited a typical type IV N$_2$ physisorption isotherm and contained mesopores centered at 40 nm. Also hierarchical palladium-containing zeolite β[72] and vanadium-containing AlPO-5[73] have been reported by resin-macrotemplating.

Use of Solid Biological Templates. Another interesting approach for the preparation of hierarchical zeolites is by use of biological templates, which offer a wide range of different material shapes. So far, a few examples of using solid biological templates have appeared to illustrate the possibilities for controlling the morphology of zeolite materials. They represent an attractive alternative compared to the standard templates such as polymers, carbons, or other synthetic templates, because many biological templates are abundant and often relatively inexpensive. Mann et al.[74] demonstrated how organized bacterial superstructures can

be used as 3D templates for the fabrication of ordered inorganic–organic fibrous composites.[74,75] They prepared MCM-41 silica-based fibers containing hierarchically organized pore structures at the meso- and microscopic length scales.[74] Bacterial templates were also applied to create hierarchically structured zeolite fibers containing ordered pores at the meso- and microscopic length scales.[76] The stable aqueous dispersion of preformed zeolite nanoparticles as building blocks for the infiltration of a bacterial supercellular thread was used by reversible swelling. Macroscopic bacterial threads were produced from cell cultures of mutant FJ7 strain of *Bacillus subtilis*. The final zeolite fibers showed a high surface area and a unidirectional patterned architecture. Along the same lines, hierarchical MFI zeolites were prepared through templating with wood cells giving materials with controlled micro-, meso-, and macropores that are clearly replicas of the original biological template.[77] Moreover, the leaves and stems of *Equisetum arvense*, a plant rich in amorphous silica, has been used to produce hierarchical MFI and BEA structures with order at all three levels.[78–80]

Finally, starch gels have also been used a solid template to fabricate zeolite materials with a hierarchical micro-, meso-, macropore organization.[81] The macroporous monoliths consisting of a continuous mesoporous framework of microporous silicalite were prepared by incorporating 50 nm sized zeolite nanoparticles into freshly prepared viscous starch gels, followed by air-drying and calcination. Macropores with sizes between 0.5 and 50 μm were created by varying the amount of starch and the starch/silicalite weight ratio. Mesoporous thin films of microporous silicalite, 2–15 μm in thickness, were also prepared by using gels containing low concentrations of starch (about 2 wt %).

Supramolecular Templating

In the supramolecular templating method, an organized assembly of surfactant molecules is used as the template for creating intercrystalline or intracrystalline meso-/macropores in a zeolite material. Thus, in all supramolecular templating approaches to mesoporous zeolites, the zeolite crystal is in direct contact with the supramolecular template when it is starts being removed from the zeolite material to generate the porosity.

Direct Crystallization of Zeolites in the Presence of Supramolecular Templates. Soon after the discovery of the mesoporous molecular sieves,[82,83] Beck et al. more systematically explored the use of alkyltrimethylammonium surfactants to serve as structure-directing agents, or templates, for the formation of microporous or mesoporous molecular sieve frameworks[84] to elucidate which factors favor molecular and supramolecular templating. An early attempt to prepare a mesoporous aluminosilicate material that possessed microporosity and acidity analogous to zeolites via dual templating, i.e., using both molecular and supramolecular templates, in a one-step synthesis was reported by Karlsson et al.[85] This approach is based on the idea that the molecular templates could direct zeolite crystallization in the mesopore walls while the mesoporous structure was simultaneously formed according to the supramolecular templating mechanism of the surfactant micelles. The group investigated

whether simultaneously supramolecular aggregation and molecular templating by using mixtures of alkyltrimethylammonium surfactants with different chain lengths could be was achieved. However, it turned out that the two templating systems worked in a competitive, rather than cooperative, manner, resulting in the formation of bulk zeolite without any mesoporosity, amorphous mesoporous material, or their physical mixtures.

Lamellar surfactant-directed silicate mesophases with molecularly ordered inorganic frameworks were prepared by Chmelka et al. Prior to hydrothermal treatment at 135 °C, these materials possessed lamellar mesostructural order with amorphous silica frameworks. However, hydrothermal treatment/calcination of these thin fragile materials at temperatures >140 °C, resulted in decomposition of the surfactant, leading to subsequent degradation of the framework order and therefore loss of mesoporosity.[86,87] Thus, it is not straightforward to obtain crystalline zeolites containing both micro- and mesoporous structures in a single phase if the aluminosilicate gel is directly crystallized in the presence of both ordinary organic mesopore-directing surfactants and molecular templates for the zeolite. However, Ryoo et al. elegantly circumvented this difficulty by developing a direct synthesis route to mesoporous zeolites with easily tuned, uniform mesopores using amphiphilic organosilanes, $[(CH_3O)SiC_3H_6N(CH_3)_2C_nH_{2n+1}]Cl$, as supramolecular templates.[88] Designed in this manner, the surfactants are not expelled from the aluminosilicate sphere during the zeolite crystallization process, making it possible for the surfactants to transform the zeolite crystal growth into a mesoporous structure. In a typical synthesis, the amphiphilic organosilane is added to the initial synthesis composition of MFI zeolite containing the tetrapropylammonium ion as a structure-directing agent for the MFI zeolite. An equivalent synthesis principle was applied to the synthesis of mesoporous LTA zeolite crystals.[88] The mesopore diameters of the mesoporous MFI zeolite crystals could be systematically varied by changing the chain length of the organosilane and/or the hydrothermal synthesis temperature. For $n = 12, 16$, and 18, pore diameters of 2.1, 3.1, and 3.9 nm, respectively were obtained, but a mesopore diameter up to 20 nm could be obtained under proper synthesis conditions. The mesoporous MFI zeolite crystals exhibited superior catalytic activity and selectivity in the jasminaldehyde and vesidryl synthesis reactions compared to a purely microporous MFI zeolite and Al-MCM-41. In addition, these hierarchical zeolite crystals have also shown a remarkably high resistance to deactivation in some catalytic applications.[89] Ryoo et al. later extended the synthesis strategy, using organosilane surfactants as a supramolecular template, to also comprise aluminophosphate compositions.[90] The resulting aluminophosphates exhibited mesoporous structures and in the proposed synthesis mechanism, the organic tail of the surfactant directs the mesoporous structure while the silica moiety is incorporated in the resultant aluminophosphate frameworks (see Figure 5).

Surfactant-Mediated Assembly of Zeolite Seeds into Mesoporous Structures. After the discovery of mesoporous MCM-41 molecular sieves,[91] it was found that the incorporation of aluminum into the framework introduced mild acidic

Reviews

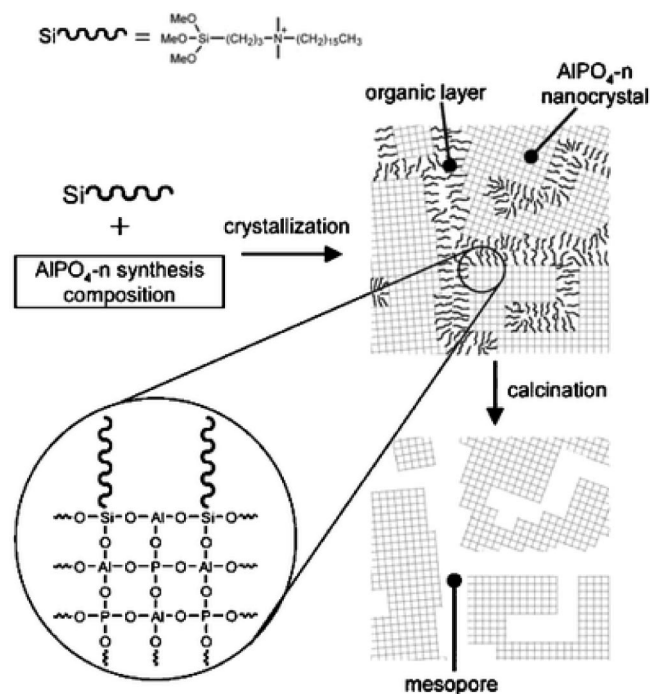Chem. Mater., Vol. 20, No. 3, 2008   953

Figure 5. Proposed synthesis mechanism for hierarchical aluminophosphate crystals (HP-ALPO-*n*) prepared by supramolecular templating. Reprinted with permission from ref 90. Copyright 2006 Royal Society of Chemistry.

functionality. However, it can also lead to a loss of structural integrity in the mesoporous aluminosilicate materials because of the amorphous nature of their frameworks and relatively thin walls.[92–94] Metal-supported MCM-41 catalysts have yielded promising results in reactions such as hydrocracking, hydrodesulfurization, and hydrodenitrogenation because of their high surface areas and regular pore dimensions.[95–98] But the lower thermal, hydrothermal, and mechanical stability and the low acidity of M41S materials seems to limit their practical catalytic applications.[8] Because these parameters are critically important for the potential applications of mesoporous molecular sieves in catalysis, significant efforts have been made to solve this problem. Thus, many different synthesis procedures were designed to improve the acidity and hydrothermal stability of ordered mesoporous materials.[21] Recently, important advances have been made in improving the structural integrity of Al-MCM-41 through direct assembly[99] and postsynthesis modification methods.[100–103] However, one of the most promising strategies for improving the structural order, hydrothermal stability, and acidity of mesoporous aluminosilicates was suggested by Pinnavaia et al. The approach is based on the surfactant-directed assembly of the nanosized aluminosilicate precursors that normally nucleate the formation of conventional microporous zeolites. These protozeolitic nanoclusters, also known as zeolite seeds, are supposed to promote zeolite nucleation by admitting AlO_4 and SiO_4 connectivities that resemble the secondary structural units in crystalline zeolites.[104] Usually, they are particles 10−50 nm in size that can be synthesized simply by reducing the synthesis time normally required for the preparation of micrometer-sized zeolite crystals.[105] The nanosized zeolite seeds were used as building blocks, which were directly assembled into hexagonal, cubic, wormhole, and foamlike

framework structures using supramolecular templating.[106] This method has been applied for the controlled assembly of steam-stable aluminosilicate mesostructures from zeolite FAU, MFI, and BEA seeds.[105,107–110] For the preparation of these templated mesostructures, a variety of different assembly conditions were applied.[111] Particularly, it was shown that the obtained MSU (Michigan State University) mesoporous materials with FAU zeolite seeds have a unique hydrothermal stability[105] that is attributed to the assembly of the Na^+-nucleated zeolite seeds under hydrothermal conditions in the presence of cetyltrimethylammonium ions. This afforded hexagonal MSU-S mesostructures with Si:Al ratios in the range of 1.6:1 to 10:1. The replacement of Na^+ by NH_4^+ ions in the as-made materials followed by calcination yielded exceptionally acidic and steam-stable mesostructures. However, the resulting materials were found to contain some occluded carbon, which is formed during the calcination process. This occluded carbon also contributes to the structural stability, which was illustrated by the observation that calcined samples with lower carbon contents exhibited a larger loss in surface area and pore volume upon steaming. Therefore, the steam-stability at 800 °C was in part a consequence of the exceptional acidity of a framework that resulted in the formation of structure-stabilizing carbon by partial template decomposition, and not entirely the result of a stable aluminosilicate framework.[107]

The same method was also applied for the preparation of mesostructures with MFI and BEA zeolitic seeds, which were formed using the typical molecular organic structure directing agents, such as tetrapropylammonium (TPA^+) and tetraethylammonium (TEA^+) ions, respectively.[106,112] The resulting mesoporous, Al-MSU-S with MFI zeolite seeds (Al-MSU-S_{MFI}) and Al-MSU-S with BEA zeolite seeds (Al-MSU-S_{BEA}) are remarkably steam-stable even in the absence of occluded carbon.[106] Additionally, it was shown that increasing the steaming temperature up to 800 °C does not lead to destruction of the long-range hexagonal order of the MSU-S aluminosilicate mesostructures and that substantial mesoporosity was maintained whereas the mesoporosity of MCM-41 was completely lost by the same treatment.[100] MSU materials containing LTZ seeds have also been prepared,[113] and the idea of using zeolite seeds as precursors to assemble hydrothermally stable and strongly acidic large pore mesoporous materials has been extended more recently to include SBA-15 under acidic assembly conditions.[114] Similarly, it has been shown that by using essentially the same synthesis strategy, a one-step synthesis of a highly stable mesoporous molecular sieve, MMS-H, with a structure analogous to MCM-48 but also containing zeolite secondary building units, could be obtained.[115–118] The MMS-H material was synthesized by first preparing a micellar solution of the surfactants cetyltrimethylammonium bromide and 1,3-diacetoxy-1,1,3,3-tetrabutyltin oxide polyethylene glucol dodecyl ether (Brij 30). Then the zeolite secondary building units and mesoporous phase were formed in situ by adding tetrapropylammonium hydroxide followed by crystallization. Adsorption/desorption curves of calcined MMS-H samples exhibited typical type IV isotherms with a broad hysteresis loop characteristic of capillary condensation in mesoporous

channels. These new materials possess uniform mesopores with a bimodal pore size distribution and pore sizes of 2.3–2.6 and 3.6–3.7 nm, respectively. Typical BET surface areas of about 1000 m^2/g and wall thicknesses of about 1.6 nm are observed, which is somewhat larger than that of conventional MCM-48 materials having a wall thickness of typically 0.8–1.2 nm. The hydrothermal stability of the MMS-H material was also examined, and it showed a superior stability compared to a physical mixture of mesoporous Al-MCM-48 molecular sieve and microporous ZSM-5 zeolite.

Related families of materials are the cocalled MAS/MTS materials[119–125] and mesoporous TUD-1 containing zeolite nanocrystals.[126] MAS and MTS materials are mesoporous aluminosilicates or titanosilicates formed by assembly of zeolite nanoclusters. To date, several types of MAS and MTS materials have been prepared using this methodology. Seeds of zeolite β have been utilized for the assembly of MAS-5[119] and MAS-7[120] using CTAB and Pluronic P123 to guide the assembly processes, respectively. Pluronic P123 have also been used to assemble MAS-9[121] and MTS-9[120,122] from MFI-structured ZSM-5-type and TS-1-type seeds. MAS-3 and MAS-8 have been assembled from zeolite L-type seeds and Pluronic P123 in alkaline and acidic solution, respectively.[123] Using CTAB, researchers have assembled MTS-5 and MTS-8 from TS-1-type seeds in alkaline and acidic solution, respectively.[124] Similarly, it is also possible to prepare ordered micro/mesoporous composite materials containing zeolite nanocrystals as thin films by spin-coating solutions containing zeolite seeds and solutions containing silica/surfactants, simultaneously.[127,128]

Surfactant-Mediated Coating of Zeolite Crystals with Mesoporous Materials. In 1996, it was reported by van Bekkum et al. that zeolite Y crystals can be coated with a thin layer of a mesoporous MCM-41-type material.[129] The coating procedure involved impregnating FAU crystals with CTA-Cl and subjecting the material to MCM-41 synthesis conditions. This resulted in FAU crystals overgrown with 5–20 nm thick layers of MCM-41 structured materials. The prepared material exhibited higher conversion of heavy molecules in vacuum gas oil cracking than USY. Recently, a MOR/MCM-41 was reported by a similar procedure.[130] However, in a comparative study of the catalytic performance in palm oil cracking of MCM-41/β materials prepared using this methodology with an MCM-41/β material prepared by the seed-assembly methodology described above, it was shown that the material prepared by seed-assembly exhibited higher conversion as well as higher selectivity toward liquid gasoline.[131]

Delamination of Layered Zeolite Structures. For some zeolite materials, it is possible to rationally design nanosized zeolite crystals by an approach called delamination.[132–134] It has been found by Corma et al. that zeolites with layered precursors, such as MCM-22 or ferrierite, can be synthesized as lamellar precursors with a surfactant intercalated between two neighboring zeolite layers.[135–138] Thus, by completely swelling the layered zeolite precursor, the individual zeolite layers are separated or exfoliated while the structure of the layers is preserved. Upon removal of the surfactant swelling
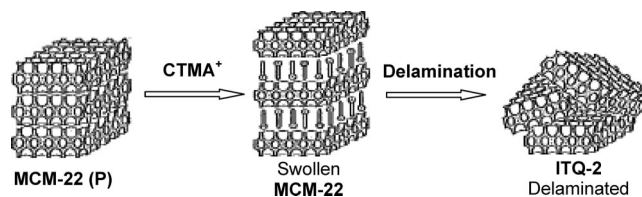

Figure 6. Scheme for the preparation of delaminated material ITQ-2 from a lamellar zeolite precursor (MCM-22 (P)). Adapted from ref 134.

agent, the intercalated structure collapses to form a material composed of zeolite sheets that are packed together in such a way that that essentially all active sites are directly accessible from the external surface as illustrated in Figure 6.[136]

Thus, the delaminated or exfoliated zeolites are sheetlike structures that are nanosized in one direction and significantly larger in the other two directions. Accordingly, they often show significant mesoporosity. By adding suitable inorganic guest molecules functioning as pillars, control of the interlayer distance can also be achieved. These materials possess a high thermal/hydrothermal stability and acidity, which is characteristic for zeolite materials and the accessibility of the acid sites was found to be significantly improved even for larger organic molecules.[135] Accordingly, delaminated zeolites exhibited improved properties in a wide range of catalytic applications.[139–143] The main role of the surfactant is to separate the individual zeolite layers by swelling the layered precursor, and in the swollen material, the interlayer distance is clearly determined by the surfactant. During removal of the surfactant, the layered zeolite structure must necessarily collapse unless pillars are present; therefore, there is only limited control over the resulting pore size. However, it is clear that the porosity of the sheetlike structure somehow reflects the use of the delaminating agent.

Use of Microemulsions and Reverse Micelles to Prepare Nanosized Zeolite Crystals. Another example of supramolecular templating of mesoporous zeolites is the use of zeolite crystallization in microemulsions or reverse micelles. Microemulsions or reverse micelles can successfully function as nanoreactors for the zeolite growth[144] in a completely analogous way to the voids in porous carbon materials in the confined space synthesis method (Figure 3). Thus, in the presence of microemulsions or reverse micelles, zeolite crystals can form only with a size smaller than that of the individual microemulsion droplets and that provides a convenient approach to controlling the crystal size and thereby to some extent the pore size. Reverse micelles prepared from a surfactant in an oil–water mixture were originally used to attempt to control the crystallization of a microporous zinc phosphate.[145] Later, Lin and Yates[146] used microemulsions to control the size of silicalite-1. In their work, the microemulsions were prepared by mixing the synthesis gel, an aqueous phase, an oil phase, toluene cetyltrimethylammonium bromide, and *n*-butanol. Zeolite crystals obtained from the microemulsions were found to exhibit relatively narrow size distributions. Similarly, Lee and Shantz also used microemulsions for zeolite synthesis and used the method to form platelet aggregates and spheres of silicalite-1,[147] but apparently with limited control of the

Reviews

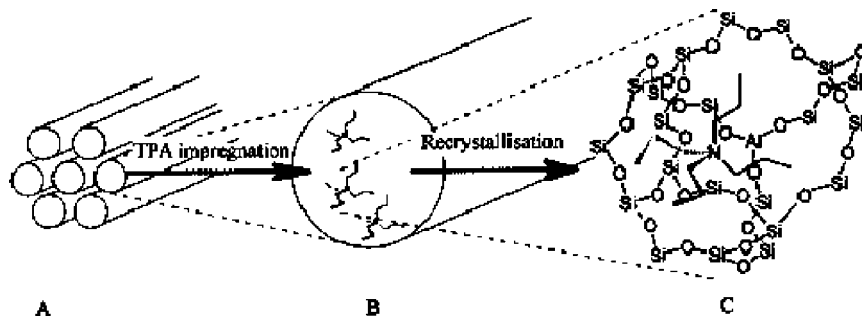*Chem. Mater., Vol. 20, No. 3, 2008* 955

Figure 7. Schematic representation of the pore wall crystallization approach. An ordered mesoporous material is impregnated with a zeolite structure-directing agent and subjected to hydrothermal crystallization conditions resulting in partial crystallization of the mesoporous silica to zeolite structural units. Reprinted with permission from ref 148. Copyright 2001 American Chemical Society.

porosity. They used a microemulsion of heptane, surfactant, butanol, and the synthesis gel. Just as is the case for the delamination method, it is not completely clear to what extent the surfactant used in the microemulsion and reverse micelle techniques controls or influences the pore size in the resulting hierarchical zeolite material.

Indirect Templating

In the categorization of methods and materials in Figure 2, hierarchical zeolite materials formed by an ordered transformation of another templated mesoporous material into a hierarchical zeolite or by a controlled deposition of a zeolite onto a templated material are also considered to be templated, albeit indirectly. There are only a few different preparative approaches belonging to the category, the majority of which related to partial (secondary) zeolite crystallization of ordered mesoporous materials.

Partial Crystallization of Preformed Mesoporous Materials. Zeolite materials with hierarchical porosity can be produced by crystallization of mesoporous molecular sieves such as MCM-41 in the presence of appropriate molecular zeolite structure-directing agents. In our categorization of materials, they can be considered supported zeolite crystals when a partial crystallization leads to nanosized zeolite crystals supported on (or incorporated into) an amorphous mesoporous matrix. The generalized process is shown schematically in Figure 7, and it comprises the following two steps:

(i) assembly of an (amorphous) mesoporous phase by templating;

(ii) partial (secondary) crystallization of the amorphous material to a zeolite phase.

The "reverse" process, i.e., surfactant-mediated assembly of preformed zeolite seeds into mesoporous zeolite materials, was dealt with in the previous section. In its prototypical form, i.e., in the absence of templates to support the mesoporous material during zeolite crystallization, the indirect templating approach requires delicate optimization of synthesis conditions because zeolite crystallization conditions are generally quite severe (strong base and high temperatures). As will be shown, several measures are usually taken to ensure mesoporosity in the resulting zeolite composite material. Typically, they include

(i) applying less severe zeolite crystallization conditions and/or more stable, i.e., thicker-walled, starting materials;

(ii) retarding the disintegration of the mesoporous phase by adding supporting surfactants during the (secondary) zeolite crystallization step;

(iii) filling the mesoporous phase with carbon affording, a so-called CMK material, and applying this for the zeolite synthesis (in such a case the templating method is considered to be solid templating as discussed above).

The synthetic approach of partially crystallizing ordered mesoporous silicates was conceptually introduced in 1997 by Jansen et al., who showed that hexagonally ordered mesoporous silica ion-exchanged with tetrapropyl ammonium (TPA) cations can be partially crystallized in glycerol to afford mesoporous materials containing very small protozeolitic, or embryonic ZSM-5, tectosilicate structures within the pore walls, as evidenced by an absorption at ca. 550 cm^{-1} in the FTIR spectrum.[149]

The approach was further developed with the successful crystallization of true zeolite structural units (visible by XRD) in the pore walls of mesoporous silicates. This was achieved by Huang et al. who reported a procedure for the preparation of MCM-41 containing small ZSM-5 crystals in the pore walls.[150] First, a zeolite synthesis gel containing the surfactant cetyltrimethylammonium bromide in addition to the zeolite synthesis gel components (water glass, sodium aluminate, and TPA-Br) was allowed to self-assemble into a hexagonally ordered mesoporous silica by heating the gel to 100 °C at pH 11 for 2 days. Subsequently, the afforded MCM-41 material containing TPA cations was heated to 125 °C at pH 9.5 for a period of 1–12 days. The latter treatment resulted in the partial transformation of the MCM-41 material into small ZSM-5 crystals. With a crystallization time of 2 days, a disordered hexagonal mesoporous silicate containing small ZSM-5 crystals was obtained; however, even more prolonged crystallization times caused the hexagonal mesoporous structure to become increasingly disordered and eventually transform into a lamellar structure that was not stable under calcination. At about the same time as Huang et al. reported synthesis of ZSM-5/MCM-41 composites, van Bekkum et al. reported that crystallization of ZSM-5 from MCM-41 impregnated with TPA at 170 °C for only 1 h caused the mesoporous framework to collapse along with the appearance of small ZSM-5 peaks in the XRD pattern.[148] However, if the crystallization step is carried out in the presence of the surfactant hexadecylamine, the collapse of the mesoporous silicate can be retarded, resulting in a material containing
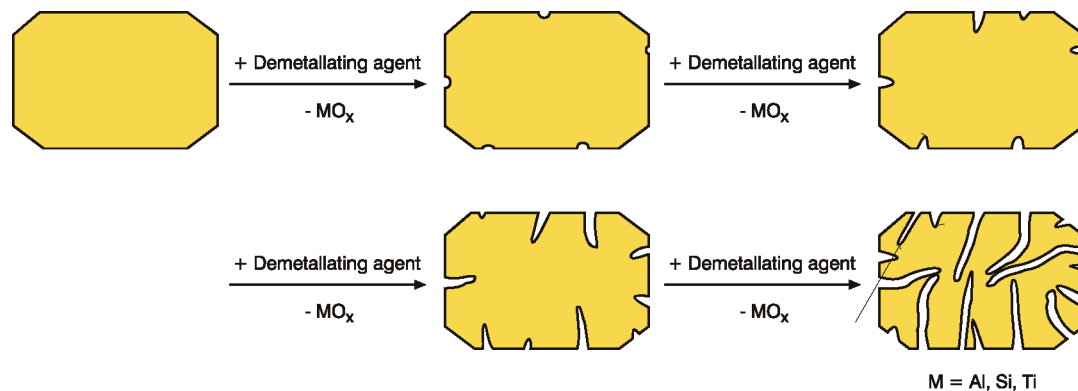
Figure 8. Nontemplated demetalation of zeolites to generate mesoporous zeolite crystals.

small zeolite crystals while retaining some degree of mesoporosity. Nonetheless, hydrothermal treatment for 2 h caused the mesoporous silicate to collapse even in the presence of the supporting surfactant.

A related class of materials was reported by Trong On and Kaliaguine in 2001.[151,152] These SBA-15/MFI composite materials, the so-called UL-ZSM-5[151] and UL-TS-1,[152] were synthesized using larger-pore SBA-15 as the starting material instead of smaller-pore MCM-41. By applying thick-walled mesoporous materials and carrying out the zeolite crystallization step at comparatively low temperatures (120 or 130 °C), they were able to produce materials exhibiting large mesopore volumes (1.25–1.83 cm^3/g) and high degrees of zeolite crystallinity (up to 42% after 5 days of hydrothermal treatment) at the same time.[151] The materials were synthesized by impregnation of TPA-OH onto calcined SBA-15 with the desired elemental composition and subsequent hydrothermal treatment. For the synthesis of UL-ZSM-5, hydrothermal treatment was carried out at 130 °C for a period of 1–5 days, resulting in an increasingly crystalline product with ZSM-5 structure retaining some of the mesoporosity of the starting material. The synthesis of UL-TS-1 from a titanium-containing SBA-15 starting material was also reported by the same authors.[152]

A mesoporous composite material containing ZSM-5 very similar to those described above was reported by Hidrobo et al.[153] A mesoporous aluminosilicate prepared by hydrothermal treatment of an aluminosilicate gel also containing the biopolymer chitosan as mesopore template was impregnated with TPA-OH and crystallized at 160 °C for 3 days. After calcination, a mesoporous material containing ZSM-5 crystals was obtained.

Deposition of Zeolite Seeds onto Templated Mesoporous Materials. Composite materials comprising zeolites dispersed onto mesoporous materials have been produced by impregnating preformed large-pore mesoporous materials such as SBA-15[154] or mesostructured cellular foams (MCFs)[155] with zeolite seeds and subsequently subjecting the seeded materials to hydrothermal treatment conditions. Starting from SBA-15, the procedure resulted in a highly mesoporous SBA-15/ZSM-5 composite material with very uniform mesopore size distribution centered at 5.4 nm.[154] A similar procedure starting from siliceous MCF allowed for the preparation of mesoporous ZSM-5 and NaY materials, however, with much larger mesopores (15.5–17.5 nm diam-

eter).[155] Also, very small beta seeds supported on MCM-41 were prepared by impregnation using a colloidal beta seed solution.[156]

Zeolitization of Diatomaceous Earth. Also silica-rich diatomaceous earth has been applied for the synthesis of mesoporous zeolites. The synthesis involves attaching zeolite seeds to the surface of diatoms and crystallizing the diatom-supported seeds into zeolite crystals retaining the basic morphology of the diatom.[157–160] Because diatoms are very rich in silica, they are used as a source of silicon at the same time. Thus, the majority of the silicon in the zeolite comes from the diatoms rather than from the zeolite synthesis gel mixture. As a multitude of diatom species are known, the application of these can be envisaged to provide excellent possibilities for tailoring hierarchical porosity in zeolites.

Nontemplated Approaches to Mesoporous Zeolites

In addition to the templating methods used to prepare mesoporous zeolites that are discussed extensively above, it should be noted that several nontemplated approaches also exist. It is outside the scope of the present review to discuss these in detail but it is interesting to note that nontemplated routes to all the three categories of hierarchical zeolite materials defined in Figure 1 have been reported. For the preparation of hierarchical zeolite crystals, the demetalation approach seems to be the only viable nontemplated route to produce additional intracrystalline porosity in zeolite crystals. Generally, the demetalation method involves the synthesis of a conventional, purely microporous zeolite, which is then treated chemically to preferentially extract one of the constituent metallic elements of the zeolite. The most well-studied demetalation methods are dealumination and desilication and recent reviews gives excellent accounts of state-of-the art for these methods.[21–23] Recently, detitanation was also reported as a means to introduce intracrystalline mesoporosity in titanosilicate materials,[161–163] which could indicate that the full scope of the demetalation approaches has not yet been fully explored. Figure 8 illustrates the basic principle of the demetalation approach.

It is clear that mesopores result from demetalation only if the dissolution process proceeds in a quite special way that clearly cannot involve complete dissolution of the zeolite crystals at the same rate from all faces of the parent crystal. Moreover, it is seen that the obtained mesoporosity depends

Reviews

Chem. Mater., Vol. 20, No. 3, 2008 957

directly on the amount of dissolved material, and that there is a priori no way to directly control the pore size. Typically, the conditions required to partly dissolve zeolite crystals are quite harsh because zeolites are typically quite stable materials. Thus, the dissolution process usually involves strong acids or bases, or strongly complexing agents.[21–23,161] The selective extraction process leads to removal of some of the metallic or semimetallic components of the zeolite, typically in the form of soluble oxoanions, but it can also be in the form of complexed species. Originally, the dealumination method has attracted most attention because the importance of this method in producing ultrastable zeolite Y crystals for industrial used in catalytic cracking.[22] However, the selective extraction of silicon from zeolite crystals has been known for a long time,[164–169] but recently a series of systematic studies of this approach by Groen, Mouljin, Perez-Ramirez, and co-workers[170–173] has provided detailed insight into the synthesis factors that control the porosity and into the properties of these materials, especially the improved diffusion[173] and the enhanced catalytic properties in some applications.[174]

For the preparation of nanosized zeolite crystals, several nontemplated methods have been reported and these methods were recently carefully reviewed.[175] Typically, these methods involve synthesis of the zeolite nanocrystals from clear solutions and gels under experimental conditions that are controlled to favor nucleation over crystal growth. Even though it is often possible to rationalize why a given synthesis scheme leads to nanosized zeolites, there appear to be few versatile methods that allow the use of a certain preparative protocol to yield a wide range of different mesoporous zeolites. Rather, it appears that special synthesis schemes have to be developed for each desired zeolite material.

Finally, it is also possible to produce supported zeolite crystals by many different nontemplated routes. Actually, most industrial zeolite catalysts are indeed supported zeolite crystals produced simply because pure zeolites cannot easily be shaped into tablets or extrudates of sufficient mechanical strength for industrial applications or because the zeolite itself is too active to be useful in the pure form for the desired catalytic application. The industrial supported zeolite crystal catalysts are normally produced by extrusion of a zeolite-support composite paste obtained by careful mixing of the constituents, possibly with inclusion of various additives or by spray-drying an appropriately prepared slurry of the zeolite and the support(s) and any required binders. Thus, there are numerous examples in the catalytic literature of supported zeolite crystals acting as heterogeneous catalysts in a very wide range of reactions.[2,3]

Concluding Remarks

During the past decade, hierarchical zeolites materials and methods for their preparation have attracted continually increasing attention. Much of this attention can be attributed to the fundamental interest in developing preparative methods that allow careful tailoring of the properties of solid materials but also to the technical interest in developing heterogeneous zeolite catalysts with improved accessibility of the active sites located inside the micropores. Today, numerous pre-

parative approaches have been reported to yield different hierarchical zeolite materials featuring intracrystalline micropores and intracrystalline or intercrystalline meso-/macropores. Here, we have tried to categorize both the hierarchical zeolite materials and the methods available for their synthesis and give a detailed overview of the available literature described templating approaches to hierarchical zeolites, and to mesoporous zeolites in particular. In our categorization, we distinguish between three distinctly different types of hierarchical zeolite materials, the hierarchical zeolite crystals, the nanosized crystals, and the supported zeolite crystals. For the templating approaches available to synthesize hierarchical zeolites, we categorize these methods as solid templating, supramolecular templating, and indirect templating. Hopefully, this terminology can be useful in the future development of the field. From the detailed discussion of the materials and the methods given above, it should be clear that it is simple to use the present scheme to categorize the vast majority of the currently published materials and templating approaches. However, it is also clear that in some cases, it is not straightforward to directly establish to which category a given hierarchical zeolite material belongs. However, this typically arises when there is only limited characterization of the material, so that it is not possible to determine whether the material is adequately described as hierarchical zeolite crystals or nanosized zeolite crystals or supported zeolite crystals. Often efficient discrimination between the three categories of hierarchical zeolite materials cannot be done solely on the basis of measured pore size distributions and X-ray diffraction studies of the materials but typically also requires careful electron microscopy studies. Thus, in future characterization studies of new hierarchical zeolite materials, the present categorization can be used as a tool to help select the techniques that will provide the information required to give a detailed description of the structure of the material, and the reasons for its hierarchical porosity. It is noted that hierarchical zeolite materials that are actually hybrids between, or physical mixtures of, the prototypical materials in the categorization can easily be envisaged. This could be hierarchical nanosized zeolite crystals or supported nanosized zeolite crystals, both of which are in fact already known, but also hierarchical supported zeolites could be easily prepared.

Whereas the categorization of the materials is usually straightforward provided that sufficiently detailed characterization is available, it is often more difficult to correctly categorize the templating method into one of the three types. For solid templating and supramolecular templating, the challenge is clearly not to establish whether, for example, a solid or a supramolecular assembly of surfactants is present during zeolite synthesis. Rather, it can be quite difficult to firmly establish to what extent the solid or the supramolecular assembly of surfactants actually acts as template and thereby directly controls the size and shape of the meso-/macropores in the resulting hierarchical zeolite material. This challenge is even more pronounced for the indirect templating method, because here the original template is no longer present when the hierarchical zeolite material is formed. However, if the hierarchical zeolite is formed in, for example, a pseudomor-

phic transformation of another templated mesoporous material, the resulting material can still be considered to be templated, albeit indirectly. Similarly, zeolite nanocrystals or seeds deposited carefully onto the pore walls of a templated mesoporous material can be considered a templated hierarchical zeolite material even though the template is not present during the deposition. However, in practice, it turns out that by the indirect templating method, some disorder is typically introduced when, for example, the pore walls of mesoporous molecular sieves or diatoms are crystallized into zeolites, and this clearly makes it difficult to establish in which cases the term templating is properly used. However, the problem of introducing some disorder during synthesis is not unique for the indirect templating method because often some disorder is also introduced when a solid or a supramolecular template is removed. This disorder can be either a structural collapse as in the case of the delamination or it can be a partial amorphization of the zeolite crystal. Again, this is not a problem for the present categorization of templating methods but it pinpoints the necessity to carefully characterize the synthesized hierarchical zeolite materials to clearly identify the role of the template and fully understand to what extent it controls the resulting pore size distribution. It is noted that it is not only for fundamental reasons that it is desirable to clearly understand and control the factors that determine the pore structure of hierarchical zeolites. When these materials are used as heterogeneous catalysts, it is typically desirable to maximize the accessibility of the active sites to fully utilize the catalytic potential of the material and at the same time to minimize the volume of void space in the material since this leads to a lower catalytic activity on a volume basis, which is often the industrially important parameter. Thus, the optimal porosity is often a compromise between accessibility and the volumetric density of active site, and this compromise can be quite different from reaction to reaction, and even for the same reaction it can vary significantly from one set of reaction conditions to another. Recently, it has been convincingly demonstrated using different probe molecules that both templated and nontemplated hierarchical zeolites do, as expected, exhibit significantly faster diffusion than conventional zeolites featuring only micropores.[50,173,176] Thus, it seems reasonable to attribute the improved performance of hierarchical zeolite catalysts observed in numerous cases to the improved mass-transport properties. Some examples of this are given in the discussion above. However, so far, mesoporous zeolite crystals prepared by solid templating with carbon nanoparticles have been the most extensive studied examples of templated zeolite catalysts, and significantly improved performance has been observed in a number of acid-catalyzed hydrocarbon reactions,[176–180] but also in important environmental technologies[181,182] and in some selective oxidations.[43,183] Similarly, there are also several examples that nanosized zeolite crystals prepared by supramolecular templating of zeolite seeds yields, for example, improved hydrocarbon conversion catalysts[123,184–186] and recently, remarkable catalytic activities were reported for mesoporous zeolite crystals synthesized by supramolecular templating.[88,89] The fact that improved catalytic performances are also observed

in several examples using hierarchical zeolite catalysts prepared by nontemplated methods[179] supports the notion that the enhanced activity and/or selectivity can be attributed to the presence of a hierarchical structure with increased accessibility of the active sites. Thus, it appears likely that in the coming years, hierarchical zeolite materials will continue to attract increasing attention. This will undoubtedly lead to an even more detailed insight into the materials and templating methods described here, but hopefully also to completely new discoveries. Furthermore, the use of mesoporous zeolites as catalysts is also expected to gain importance in the coming years and it will be interesting to see if the possibilities for templating mesoporous zeolites will lead to significantly improved or maybe even completely new heterogeneous catalysts.

References

(1) Sing, K. S. W.; Everett, D. H.; Haul, R. A. W.; Moscou, L.; Pierotti, R. A.; Rouquérol, J.; Siemieniewska, T. *Pure Appl. Chem.* **1985**, *57*, 603.
(2) Cejka, J.; van Bekkum, H., Eds. *Zeolites and Ordered Mesoporous Materials: Progress and Prospects*; Studies in Surface Science and Catalysis 157C; Elsevier: Amsterdam, 2005.
(3) van Steen, E.; Claeys, M.; Callanan, L. H., Eds. *Recent Advances in the Science and Technology of Zeolites and Related Materials*; Studies in Surface Science and Catalysis 154B; Elsevier: Amsterdam, 2005.
(4) Kesraouiouki, S.; Cheeseman, C. R.; Perry, R. *J. Chem. Technol. Biotechnol.* **1994**, *59*, 121.
(5) Bailey, S. E.; Olin, T. J.; Bricka, R. M.; Adrian, D. D. *Water Res.* **1999**, *33*, 2469.
(6) Chen, N. Y.; Degnan, T. F. *Chem. Eng. Prog.* **1988**, *84*, 32.
(7) Corma, A. *Chem. Rev.* **1995**, *95*, 559.
(8) Corma, A. *Chem. Rev.* **1997**, *97*, 2373.
(9) Davis, M. E. *Nature* **2002**, *417*, 813.
(10) Stein, A. *Adv. Mater.* **2003**, *15*, 763.
(11) Tsapatsis, M. *AIChE J.* **2002**, *48*, 654.
(12) Zhang, X. H.; Li, W. Z.; Xu, H. Y. *Prog. Chem.* **2004**, *16*, 728.
(13) Xu, X. W.; Wang, J.; Long, Y. C. *Sensors* **2006**, *6*, 1751.
(14) Cundy, C. S.; Cox, P. A. *Chem. Rev* **2003**, *103*, 663.
(15) Cundy, C. S.; Cox, P. A. *Microporous Mesoporous Mater.* **2005**, *82*, 1.
(16) Hunger, M. *Microporous Mesoporous Mater.* **2005**, *82*, 241.
(17) Keil, F. J.; Krishna, R.; Coppens, M. O. *Rev. Chem. Eng.* **2000**, *16*, 71.
(18) McLeary, E. E.; Jansen, J. C.; Kapteijn, F. *Microporous Mesoporous Mater.* **2006**, *90*, 198.
(19) Miyamoto, A.; Kobayashi, Y.; Elanany, M.; Tsuboi, H.; Koyama, M.; Endou, A.; Takaba, H.; Kubo, M.; Del Carpio, C. A.; Selvam, P. *Microporous Mesoporous Mater.* **2007**, *101*, 324.
(20) Weitkamp, J., Ernst, S., Puppe, L. In *Catalysis and Zeolites*; Weitkamp, J., Puppe, L., Eds.; Springer: New York, 1999; p 327.
(21) Tao, Y.; Kanoh, H.; Abrams, L.; Kaneko, K. *Chem. Rev.* **2006**, *106*, 896.
(22) van Donk, S.; Janssen, A. H.; Bitter, J. H.; de Jong, K. P. *Catal. Rev.* **2003**, *45*, 297.
(23) Groen, J. C.; Moulijn, J. A.; Perez-Ramirez, J. *J. Mater. Chem.* **2006**, *16*, 2121.
(24) Groen, J. C.; Peffer, L. A. A.; Moulijn, J. A.; Perez-Ramirez, J. *Chem.—Eur. J.* **2005**, *11*, 4983.
(25) Cejka, J.; Mintova, S. *Catal. Rev.—Sci. Eng.*, **2007**, in press.
(26) Hartmann, M. *Angew. Chem., Int. Ed.* **2004**, *43*, 5880.
(27) Drews, T. O.; Tsapatsis, M. *Curr. Opin. Colloid Interface Sci.* **2005**, *10*, 233.
(28) Tosheva, L.; Valtchev, V. P *C. R. Chim.* **2005**, *8*, 475.
(29) Schüth, F. *Annu. Rev. Mater. Res.* **2005**, *35*, 209.
(30) Schüth, F. *Angew. Chem., Int. Ed.* **2003**, *42*, 3604.
(31) Meynen, M.; Cool, P.; Vansant, E. F. *Microporous Mesoporous Mater.* **2007**, *104*, 26.
(32) Kirchhock, C. E. A.; Kremer, S. P. B.; Vermant, J.; van Tendeloo, G.; Jacobs, P. A.; Martens, J. A. *Chem.—Eur. J.* **2005**, *11*, 4306.
(33) Holland, B. T.; Abrams, L.; Stein, A. *J. Am. Chem. Soc.* **1999**, *121*, 4308.
(34) Tosheva, L.; Valtchev, V.; Sterte, J. *Microporous Mesoporous Mater.* **2000**, *35–36*, 621.
(35) Madsen, C.; Jacobsen, C. J. H. *Chem. Commun.* **1999**, 673.
(36) Schmidt, I.; Madsen, C.; Jacobsen, C. J. H. *Inorg. Chem.* **2000**, *39*, 2279.
(37) Jacobsen, C. J. H.; Madsen, C.; Janssens, T. V. W.; Jakobsen, H. J.; Skibsted, J. *Microporous Mesoporous Mater.* **2000**, *39*, 393.
(38) Tao, Y.; Kanoh, H.; Kaneko, K. *J. Phys. Chem. B* **2003**, *107*, 10974.

Reviews

Chem. Mater., Vol. 20, No. 3, 2008 959

(39) Jacobsen, C. J. H.; Madsen, C.; Houzvicka, J.; Schmidt, I.; Carlsson, A. *J. Am. Chem. Soc.* **2000**, *122*, 7116.

(40) Jacobsen, C. J. H.; Houzvicka, J.; Carlsson, A.; Schmidt, A. *Stud. Surf. Sci. Catal.* **2001**, *135*, 167.

(41) Pavlackova, Z.; Kosova, G.; Zilkova, N.; Zukal, A.; Cejka, J. *Stud. Surf. Sci. Catal.* **2006**, *162*, 905.

(42) Kustova, M. Y.; Kustov, A. L.; Christensen, C. H. *Stud. Surf. Sci. Catal.* **2005**, *158*, 255.

(43) Kustova, M. Yu.; Hasselriis. ; Christensen, C. H *Catal. Lett.* **2004**, *96*, 205.

(44) Wei, X.; Smirniotis, P. G. *Microporous Mesoporous Mater.* **2006**, *89*, 170.

(45) Egeblad, K.; Kustova, M.; Klitgaard, S. K.; Zhu, K.; Christensen, C. H. *Microporous Mesoporous Mater.* **2007**, *101*, 214.

(46) Chou, Y. H.; Cundy, C. S.; Garforth, A. A.; Zholobenko, V. L. *Microporous Mesoporous Mater.* **2006**, *89*, 78.

(47) Schmidt, I.; Boisen, A.; Gustavsson, E.; Ståhl, K.; Pehrson, S.; Dahl, S.; Carlsson, A.; Jacobsen, C. J. H. *Chem. Mater.* **2001**, *13*, 4416.

(48) Boisen, A.; Schmidt, I.; Carlsson, A.; Dahl, S.; Brorson, M.; Jacobsen, C. J. H. *Chem. Commun.* **2003**, 958.

(49) Janssen, A. H.; Schmidt, I.; Jacobsen, C. J. H.; Koster, A. J.; de Jong, K. P. *Microporous Mesoporous Mater.* **2003**, *65*, 59.

(50) Kustova, M.; Egeblad, K.; Christensen, C. H.; Kustov, A. L.; Christensen, C. H. *Stud. Surf. Sci. Catal.* **2007**, in press.

(51) Kim, S.-S.; Shah, J.; Pinnavaia, T. J. *Chem. Mater.* **2003**, *15*, 1664.

(52) Li, H.; Sakamoto, Y.; Liu, Z.; Ohsuna, T.; Terasaki, O.; Thommes, M.; Che, S. *Microporous Mesoporous Mater.* **2007**, doi: 10.1016/j.micromeso.2007.02.054.

(53) Ryoo, R.; Joo, S. H.; Jun, S. *J. Phys. Chem. B* **1999**, *103*, 7743.

(54) Cho, S. I.; Choi, S. D.; Kim, J.-H.; Kim, G.-J. *Adv. Funct. Mater.* **2004**, *14*, 49.

(55) Yang, Z.; Xia, Y.; Mokya, R. *Adv. Mater.* **2004**, *16*, 727.

(56) Sakhtivel, A.; Huang, S.-J.; Chen, W.-H.; Lan, Z.-H.; Chen, K.-H.; Kim, T.-W.; Ryoo, R.; Chiang, A. S. T.; Liu, S.-B. *Chem. Mater.* **2004**, *16*, 3168.

(57) Zhang, Y.; Okubo, T.; Ogura, M. *Chem. Commun.* **2005**, 2719.

(58) Ogura, M.; Zhang, Y.; Elangovan, S. P.; Okubo, T. *Microporous Mesoporous Mater.* **2007**, *101*, 224.

(59) Chu, X.-Z.; Zhou, Y.-P.; Zhang, Y.-Z.; Su, W.; Sun, Y.; Zhou, L. *J. Phys. Chem. B* **2006**, *110*, 2596.

(60) Zhu, K.; Egeblad, K.; Christensen, C. H. *Eur. J. Inorg. Chem.* **2007**, doi: 10.1002/ejic.200700218.

(61) Kustova, M.; Egeblad, K.; Zhu, K.; Christensen, C. H. *Chem. Mater.* **2007**, *19*, 2915.

(62) Katsuki, H.; Furuta, S.; Watari, T.; Komarneni, S. *Microporous Mesoporous Mater.* **2005**, *86*, 145.

(63) Tao, Y.; Kanoh, H.; Kaneko, K. *J. Am. Chem. Soc.* **2003**, *125*, 6044.

(64) Tao, Y.; Kanoh, H.; Hanzawa, Y.; Kaneko, K. *Colloids Surf., A* **2004**, *241*, 75.

(65) Tao, Y.; Kanoh, H.; Kaneko, K. *Langmuir* **2005**, *21*, 504.

(66) Tao, Y.; Hattori, Y.; Matumoto, A.; Kanoh, H.; Kaneko, K. *J. Phys. Chem. B* **2005**, *109*, 194.

(67) Lee, Y.-J.; Lee, J. S.; Park, Y. S.; Yoon, K. B. *Adv. Mater.* **2001**, *13*, 1259.

(68) Li, W.-C.; Palkovits, R.; Schmidt, W.; Spliethoff, B.; Schüth, F. *J. Am. Chem. Soc.* **2005**, *127*, 12595.

(69) Xiao, F.-S.; Wang, L.; Yin, C.; Lin, K.; Di, Y.; Li, J.; Xu, R.; Su, D. S.; Schlögl, R.; Yokoi, T.; Tatsumi, T. *Angew. Chem., Int. Ed.* **2006**, *45*, 3090.

(70) Wang, H.; Pinnavaia, T. J. *Angew. Chem., Int. Ed.* **2006**, *45*, 7603.

(71) Rhodes, K. H.; Davis, S. A.; Caruso, F.; Zhang, B.; Mann, S. *Chem. Mater.* **2000**, *12*, 2832.

(72) Naydenov, V.; Tosheva, L.; Sterte, J. *Chem. Mater.* **2002**, *14*, 4881.

(73) Naydenov, V.; Tosheva, L.; Sterte, J. *Microporous Mesoporous Mater.* **2003**, *66*, 321.

(74) Davis, S. A.; Burkett, S. L.; Mendelson, N. H.; Mann, S. *Nature* **1997**, *385*, 420.

(75) Davis, S. A.; Patel, H. M.; Mayes, E. L.; Mendelson, N. H.; Franco, G.; Mann, S. *Chem. Mater.* **1998**, *10*, 2516.

(76) Zhang, B.; Davis, S. A.; Mendelson, N. H.; Mann, S. *Chem. Commun.* **2000**, 781.

(77) Dong, A.; Wang, Y.; Tang, Y.; Ren, N.; Zhang, Y.; Yue, Y.; Gao, Z. *Adv. Mater.* **2002**, *14*, 926.

(78) Valtchev, V.; Smaihi, M.; Faust, A.-C.; Vidal, L. *Angew. Chem., Int. Ed.* **2003**, *42*, 2782.

(79) Valtchev, V.; Smaihi, M.; Faust, A.-C.; Vidal, L. *Chem. Mater.* **2004**, *16*, 1350.

(80) Valtchev, V.; Smaihi, M.; Faust, A.-C.; Vidal, L. *Stud. Surf. Sci. Catal.* **2005**, *154A*, 588.

(81) Zhang, B.; Davis, S. A.; Mann, S. *Chem. Mater.* **2002**, *14*, 1369.

(82) Kresge, C. T.; Leonowicz, M. E.; Roth, W. J.; Vartuli, J. C.; Beck, J. S. *Nature* **1992**, *359*, 710–712.

(83) Yanagisawa, T.; Shimizu, T.; Kuroda, K.; Kato, C. *Bull. Chem. Soc. Jpn.* **1990**, *63*, 988.

(84) Beck, J. S.; Vartuli, J. C.; Kennedy, G. J.; Kresge, C. T.; Roth, W. J.; Schramm, S. E. *Chem. Mater.* **1994**, *6*, 1816.

(85) Karlsson, A.; Stöcker, M.; Schmidt, R. *Microporous Mesoporous Mater.* **1999**, *27*, 181.

(86) Christiansen, S. C.; Zhao, D.; Janicke, M. T.; Landry, C. C.; Stucky, G. D.; Chmelka, B. F. *J. Am. Chem. Soc.* **2001**, *123*, 4519.

(87) Hedin, N.; Graf, R.; Christiansen, S. C.; Gervais, C.; Hayward, R. C.; Eckert, J.; Chmelka, B. F. *J. Am. Chem. Soc.* **2004**, *126*, 9425.

(88) Choi, M.; Cho, H. S.; Srivastava, R.; Venkatesan, C.; Choi, D.; Ryoo, R. *Nat. Mater.* **2006**, *5*, 718.

(89) Srivastava, R.; Choi, M.; Ryoo, R. *Chem. Commun.* **2006**, *43*, 4489.

(90) Choi, M.; Srivastava, R.; Ryoo, R. *Chem. Commun.* **2006**, *42*, 4380.

(91) Beck, J. S.; Vartuli, J. C.; Roth, W. J.; Leonowicz, M. E.; Kresge, C. T.; Schmitt, K. D.; Chu, C. T. W.; Olson, D. H.; Sheppard; McCullen, S. B.; Higgins, J. B.; Schlenker, J. L. *J. Am. Chem. Soc.* **1992**, *114*, 10834.

(92) Chen, C. Y.; Li, H. X.; Davis, M. E. *Microporous Mater.* **1993**, *2*, 17.

(93) Borade, R. B.; Clearfield, A. *Catal. Lett.* **1995**, *31*, 267.

(94) Luan, Z. H.; Cheng, C. F.; He, H. Y.; Klinowski, J. *J. Phys. Chem.* **1995**, *99*, 10590.

(95) Corma, A.; Martinez, A.; Martinez Soria, V.; Monton, J. B. *J. Catal.* **1995**, *153*, 25.

(96) Landau, M. V.; Vradman, L.; Herskowitz, M.; Koltypin, Y.; Gedanken, A. *J. Catal.* **2001**, *201*, 22.

(97) Klimova, T.; Calderon, M.; Ramirez, J. *Stud. Surf. Sci. Catal.* **2001**, *135*, 4280.

(98) Shanthi, K.; Sasi Rekha, N. R.; Moheswari, R.; Sivakumar, T. *Stud. Surf. Sci. Catal.* **2001**, *135*, 4296.

(99) Janicke, M. T.; Landry, C. C.; Chistiansen, S. C.; Brirtalan, S. B.; Stucky, G. D.; Chmelka, B. F. *Chem. Mater.* **1999**, *11*, 1342.

(100) Hamdan, H.; Endud, S.; He, H.; Mohd Muhid, M. N.; Klinowski, J. *J. Chem. Soc., Faraday Trans.* **1996**, *92*, 2311.

(101) Mokaya, R.; Jones, W. *Chem. Commun.* **1997**, 2185.

(102) Ryoo, R.; Jun, S.; Kim, J. M.; Kim, M. J *Chem. Commun.* **1997**, 2225.

(103) Ryoo, R.; Ko, C. H.; Howe, R. F. *Chem. Mater.* **1998**, *9*, 1607.

(104) Lobo, R. F.; Zones, S. I.; Davis, M. E. *J. Inclusion Phenom.* **1995**, *21*, 47.

(105) Liu, Y.; Zhang, W.; Pinnavaia, T. J. *J. Am. Chem. Soc.* **2000**, *122*, 8791.

(106) Liu, Y.; Pinnavaia, T. J. *J. Mater. Chem.* **2002**, *12*, 3179.

(107) Liu, Y.; Zhang, W.; Pinnavaia, T. J. *Angew. Chem., Int. Ed.* **2001**, *40*, 1255.

(108) Agundez, J.; Diaz, I.; Marquez-Alvarez, C.; Perez-Pariente, J.; Sastre, E. *Chem. Commun.* **2003**, *150*.

(109) Prokesova, P.; Mintova, S.; Cejka, J.; Bein, T. *Mater. Sci. Eng., C* **2003**, *23*, 1001.

(110) Guo, W.; Xiong, C.; Xua, Z.; Huang, L.; Li, Q. *J. Mater. Chem.* **2001**, *11*, 1886.

(111) Liu, Y.; Pinnavaia, T. J. *J. Mater. Chem.* **2004**, *14*, 1099.

(112) Bagshaw, S. A.; Baxter, N. I.; Drew, D. R. M.; Hosie, C. F.; Yuntong, N.; Jaenicke, S.; Khuan, C. G. *J. Mater. Chem.* **2006**, *16*, 2235.

(113) Bagshaw, S. A.; Jaenicke, S.; Khuan, C. G. *Catal. Commun.* **2003**, *4*, 140.

(114) Liu, Y.; Pinnavaia, T. J. *Chem. Mater.* **2002**, *14*, 3.

(115) Sakthivel, A.; Huang, S.; Chen, W.; Lan, Z.; Chen, K.; Lin, H.; Mou, C.; Liu, S. *Adv. Funct. Mater.* **2005**, *15*, 253.

(116) Prokesova, P.; Mintova, S.; Cejka, J.; Bein, T. *Microporous Mesoporous Mater.* **2003**, *64*, 165.

(117) Xia, Y.; Mokaya, R. *J. Mater. Chem.* **2004**, *14*, 863.

(118) Xia, Y.; Mokaya, R. *J. Mater. Chem.* **2004**, *14*, 3427.

(119) Zhang, Z.; Han, Y.; Zhu, L.; Wang, R.; Yu, Y.; Qiu, S.; Zhao, D.; Xiao, F. S. *Angew. Chem., Int. Ed.* **2001**, *40*, 1258.

(120) Han, Y.; Xiao, F.-S.; Wu, S.; Sun, Y.; Meng, X.; Li, D.; Lin, S.; Deng, F.; Ai, X. *J. Phys. Chem. B* **2001**, *105*, 7953.

(121) Han, Y.; Wu, S.; Sun, Y.; Li, D.; Xiao, F. S.; Liu, J.; Zhang, X. *Chem. Mater.* **2002**, *14*, 1144.

(122) Xiao, F.-S.; Han, Y.; Xu, Y.; Meng, X.; Yang, M.; Wu, S. *J. Am. Chem. Soc.* **2002**, *124*, 888.

(123) Di, Y.; Yu, Y.; Sun, Y.; Yang, X.; Lin, S.; Zhang, M.; Li, S.; Xiao, F.-S. *Microporous Mesoporous Mater.* **2003**, *62*, 221.

(124) Lin, K.; Sun, Z.; Lin, S.; Jiang, D.; Xiao, F.-S. *Microporous Mesoporous Mater.* **2004**, *72*, 193.

(125) Sun, Y.; Han, Y.; Yuan, L.; Ma, S.; Jiang, D.; Xiao, F. S. *J. Phys. Chem. B* **2003**, *107*, 1853.

(126) Waller, P.; Shan, Z.; Marchese, L.; Tartaglione, G.; Zhou, W.; Jansen, J. C.; Maschmeyer, T. *Chem.—Eur. J.* **2004**, *10*, 4970.

(127) Petkov, N.; Mintova, S.; Jean, B.; Metzger, T. H.; Bein, T. *Chem. Mater.* **2003**, *15*, 2240.

(128) Petkov, N.; Hölzl, M.; Metzger, T. H.; Mintova, S.; Bein, T. *J. Phys. Chem. B* **2005**, *109*, 4485.

(129) Kloetstra, K. R.; Zandbergen, H. W.; Jansen, J. C.; van Bekkum, H. V. *Microporous Mesoporous Mater.* **1996**, *6*, 287.

(130) Wang, S.; Dou, T.; Li, Y.; Zhang, Y.; Li, X.; Yan, Z. *Catal. Commun.* **2005**, *6*, 87.

(131) Ooi, Y.-S.; Zakaria, R.; Mohamed, A. R.; Bhatia, S. *Appl. Catal., A* **2004**, *274*, 15.

(132) Corma, A.; Fornes, V.; Pergher, S. B.; Maesen, Th. L.; Buglass; J, G. *Nature* **1998**, *396*, 353.

(133) Corma, A.; Fornes, V.; Rey, F. *Adv. Mater.* **2002**, *14*, 71.

(134) Cejka, J. *Stud. Surf. Sci. Catal.* **2005**, *157*, 111.

(135) Corma, A.; Fornes, V.; Guil, J. M.; Pergher, S.; Maesen, Th. L.; Buglass, J. G. *Microporous Mesoporous Mater.* **2000**, *38*, 301.

(136) Corma, A.; Fornes, V.; Martinez-Triguero, J.; Pergher, S. B. *J. Catal.* **1999**, *186*, 57.

(137) Corma, A.; Diaz, U.; Domine, M. E.; Fornes, V. *Chem. Commun.* **2000**, 137.
(138) Corma, A.; Diaz, U.; Domine, M. E.; Fornes, V. *Angew. Chem., Int. Ed.* **2000**, *39*, 1499.
(139) Gomez, M. V.; Cantin, A.; Corma, A.; de la Hoz, A. *J. Mol. Catal. A: Chem.* **2005**, *240*, 16.
(140) Corma, A.; Botella, P.; Mitchell, C. *Chem. Commun.* **2004**, *17*, 2008.
(141) Corma, A.; Martiınez, A.; Martinez-Soriay, V. *J. Catal.* **2001**, *200*, 259.
(142) Climent, M. J.; Corma, A.; Iborra, S. *J. Catal.* **2005**, *233*, 308.
(143) Climent, M. J.; Corma, A.; Velty, A. *Appl. Catal. A: Gen.* **2004**, *263*, 155.
(144) Schacht, S.; Huo, Q.; Voigt-Martin, I. G.; Stucky, G. D.; Schuth, F. *Science* **1996**, *273*, 768.
(145) Dutta, P. K.; Jakupca, M.; Narayana, K. S.; Salvati, L. *Nature* **1995**, *374*, 44.
(146) Lin, J. C.; Yates, M. Z. *Langmuir* **2005**, *21*, 2117.
(147) Lee, S.; Shantz, D. F. *Chem. Mater.* **2005**, *17*, 409.
(148) Verhoef, M. J.; Kooyman, P. J.; van der Waal, J. C.; Rigutto, M. S.; Peters, J. A.; van Bekkum, H. *Chem. Mater.* **2001**, *13*, 683.
(149) Kloetstra, K. R.; van Bekkum, H.; Jansen, J. C. *Chem. Commun.* **1997**, 2281.
(150) Huang, L.; Guo, W.; Deng, P.; Xue, Z.; Li, Q. *J. Phys. Chem. B* **2000**, *104*, 2817.
(151) Trong On, D.; Kaliguine, S. *Angew. Chem., Int. Ed.* **2001**, *40*, 3248.
(152) Trong On, D.; Lutic, D.; Kaliguine, S. *Microporous Mesoporous Mater.* **2001**, *44–45*, 435.
(153) Hidrobo, A.; Retuert, J.; Araya, P.; Wolf, E. *J. Porous Mater.* **2003**, *10*, 231.
(154) Trong On, D.; Kaliaguine, S. *Angew. Chem., Int. Ed.* **2002**, *41*, 1036.
(155) Trong On, D.; Kaliaguine, S. *J. Am. Chem. Soc.* **2003**, *125*, 618.
(156) Mavrodinova, V.; Popova, M.; Valchev, V.; Nickolov, R.; Minchev, Ch. *J. Colloid Interface Sci.* **2005**, *286*, 286.
(157) Anderson, M. W.; Holmes, S. M.; Hanif, N.; Cundy, C. S. *Angew. Chem., Int. Ed.* **2000**, *39*, 2707.
(158) Holmes, S. M.; Plaisted, R. J.; Crow, P.; Foran, P.; Cundy, C. S.; Anderson, M. W. *Stud. Surf. Sci. Catal.* **2001**, *135*, 296.
(159) Wang, Y. J.; Tang, Y.; Wang, X. D.; Dong, A. G.; Shan, W.; Gao, Z. *Chem. Lett.* **2001**, 1118.
(160) Wang, Y.; Tang, Y.; Dong, A.; Wang, X.; Ren, N.; Gao, Z. *J. Mater. Chem.* **2002**, *12*, 1812.
(161) Gao, Y.; Yoshitake, H.; Wu, P.; Tatsumi, T. *Microporous Mesoporous Mater.* **2004**, *70*, 93.
(162) Pavel, C. C.; Schmidt, W. *Chem. Commun.* **2006**, 882.
(163) Pavel, C. C.; Park, S. H.; Dreier, A.; Tesche, B.; Schmidt, W. *Chem. Mater.* **2006**, *18*, 3813.
(164) Chang, C. D.; Chu, C.T.W. U.S. Patent 4594 333, 1986.
(165) Dessau, R. M.; Valyocsik, E. W.; Goeke, N. H. *Zeolites* **1992**, *12*, 776.
(166) Lietz, G.; Schnabel, K. H.; Peuker, C.; Gross, T.; Storek, W.; Völter, J. *J. Catal.* **1994**, *148*, 562.
(167) Garces, J. M.; Millar, D. M. U.S. Patent 6017508, 1998.
(168) Drake, C. A.; Wu, A. H. U.S. Patent 5952259, 1999.
(169) Ogura, M.; Shinomiya, S. Y.; Tateno, J.; Nara, Y.; Kikuchi, E.; Matsukata, H. *Chem. Lett.* **2000**, 82.
(170) Groen, J. C.; Peffer, L. A. A.; Moulijn, J. A.; Perez-Ramirez, J. *Colloids Surf., A* **2004**, *241*, 53.
(171) Groen, J. C.; Jansen, J. C.; Moulijn, J. A.; Perez-Ramirez, J. *J. Phys. Chem. B* **2004**, *108*, 13062.
(172) Groen, J. C.; Peffer, L. A. A.; Moulijn, J. A.; Pérez-Ramírez, J. *Mircopor. Mesopor. Mater.* **2003**, *60*, 1.
(173) Groen, J. C.; Zhu, W.; Brouwer, S.; Huynink, S. J.; Kapteijn, F.; Mouljin, J. A. *J. Am. Chem. Soc.* **2007**, *129*, 355.
(174) Groen, J. C. Mesoporous Zeolites Obtained by Desilication. Ph.D. Thesis, University of Delft, Delft, The Netherlands, 2007; ISBN 978–90–9021–739–0.
(175) Tosheva, L.; Valtchev, V. P. *Chem. Mater.* **2005**, *17*, 2494–170.
(176) Christensen, C. H.; Johannsen, K.; Törnqvist, E.; Schmidt, I.; Topsøe, H.; Christensen, C. H., *Catal. Today* **2007**, doi:10.1016/j.cat-tod.2007.06.082.
(177) Houzvicka, J.; Schmidt, I.; Jacobsen, C. J. H. *Stud. Surf. Sci. Catal.* **2001**, *135*, 158.
(178) Christensen, C. H.; Johannsen, K.; Schmidt, I.; Christensen, C. H. *J. Am. Chem. Soc.* **2003**, *125*, 13370.
(179) Christensen, C. H.; Schmidt, I.; Christensen, C. H. *Catal. Commun.* **2004**, *5*, 543.
(180) Christensen, C. H.; Schmidt, I.; Carlsson, A.; Herbst, K.; Johannesen, K. *J. Am. Chem. Soc.* **2005**, *127*, 8098.
(181) Kustova, M.; Kustov, A.; Rasmussen, S. B.; Christensen, C. H. *Appl. Catal., B* **2006**, *67*, 60.
(182) Kustov, A. L.; Hansen, T. W.; Kustova, M.; Christensen, C. H., *Appl. Catal., B*, accepted **2007**.
(183) Schmidt, I.; Krogh, A.; Wienberg, K.; Carlsson, A.; Brorson, M.; Jacobsen, C. J. H. *Chem. Commun.* **2000**, 2157.
(184) Triantafyllidis, K. S.; Lappas, A. A.; Vasalos, I. A.; Liu, Y.; Wang, H.; Pinnavaia, T. J. *Catal. Today* **2006**, *112*, 33.
(185) Frunz, L.; Prins, R.; Pirngruber, G. D. *Microporous Mesoporous Mater.* **2006**, *88*, 152.
(186) Zhu, L.; Xiao, F. S.; Zhang, T.; Sun, Y. Y.; Han, Y.; Qiu, S. L. *Catal. Today* **2001**, *68*, 209.

15 Mesoporous zeolite crystals

**Kresten Egeblad[1], Christina Hviid Christensen[2], Marina Kustova[1, 2]
and Claus Hviid Christensen[1]**
[1]Center for Sustainable and Green Chemistry, Department of Chemistry, Building 206
Technical University of Denmark, DK-2800 Lyngby, Denmark; [2]Haldor Topsøe A/S
Nymøllevej 55, DK-2800 Lyngby, Denmark

Abstract

   *Much of the success of zeolites as heterogeneous
catalysts can be attributed to the possibilities for
tailoring the intrinsic properties of the zeolite, such as
the number and strength of the acid sites, the redox
properties, the hydrophobicity/hydrophilicity of the
micropores and the pore architecture. In particular,
the availability of a wide range of zeolite structures
with different pore sizes and pore geometries makes it
possible to conduct shape selective catalysis, which
represents one of the most significant triumphs in the
history of zeolite science. However, in many cases it
appears that the sole presence of micropores in zeolite
catalysts can significantly hinder efficient diffusion of
reactants, intermediates and products to and from the
active sites located inside the zeolite crystals. In effect,*

Correspondence/Reprint request: Dr. Claus Hviid Christensen, Center for Sustainable and Green Chemistry, Department of
Chemistry, Building 206, Technical University of Denmark, DK-2800 Lyngby, Denmark

the zeolite catalyst is not optimally utilized in the given catalytic process since the catalytic reaction will occur in a diffusion-limited regime. Thus, several strategies have been pursued to increase the accessibility of the active sites. Recently, the use of so-called hierarchical zeolite catalysts featuring both micropores and mesopores has attracted significant attention. Here, the currently most common and versatile approaches for introducing mesoporosity into zeolite crystals are highlighted and compared. Generally, mesoporosity can be introduced in two conceptually different ways. One method involves the synthesis of a purely microporous zeolite, which is then treated chemically to preferentially extract one of the constituent (semi)metallic elements of the zeolite, here this approach is called demetallation. This can be preferential extraction of aluminum (dealumination), silicon (desilication), or titanium (detitanation). The other method is based on crystallization of the zeolite in the presence of an auxiliary mesopore template that is subsequently removed after the crystallization. Typically, the auxiliary mesopore template is a porous carbon that is removed from the zeolite after crystallization simply by calcination. With the resulting hierarchical zeolite materials, there are several reports on improved diffusion and also of improved catalytic performance. Here, examples of improved acidic, redox and bifunctional catalysts are presented, and some possibilities for achieving both higher activity and selectivity at the same time, and also higher activity and simultaneously a longer catalyst lifetime are discussed to illustrate the fundamental concepts.

1. Introduction

Zeolites are aluminosilicates featuring intracrystalline micropores, and the size and geometry of these micropores are defined entirely by the crystallographic structure of the zeolite. In other words, the micropores appear as the voids between the non-close packed oxygen atoms in the unit cell. Today, more than 170 such different zeolite structure types have been identified and currently several new structures appear each year. Much of the success of zeolites in research laboratories and in industry can be attributed to the presence of these well-defined micropores that are responsible for the molecular sieve effect. Zeolites have structures in which all atoms can be considered to be surface atoms and therefore they exhibit very large specific surface areas. The pore volume of the zeolite micropores is obviously also defined by the structure of the unit cell [1]. To fully appreciate the pore system of a typical zeolite, it is instructive to estimate the total pore length present in e.g., 1 g of zeolite. This can be easily calculated from the micropore volume and the average micropore diameter by assuming cylindrical pores as given in Fig. 1.

From this simple calculation, it is clear that diffusion in zeolites is not at all a simple phenomenon. First of all, the pore size of the zeolite is comparable to that of typical small molecules. Therefore, diffusion often occurs by so-called configurational diffusion, which is much slower than Knudsen diffusion. In this diffusion regime, the molecules are almost constantly in contact with the pore walls and it is clear that a molecule diffusing through one micropore will essentially block that pore completely from any mass transport in the opposite direction. Secondly, the diffusion path length can be quite long as illustrated in Fig. 1. A typical zeolite crystal has a characteristic size of about 1-10 μm but they can be both significantly smaller and larger.
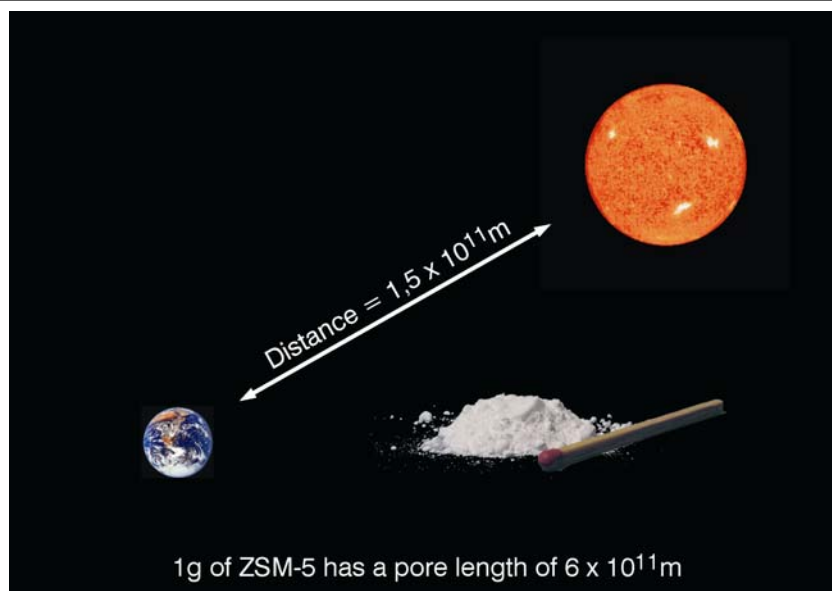
1g of ZSM-5 has a pore length of 6×10^{11} m

Figure 1. The total pore length in 1 g of MFI-structured zeolite is comparable to 4 times the distance from the Earth to the sun. This is calculated assuming cylindrical pores with diameter 5.5 Å and a micropore volume of 0.13 ml/g.

In heterogeneous catalysis, it is very interesting to combine the molecular sieve effect with a catalytic effect. When this is done and the catalytically active sites are located preferentially or exclusively inside the micropores of the zeolite, it is possible to obtain shape-selective catalysts. With these catalysts, it is possible to conduct highly selective catalytic transformations based on the complete exclusion, or strongly hindered diffusion, of certain reactants, intermediates or products; or on the sterically confined reaction space present in the zeolite micropores favoring one reaction path (transition state) over another [2].

Often, the catalytically active sites in zeolite micropores are acid sites that result from the charge compensation of the framework with protons, which is necessary when e.g., Al^{3+} substitutes Si^{4+} in the framework. However, it can also be redox active sites resulting when the charge compensation is done with redox active ions such as Fe(III) or Cu(II) rather than protons [3]. Additionally, it is also possible to incorporate several redox active metals ions directly into the framework structure, e.g., Ga, Ti, V, Mn, Fe etc. [1]. In many cases, even bifunctional catalyst systems can be designed by combining e.g. acid catalysis with redox catalysis. Thus, it is not surprising that zeolite catalysts attract significant attention in many areas of heterogeneous catalysis both for purely fundamental reasons since they can be tailored quite accurately to allow careful and systematic studies of a range of reactions but also in numerous industrial applications where they can be active, selective, durable, and relatively inexpensive catalysts. However, in many cases the sole presence of micropores also imposes significant limitations on the range of reactions that are efficiently catalyzed by zeolite catalysts. It is

clear that if the zeolite catalyst could in principle transform the reactant(s) into the desirable product(s) at a rate higher than the rate of diffusion of reactants, intermediates and products in the zeolite or faster than the rate of adsorption/desorption; then the overall reaction rate will be limited by the rate of diffusion. Thus, the reaction is in a diffusion-limited regime. Obviously, the diffusion limitation will usually be most pronounced for reactions involving larger molecules such as heavy hydrocarbons or carbohydrates that diffuse very slowly through the zeolite micropores and for larger zeolite crystals where the diffusion path is longer.

Several strategies have been proposed to alleviate this problem. Generally, the challenge is to improve the accessibility of the active sites without altering its nature. This can be achieved during or after the zeolite synthesis by introducing mesopores directly into the zeolite crystals, by synthesizing nanosized zeolite crystals, or by supporting zeolite crystals on a mesoporous support material. Fig. 2 provides a schematic illustration of these different materials and it also categorizes various preparative methods that can be used to obtain these hierarchical materials, which all feature (at least) two distinctly different kinds of porosities [4]. The materials are termed hierarchical since they have porosity in at least two different size ranges. At the lowest level, the typical intracrystalline zeolite micropores can be recognized. At a higher level, the larger mesopores can be categorized as either intracrystalline or intercrystalline mesopores or voids when the mesopores are situated inside the zeolite crystals or between the zeolite crystals, respectively.

Several recent reviews highlighting some of these methodologies and the properties of the resulting materials can be found in the literature [4-9].
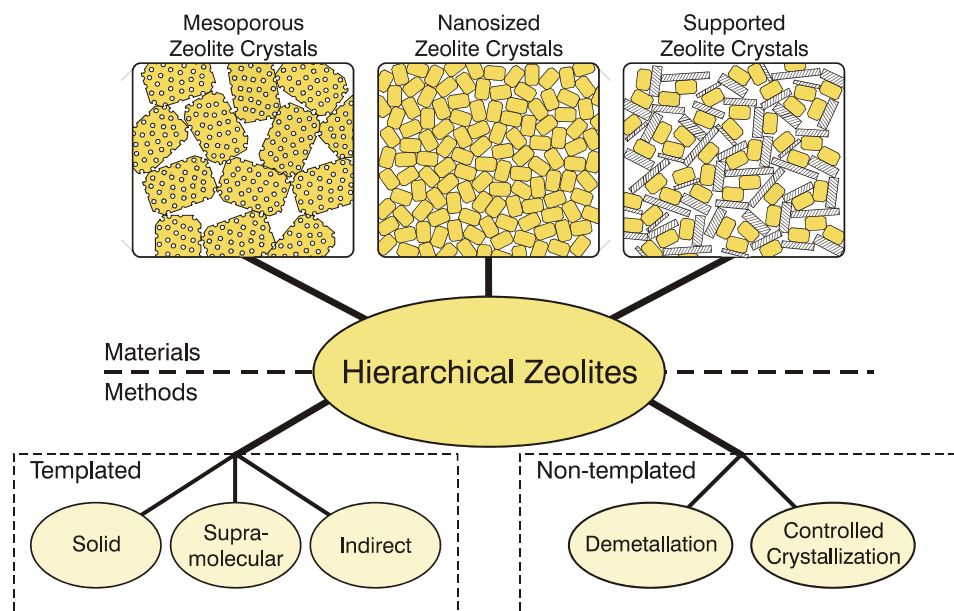

Figure 2. Categorization of classes of hierarchical zeolites materials and the methods used for their preparation, see [4] for more details.

Here, we highlight the preparation and characterization of mesoporous zeolite crystals, i.e., zeolites with intracrystalline mesoporosity, and their performance as heterogeneous catalysts. Mesoporous zeolite crystals are crystalline materials that apart from the micropore system characteristic of the particular zeolite structure also feature an additional intracrystalline system of mesopores that facilitates mass transport to and from the active sites. This is shown to be very useful in a range of catalytic transformations, and we give examples of improved acidic, redox and bifunctional catalysts, and focus on selected cases chosen to pinpoint the possibilities for achieving *both* higher activity and selectivity at the same time and *both* higher activity and simultaneously a longer catalyst lifetime.

2. Synthesis of mesoporous zeolite crystals

Currently, intracrystalline mesoporosity can be introduced into zeolite crystals by three conceptually different approaches. One approach involves the synthesis of a purely microporous zeolite, which is then treated chemically to preferentially extract one of the constituent metallic or semi-metallic elements of the zeolite. Currently, this can be preferential extraction of aluminum (dealumination) [5,6], silicon (desilication) [5-8], or titanium (detitanation) [10,11]. The second approach is based on crystallization of the zeolite in the presence of an auxiliary mesopore template that is subsequently removed after the crystallization [12,13]. Typically, the auxiliary mesopore template is a porous carbon that is removed from the zeolite after crystallization simply by calcination [13] but it can also be a supramolecular template [14]. Using the terminology introduced in Fig. 2, the selective extraction approach can be considered a non-templated route to mesoporous zeolite crystals and the carbon-templating approach represents a solid-templated route [4].

Here, we focus on the preparation of mesoporous zeolites by alkaline post-treatment, typically called desilication [7] and by carbon-templating [13] since currently these methods are attracting most attention. Moreover, these two approaches also appear to be the, by far, most versatile and inexpensive methods for introducing significant mesoporosity in zeolites. They should both be useful for a broad range of zeolite frameworks and they both also provide some possibilities for tailoring the porosity of the resulting materials. Finally, introduction of mesopores in zeolites by desilication or by carbon-templating is expected to only marginally change the intrinsic catalytic properties of the parent zeolite even though this has not yet been thoroughly investigated. Contrary to this, it is clear that e.g. dealumination will lead to significant changes in both the number and the strength of the acid sites. Furthermore, it typically also changes the hydrothermal stability of the zeolite. Thus, the use of mesoporous zeolites prepared by desilication or by carbon-templating makes it possible to study how improved mass transport influence the performance of a specific zeolite in a given application without having to consider the influence of other major changes in the intrinsic catalytic properties.

Demetallation of zeolite crystals

One approach to produce zeolite crystals with intracrystalline mesopores comprises the, more or less, selective dissolution of some part of a conventionally prepared zeolite by use of a chemical reagent. Typically, the conditions required to partly dissolve zeolite

crystals are quite harsh since zeolites are typically quite stable materials. Thus, the dissolution process usually involves strong acids or bases, or strongly complexing agents [6-8]. The selective extraction process leads to removal of some of the metallic or semi-metallic components of the zeolite, typically in the form of soluble oxoanions, but it can also be in the form of complexed species. Fig. 3 schematically illustrates such a dissolution process.

It is clear that mesopores are only formed if the dissolution process proceeds in a quite special way that clearly cannot involve complete dissolution of the zeolite crystals at the same rate from all faces of the parent crystal. Moreover, it is seen that the mesoporosity depends directly on the amount of material that is dissolved, and that there is no direct way of controlling the pore size. Therefore, this method is categorized as a non-templated approach for introducing mesopores in zeolites [4]. Here, we will use the term demetallation to describe all methods for preparing mesoporous zeolites from their conventional microporous counterparts, which involve a selective dissolution of one component of the parent zeolite crystal. Historically, dealumination has been the prototypical example of such a selective dissolution process that leads to mesoporous zeolites, and specifically the dealumination of zeolite Y has received significant attention due to its enormous industrial importance [6]. However, the selective dissolution of silicon from zeolites by strong base, the so-called desilication has also been known for many years [15,16]; and quite recently it was shown that titanium can be selectively extracted from certain titanium-silicates by use of hydrogen peroxide in what might be called a detitanation [11,17]. So far, there are only few examples of porosity being introduced by detitanation but they clearly illustrate that the use of demetallation can be considered a quite general approach to produce hierarchical materials and probably even completely new methods will emerge. Several different methods can be used to perform dealumination of zeolites, and they have recently been carefully reviewed [6]. Typically, dealumination is conducted simply by steaming the zeolite at high temperatures but it can
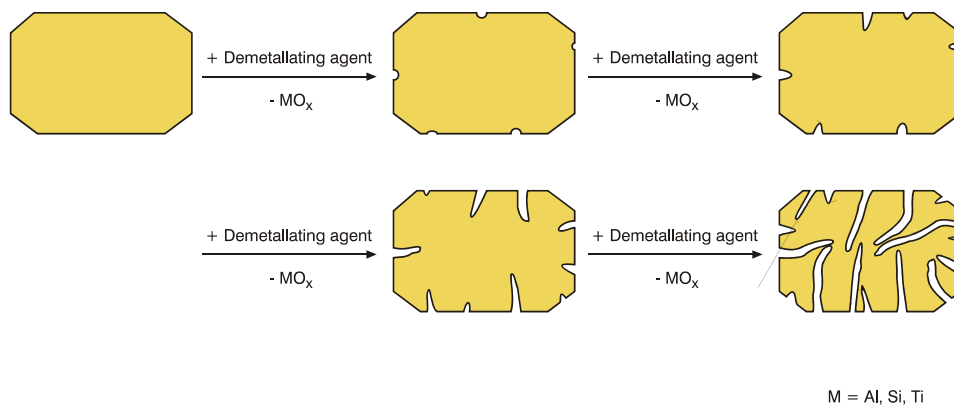

Figure 3. Schematic illustration of the demetallation method used for introduction of mesopores by more or less selective dissolution of part of the zeolite crystal. The extraction is conducted as a post-synthesis treatment and the demetallating agent used is typically a strong acid or base, or a complexing agent.

also be achieved by treating certain aluminum-containing zeolites with strong acid, with complexing agents such as EDTA, or with silicon tetrachloride. Often however, dealumination is not conducted mainly to improve mass transport in the zeolite catalyst but rather to improve hydrothermal stability and/or to modify the acidic properties of the zeolite [6]. In fact, it has been shown by sophisticated transmission electron microscopy techniques that the mesoporosity introduced by dealumination does not significantly lead to any improved accessibility of the zeolite acid sites [18]. Moreover, it is obvious that dealumination has a somewhat limited scope in catalysis since it can only be used to introduce significant mesoporosity in zeolites that has relatively high aluminum concentrations. However, even in such favorable situations dealumination is often not a viable route to create mesoporosity since it will simultaneously lead to a dramatic lowering of the number of acid sites that are typically desirable for catalysis. Therefore, it can be considered quite natural that desilication has attracted rapidly increasing attention over the last years as an alternative method for introducing mesopores in zeolites. The method is attractive since, first of all, most zeolites have high concentrations of silicon and therefore relatively high mesoporosities can be achieved by the selective extraction of silicon from the zeolite framework. Secondly, extraction of silicon does not *per se* lead to any change in the number of acid sites. Even though the term desilication was only coined recently, it is clear that the method has attracted significant attention in industrial laboratories for more than two decades [15,16]. In the patent literature, numerous zeolites have been subjected to various base treatments [19,20] to selective extract silicon; and in several cases improved catalytic performance in different catalytic reactions is reported [15]. In the open literature, the first report of selective dissolution of silicon by base treatment appeared in 1992 by Dessau et al. [21]. They attributed the preferential dissolution of Si from the zeolite to the kinetic resistance of Si-O-Al linkages towards base hydrolysis. Soon after, Lietz et al. [22] also demonstrated that silicon can be selectively dissolved from zeolite crystals but it was not until Ogura and coworkers in a series of papers [23,24] showed transmission electron microscopy images of the materials and reported the porosities of the resulting materials that the field truly gained momentum. During the last few years, the group of Groen, Perez-Ramirez and Mouljin in a series of papers [7,8,25,26] has explored the scope of the desilication method and provided a detailed fundamental understanding of the factors that determine the mesoporosity of the resulting zeolite materials. The effect of variation in temperature, type of base, base concentration, digestion time and Si/Al ratio of the zeolite has been investigated in detail [26-28]. Obviously, all these factors are important and must be optimized individually to tailor the zeolite to any given application. However, whereas the experimental conditions for conducting the desilication can be varied within quite broad ranges, it is noteworthy that the Si/Al content of the zeolite is quite decisive for the outcome of the desilication [27]. Typically, the best results are obtained with zeolites having Si/Al ratios between 20 and 50. For these materials, it is often possible to achieve mesopore surface areas in the range of 50-250 m^2/g with an average pore diameter of about 10-40 nm without any noticeable loss of microporosity compared to that of the parent zeolite. The reason for this behavior is actually quite simple. The desilication method relies on the selective dissolution of silicon from the zeolite. For zeolites with very high silicon concentrations, the zeolite crystals simply dissolve starting from the external surface and continue with more or less the same rate from all faces until the

entire crystal is dissolved. This clearly does not lead to any intracrystalline mesoporosity. For zeolites with high aluminum concentrations, it is essentially impossible to dissolve any part of the zeolite crystal since Si-O-Al linkages are found frequently at all crystal faces, and these structural units are not attacked at any noticeable rate [21]. Only for intermediate Si/Al ratios is it possible for the base to dissolve significant amounts on Si-O-Si linkages and thereby "dig" into the zeolite crystal. In this way, the resulting intracrystalline mesopores are formed when the part of the zeolite crystal that is not protected by the presence of Si-O-Al linkages is gradually dissolved. It has been shown that only negligible amounts of aluminum are transferred to the alkaline solution during the treatment and consequently, the Si/Al ratio of the zeolite gradually decreases during desilication. So far, the method has been mostly applied to ZSM-5 but successful reports of the desilication of other zeolites, including zeolite beta [26] and mordenite [26] are currently appearing. Thus, the desilication method seems to be a useful, simple and quite versatile method for introducing mesoporosity in zeolites. It is relatively inexpensive and significant mesoporosity can be achieved provided that the parent zeolite contains a reasonable amount of silicon.

Carbon-templating of mesoporous zeolite crystals

The carbon-templating approach to mesoporous zeolites was first reported by a research group at Haldor Topsøe A/S in 2000 [13]. This approach is fundamentally different from the demetallation approach since it involves the use of an auxiliary mesopore template that is removed after crystallization of the zeolite. In the categorization of methods for producing hierarchical zeolites shown in Fig 2, it is considered a hard-templating method [4]. Fig 4 illustrates schematically that carbon particles encapsulated by a zeolite crystal can be removed by combustion to produce a zeolite crystal, which has now pores where the carbon particles were originally located [13].

In this way, the carbon particles have effectively been used as mesopore templates. Obviously, the method requires that the zeolite grows almost exclusively in the pores of the carbon material since all zeolite material that crystallizes outside the carbon will exhibit no extra porosity after removal of the carbon template. Thus, it is essential that the zeolite synthesis gel efficiently fills all the pores or void volumes of the carbon template before
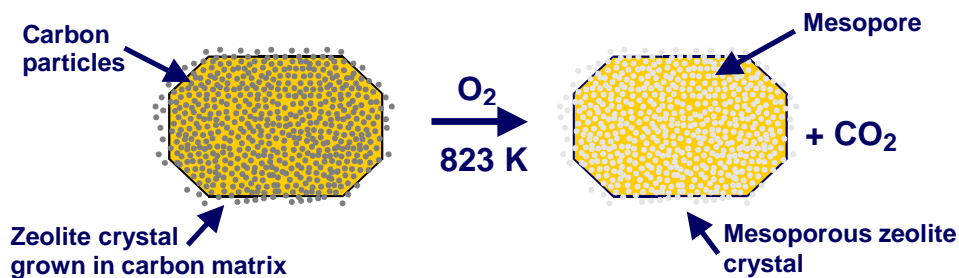

Figure 4. Schematic illustration of the carbon-templating route to mesoporous zeolite. The zeolite is crystallized in the pore system of a suitable carbon that acts as a mesopore template. The carbon is removed by combustion after the zeolite crystallization [Adapted from Ref. 13].

crystallization. Typically, zeolite gels are quite viscous and therefore it is often not straightforward to load them into the carbon material. In some special cases, when the zeolite gel has very low viscosity as e.g. the ZSM-12 gel, it is possible to simply impregnate the carbon with the zeolite gel using the traditional incipient wetness impregnation technique [29]. However, in most cases it is necessary to directly synthesize the zeolite gel inside the pores of the porous carbon. This typically involves at least two incipient wetness impregnations with zeolite gel precursors and an intermediate evaporation of the impregnation solvent to open the pore volume for the subsequent impregnation. Furthermore, not all carbons are suitable as mesopore templates. First of all, the carbon needs to have an average pore diameter that is sufficiently large so the zeolite crystal can nucleate and grow inside the pores. This is apparently not possible with pure microporous carbons probably because the unit cell sizes of most zeolites are larger than the pore size of the microporous carbons. So far, most mesoporous zeolites have been grown using carbon templates with average pore diameters above 10 nm. It is quite clear that the pore size of the zeolite to a large extent is determined by the particle size of the carbon. However, in practice the zeolite does not encapsulate individual carbon particles to any significant extent. If that did occur, the resulting zeolite would mostly have meso-cavities rather than mesopores. Instead, the zeolite crystals grow inside the porous carbon and fill the void space between the packed carbon particles. When the carbon is removed, the remaining zeolite crystal is essentially the negative image of the original carbon material. Thus, it is clear that the detailed pore structure of the carbon and the carbon particle size are the main parameters for determining the mesopores structure of the zeolite. By using a carbon template with a high porosity, it is possible to impregnate a significant amount of zeolite gel into the carbon material. Therefore, a larger amount of zeolite per mass of carbon can be produced than it would be possible using a carbon template with a low porosity. On the other hand, the use of a carbon template with a low porosity will lead to a zeolite material with higher porosity than what would result from using a carbon template with a high porosity. Thus, by proper selection of the carbon template it is in principle possible to design zeolites with any desired mesoporosity. However, this obviously requires that a suitable carbon template is available, and this will clearly not always be the case. Anyhow, the use of multi-walled carbon nanotubes as templates to prepare zeolites with straight pores of exactly the same diameter as the nanotubes has illustrated that there exist significant opportunities for designing zeolite materials with unprecedented pore systems [30,31]. In any case, special attention must be paid to the step involving removal of the carbon template by a more or less controlled combustion. Typically, the carbon-template is removed together with any structure directing agent used for the crystallization of the zeolite in a simple calcination, and here it is advantageous if the carbon can be removed at only moderate temperatures. Clearly, combustion of the relative large amounts of carbon present in the composite materials generates significant heat and if this is not handled properly, it can lead to significant loss of the zeolite crystallinity and in severe cases to the formation of a purely amorphous material. There are several ways to control the combustion of the carbon template, including a slow calcination of only thin layers of the composite zeolite-carbon material, use of dilute air or calcination in a fluid-bed furnace. So far, the carbon templating method has been used to prepare a range of different zeolites, including ZSM-5 [13], ZSM-11 [32], ZSM-12 [29,33], zeolite Y [34], and zeolite beta [35]. Most recently, it was shown that the carbon-templating approach to mesoporous zeolites

can also be conducted in a quite different way [36]. The methodology is shown schematically in Fig. 5.

First, a mesoporous silica is impregnated with a concentrated solution of sugar (or any suitable carbohydrate or carbohydrate derivative), which is then decomposed to carbon by heating in an inert atmosphere. After this, the zeolite is crystallized by entirely conventional means and the carbon template, which can be considered to be generated in-situ during the zeolite synthesis, is removed. This has several advantages. First of all, the method uses only simple chemicals that are widely available and inexpensive. Secondly, only the impregnation and decomposition of the carbohydrate are extra preparative steps compared with those required in a conventional zeolite synthesis. Thirdly, and probably most importantly, the method makes it possible to control the porosity simply by using more or less concentrated solutions of the carbohydrate. Currently, the carbon-templating method can probably be considered the most versatile route to mesoporous zeolites since it appears to be useful for preparing a wide range   of   zeolite materials with a reasonable control of the mesoporosity. In particular, it can be used to prepare zeolites of any Si/Al ratio unlike the desilication method, which is limited to Si/Al ratios in the range of about 20-50. Finally, it is noted that by use of the carbon-templating approach it is also possible to synthesize mesoporous zeotypes, such as ALPO's and SAPO's [34], which are obviously not efficiently prepared with any demetallation method.
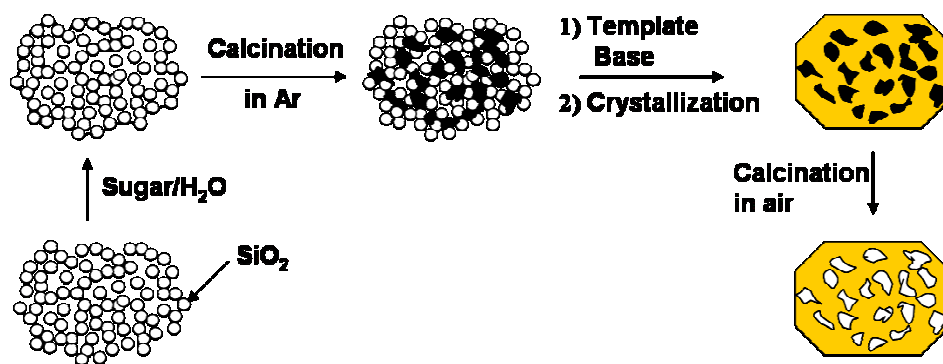

Figure 5. Principle for in-situ carbon templating. The carbon template is directly synthesized in the mesoporous silica by impregnation with a carbohydrate followed by decomposition of the carbohydrate to produce amorphous carbon that acts as a mesopore template [Adapted from Ref. 36].

3. Properties of mesoporous zeolite crystals

Here, we will describe the properties of mesoporous zeolite crystals obtained by desilication and by carbon-templating, and we will highlight the most common methods used for characterization of this class of zeolite materials. It is shown that mesoporous zeolite crystals produced by both desilication and carbon-templating are phase-pure and highly crystalline zeolite materials composed of single crystals featuring intracrystalline mesopores interconnected with the crystallographic micropore system characteristic of

zeolites. Furthermore, it is shown that these materials are highly acidic and that diffusion in such crystals is much faster than in conventional zeolite crystals.

Techniques applied for characterization of mesoporous zeolite crystals

A range of different techniques have been applied to investigate the nature of mesoporous zeolite materials with intracrystalline mesoporosity. The most common ones along with a short description of the type of information they provide are listed in Table 1.

Physisorption measurements, typically using N_2 or Ar as the adsorbate, are often used to probe the pore characteristics of porous materials [37,38]. An instructive review on the application of physisorption techniques to investigate materials with combined micro- and mesoporosity covering also the most common pitfalls of data interpretation has recently been published [37]. Physisorption measurements can reveal information about the textural properties of microporous and mesoporous materials, e.g. surface areas and pore volumes. For materials with combined micro- and mesoporosity, characterization of the porosity using N_2 or Ar physisorption is often accompanied by other types of investigations as well, in order to get a more detailed picture. Mercury intrusion porosimetry is frequently used to investigate the nature of the porosity that is not in the micropore region, i.e. whether the material is mesoporous or macroporous as well. Mercury intrusion experiments also reveal information about the accessibility of the additional porosity from the external surface of the zeolite crystals. Electron microscopy, particularly scanning electron microscopy but also transmission electron microscopy, is used routinely to study the porosity of mesoporous zeolites since these methods provide a

Table 1. Characterization techniques commonly applied to mesoporous zeolites.

Technique	Information
N_2 and Ar physisorption measurements	Porosity (micro- and mesopores), surface area
Hg intrusion porosimetry (MIP)	Porosity (meso- and macropores)
X-ray diffraction (XRD) on powdered samples	Framework structure type, phase purity, crystallinity
Scanning electron microscopy (SEM)	Morphology, material crystallinity and homogeneity, nature of porosity
Transmission electron microscopy (TEM)	Morphology, crystallinity of individual crystals, nature of porosity
Temperature programmed desorption of chemisorbed ammonia	Framework aluminum content
FTIR spectroscopy of chemisorbed pyridine	Brønsted and Lewis acidity
^{27}Al MAS NMR spectroscopy	Framework aluminum content

direct and very visual image of the individual crystals. Thus, it is often very easy to see whether the mesoporosity of a particular sample results from packing of nanosized crystals or from additional pores within the individual crystals. This central information is not easily available by any other technique or combination of techniques.

X-ray diffraction is used to determine the structural properties of mesoporous zeolite materials, since it can be directly determined from powder XRD patterns, which phases are present and in which relative amounts. Thus, XRD is used to verify that the desired zeolite material is obtained after synthesis as well as to establish the phase-purity of the material [39].

Electron microscopy imaging of the individual crystals of a mesoporous zeolite material reveals a wealth of important information about the sample. Scanning electron microscopy provides information about the homogeneity of the material since the size and morphology of the individual zeolite crystals are easily and directly visualized. Transmission electron microscopy can also be used for this type of investigation. However, TEM is a far more tedious and time-consuming technique than SEM for studying a larger number of zeolite crystals. Therefore, TEM is optimally used to investigate representative individual crystals in more detail and with higher resolution rather than for statistical analyses of the mesoporous materials [40].

The acidic properties of mesoporous zeolite crystals are correlated with the framework concentration of aluminum relative to silicon. However, rather than determining the aluminum content by bulk elemental analyses, techniques such as ICP, chemisorption and spectroscopic techniques, or a combination of those, are often used. Thus, the aluminum content and hence acidic properties, are normally determined by temperature programmed desorption of chemisorbed NH_3, IR spectroscopy on chemisorbed pyridine or by ^{27}Al MAS NMR spectroscopy, since these techniques can all be used to specifically probe the framework aluminum concentration [41,42].

Textural properties

Physical gas adsorption, or physisorption, of N_2 or Ar is the most widely applied technique used for determining the surface area and porosity of solid materials since measurements of adsorption at the gas/solid interface provide a wealth of information on the textural properties of solid surfaces. Most N_2 physisorption isotherms for solid materials can be classified as one of Types I-VI according to the IUPAC classification system [43]. In this classification, N_2 physisorption isotherms for conventional zeolites are classified as Type I isotherms indicating that these are microporous solids with very limited mesoporosity, whereas the isotherms for zeolites with larger amounts of mesoporosity in addition to the micropores, i.e. mesoporous zeolite crystals, are typically classified as Type IV isotherms. Due to the crystallographically well-defined micropore system characteristic of zeolites, all zeolite materials show gas uptake capacities at low relative pressures corresponding to the filling of the micropores. After complete filling, the gas uptake capacity of conventional zeolites is very limited, indicating that no additional porosity exist in the mesopore region (2-50 nm diameter). Type IV isotherms are characterized by exhibiting hysteresis between the adsorption and desorption branches of the isotherms due to capillary condensation of the adsorbate in mesopores of the adsorbent. The specific form of the hysteresis loop is a further source of information, which is covered in detail elsewhere [43]. The physisorption isotherms associated with

mesoporous zeolite materials consisting of single-crystals with intracrystalline mesoporosity prepared by either desilication or carbon-tempating are typical type IV isotherms [8,25,33,44-46]. As an example, Fig. 6 shows the physisorption isotherms and pore-size distribution calculated by the BJH method [44] of a ZSM-5 material before and after desilication [25].

As evident from Fig. 6a, the physisorption isotherm obtained for the non-treated ZSM-5 (squares) can be classified as a type I isotherm. However, after subjecting the sample to desilication, a material exhibiting also a typical type IV physisorption isotherm is obtained (triangles). BJH pore-size distributions of the same samples before and after alkaline treatment are shown in Fig. 6b. The non-treated sample (squares) shows only little porosity in the mesopore region, however, the desilicated sample (triangles) clearly contain mesopores centered around 30 nm. Thus, the desilication methodology is clearly capable of inducing mesopore formation in non-mesoporous zeolites. For comparison, Fig. 7 shows the physisorption isotherm and corresponding BJH pore-size distribution of a mesoporous silicalite-1 material prepared by carbon-templating using a pre-formed carbon as the mesopore template [45].

The isotherm obtained for the mesoporous silicalite-1 single-crystal material shown in Fig. 7 exhibits hysteresis in two ranges of relative pressures, from above P/P_0 of ca. 0.9 and in the range of ca. 0.1-0.3. The hysteresis loop in the lower pressure region is commonly observed for silicalite-1 materials and it is the result of a phase transformation of N_2 inside the micropores. Sometimes this is erroneously attributed to the presence of smaller mesopores [37]. The hysteresis loop at higher relative pressure indicates that the sample contains mesoporosity. From the BJH pore-size distribution shown in the inset it is seen that the material shows a quite narrow mesopore size distribution, which is often found for mesoporous zeolite crystals prepared by carbon-templating.

From physisorption measurements, it is possible to calculate the pore volume and surface area of mesoporous zeolites. If a mesoporous zeolite sample contains no appreciable
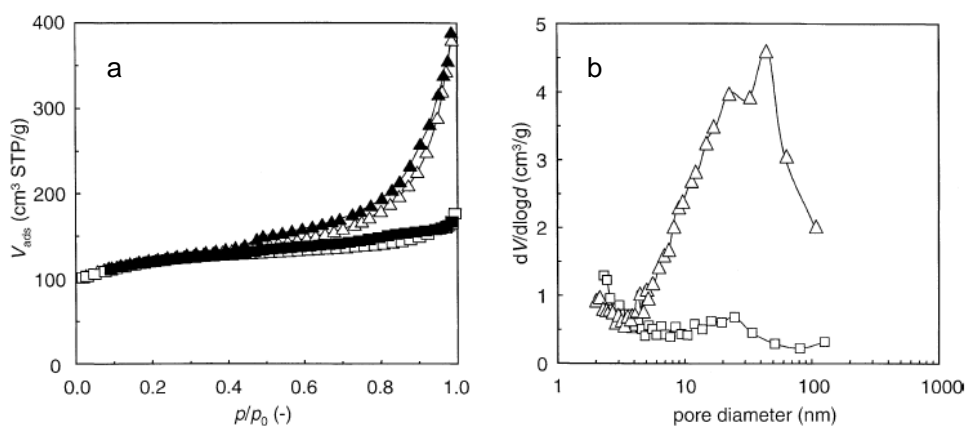

Figure 6. Physisorption isotherms (a) and BJH pore-size distributions (b) for conventional (squares) and mesoporous (triangles) ZSM-5 prepared by desilication [Reprinted with permission from Ref. 25. Copyright (2004) Elsevier].
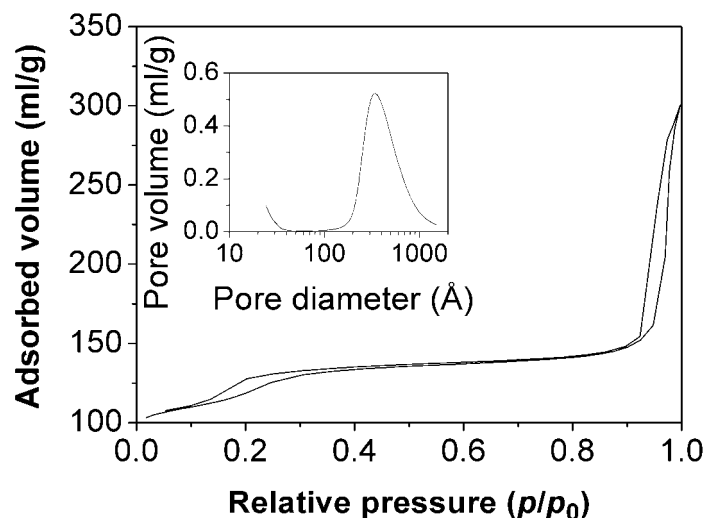
Figure 7. Physisorption isotherm and BJH pore-size distribution for mesoporous silicalite-1 prepared by carbon-templating [Adapted from Ref. 45].

amount of macroporosity, the mesopore volume, i.e. the pore volume of a sample that results from mesopores, is determined by subtracting the micropore volume (calculated by the *t*-plot method [47] from the total pore volume (total volume of gas adsorbed at a relative pressure of 0.99). Mesopore volumes of zeolite materials with intracrystalline porosity are typically in the range 0.2-1.0 ml/g. It is noted that the BET method is *not* applicable to determine the surface area in the zeolite micropores since the assumptions of this method are not fulfilled for these materials. However, often the BET area is still given to provide a "fingerprint" of the given zeolite material. The porosity of mesoporous zeolites has also been investigated using mercury intrusion porosity measurements. In general, mesopore sizes and volumes determined by Hg intrusion measurements are in excellent accordance with mesopore sizes and volumes determined by N_2 physisorption measurements [36,48]. Thus, Hg intrusion porosimetry measurements confirm that the mesopores of mesoporous zeolite crystals are fully accessible and distributed throughout the individual crystals but it clearly does not provide information about the micropores.

Structural chemistry

The most prominent and straight-forward method of investigating the structure and crystallinity of mesoporous zeolite single crystal materials is by X-ray diffraction of powdered samples [8,25,32,35]. The XRD patterns of mesoporous zeolites obtained by desilication as well as by carbon-templating reveal that these materials are indeed highly crystalline and can be synthesized as completely phase-pure materials. Representative XRD patterns of mesoporous ZSM-5 samples obtained by both techniques as well as of conventional micron-sized ZSM-5 and nanosized ZSM-5 samples are shown in Fig. 8.

As seen in the XRD patterns of the ZSM-5 samples, all materials consist exclusively of highly crystalline MFI-structured material. Further analyses of the XRD patterns of the

mesoporous samples reveal that the peaks are broader than in the conventional micron-sized zeolite sample, see Fig. 9.

In fact, they are as broad as the peaks in the pattern obtained from the nanosized zeolite sample. Thus, crystal size determination by use of the Scherrer equation would falsely suggest the crystal size of the mesoporous zeolites to be in the nanosized range. However, the Scherrer equation merely provides information about the mean size of the coherently diffracting entities in the crystal, i.e., the mean crystal size. For most crystals, this crystal size is in reasonable agreement with the true crystal size, however, in mesoporous zeolite crystals the longer-range ordering is disturbed by the presence of non-crystallographic voids, or mesopores. Thus, XRD cannot be applied to determine whether
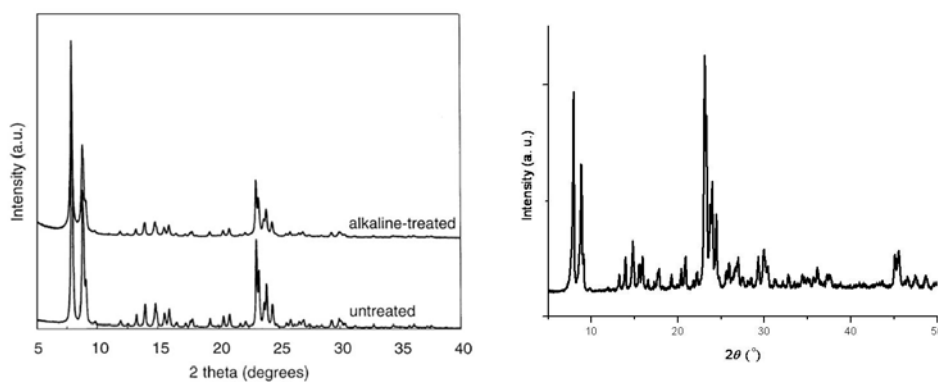

Figure 8. Representative XRD patterns of mesoporous and conventional ZSM-5 single crystal materials (a) before and after desilication and (b) prepared by carbon-templating [(a) Reprinted with permission from Ref. 25. Copyright (2004) Elsevier].
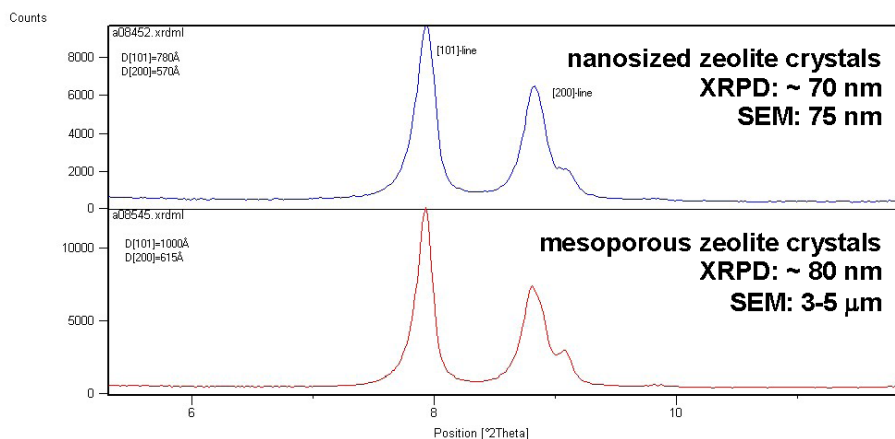

Fig. 9. Close-up on the [101] and [200]-reflections in XRD patterns of nanosized zeolite crystals and carbon-templated mesoporous zeolite single crystals.

the mesopores in mesoporous zeolite materials are intercrystalline or intracrystalline, i.e. whether the individual crystals are nanosized or mesoporous. To determine the size of the individual crystals of mesoporous zeolite materials, more direct imaging techniques such as scanning electron microscopy and transmission electron microscopy must be used. Scanning electron microscopy in particular is frequently used to determine the size and morphology of the individual crystals of a particular zeolite sample as it is often directly visible whether the sample consists of agglomerates of nanosized crystals or contains larger porous crystals [33,35,46,49,50]. Typical low and high magnification scanning electron microscopy images of a mesoporous ZSM-5 sample synthesized by carbon-templating are shown in Fig. 10.

As seen in Fig. 10, mesoporous zeolite crystals prepared by carbon-templating exhibit a sponge-like morphology but at the same time, they retain the coffin-like shape characteristic of MFI-structured zeolites. As evident from the SEM images of themesoporous ZSM-5 sample shown in Fig. 10, it is possible with the carbon-templating methodology to obtain mesoporous zeolite samples with a very homogeneous crystal size distribution. In general, the crystal sizes of mesoporous zeolite crystals prepared by carbon-templating are in the range of 1-5 µm but nano-sized mesoporous zeolite crystals have indeed also been reported [51]. Since mesopore generation by desilication is a post-synthesis chemical treatment, the crystal size distribution of the mesoporous zeolite crystals produced by desilication should directly reflect that of the parent material. However, as discussed above, the framework Si/Al ratio of the parent zeolite greatly determines the porosity obtained via desilication. Thus, by the alkaline treatment procedure it is as easy to produce mesoporous zeolite materials consisting of large crystals as it is to produce the parent zeolite with desired framework Si/Al ratios. In general, as shown in Fig. 11, mesoporous ZSM-5 crystals produced by desilication of conventional zeolite samples with framework Si/Al ratios in the range 20-50 retain the morphology of the parent sample. However, as the SEM image shown in Fig. 11c shows, excessive alkaline treatment of zeolite samples even with an optimal framework Si/Al is destructive for the crystals [49].
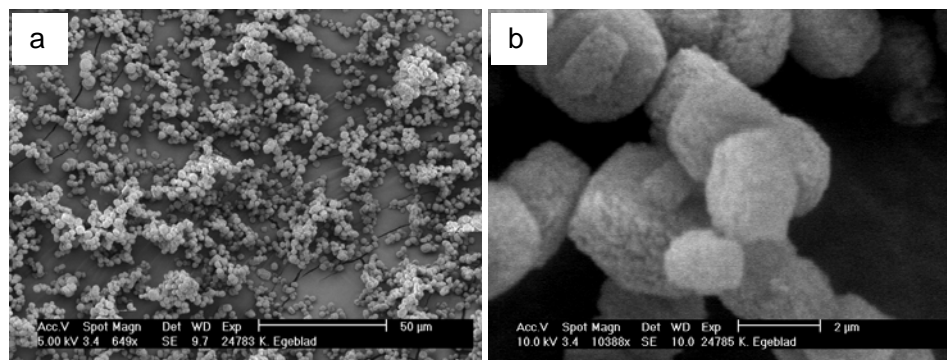

Figure 10. Scanning electron microscopy images of a mesoporous ZSM-5 sample produced by carbon-templating recorded at (a) low magnification and (b) high magnification [Adapted from Ref. 45].
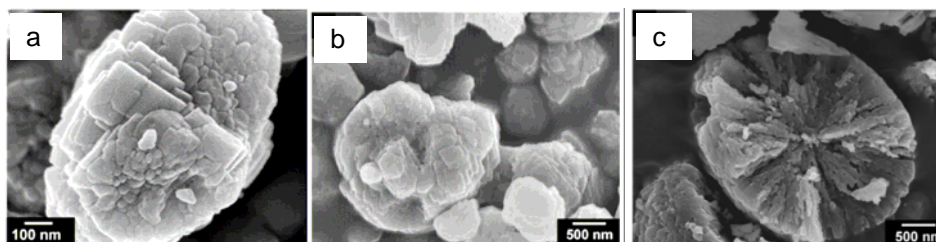
Figure 11. SEM images of (a) non-treated ZSM-5 crystals (Zeolyst, CBV8020, NH$_4$) with framework Si/Al=37, (b) same sample after optimal alkaline treatment (10 cm^3 of 0.2 M NaOH and 330 mg of zeolite, 338 K, 30 min) and (c) sample after excessive alkaline treatment (50 cm^3 of 0.2 M NaOH and 330 mg of zeolite, 338 K, 30 min) [Reprinted in part with permission from Ref. 49. Copyright (2007) American Chemical Society].

Transmission electron microscopy is also frequently used to study mesoporous zeolite materials [13,23,28,30,36,52-54]. Comparison of transmission electron microscopy images of conventional zeolites with mesoporous zeolites prepared by either carbon-templating or desilication very visibly reveals the porosities of the individual crystals; conventional zeolite crystals appear to be dense exhibiting no distinct contrast difference throughout the crystals whereas mesoporous zeolite crystals show pronounced contrast differences and therefore appear to be sponge-like rather than dense. Typical TEM images of mesoporous zeolite crystals prepared by either of the two methods are shown in Fig. 12. For comparison is also shown in Fig. 12, a TEM image of conventional zeolite crystals.

The contrast difference seen in the TEM images in Fig. 12 is due to less absorption of the electron beam by passage through a mesoporous crystal than through a conventional crystal. Thus, an electron beam transmitted through a mesoporous zeolite crystal encounters fewer atoms than an electron beam transmitted through a conventional zeolite crystal of equal thickness. As mesoporous zeolite crystals are composed of crystalline domains and void domains distributed more or less randomly throughout the crystals, these crystals appear to be white-spotted particles in TEM images, indicating that mesoporous zeolite crystals prepared by either carbon-templating or desilication contain intracrystalline porosity. Cross-sectional (3D-)TEM images of mesoporous zeolite crystals prepared by carbon-templating clearly show that the mesopore system extends throughout the entire crystals starting at the external surface. Final proof of the single-crystalline nature of mesoporous zeolite crystals has also been provided by careful TEM studies using the selected area electron diffraction technique on individual crystals in the powdered samples. As shown in Fig. 13, the electron diffraction pattern obtained from an isolated mesoporous ZSM-5 particle is an array of reflections rather than concentric circles.

This diffraction pattern that can be completely ascribed to a twinned MFI crystal and this unambiguously proves that mesoporous zeolite crystals prepared by carbon-templating are indeed single crystals rather than agglomerates of nanosized crystals. A similar verification of the single crystalline nature of the mesoporous zeolite crystals can also be obtained by careful inspection of high-resolution images of smaller crystals [55]. Here, it is easily seen that lattice fringes extend throughout the entire crystal.
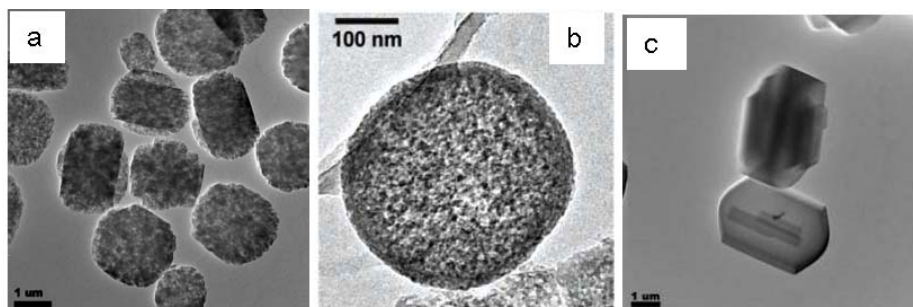
Figure 12. TEM images of (a) mesoporous silicalite-1 prepared by carbon-templating, (b) mesoporous ZSM-5 prepared by alkaline treatment and (c) conventional silicalite-1 crystals [(a and c) adapted from Ref. 45; (b) Reprinted in part with permission from Ref. 28. Copyright (2005) American Chemical Society].
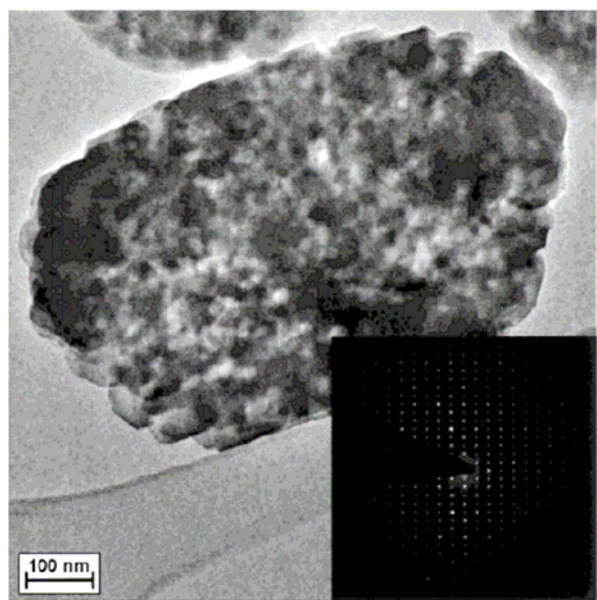

Figure 13. TEM image and selected area electron diffraction pattern of a mesoporous ZSM-5 crystal prepared by carbon-templating [Adapted from Ref. 13].

Acidic properties

Of particular importance for the properties of mesoporous zeolites is the framework Si/Al ratio, since this to a large extent determines the acidity of the material. Substitution of framework silicon ions (Si^{4+}) with aluminum ions (Al^{3+}) in mesoporous zeolite crystals requires also the presence of non-framework cations to compensate for the lower charge of aluminum. Normally, sodium or potassium ions function as the charge-compensating cations after synthesis since zeolites are often crystallized from alkaline gels. However, if

the charge-compensating cations are H^+-ions, the zeolite will have Brønsted acidity. Mesoporous zeolite crystals with acidic properties may be easily obtained via standard ion-exchange procedures of, e.g., the Na-form with NH_4^+-ions followed by calcination to desorb ammonia. The most straightforward method for determining the acidity of mesoporous as well as conventional zeolite materials with limited mesoporosity is temperature-programmed desorption of chemisorbed ammonia (NH_3-TPD). Using NH_3-TPD, a measure of both the number and strength of the acid sites can be estimated. By the carbon-templating procedure, mesoporous zeolite crystals have been prepared with framework Si/Al ratios from ca. 25 and higher. However, by careful choice of aluminum source it is possible to produce more acidic mesoporous zeolite materials. Table 2 lists NH_3 desorption capacities and results of elemental analyses of mesoporous zeolite crystal materials prepared from different aluminum sources [56].

As seen in Table 2, when sodium aluminate is used as aluminum source, a discrepancy between Si/Al ratios determined by NH_3-TPD and Si/Al ratios determined by elemental analysis is observed, indicating that not all of the aluminum in the mesoporous zeolite crystals is present in the framework, as only framework aluminum contributes significantly to the acidity. However, it could also indicate a different ratio of Brønsted and Lewis acid sites. Anyhow, when aluminum isopropoxide is used instead, much more aluminum appears to be incorporated into the framework, resulting in an overall higher total acidity as measured by ammonia-TPD. Thus, Table 2 shows that zeolite crystals with

Table 2. Aluminum contents determined by NH_3 TPD and elemental analyses of mesoporous ZSM-5 prepared from different aluminum sources by carbon-templating.

Sample	Aluminum Source	Si/Al ratio[a]	Al content, μmol/g	Amount of NH_3 desorbed, μmol/g	Si/Al ratio[b]
ZSM-5	aluminum isopropoxide	14.4	870	740	16.6
ZSM-5	aluminum isopropoxide	31.2	529	464	32.3
ZSM-5	sodium aluminate	16.8	825	350	43.9
ZSM-5	sodium aluminate	34.3	451	336	46.9

[a] Elemental analysis results
[b] NH_3-TPD results

substantial amount of acid sites (> 700 µmol/g) may be prepared by carbon-templating and that the framework Si/Al content should not exclusively be determined by bulk elemental analysis techniques. The acidity range possible to achieve for mesoporous zeolite crystal materials prepared by desilication is more limited due to the fact that mesopore generation by this procedure is very much dependent on the Si/Al ratio of the parent zeolite. As pointed out previously, the framework Si/Al content of the parent zeolite before alkaline treatment, should be in the approximate range 20-50 in order to achieve reasonable mesopore content. However, since desilication results in preferential extraction of silicon from the framework, the aluminum concentration relative to silicon gradually increases during the alkaline treatment. This is shown in Fig. 14 for mesoporous MFI and MOR prepared by alkaline treatment [57]. Clearly, the NH_3-TPD method does not provide information on the relative amounts of Brønsted and Lewis acid sites, and such studies have not yet been reported for mesoporous zeolite crystals.

The framework aluminum concentration of mesoporous zeolites have also been investigated using FTIR spectroscopy of pyridine chemisorbed onto acid sites and by ^{27}Al MAS NMR spectroscopy. In general, good agreement is found for aluminum concentrations determined by these methods in comparison with NH_3-TPD results as shown in Table 3.
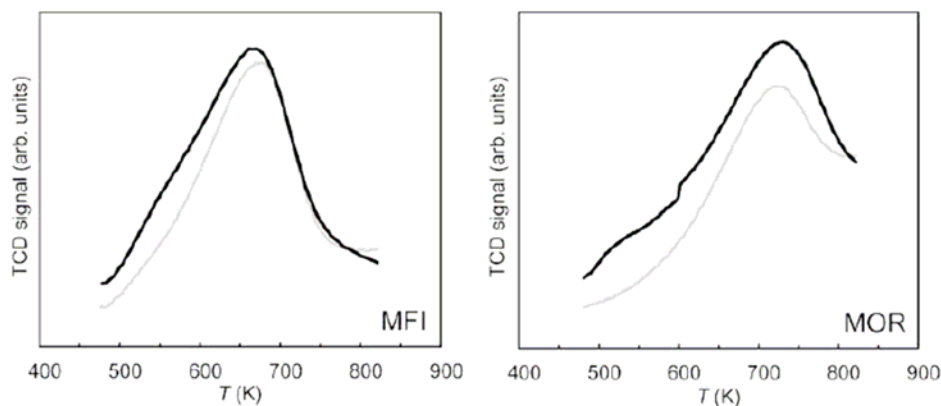

Figure 14. NH_3-TPD curves for mesoporous (black line) and conventional (grey line) zeolite crystals of MFI and MOR structure type [Reprinted with permission from Ref. 57. Copyright (2007) Elsevier].

Table 3. Aluminum content determined by NH_3-TPD, IR of chemisorbed pyridine and ^{27}Al MAS NMR of conventional and mesoporous ZSM-5 prepared by carbon-templating.

Sample	NH_3-TPD	pyridine-IR	^{27}Al NMR
Conventional	71	70	70
Mesoporous	116	110	120

Diffusional properties

The diffusion of gases and liquids into and out of zeolite crystals is of central importance for catalytic application of zeolites. Often, mass transfer limitations are imposed onto catalytic reactions when purely microporous (conventional) zeolite catalysts are used as mentioned above. Thus, the main purpose of introducing additional mesoporosity into individual zeolite crystals is to enhance the rate of diffusion of reactants, intermediates and products within the individual zeolite crystals. The diffusional properties of mesoporous zeolite crystal materials compared to conventional zeolites have been investigated by gas adsorption and desorption experiments and by diffusion of liquids in zeolite crystals. Fig. 15 shows the results of gas diffusion experiments for mesoporous and conventional ZSM-5 crystals as a function of time.

As seen in Fig. 15, mesoporous ZSM-5 prepared by desilication shows much faster neo-pentane adsorption capabilities than conventional, non-treated ZSM-5: 50% of the maximum neopentane uptake is achieved after only 2 min. for the mesoporous sample and after approximately 120 min. for the conventional sample. From these data, the average characteristic diffusion time was determined to be more than 2 orders of magnitude shorter in the mesoporous sample than in the conventional sample [58]. Fig. 16 shows that also desorption of *i*-butane out of saturated ZSM-5 crystals is much faster for carbon-templated mesoporous zeolite crystals than for conventional zeolite crystals [59].

Likewise, comparative experiments with diffusion of liquids adsorbed onto mesoporous and conventional silicalite-1 materials have been conducted [29]. These experiments clearly show that also diffusion of molecules out of mesoporous zeolite crystals into a liquid is much faster than out of conventional crystals. Fig. 17 shows the results of diffusion experiments with *n*-hexadecane (at different loadings) and mesitylene out of mesoporous and conventional silicalite-1 crystals.
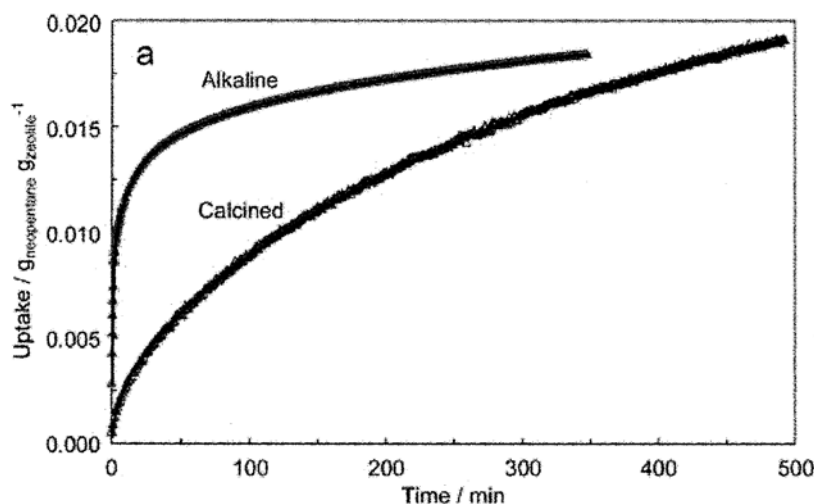

Figure 15. Adsorption of neopentane in alkaline treated ZSM-5 [Reprinted in part with permission from Ref. 58. Copyright (2006) American Chemical Society].
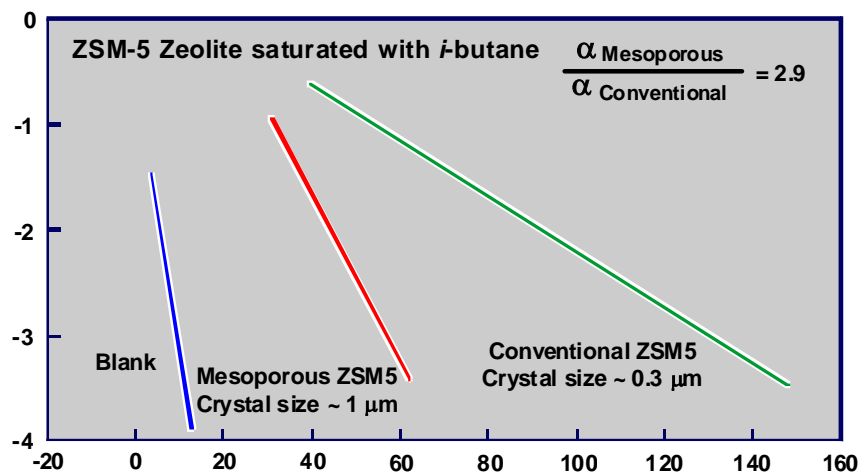
Figure 16. Desorption of *i*-butane in carbon-templated ZSM-5 [Adapted from Ref. 59].
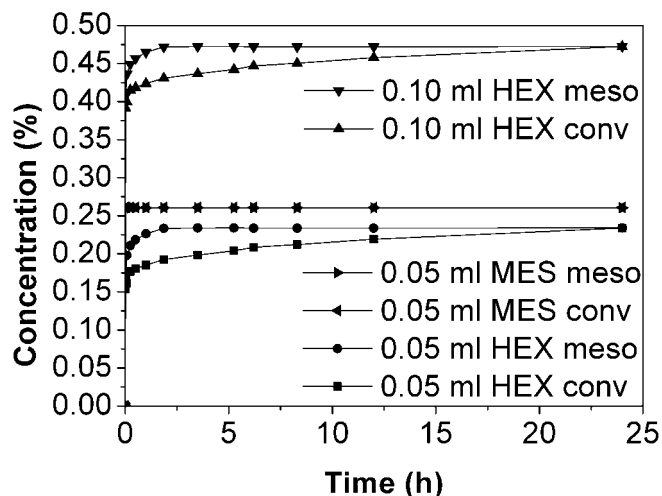

Figure 17. Diffusion of *n*-hexadecane and mesitylene in mesoporous and conventional silicalite-1 crystals [Adapted from Ref. 29].

It can be seen from Fig. 17 that diffusion of *n*-hexadecane is much faster out of mesoporous than out of conventional silicalite-1, as the concentration of *n*-hexadecane in *n*-hexane increases much more rapidly for the mesoporous sample regardless of the amount of *n*-hexadecane adsorbed in the zeolite micropores prior to the diffusion experiment. It is also seen that mesitylene is too bulky a molecule to penetrate to the micropore system of silicalite-1, since no change in concentration is observed over time demonstrating that the mesitylene is only adsorbed on the external surface of the zeolite materials.

4. Applications of mesoporous zeolite catalysts

In industry, zeolite catalysts are primarily used for catalytic fuel-upgrading in refineries and for the production of various petrochemicals [60,61]. The success of zeolite catalysts can primarily be attributed to the presence of micropores with well-defined sizes and geometries that are the explanation for the shape-selectivity exhibited by such catalysts. Unfortunately, in many cases, the sole presence of micropores can also be a significant limitation [13,62-65] because mass transport to and from the active sites located within the micropores is relatively slow resulting in part of the zeolite crystal not being used efficiently for catalysis as shown in Fig. 18.
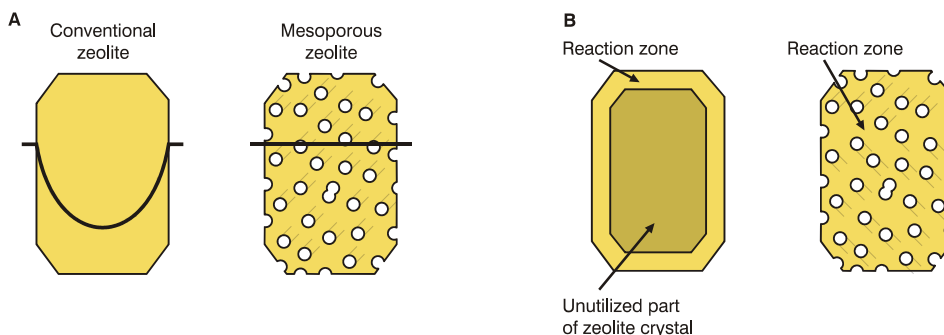

Figure 18. Improved transport properties of mesoporous zeolites over conventional zeolites. Compared to conventional zeolite single crystals, all of the mesoporous zeolite single crystal is utilized efficiently in the catalytic reaction [Adapted from Ref. 59].

Thus, much of the interest in mesoporous zeolites is motivated by the desire to overcome this diffusion limitation by improving the transport of reactants, intermediates and products to and from the active sites located inside the zeolite micropores by creating an additional mesopore system in the zeolite catalyst. As discussed above, mesoporous zeolite crystals combine in each individual crystal, the crystallographic, intracrystalline micropore system typical of zeolites, with a non-crystallographic, intracrystalline mesopore system, resulting in a bimodal pore size distribution [13]. This combination of micro- and mesopores in the mesoporous zeolite catalysts is expected to give rise to improved catalytic activities due the improved diffusion demonstrated in Figs. 15, 16, and 17, which lead to more constant concentration profiles through the mesoporous zeolite crystal during operation in steady-state catalytic reactors. This is shown schematically in Fig. 18a [59]. In the presence of a significant diffusion limitation, the conventional zeolite catalyst can have a very low concentration of reactants in the interior of the zeolite and consequently, only a narrow reaction zone is utilized for catalysis as schematically depicted in Fig. 18b. This is clearly less pronounced or not an issue at all in the mesoporous zeolite crystals.

Mesoporous zeolites as acidic catalysts

Today, there are several examples that the improved transport properties of the mesoporous zeolite catalysts actually results in an increased catalytic activity and/or

selectivity and/or catalyst lifetime [32,66-68]. As an example of an acid-catalyzed reaction, alkylation of benzene with ethylene has been studied in some detail [59,66] using comparable conventional zeolites and mesoporous zeolite crystals prepared by carbon-templating. Alkylation of benzene with ethylene is a major industrial process responsible for production of essentially all ethylbenzene, which in turn is used almost exclusively as an intermediate for styrene production. In the catalytic alkylation of benzene with ethylene to form ethylbenzene, mesoporous H-ZSM-5 zeolite catalysts exhibit both significantly improved catalytic activities and selectivities compared to conventional H-ZSM-5 zeolite catalysts as shown in Fig. 19 [66].

In fact, the selectivity to ethylbenzene is increased by up to 10 % for the mesoporous zeolite catalyst depending on the benzene conversion. The observed activity difference can be attributed to the improved mass transport of reactants and products resulting from the bimodal pore size distribution of the mesoporous catalyst. The ethylbenzene activity measurements were conducted at reaction conditions comparable to those practiced in industrial processes, but generally at somewhat lower conversions. Hence, the observed effect of the enhanced mass transport in the mesoporous catalyst samples could be even larger than shown here.

The experimental evidence for improved mass transfer in mesoporous zeolite catalysts is furthermore supplemented by a classical evaluation of the diffusion properties of ethylbenzene, benzene and ethylene during catalytic ethylation of benzene [59]. The mass transport of both benzene and ethylbenzene in a conventional zeolite single crystal is diffusion-limited whereas in the case of a mesoporous zeolite single crystal, the mass transport of neither benzene nor ethylbenzene is diffusion-limited. Thus, the improved selectivity to the mono-ethylated product is ascribed to the concentration profile of ethylbenzene. In the conventional sample, the ethylbenzene concentration is relatively high in the interior of the single crystal as shown in Fig. 20, thereby favoring formation of di-alkylated (or even poly-alkylated) products. In the mesoporous zeolite crystal, diffusion is so fast that the ethylbenzene concentration throughout the crystal is kept very
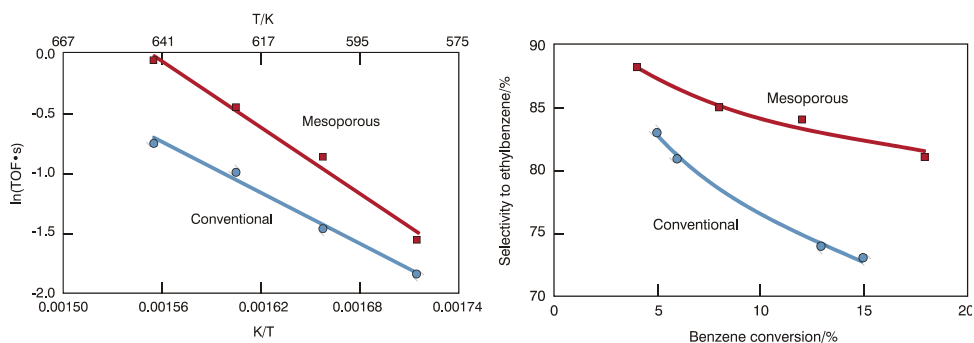

Figure 19. *Left*: Arrhenius plot illustrating the activity difference between conventional and mesoporous H-ZSM-5 zeolite catalysts. The activities are expressed as turn-over frequencies using the Si/Al ratio as a measure of the number of active sites. *Right*: Selectivity to ethylbenzene for mesoporous zeolite and conventional zeolite catalysts obtained at 583-643 K and 2.5 bar [Adapted from Ref. 66].
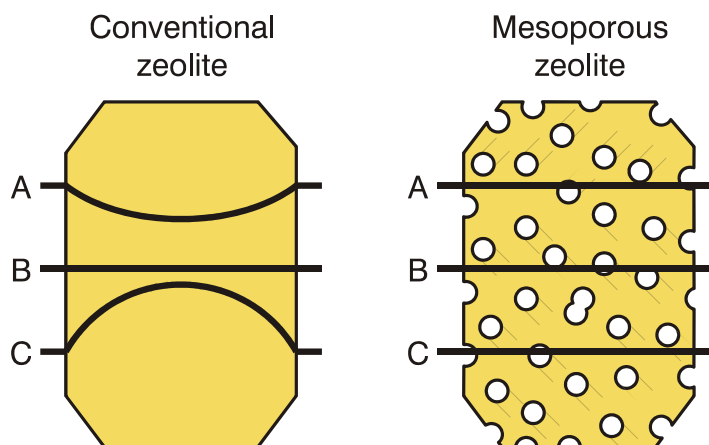
Figure 20. Reactants and product profiles for benzene (A), ethylene (B) and ethylbenzene (C) in the catalytic ethylation of benzene for both conventional and mesoporous zeolite crystal catalysts [Adapted from Ref. 59].

close to that of the gas phase. Consequently, whenever a benzene molecule is ethylated in the mesoporous zeolite catalyst, it can easily diffuse away before it undergoes a second alkylation and thus, di-alkylation is suppressed relatively to that in the conventional sample. Moreover, the entire mesoporous zeolite single crystal is effectively utilized for catalysis with both reactants present in their optimal concentrations throughout the crystal, whereas the interior of the conventional catalyst is partly depleted for benzene. The concentration profiles of benzene (A), ethylene (B) and ethylbenzene (C) under reaction conditions, in both a conventional and a mesoporous zeolite crystal can be illustrated as shown schematically in Fig. 20.

Thus, this illustrates that both improved activity and improved selectivity can be achieved at the same time by utilizing mesoporous zeolite catalysts. Interestingly, completely analogous results were recently reported [26] by use of desilicated mordenite in the liquid-phase alkylation of benzene; see Table 4, entry 1. There are also several other examples of improved performance using mesoporous zeolites. Superior activity of mesoporous H-ZSM-11 zeolite catalyst over comparable conventional zeolite catalyst was reported in the catalytic cracking and isomerization of n-hexadecane, see Table 4, entry 2 [32] and in this particular reaction, it was also shown that both higher activity and better resistance to deactivation could be achieved simultaneously. The reason appears to be that the deactivation is slower since more carbon deposition is required to completely block diffusion in the micropores of the mesoporous zeolite. In other words, there are many pore mouths that must be blocked before the active sites are no longer accessible In another example, the trans-alkylation reaction of biphenyl and p-diisopropylbenzene, recrystallized mordenite catalysts showed improved catalytic activity due to high zeolitic acidity combined with improved accessibility of active sites and easier transport of bulky molecules provided by the presence of mesopores, see Table 4, entry 3 [69]. Most recently, mesoporous ZSM-5 zeolite synthesized using amphiphilic organosilanes as a mesopore-directing agent showed outstanding catalytic activity in jasminaldehyde and

Table 4. Examples of improved performance of acidic mesoporous zeolite catalysts.

Catalytic reaction	Mesopore introduction	Zeolite framework type	Reference
Liquid phase ethylation of benzene	Desilication	Mesoporous MOR	Groen et al. [26]
Catalytic cracking and isomerization	Solid templating	Mesoporous MEL	Kustova et al. [32]
Transalkylation	Assembly of crystals	Mesoporous MOR	Ivanova et al. [69]
Aldol condensation	Supramolecular	Mesoporous MFI	Ryoo et al. [70]
Claisen-Schmidt condensation	Supramolecular	Mesoporous MFI	Ryoo et al. [70]
Methanol to olefins (MTO)	Solid templating	Mesoporous MFI	Janssens et al. [71]

vesidryl syntheses involving large organic molecules in which diffusion constraints and/or adsorption of reactant molecules onto the strong acid sites are normally the main concern; see Table 4, entries 4 and 5 [70].

Deactivation by coke formation is often a serious problem in many industrial processes in which organic molecules are converted over catalysts based on zeolites. Recently, an improved lifetime of mesoporous H-ZSM-5 catalyst over comparable conventional zeolite was also reported in the MTO/MTH (methanol-to-olefins/methanol-to-hydrocarbons) process that converts methanol into olefins or other hydrocarbons [71]. In this reaction, the rate of deactivation is of crucial importance for operating the overall process; see Table 4, entry 6.

Thus, there are already a number of reports suggesting that mesoporous zeolite catalysts can provide important advantages in several acid-catalyzed reactions and probably more will appear in the coming years.

Mesoporous metal-zeolite catalysts

Zeolites can also be used as redox catalysts by proper introduction of redox active metals using either isomorphous substitution of the desired metal ion into the zeolite framework, e.g. Ti, V, Ga, Mn, or by use of charge-compensating transition metal ions such as Cu and Fe in ion-exchange positions [5,61]. In 1983, Taramasso et al. reported the synthesis of the titanium-substituted analogue of silicalite-1 [72], which has later proven to be an extremely useful oxidation catalyst, particularly with aqueous hydrogen peroxide as the oxidant. In these systems, titanium isomorphously substitutes silicon in the framework. Mesoporous titanosilicalite-1 (TS-1) catalysts obtained by the carbon-templating route were shown to be very active in the epoxidation of oct-1-ene and were significantly more active in the epoxidation of cyclohexene than conventional TS-1 [67]. Mesoporous titanosilicalite-2 (TS-2) catalysts also obtained using the carbon-templating

route showed good performance in the epoxidation of oct-1-ene and styrene with regard to selectivity in comparison with conventional microporous catalysts [32]. As an example of the use of redox catalyst with transition metal ions in ion-exchange positions, Cu-exchanged zeolites often show remarkable NO decomposition activities. Since the original discovery of the Cu/ZSM-5 catalysts by Iwamoto and coworkers in 1986 [73], significant efforts have been devoted to the understanding f the reasons for the superior performance of this catalyst in comparison with other copper-containing systems [74,75]. Recently, it was reported that introduction of mesoporosity into the conventional zeolite materials by carbon-templating leads to a significant improvement of the catalytic activity of both Cu/ZSM-5 and Cu/ZSM-11 in direct NO decomposition [76]. Specifically, the mesoporous Cu/ZSM-11 catalyst was found to be about twice as active as the mesoporous Cu-ZSM-5 catalyst. Apparently, it is a preferential formation of the active sites and/or an improved accessibility of the active sites in the mesoporous zeolite crystals, which is responsible for the observed activity increase. Fig. 21 illustrates how the active species located in ion-exchange positions, either as monomeric or dimeric Cu-entities significantly decrease access to the pore system.

Therefore, the introduction of mesopores into the metal-zeolite catalyst is expected to give improved performance even if the reactant and product molecules are very small since in these materials, the active sites can be reached through several different mesopores. As an example of a bifunctional catalyst featuring metal particles dispersed on the zeolite, mesoporous platinum-containing zeolite catalysts prepared by carbon- templating showed good performance in the cracking and isomerization of n- hexadecane, and were significantly more active than similar, conventional zeolite catalysts [77]. Also, Mo-modified zeolite catalysts prepared by desilication had better catalytic performance in the conversion of methane to aromatics than conventional Mo/HZSM-5 catalyst [78]. Some attention has also been devoted to mesoporous Fe-zeolite catalysts for selective catalytic reduction (SCR) and for direct decomposition of N_2O. In a series of comparable mesoporous and conventional Fe/HZSM-5 and Fe/HZSM-12 catalysts with different iron contents, it was shown that with similar Fe contents, the activity of the mesoporous catalyst in NO SCR with NH_3 was significantly higher than for conventional Fe-zeolite samples [79]. Moreover, it was observed that the maximum activity was observed at significantly higher iron-loadings on the mesoporous zeolite than on the conventional zeolite as shown in Fig. 22.
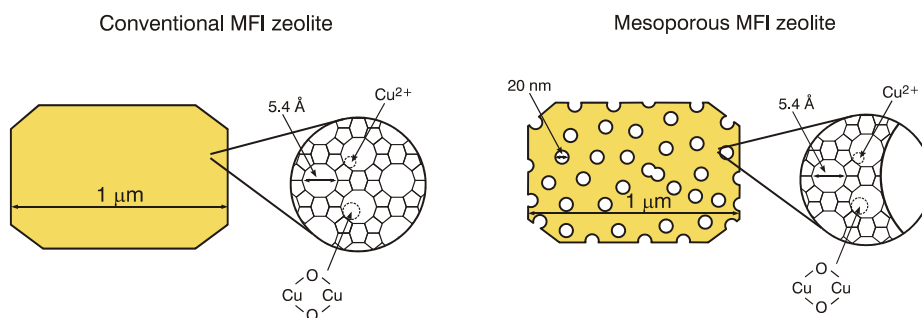

Figure 21. Illustration of the limited accessibility of the active sites in Cu-exchanged MFI-zeolite assuming an active site based on Cu^{2+} or on $Cu_2O_2^{2+}$.
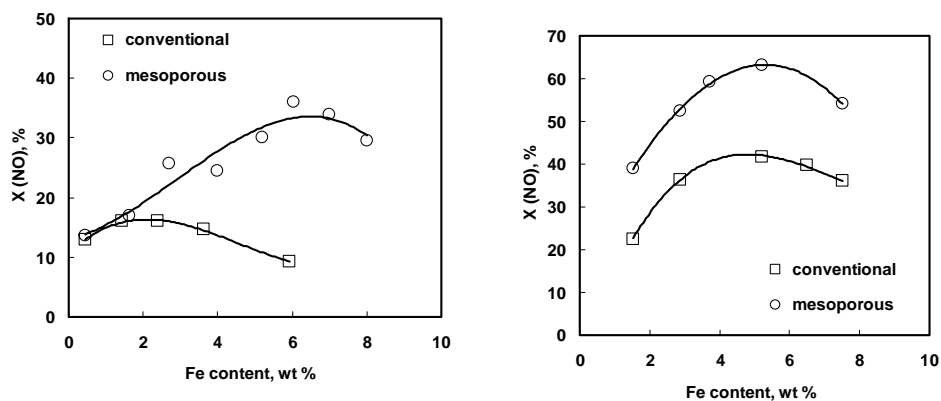
Figure 22. Effect of Fe loading on NO conversion over conventional (○) and mesoporous (□) Fe/HZSM-5 (*left*) and Fe/HZSM-12 (*right*) catalysts. Reaction conditions: 50 mg of catalyst, T=623 K, 1000 ppm NO, 1100 ppm NH_3, 3.5 % O_2, 3% H_2O balanced with N_2 (total flow rate 300 ml/min) [Adapted from Ref. 79].
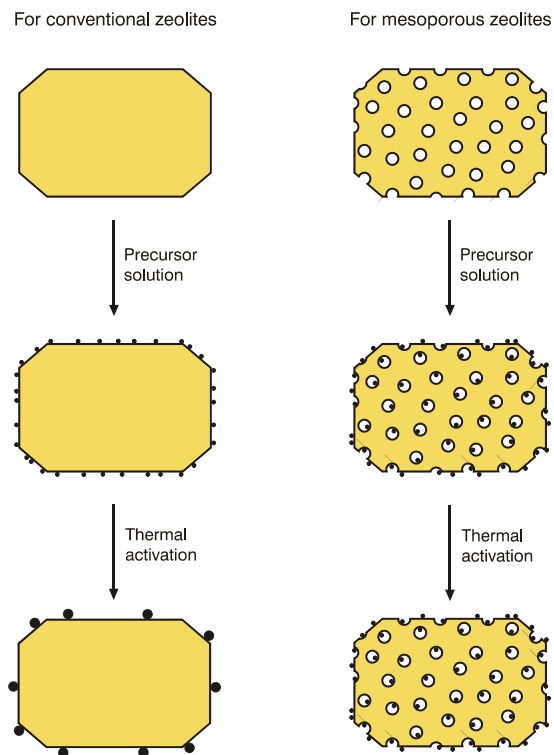

Figure 23. Improved dispersion of a metallic component is possible in a mesoporous zeolite that has a significantly larger external surface area available for the metal (or metal oxide, sulfide, carbide, nitride etc.) [Adapted from Ref. 52].

This strongly suggests that it is easier to disperse a metallic component on a mesoporous zeolite than on conventional zeolite crystals as shown schematically in Fig. 23 [52].

Finally, it was also shown that mesoporous Fe-zeolites prepared by desilication were significantly more active in the decomposition of N_2O than samples prepared from the parent zeolite [80]. Again this was ascribed to a better accessibility of the active sites. Thus, it is clear that also in metal-zeolite catalysts there can be significant advantages associated with the use of a catalyst based on a mesoporous zeolite and further developments seem probable in this area.

5. Summary and outlook

Zeolites and zeotypes are among the most studied families of heterogeneous catalysts and they have been shown to be useful catalysts for an overwhelming range of important catalytic reactions. This success can be attributed to the possibilities for tailoring the intrinsic catalytic properties of zeolites by carefully controlling e.g., the strength and number of acid sites, the pore size and pore geometry, the redox properties etc. However, in many cases the sole presence of micropores in zeolite catalysts results in too low catalytic activities and/or selectivities for industrial applications because of the hindered diffusion of reactants, intermediates and products in the zeolite. Finding ways to circumvent this diffusion limitation has attracted significant attention for many years in both industrial and academic research laboratories. In particular, the possibilities for tailoring the extrinsic properties of the zeolite e.g., by introducing mesopores in otherwise purely microporous crystalline materials to facilitate mass-transport to and from the active sites have been widely investigated. Overall, there are three approaches to achieve such an improved mass transport without altering the microporous structure, namely by the introduction of mesopores in individual zeolites crystals, by the synthesis of nanosized zeolite crystals or by supporting nanosized zeolite crystals on suitable support materials. Here, we have focused our attention on the first approach, which appears to be the most versatile and also the currently most studied procedure to design zeolite catalysts with improved accessibility. Currently, there are two conceptually different methods to synthesize mesoporous zeolite crystals and they were both discovered in industrial laboratories. The first method involves the conventional synthesis of a purely microporous zeolite, which then in one or more post-treatment steps is treated chemically to preferentially extract one of the constituent elements of the zeolite. This can be preferential extraction of aluminum (dealumination), silicon (desilication), or titanium (detitanation). The second method is based on crystallization the zeolite in the presence of an auxiliary mesopore template that is subsequently removed after the crystallization. Typically, the auxiliary mesopore template is carbon, which is removed from the zeolite after crystallization simply during the calcination step that is often required to remove the structure-directing agent necessary to form certain zeolites. It is shown that by these approaches it is possible to a large extent to design zeolites with both carefully controlled intrinsic and extrinsic properties in order to optimize performance in a given catalytic application. With these materials, it is possible to combine many of the typical advantages of zeolite catalysts and catalysts based on mesoporous molecular sieves, such as MCM-41, FSM-16 and SBA-15.

In particular, it is demonstrated that catalysts with *both* improved activity and selectivity can result, and in other cases also catalysts with *both* improved activity and catalyst life-time. Since it is only within the last few years that reproducible preparative routes to these materials have appeared in the open literature, it is anticipated that mesoporous zeolites will continue to attract significant attention in the coming years, and that this will lead to new opportunities for improving current zeolite catalysts but also to extend the number of successful applications of this intriguing family of materials.

6. Acknowledgements

7. References

1. Čejka, J., van Bekkum, H., Corma, A., Schüth, F. (Eds.) 2007, Introduction to Zeolite Science and Technology, 3. ed., Elsevier; Stud. Surf. Sci. Catal. 2007 vol. 168.
2. Weitkamp, J., Ernst, S., Puppe, L. 1999, Catalysis and Zeolites, Springer.
3. Dyer, A., 2007, Stud. Surf. Sci. Catal., 168, 525.
4. Egeblad, K., Christensen, C. H., Kustova, M., Christensen, C. H., 2008, Chem. Mater. Accepted, DOI: 10.1021/cm702224p.
5. Tao, Y., Kanoh, H., Abrams, L., Kaneko, K., 2006, Chem. Rev., 106, 896.
6. van Donk, S., Janssen, A. H., Bitter, J. H., de Jong, K. P., 2003, Catal. Rev., 45, 297.
7. Groen, J.C., Moulijn, J.A., Perez-Ramirez, J. 2006, J. Mater. Chem., 16, 2121
8. Groen, J.C., Peffer, L.A.A., Moulijn, J.A., Perez-Ramirez, J. 2005, Chem. Eur. J., 11, 4983
9. Čejka, J., Mintova, S., 2007, Catal. Rev., 49, 1.
10. Gao, Y. ; Yoshitake, H. ; Wu, P. ; Tatsumi, T. 2004, Micropor. Mesopor. Mater., 70, 93.
11. Pavel, C. C., Schmidt, W., 2006, Chem. Commun. 882.
12. Holland, B.T., Abrams, L., Stein, A. 1999, J. Am. Chem. Soc., 121, 4308.
13. Jacobsen, C.J.H., Madsen, C., Houzvicka, J., Schmidt, I., Carlsson, A. 2000, J. Am. Chem. Soc., 122, 7116.
14. Choi, M., Srivastava, R., Ryoo, R. 2006, Chem. Commun., 42, 4380.
15. Chang, C.D., Chu, C.T.W. 1986, U.S. Patent 4,594,333.
16. Chang, C.D., Chu, C.T.-W., Chu, P., Dessau, R.M., Garwood, W.E., Kuehl, G.H., Miale, J.N., Shihabi, D.S. 1989, U.S. Patent 4,876,228.
17. Pavel, C. C., Park, S. H., Dreier, A., Tesche, B, Schmidt, W., 2006, Chem. Mater., 18, 3813.
18. Janssen, A. H., Koster, A. J., de Jong, K. P., 2001, Angew. Chem. Int. Ed. 40, 1102.
19. Drake, C. A., Wu, A. H., 1999, U.S. Patent 5,952,259.
20. Garces, J. M., Millar, D. M., 1998, U.S. Patent 6,017,508.
21. Dessau, R.M., Valyocsik, E.W., Goeke, N.H. 1992, Zeolites, 12, 776
22. Lietz, G., Schnabel, K. H., Peuker, C., Gross, T., Storek, W., Völter, J., 1994, J. Catal., 148, 562.
23. Ogura, M., Shinomiya, S.Y., Tateno, J., Nara, Y., Kikuchi, E., Matsukata, H. 2000, Chem. Lett., 82.
24. Ogura, M., Shinomiya, S.Y., Tateno, J., Nara, Y., Nomura, M., Kikuchi, E., Matsukata, H. 2001, Appl. Catal. A, 219, 33.
25. Groen, J.C., Peffer, L.A.A., Moulijn, J.A., Perez-Ramirez, J. 2004, Colloids. Surf. A, 241, 53
26. Groen, J. C., Ph. D. Thesis, 2007, Mesoporous Zeolites Obtained by Desilication, Delft University.
27. Groen, J.C., Jansen, J.C., Moulijn, J.A., Perez-Ramirez, J. 2004, J. Phys. Chem. B, 108, 13062.
28. Groen, J.C., Bach, T., Ziese, U., Paulaime-van Donk, A.M., de Jong, K.P., Moulijn, J.A., Perez-Ramirez, A. 2005, J. Am. Chem. Soc., 127, 10792.

29. Kustova, M., Egeblad, K., Christensen, C.H., Kustov, A.L., Christensen, C.H. 2007, Stud. Surf. Sci. Catal., 170A, 267.
30. Janssen, A.H., Schmidt, I., Jacobsen, C.J.H., Koster, A.J., de Jong, K.P. 2003, Micropor. Mesopor. Mater., 65, 59.
31. Schmidt, I., Boisen, A., Gustavsson, E., Ståhl, K., Pehrson, S., Dahl, S., Carlsson, A., Jacobsen, C.J.H. 2001, Chem. Mater., 13, 4416.
32. Kustova, M.Y., Hasselriis, P. and Christensen, C.H., 2004, Catal. Lett., 96, 205.
33. X. Wei, P. G. Smirniotis, 2005, Micropor. Mesopor. Mater., 89, 170.
34. Tao, Y., Kanoh, H., Kaneko, K. 2003, J. Phys. Chem. B, 107, 10974.
35. Egeblad, K., Kustova, M.K., Klitgaard, S.K., Zhu, K., Christensen, C.H. 2007, Micropor. Mesopor. Mater., 101, 214.
36. Kustova, M., Egeblad, K., Zhu, K., Christensen, C.H. 2007, Chem. Mater., 19, 2915.
37. Groen, J.C., Peffer, L.A.A., and Pérez-Ramírez, J., 2003, Mircopor. Mesopor. Mater., 60, 1.
38. Thommes, M., 2007 Stud. Surf. Sci. Catal. 168, 495.
39. Morris, R. E., Wheatley, P. S., 2007, Stud. Surf. Sci. Catal. 168, 375.
40. Terasaki, O., Ohsuna, T., Liu, Z., Sakamoto, Y., Ruan, J., Che, S. 2007, Stud. Surf. Sci. Catal. 168, 477.
41. Lercher, J. A., Jentys, A., 2007, Stud. Surf. Sci. Catal. 168, 435.
42. Gedeon, A., Fernandez, C., 2007, Stud. Surf. Sci. Catal. 168, 403.
43. Sing, K.S.W., Everett, D.H., Haul, R.A.W., Moscou, L., Pierotti, R.A., Rouquérol, J., Siemieniewska, T. 1985, Pure & Appl. Chem., 57, 603.
44. Barret, P., Joyner, L.G., Halenda, P.P. 1951, J. Am. Chem. Soc., 73, 373.
45. Zhu, K., Egeblad, K., Christensen, C.H. 2007, Eur. J. Inorg. Chem., 25, 3955.
46. Wei, X., Smirniotis, P.G. 2006, Micropor. Mesopor. Mater., 97, 97.
47. Lippens, B.C., Linsen, B.G., de Boer, J.H. 1964, J. Catal., 3, 32.
48. Groen, J.C., Brouwe, S., Peffer, L.A.A., Pérez-Ramírez, K., 2006, Part. Part. Syst. Charact., 23, 101.
49. Groen, J.C., Moulijn, J.A., Perez-Ramirez, J. 2007, Ind. Eng. Chem. Res., 46, 4193.
50. Chou, Y.H., Cundy, C.S., Garforth, A.A., Zholobenko, V.L. 2006, Micropor. Mesopor. Mater., 89, 78.
51. Jacobsen, C. J. H., Houzvicka, J., Carlsson, A., Schmidt, I., 2001, Stud. Surf. Sci. Catal., 135, 167.
52. Christensen, C.H., Schmidt, I., Carlsson, A., Johannsen, K., Herbst, K. 2005, J. Am. Chem. Soc., 127, 8098.
53. Tao, Y. S., Kanoh, H., Kaneko, K., 2004, J. Phys. Chem. B, 107, 10974.
54. Kim, S., Shah, J., Pinnavaia, T.J., 2003, Chem. Mater., 15, 1664.
55. Jacobsen, C. J. H., Houzvicka, J., Carlsson, A., Schmidt, I., 2001, Stud. Surf. Sci. Catal. 135,167.
56. Kustova, M.Yu., Kustov, A.L., Christensen, C.H. 2005, Stud. Surf. Sci. Catal., 158B, 255.
57. Groen, J.C., Peffer, L.A.A., Moulijn, J.A., Perez-Ramirez, J. 2004, Micropor. Mesopor. Mater., 69, 29.
58. Groen, J.C., Zhu, W., Brouwer, S., Huynink, S.J., Kapteijn, F., Moulijn, J.A., Perez-Ramirez, J. 2006, J. Am. Chem. Soc., 129, 355.
59. Christensen, C.H., Johannsen, K., Törnqvist, E., Schmidt, I., Topsøe, H. and Christensen, C.H., 2007, Catal. Today, 128, 117.
60. Cundy, C.S. and Cox, P.A., 2003, Chem. Rev., 103, 663.
61. Corma, A., 1997, Chem. Rev., 97, 2372.
62. van Donk, S., Broersma, A., Gijzeman, O.L.J., van Bokhoven, J.A., Bitter, J.H. and de Jong, K.P., 2001, J. Catal., 204, 272.
63. Herrmann, C., Haas, J. and Fetting, F., 1987, Appl. Catal., 35, 299.
64. Pérez-Ramírez, J., Kapteijn, F., Groen, J.C., Domenech, A., Mul, G. and Moulijn, J.A., 2003, J. Catal, 214, 33.

65. Nesterenko, N.S., Thibault-Starzyk, F., Montouillout, V., Yuschenko, V.V., Fernandez, C., Gilson, J.P., Fajula, F. and Ivanova, I.I., 2004, Microporous Mesoporous Mater., 71, 157.
66. Christensen, C.H., Johannsen, K., Schmidt I. and Christensen C.H., 2003, J. Am. Chem. Soc., 125, 13370.
67. Schmidt, I. Krogh, A., Wienberg, K., Carlsson, A., Brorson, M. and Jacobsen, C.J.H., 2000, Chem. Commun., 215.
68. Melian-Cabrera, I., Espinosa, S., Groen, J.C., Linden, B., Kapteijn, F. and Mouljin, J.A., 2006, J. Catal., 238, 250.
69. Ivanova, I.I., Kuznetsov, A.S., Ponomareva, O.A., Yuschenko, V.V. and Knyazeva, E.E., 2005, Stud. Surf. Sci. Catal., 158, 121.
70. Choi, M., Cho, H.S., Srivastava, R., Venkatesan, C., Choi, D. and Ryoo, R., 2006, Nat. Mater. 5, 718.
71. Janssens, T.V.W., Dahl, S., Christensen, C.H., 2006, US Patent 7,078,578.
72. Taramassso, M., Perego, G., Notari, B., 1983, US Patent, 4 410 501.
73. Iwamoto, M., Furukawa, H., Mine, Y., Uemura, F., Mikuriya S., Kagawa, S., 1986, J. Chem. Soc., Chem. Commun., 1272.
74. Iwamoto, M., Yahiro, H., Tanda, K., Mizuno, N., Mine, Y., Kagawa, S., 1991, J. Phys. Chem., 195, 3727.
75. Li, Y., Hall, W. K., 1991, J. Catal., 129, 202.
76. Kustova, M. Yu., Rasmussen, S. B., Kustov, A., Christensen, C. H., 2006, Appl. Catal. B, 67, 60.
77. Christensen, C. H., Schmidt, I., Christensen, C. H., 2004, Catal. Commun., 5, 543.
78. Su, L., Liu, L., Zhuang, J., Wang, H., Li, Y., Shen, W., Xu, Y., Bao, X., 2003, Catal. Lett., 91, 155.
79. Kustov, A. L., Egeblad, K., Kustova, M., Hansen, T. W., Christensen, C. H., 2007, Top. Catal. 45, 159
80. Groen, J. C., Brückner, A., Berrier, E., Maldonado, L., Mouljin, J. A., Perez-Ramirez, J., 2006, J. Catal. 243, 212.

Tailoring the porosity of hierarchical zeolites by carbon-templating

Kake Zhu,[a] Kresten Egeblad,[a] Claus H. Christensen[a]

[a]*Center for Sustainable and Green Chemistry, Department of Chemistry, Technical University of Denmark, Building 206, DK-2800 Lyngby, Denmark*

Abstract

We report the synthesis and characterization of a series of hierarchical porous zeolite single crystal materials with a range of porosities made available by carbon-templating using differently-sized carbon particles as templates for the additional non-micropore porosity. The materials were prepared by adsorption of the required zeolite synthesis gel components onto various commercially available carbon black powders followed by crystallization of the zeolite crystals in the presence of the inert carbon matrix and subsequent removal of the carbon particles embedded in the zeolite crystals by combustion. It is shown that the additional porosity of the hierarchical zeolites can be tailored by encapsulation of the differently-sized carbon particles during crystallization.
Keywords: carbon-templating, mesoporous zeolite single crystals, hierarchical zeolites.

1. Introduction

Hierarchical zeolite crystals featuring intracrystalline porosity in addition to the structural micropore system characteristic of zeolites have attracted significant attention in recent years as a new and growing family of zeolite materials which offers greatly enhanced diffusion properties in comparison with purely microporous zeolites [1-3]. These materials may be prepared by either alkaline treatment of conventional zeolite crystals with certain Si/Al-ratios [4] or by directly crystallizing the zeolite in the presence of an auxiliary carbon matrix which is removed by combustion after synthesis [5-8]. So far, most reports concerning carbon-template synthesis of hierarchical zeolite crystals have focused on the application of 12 nm carbon black particles (BP2000). Here, we describe the synthesis and characterization of a series of hierarchical silicalite-1 crystal materials with different porosities made available by carbon-templating. It is shown that the porosity can be tailored by the use of different carbon particles. Moreover we show that pre-adsorption of sodium citrate onto the carbon powders prior to adsorption of the synthesis gel components leads to zeolites with increased pore volumes and crystal sizes.

2. Experimental

2.1. Sample synthesis

Hierarchical silicalite-1 samples were synthesized by modified literature procedures using different carbon powders as templates. Briefly, carbon powders (Raven carbons, supplied by Columbia Chemical Corporation: RV500, RV1200, RV5000 and RV7000; Black Pearls, supplied by Cabot Corporation: BP2000. See Table 1 for textural properties of the applied carbons and the amounts of carbons in the synthesis gels) were impregnated with mixtures of tetrapropyl ammonium hydroxide (TPAOH, 3.44 g, 40 wt%), water (0.5 g) and ethanol (3.03 g) and left to dry overnight. On the following day,

the carbons were impregnated with tetraethyl orthosilicate (TEOS, 3.87 g) and left to hydrolyze in air overnight before being crystallized under hydrothermal conditions. After crystallization, the organic template and the auxiliary carbon template were removed by combustion.

Table 1. Textural properties of the applied carbon templates.

	RV500	RV1200	RV7000	RV5000[b]	BP2000[c]
Particle size (nm)[a]	53	20	11	8	12
V_{total} (ml/g)	0.07	0.19	0.89	-	1.4
Amount of carbon in gel (g)	11.2	16.0	8.0	3.0	2.0

[a] Carbon particle sizes were taken from the data sheets provided by the suppliers.
[b] RV5000 was heated to 600 °C in N_2 prior to synthesis. RV5000H denotes the sample synthesized from this carbon. For this carbon, the amount of components in the gel were 1.7 g TPAOH, 1.5 g ethanol, 0.3 g H_2O and 2.0 g TEOS.
[c] BP2000 pre-treated in two different ways was used as starting material for two different silicalite-1 materials: BP2000H denotes BP2000 heated to 600 °C in N_2 prior to application in zeolite synthesis; BP2000C denotes BP2000 (4 g) impregnated with sodium citrate (1.5 g in 200 ml H_2O) prior to application in zeolite synthesis.

2.2. Sample characterization

All samples were characterized by X-ray diffraction (XRD), nitrogen physisorption and scanning electron microscopy (SEM) techniques. The XRD measurements were conducted on a Philips PW 3710 X-ray Diffractometer. Nitrogen adsorption and desorption isotherms were measured at liquid nitrogen temperature on a Micromeritics ASAP 2020 apparatus. Prior to physisorption measurements, all samples were outgassed under vacuum at 200 °C overnight. Total surface areas were calculated according to the BET method. Micropore volumes were calculated by the *t*-plot method. Total pore volumes were estimated from the amount of N_2 adsorbed at $p/p_0 = 0.99$. Meso-/macropore volumes were calculated by subtracting micropore volumes from total pore volumes. SEM analyses were performed on a Philips XL20 FEG. The calcined samples were placed on a carbon film and Pt was evaporated on the samples for approximately 20 minutes in order to achieve sufficient conductivity.

3. Results and discussion

All samples produced by the above methods resulted in completely phase-pure zeolite samples. However, all attempts to produce silicalite-1 using RV5000 as the carbon template failed.

The pore size distributions derived from physisorption measurements (desorption data) of the resultant zeolite samples are shown in Fig. 1 and the the data obtained from these measurements are listed in Table 2. For all samples, the isotherms obtained (not shown) are typical type IV isotherms according to the IUPAC classification. As seen in Fig. 1, all samples contain porosity in addition to the micropores characteristic of zeolite structures. From the pore size distribution plots shown in Fig. 1 it is seen that the additional porosity of the zeolite samples are highly dependent on the carbon template as well as the method of pretreatment applied. Application of RV 500 in which the carbon particle size is 53 nm, for instance, resulted in a predominantly macroporous zeolite sample with a very broad pore size distribution centered around 55 nm. Despite the difference in the size of the carbon particles of RV 1200 and RV 7000, 20 and 12 nm, respectively, application of both of these carbons resulted in zeolite samples which contained both mesopores and macropores but for which the pore size distributions (centered around 35 nm) were quite similar. This points to the conclusion that the

porosity is produced from aggregates of carbon particles, which are encapsulated during synthesis rather than from individual carbon particles. From Fig. 1b it is seen that RV5000 and BP2000 carbons pretreated in various ways also can be applied to produce zeolite samples with additional porosity. For instance, application of preheated RV5000 results in a predominantly mesoporous silicalite-1 material with pore size distribution centered around 30 nm whereas application of RV5000 as received from the supplier did not result in silicalite-1 at all. In this case, the preheating probably removes any funtional groups are present on the surface of the carbon, so that these no longer influence the crystallization of the zeolite phase. Also with preheated BP2000 as well as with citrate-pretreated BP2000, it is possible to produce mesoporous silicalite-1 materials, in both cases with pore size distributions centered around 25 nm.

Table 2. Data derived from physisorption measurements (desorption data).

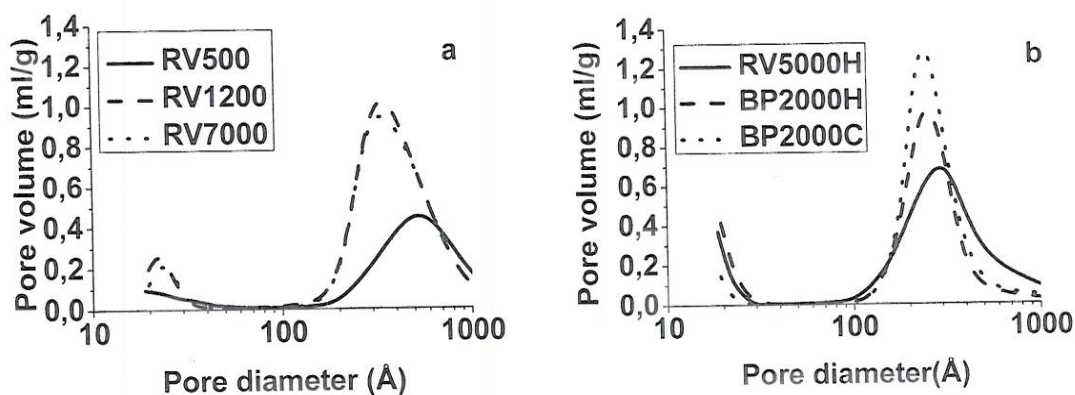|	RV500	RV1200	RV7000	RV5000H	BP2000H	BP2000C
S_{BET} (m^2/g)	405	360	357	391	395	388
V_{total} (ml/g)	0.25	0.55	0.59	0.41	0.37	0.42
V_{micro} (ml/g)	0.14	0.11	0.11	0.079	0.10	0.068
$V_{meso+macro}$ (ml/g)	0.11	0.44	0.48	0.33	0.27	0.35

Figure 1. Pore size distributions of hierarchical silicalite-1 samples synthesized from various carbon precursors (desorption data).

All samples were analysed by SEM in order to study the morphology as well as the homogeneity of the individual crystals. For all zeolite samples, except the one produced from RV5000H, the crystals featured the characteristic sponge-like morphology of carbon-templated mesoporous zeolite single crystals [5]. In Fig. 2, SEM images of the mesoporous zeolite samples produced from RV5000H and BP2000C are shown. Clearly, the RV5000H templated zeolite sample (Fig. 2a) looks different from all the other samples, which are generally very similar in appearance to the BP2000C templated sample (Fig. 2b). This is most likely attributed to the very small particle size of this particular carbon template. The characteristic sponge-like morphology of the other mesoporous zeolite samples, shown for the BP2000C templated material as an example, evidences that the additional porosity of the materials is indeed intracrystalline rather than the result of packing of nanosized zeolite crystals. In general, the crystal sizes of all the materials (RV500, RV1200, RV7000 and BP2000H) were 1-2 μm long, however, as is evident from Fig. 2b, the BP2000C templated crystals are somewhat longer, namely ca. 5 μm. These extraordinarly large crystals, which to our knowledge are the largest carbon-tepmlated mesoporous zeolite crystals reported yet, can only be

explained by the citrate pretreatment method, since application of both BP2000 and BP2000H produced mesoporous materials with crystal sizes of about 2 μm.
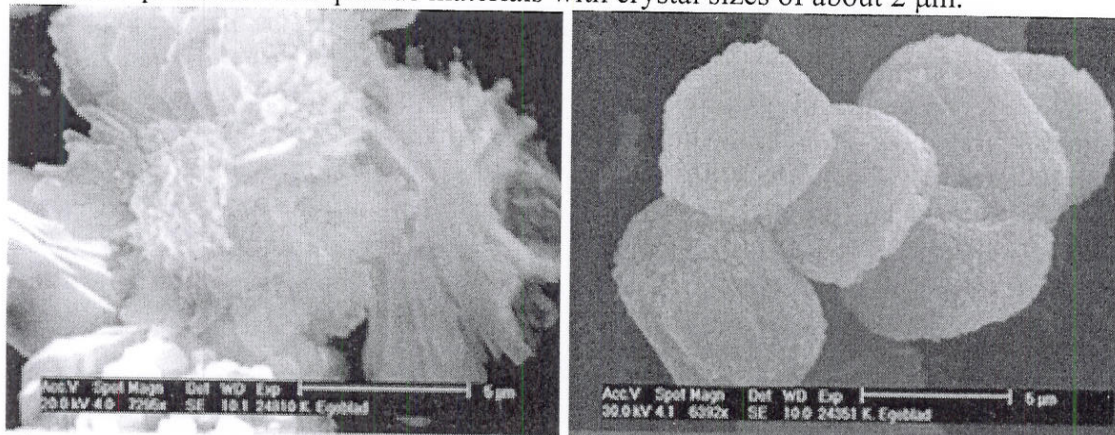

Figure 2. SEM images of RV5000H and BP2000C templated mesoporous zeolite samples.

4. Conclusion

We have shown that hierarachical silicalite-1 samples can be produced by carbon-templating using various commercially available carbons as the pore templates as well as from various pretreated carbon precursors. Using Raven carbons RV500, RV1200 and RV7000 it was possible to produce silicalite-1 with pores in the mesopore and macropore region. Interestingly, direct application of RV5000 as the pore template during zeolite synthesis did not result in a phase-pure zeolite sample. However, application of RV5000 as well as BP2000 preheated in a N_2 atmosphere resulted in mesoporous silicalite-1 samples. This difference is most likely due to the removal of functional groups which interfere with zeolite crystallization from the surface of the RV5000 carbon. In this study we have also shown, that pretreatment of BP2000 with sodium citrate affects crystallization in the carbon matrix since the mesoporous silicalite-1 crystals produced from this carbon are significantly larger than those obtained using unmodified BP2000.

Acknowledgements

References

[1]   Y. Tao, H. Kanoh, L. Abrams, K. Kaneko, , Chem. Rev., 106 (2006) 896
[2]   C.H. Christensen, K. Johannsen, I. Schmidt, C.H. Christensen, , J. Am. Chem. Soc., 125 (2003) 13370.
[3]   J.C. Groen, W. Zhu, S. Brouwer, S.J. Huynink, F. Kapteijn, J.A. Mouljin, , J. Am. Chem. Soc., 129 (2007) 355.
[4]   J.C. Groen, J.A. Moulijn, J. Perez-Ramirez, , J. Mater. Chem., 16 (2006) 2121.
[5]   C.J.H. Jacobsen, C. Madsen, J. Houzvicka, I. Schmidt, A. Carlsson, , J. Am. Chem. Soc., 122 (20007) 116.
[6]   K. Egeblad, C.H. Christensen, M. Kustova, C.H. Christensen, , Chem. Mater., 20 (2008) 946.
[7]   K. Egeblad, M. Kustova, S.K. Klitgaard, K. Zhu, C.H. Christensen, , Micropor. Mesopor. Mater. , 101 (2007) 214.
[8]   M. Kustova, K. Egeblad, K. Zhu, C.H. Christensen, 2007, Chem. Mater., 19, 2915

Mesoporous Carbon Prepared from Carbohydrate as Hard Template for Hierarchical Zeolites

Kake Zhu,[a] Kresten Egeblad,[a] and Claus Hviid Christensen*[a]

A mesoporous carbon prepared from sucrose was successfully employed as a hard template to produce hierarchical silicalite-1, thus providing a very simple and inexpensive route to desirable zeolite catalysts from widely available raw materials. The porous carbon was prepared by hydrothermal treatment of a mixture of sucrose and ammonia followed by carbonization of the mixture in N_2 at high temperatures. The porous carbon produced by this method was subsequently applied as a hard template in the synthesis of mesoporous silicalite-1 and removed by combustion after synthesis. X-ray diffraction (XRD), scanning electron microscopy (SEM), transmission electron microscopy (TEM), selected-area electron diffraction (SAD), thermal gravimetry (TG), differential scanning calorimetry (DSC), N_2 physisorption measurements, Hg porosimetry and CHN elemental analysis techniques were applied to investigate the porous carbon template as well as the mesoporous zeolite single-crystal material.

(© Wiley-VCH Verlag GmbH & Co. KGaA, 69451 Weinheim, Germany, 2007)

Introduction

Zeolites constitute an important class of crystalline microporous solids due to their widespread application in adsorption, separation and catalysis. Their importance stems from their unique pore structures, which make them highly selective to adsorbed molecules for separation purposes, or towards product molecules in catalysis. Moreover, they exhibit good thermal and hydrothermal stabilities during heterogeneous catalytic reactions.[1,2] However, the pore sizes of zeolites or zeolite-type materials, which are smaller than 1.5 nm, often restrict their applications due to diffusion limitations.[3]

Many strategies have been developed to overcome this problem, e.g. synthesizing larger-pore zeolite structures[4] and mesoporous molecular sieves,[5] reducing the size of the individual zeolite crystals,[6] subjecting the prepared zeolite to post-treatments like dealumination[7] and desilication,[8] as well as various hard template routes, where the template is removed after synthesis.[9] Naturally, pores created by post synthesis chemical treatments are highly dependant on the composition and structure of the original material, and a zeolite material consisting of nanosized crystals causes problems with handling during its applications. On the other hand, hard-template methods produce mesoporous zeolites with controlled porosity independent of their composition and structure, and have thus provided a general approach to solve this problem. So far, carbon blacks,[10] multiwalled carbon nanotubes,[11] carbon nanofibers,[12] carbon mesoporous molecular sieves,[13] carbon aerogels,[14–15] polymer aerogels,[16] and very recently mesoscale cationic polymers[17] have been utilized to fabricate zeolite materials which have a hierarchical pore system of intracrystalline mesopores interconnected with the conventional micropores.

Recently, mesoporous carbons have found application as hard templates for the production of very porous metal oxides such as Al_2O_3[18] and MgO.[19] Furthermore, also binary metal oxides like $MgAl_2O_4$ have been successfully prepared by this strategy.[20] More importantly, mesoporous carbons can also be employed to cast hierarchical-porous zeolites with tailored mesoporosities.[14–16] Mesoporous carbons are conventionally prepared by carbonization of a carbon precursor on a mesoporous silica template such as MCM-48,[21] SBA-15,[22] or amorphous silica,[23,24] which is subsequently removed by dissolving it in either HF or NaOH. Another category of mesoporous carbons are the carbon aerogels, which are prepared by pyrolysis of resorcinol/formaldehyde aerogels in an inert gas at high temperatures.[25–27] These methods are very costly and/or tedious. Preparation of an aerogel, for instance, entails supercritical fluid treatments making it both expensive and complex in preparation. In this paper, we report a simple and convenient way to prepare a mesoporous carbon template and its application in the synthesis of mesoporous silicalite-1. Contrary to the previously reported methods that typically rely on the availability of special and often expensive mesoporous carbons obtained from only a few suppliers, the present method only involves chemicals that are widely

[a] Center for Sustainable and Green Chemistry, Department of Chemistry, Technical University of Denmark, Building 206, 2800 Lyngby, Denmark
E-mail: chc@kemi.dtu.dk

K. Zhu, K. Egeblad, C. H. Christensen

available. The starting materials used here, sucrose and ammonia, are very inexpensive in comparison with aerogel precursors, and no sacrificial silica is needed. As carbon blacks are normally 100 times more expensive than sucrose, the outstanding features of the reported method are its simplicity, convenience and inexpensiveness.

Results and Discussion

Mesoporous Carbon Template

After hydrothermal treatment of a mixture of sucrose and ammonia for 2 d, a brown solid was obtained. N_2 physisorption measurements of this brown solid showed that it has a surface area of 34 m^2/g. In Figure 1 is shown a photographic image of the brown solid. It can be seen, that the brown solid retains the shape of the Teflon beaker in which it was produced and this allows for formation of larger zeolite objects though controlled templating.

Figure 1. Photographic image of the brown solid obtained after hydrothermal treatment of a mixture of sucrose and ammonia in a Teflon beaker. The porous carbon maintains the shape of the beaker.

From the TG and DSC measurements of the brown solid, shown in Figure 2, it can be seen that a major weight loss occurs between 400 and 500 °C. This is due to dehydration of the sucrose during decomposition. Above 500 °C, several endothermic peaks appear in the DSC profile. These are due to carbonization of the decomposed sucrose, since carbonization is an endothermic process. Hydrothermal treatment of the sucrose and ammonia mixture is necessary to obtain a porous carbon, because heating of sucrose directly causes melting and more complex decomposition, which results in non-porous carbon after thermal decomposition.
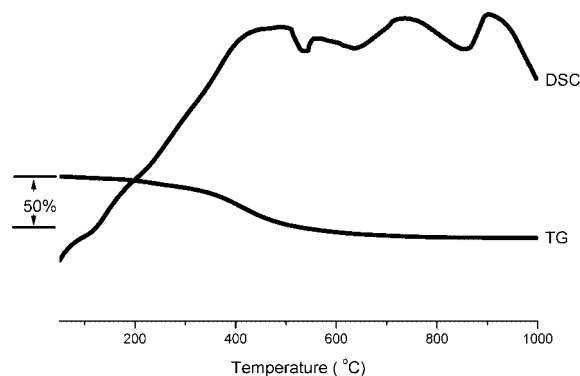

Figure 2. TG and DSC profiles of the solid obtained after hydrothermal treatment of a mixture of sucrose and ammonia.

Thermal decomposition of the brown solid at 850 °C in N_2 resulted in a porous black solid. This solid contained (by weight) 86.5% C, 1.17% N and 1.25% H, as examined by CHN elemental analysis. Thus, even after carbonization, minor amounts of nitrogen and hydrogen are present in the carbonaceous material. The remaining mass of the sample is most likely oxygen, which is not detected by this technique. Oxygen could easily be present in the carbonaceous material in the form of hydroxy groups.

N_2 adsorption and desorption isotherms of the porous black solid are shown in Figure 3. It can be seen that the isotherm contains a hysteresis loop which starts at a relative pressure of 0.8 and then rises dramatically with increasing pressure. According to the IUPAC classification of physisorption isotherms, isotherms featuring this type of hysteresis loops are classified as type IV isotherms, and are characteristic of mesoporous materials. From Figure 3 it is also evident, that the pore size distribution of the porous carbon is quite broad beginning at 10 nm and ending at more than 100 nm. Since the BET surface area of the carbon material presented here is only 416 m^2/g (further results from the physisorption analyses are listed in Table 1), the material is not superior to the known carbon aerogels, which possess surface areas above 1000 m^2/g and narrow pore size distributions.[27]
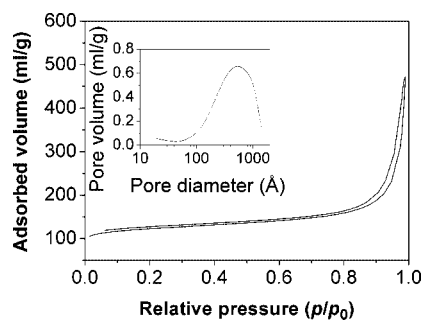

Figure 3. Nitrogen adsorption/desorption isotherms of the porous carbon obtained by carbonizing sucrose. The inset shows the pore size distribution obtained from the desorption branch of the isotherm using the BJH method.

Table 1. Surface area and porosity analyses of the mesoporous carbon template and the mesoporous silicalite-1 material obtained from it.[a]

	S_{BET} [m^2/g]	Micropore vol. [cm^3/g]	Meso- + macropore vol. [cm^3/g]	Mesopore size [nm]
Carbon	416	0.13	0.60	ca. 53
Meso silicalite-1	403	0.09	0.37	ca. 31

[a] The micropore volume is estimated from a t plot (DeBoer) and total pore volumes were calculated based on volume adsorbed at a relative pressure of $p/p_o = 0.99$, volumes of mesoporosity and macroporosity are calculated accordingly.[15]

However, given that the mesoporous carbon prepared in this way works well as a template in the synthesis of hierarchical zeolites, as will be shown later, the specific porosity properties of the material are not important.

Mesoporous Silicalite-1

After crystallization of a zeolite gel mixture adsorbed on the porous carbon and subsequent calcination of the crude product in air, a white powder was obtained. The XRD pattern obtained for this powder is shown in Figure 4: the material contains exclusively highly crystalline MFI-structured material, since no peaks from other crystalline materials are observed in the pattern and there is no amorphous background. Thus, the prepared sample is a phase-pure silicalite-1 material. The peaks in the XRD diagram shown in Figure 4 are broader than the peaks observed in XRD patterns of conventional microporous ZSM-5 samples (also of MFI framework structure). This appears to be a general phenomenon in all XRD patterns of mesoporous zeolites produced by carbon templating. Even though the overall crystal sizes are similar in conventional and mesoporous samples, the XRD line width of the mesoporous samples always shows significant broadening. Thus, it is not possible to differentiate between nanosized and mesoporous zeolite samples from XRD analyses alone. However, the line broadening is still indicative of the porous carbon functioning as a chemically inert hard template during the crystallization of the zeolite.
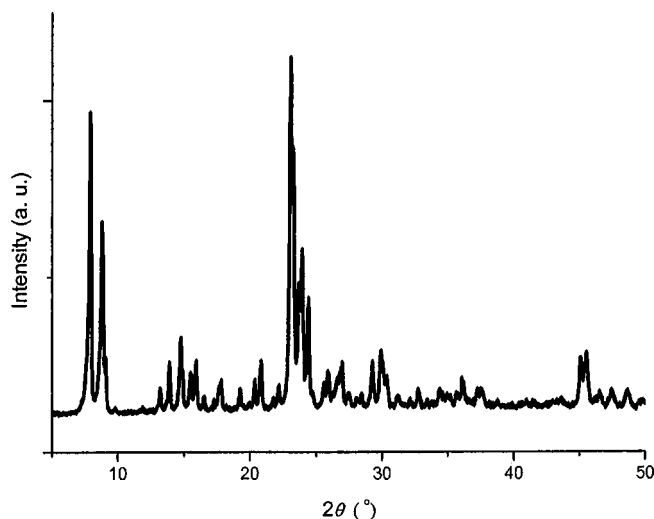
In Figure 5 is shown the nitrogen physisorption isotherms of the mesoporous silicalite-1 material. It can be seen, that the isotherms contain two hysteresis loops, one at relative pressure below 0.4 and one starting at relative pressure 0.9. The hysteresis loop at a low relative pressure is commonly observed for microporous silicalite-1 and results from a phase transformation of dinitrogen inside the micropores of the pure silica MFI structure.[9] The hysteresis loop starting at a relative pressure of 0.9 is a type IV isotherm, which indicates that the material contains mesoporosity. Besides a micropore volume of 0.09 mL/g, the material contains an additional pore volume of 0.37 mL/g, attributable to mesopores and macropores. This is calculated from the total volume of N$_2$ adsorbed by the material at a relative pressure of $P/P_o = 0.99$. The pore size distribution of the mesoporous silicalite-1 is relatively narrow and centered at 31 nm, which is comparable to mesoporous zeolites prepared from other carbon templates.[10,14–16] The findings from nitrogen physisorption are completely verified by Hg intrusion data, which also reveal that some larger macropores, which cannot be seen efficiently by physisorption, are present. They are attributed to intercrystal voids in the material. The similarity of the physisorption data and the Hg porosimetry data confirms what has been found before: the pore system of the zeolite consists of an interconnected and homogeneously distributed system of intracrystalline mesopores that completely penetrate the crystals. Thus, since the newly developed procedure presented here clearly produces a hierarchical microporous/mesoporous material, which exhibits porosity similar to that of mesoporous silicalite-1 materials prepared using carbon blacks[10] and carbon aerogels as templates,[14–16] it is preferable when considering the complex nature of the carbon aerogel preparation and its high cost.

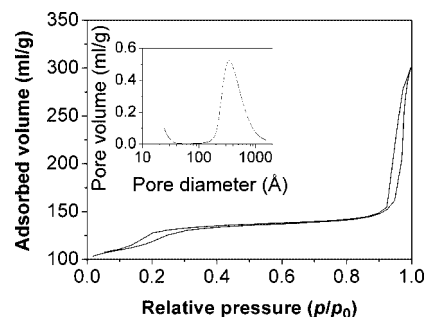Figure 4. XRD pattern of the prepared silicalite-1 material.

Figure 5. Nitrogen adsorption/desorption isotherms of the mesoporous zeolite silicalite-1 material after combustion of the carbon and organic templates. The inset shows the pore-size distribution obtained from the desorption branch of the isotherm using the BJH method.

A comparison of the pore-size distributions of the porous carbon and the silicalite-1 material (Figures 3 and 5) clearly points out that a mesoporous zeolite with a relatively narrow pore size distribution can be produced from a porous carbon having a much more broad pore size distribution. This suggests that the mesoporous silicalite-1 crystals start to grow inside the pores of the carbon matrix and during crystallization gradually encapsulate the carbon. Thus, since the porosity of the zeolite is a negative replica of the carbon template, the specific pore size distribution of this template is less important. This tendency has also been observed for mesoporous zeolites templated from different carbon blacks, since not all carbon blacks are able to efficiently produce mesoporous zeolites.[12] In this light, the route to mesoporous zeolites presented here is superior to carbon-black-based methods because, using the method reported here, it is not possible to alter the porosity of the carbon matrix by pushing aside the carbon particles during zeolite growth.

Figure 6 shows the results of SEM analyses of the prepared mesoporous silicalite-1 after combustion of the carbon and organic templates. Figure 6a shows a low-magnification SEM image of the prepared material: the sample contains only impressively homogeneously sized single crystals, which can be seen all over the sample. From the higher resolution images, shown in Figure 6b–d, it can easily be seen that the single crystals are all sponge-like in appearance, which is a characteristic feature of mesoporous zeolites. Moreover, the coffin-like morphology exhibited by the mesoporous single crystals is typical of MFI-structured crystals. Furthermore, this mesoporous silicalite-1 material is quite similar to the one reported by Jacobsen using commercially available carbon black as hard template,[10] and it is different from carbon-aerogel-templated mesoporous silicalite-1 which contains a mixture of nanosized crystals and larger mesoporous monocrystals.[14] However, in the carbon-aerogel-templated systems the zeolite properties can be influenced by the crystallizations conditions.[14–16] This can probably be ascribed to different crystallization kinetics in the various carbon matrix materials. Thus, zeolite crystallization in the confined space of the carbons leads to nanosized crystals instead of the mesoporous crystals obtained when the zeolite encapsulates the carbon particles. From the SEM analyses of the prepared zeolite material it is concluded that the present sample contains exclusively mesoporous silicalite-1 single crystals. Here, we only show the use of a specific carbon produced by carbohydrate decomposition. However, it can be envisaged that a wide range of different carbons can be produced with this approach, and that could lead to possibilities for tuning the zeolite mesopore size just as it is possible with different carbon black materials.
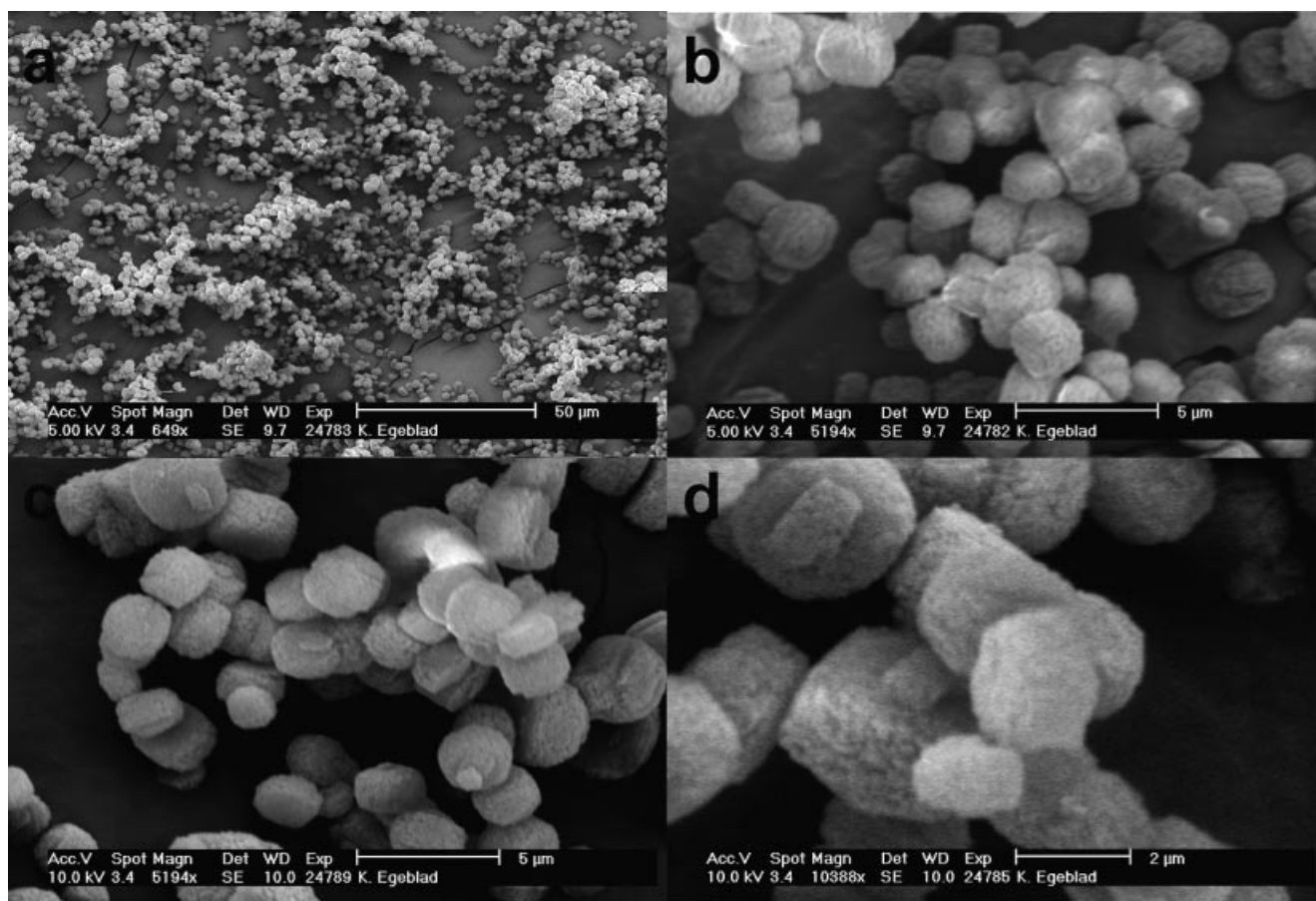

Figure 6. SEM images of the mesoporous silicalite-1 single crystals at different magnifications.

From the TEM images of the prepared mesoporous silicalite-1 material shown in Figure 7 it is evident, that the material does indeed consist of mesoporous single crystals as the sponge-like coffin shape is readily identifiable in these images. The close-up TEM image shown in Figure 7b along with the SAD pattern shown in its inset unambiguously confirms the single-crystalline nature of the materials.
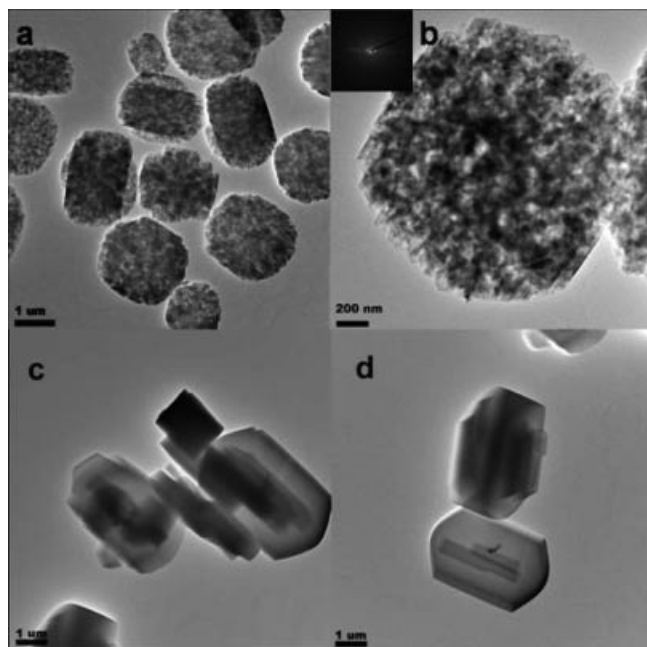

Figure 7. TEM images of the mesoporous silicalite-1 single crystals. The inset in (b) shows the SAD pattern of the area marked by a circle in the image, c) and d) show images of analogously prepared zeolite without the carbon template.

Conclusions

Mesoporous zeolite single crystals of MFI structure were synthesized from cheap and readily available starting materials using a newly developed and very simple procedure in which an in-situ prepared mesoporous carbon is used as a mesopore template during synthesis and subsequently removed by combustion. XRD, SEM, TEM, SAD and N_2 physisorption measurements of the prepared zeolite material showed that the material contained exclusively mesoporous silicalite-1 single crystals, which are very similar to those obtained using much more expensive carbon black as the mesopore template. N_2 physisorption measurements of the carbon template showed that this material was in fact mesoporous, although not as porous as carbon aerogels. However, since the carbon template can obviously be used for the synthesis of mesoporous zeolite single crystals, the specific porosity of the carbon template is perhaps not so important. Nevertheless, understanding the mechanisms leading to the mesoporous carbon as well as its specific role in templating mesoporous zeolites might lead to mesoporous zeolites with even better properties. In all, the simple procedure presented here, combined with the comparatively cheap carbon matrix, make this method attractive for the synthesis of other zeolite or zeolite-type structures or perhaps even other oxide materials.

Experimental Section

Hierarchical microporous/mesoporous silicalite-1 single crystals were obtained after combustion of a zeolite/carbon composite material, prepared by first producing a mesoporous carbon template material onto which the necessary zeolite gel components were impregnated and subjected to hydrothermal conditions.

The porous carbon template was prepared by dissolving 13.1 g of sucrose (98%, Aldrich) in a mixture of 9.6 mL of EtOH (absolute), 7.5 mL of H_2O (deionized) and 1.0 mL of ammonia (25 wt.-%, Fluka) whilst stirring at 50 °C for 1.5 h. The material was transferred to a Teflon beaker and hydrothermally treated at 180 °C for 2 d, producing a brown solid which retained the shape of the beaker. The brown solid was crushed in a mortar and transferred to a horizontal tube furnace and heated to 850 °C in a flow of N_2 for 5 h to afford a porous black carbonaceous solid.

Mesoporous silicalite-1 single crystals were prepared by sequentially impregnating the necessary zeolite gel components onto the porous black carbonaceous solid. First, a mixture of 3.4 g of TPAOH (tetrapropylammonium hydroxide, 40 wt.-%, Aldrich) and 2.0 mL of EtOH was impregnated onto 2.5 g of porous black solid and the mixture was dried in air under ambient conditions overnight. Then, the material was impregnated with 3.0 mL of TEOS (tetraethyl orthosilicate, 98%, Aldrich) which was allowed to hydrolyze in air for 1 d. After aging, the material was transferred to a Teflon beaker which was placed inside a Teflon-lined autoclave with 10.0 mL of H_2O added outside the beaker. The autoclave was hydrothermally treated at 180 °C for 3 d before the carbon and organic templates were removed by combustion at 550 °C for 24 h.

XRD was performed with a Philips PW 3710 X-ray diffractometer using Cu-K_α radiation (λ = 0.154 nm) in the 2θ range between 5 and 50° at a scanning speed of 0.6°/min.

Nitrogen adsorption/desorption isotherms were collected at liquid-nitrogen temperature (–196 °C) with a Micromeritics ASAP 2020. All samples were outgassed under vacuum at 200 °C overnight prior to measurement. The total surface area was calculated according to the BET method. Mesopore volumes were determined by the BJH method from the desorption branch of the isotherms, while micropore volumes and external surface areas were determined by using a t-plot analysis.

Hg porosimetry was measured by intrusion using a Quantachrome equipment.

SEM was performed with a Philips XL20 FEG. The calcined zeolite samples were placed on a carbon film and Pt was evaporated onto the sample for approximately 20 min to achieve sufficient conductivity.

TEM was performed with a JEM 2000FX using an accelerating voltage of 300 kV. SAD was used to obtain electron diffraction patterns from individual grains of powder. A few mg of the powdered samples were suspended in 2 mL of ethanol, and the suspension was sonicated for 1 h. Then, the suspension was allowed to settle for 15 min, before a drop was taken and dispersed on a 300 mesh copper grid coated with holey carbon film.

TG and DSC were conducted with NETZSCH STA 409 PC/PG equipment with a ramp of 20 °C/min under a nitrogen flow of 20 mL/min.

CHN elemental analysis was performed with a CE Instruments FLASH 1112 Series EA.

Acknowledgments

[1] D. W. Breck, *Zeolite Molecular Sieves*, Wiley, New York, **1974**.
[2] A. Corma, *Chem. Rev.* **1997**, *97*, 2373–2420.
[3] J. Kaerger, D. M. Ruthven, *Diffusion in Zeolites and Other Microporous Materials*, Wiley, New York, **1992**.
[4] A. G. Dong, Y. J. Wang, Y. Tang, Y. H. Zhang, N. Ren, Z. Gao, *Adv. Mater.* **2002**, *14*, 1506–1510.
[5] C. T. Kresge, M. E. Leonowicz, W. J. Roth, J. C. Vartuli, J. S. Beck, *Nature* **1992**, *359*, 710–712; D. Y. Zhao, J. L. Feng, Q. S. Huo, N. Melosh, G. H. Fredrickson, B. F. Chmelka, G. D. Stucky, *Science* **1998**, *279*, 548–552.
[6] L. Tosheva, V. P. Valtchev, *Chem. Mater.* **2005**, *17*, 2494–2513.
[7] M. Boveri, C. Marquez-Alvarez, M. A. Laborde, E. Sastre, *Catal. Today* **2006**, *114*, 217–225.
[8] J. C. Groen, J. A. Moulijn, J. Perez-Ramirez, *J. Mater. Chem.* **2006**, *16*, 2121–2131.
[9] Y. S. Tao, H. Kanoh, L. Abrams, K. Kaneko, *Chem. Rev.* **2006**, *106*, 896–910.
[10] C. J. H. Jacobsen, C. Madsen, J. Houzvicka, I. Schmidt, A. Carlsson, *J. Am. Chem. Soc.* **2000**, *122*, 7116–7117.
[11] I. Schmidt, A. Boisen, E. Gustavsson, K. Stahl, S. Pehrson, S. Dahl, A. Carlsson, C. J. H. Jacobsen, *Chem. Mater.* **2001**, *13*, 4416–4418.
[12] A. H. Janssen, I. Schmidt, C. J. H. Jacobsen, A. J. Koster, K. P. de Jong, *Microporous Mesoporous Mater.* **2003**, *65*, 59–75.
[13] Z. Yang, Y. Xia, R. Mokaya, *Adv. Mater.* **2004**, *16*, 727–732.
[14] Y. Tao, H. Kanoh, K. Kaneko, *J. Am. Chem. Soc.* **2003**, *125*, 6044–6045.
[15] W. C. Li, A. H. Lu, R. Palkovits, W. Schmidt, B. Spliethoff, F. Schuth, *J. Am. Chem. Soc.* **2005**, *127*, 12595–12600.
[16] Y. Tao, H. Kanoh, K. Kaneko, *Langmuir* **2005**, *21*, 504–507.
[17] F. S. Xiao, L. F. Wang, C. Y. Yin, K. F. Lin, Y. Di, J. X. Li, R. R. Xu, D. S. Su, R. Schlogl, T. Yokoi, T. Tatsumi, *Angew. Chem. Int. Ed.* **2006**, *45*, 3090–3093.
[18] W. C. Li, A. H. Lu, W. Schmidt, F. Schuth, *Chem. Eur. J.* **2005**, *11*, 1658–1664.
[19] J. Roggenbuck, M. Tiemann, *J. Am. Chem. Soc.* **2005**, *127*, 1096–1097.
[20] W. C. Li, M. Comotti, A. H. Lu, F. Schuth, *Chem. Commun.* **2006**, 1772–1774.
[21] M. Kruk, M. Jaroniec, R. Ryoo, S. H. Joo, *J. Phys. Chem. B* **2000**, *104*, 7960–7968.
[22] H. J. Shin, R. Ryoo, M. Kruk, M. Jaroniec, *Chem. Commun.* **2001**, 349–350.
[23] S. J. Han, M. Kim, T. Hyeon, *Carbon* **2003**, *41*, 1525–1532.
[24] K. Bohme, W. D. Einicke, O. Klepel, *Carbon* **2005**, *43*, 1918–1925.
[25] V. Bock, A. Emmerling, R. Saliger, J. Fricke, *J. Porous Mater.* **1997**, *4*, 284–297.
[26] R. W. Pekala, C. T. Alviso, F. M. Kong, S. S. Hulsey, *J. Non-Cryst. Solids* **1992**, *145*, 90–98.
[27] Y. Tao, H. Tanaka, T. Ohkubo, H. Kanoh, K. Kaneko, *Adsorpt. Sci. Technol.* **2003**, *21*, 199–203.

Communications

Versatile Route to Zeolite Single Crystals with Controlled Mesoporosity: in situ Sugar Decomposition for Templating of Hierarchical Zeolites

Marina Kustova, Kresten Egeblad, Kake Zhu, and Claus H. Christensen*

Center for Sustainable and Green Chemistry, Department of Chemistry, Technical University of Denmark, Kemitorvet, Building 206, DK-2800 Lyngby, Denmark

Zeolites are among the most widely used industrial catalysts.[1] Their superior performance can often be attributed to the existence of a well-defined system of micropores (size below 2 nm diameter) with uniform shape and size, typically of molecular dimensions. However, for some applications, the sole presence of such micropores can also result in an unacceptably slow diffusion of reactants and products to and from the active sites located inside the zeolite crystals. In such cases, a diffusion limitation is imposed on the reaction rate.[2] To overcome this limitation, researchers have pursued several different preparative strategies. One possibility is to minimize the size of the zeolite crystals,[3-6] which is often in the range of $0.5-50$ μm, and thereby shorten the diffusion path. Another possibility is to increase the pore size of the zeolite, and this approach has led to the discovery of novel

zeolites with larger pores[7-10] and ordered mesoporous materials.[11,12] The most common and successful approach so far is to introduce an additional system of mesopores (sizes between 2 and 50 nm) into each individual zeolite crystal. This is typically done by suitable posttreatments such as dealumination,[13,14] and desilication.[15-17] Recently, it was shown that mesopores can be introduced directly into the zeolite crystals, without a partially destructive posttreatment, simply by conducting the crystallization in the presence of a mesoporous carbon material.[18] The carbon particles are encapsulated by the zeolite crystals during growth. After complete crystallization, the carbon is easily removed by combustion to produce highly mesoporous zeolite single crystals that combine some of the most desirable catalytic properties of zeolites and mesoporous molecular sieves.[19]

* Corresponding author. E-mail: chc@kemi.dtu.dk.

(1) Corma, A. *Chem. Rev.* **1995**, *95*, 559.
(2) Hartmann, M. *Angew. Chem., Int. Ed.* **2004**, *43*, 5880.
(3) Jacobs, P. A.; Derouane, E. G.; Weitkamp, J. *J. Chem. Soc., Chem. Commun.* **1981**, 591.
(4) Camblor, M. A.; Corma, A.; Valencia, S. *Microporous Mesoporous Mater.* **1998**, *25*, 59.
(5) Jacobsen, C. J. H.; Madsen, C.; Janssens, T. V. W.; Jakobsen, H. J.; Skibsted, J. *Microporous Mesoporous Mater.* **2000**, *39*, 393.
(6) Tosheva, L.; Valtchev, V. P. *Chem. Mater.* **2005**, *17*, 2494.

(7) Davis, M. E.; Saldarriaga, C.; Montes, C.; Garces, J.; Crowder, C. *Nature* **1988**, *331*, 698.
(8) Freyhard, C. C.; Tsapatsis, M.; Lobo, R. F.; Balkus, K. J. *Nature* **1996**, *381*, 295.
(9) Wessels, T.; Baerlocher, C.; McCusker, L. B.; Creyghton, E. J. *J. Am. Chem. Soc.* **1999**, *121*, 6242.
(10) Corma, A.; Diaz-Cabanas, M.; Martinez-Triguero, J.; Rey, F.; Rius, J. *Nature* **2002**, *418*, 514.
(11) Kresge, C. T.; Leonowicz, M. E.; Roth, W. J.; Vartuli, J. C.; Beck, J. S. *Nature* **1991**, *359*, 710.
(12) Zhao, D.; Feng, J.; Huo, Q.; Melosh, N.; Fredrickson, G. H.; Chmelka, B. F.; Stucky, G. D. *Science* **1998**, *279*, 548.
(13) Donk, S.; Janssen, A. H.; Bitter, J. H.; Jong, K. P. *Catal. Rev.* **2003**, *45*, 297.
(14) Dutartre, R.; De Menorval, L. C.; Di Renzo, F.; McQueen, D.; Fajula, F.; Schulz, P. *Microporous Mater.* **1996**, *6*, 311.
(15) Ogura, M.; Shinomiya, S. H.; Tateno, J.; Nara, Y.; Kikuchi, E.; Matsukata, M. *Chem. Lett.* **2000**, 882.
(16) Groen, J. C.; Peffer, L. A. A.; Moulijn, J. A.; Pérez-Ramírez, J. *Colloids Surf., A* **2004**, *241*, 53.
(17) Groen, J. C.; Peffer, L. A. A.; Moulijn, J. A.; Pérez-Ramírez, J. *Microporous Mesoporous Mater.* **2004**, *69*, 29.
(18) Jacobsen, C. J. H.; Madsen, C.; Houzvicka, J.; Schmidt, I.; Carlsson, A. *J. Am. Chem. Soc.* **2000**, *122*, 7116.
(19) Christensen, C. H.; Johannsen, K.; Schmidt, I.; Christensen, C. H. *J. Am. Chem. Soc.* **2003**, *125*, 13370.
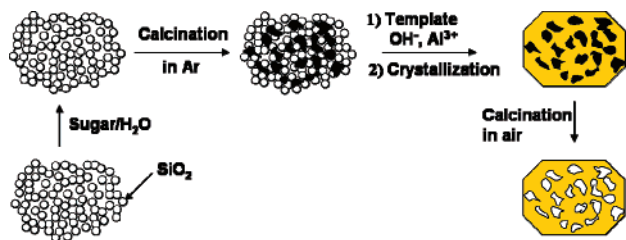
Figure 1. New route for the preparation of mesoporous zeolite single crystals using sucrose as the carbon template.

Figure 2. Controlled mesoporosity of zeolites prepared simply by varying the amount of sugar in the silica (from top C/Si = 1.75; 0.87; 0.58; 0.0).

Here, we demonstrate a simple, new, and versatile method for the preparation of mesoporous zeolites. This new method applies in situ generation of the required carbon template by decomposition of a carbohydrate directly onto the silica raw material used for the zeolite synthesis. This method significantly extends the scope of the carbon-templating approach. Most importantly, it allows careful control of the porosity of the mesoporous zeolite in a very simple manner and it does not depend on the availability of specialized carbon templates. The mesoporous zeolite single crystals resulting from the carbon-templating method have already shown promising catalytic properties in several reactions.[19−24] So far, these hierarchical zeolite structures have been reported for the MFI,[25] MEL,[20] and MTW[26] framework types and most recently also for BEA, AFI, and CHA.[27] Other synthesis schemes for preparing hierarchical zeolites have been presented as well, such as assembling zeolite seeds with organic structure directors present,[28] resin macrotemplating,[29] using carbon aerogels,[30,31] recrystallization,[32] and templating mesoporous zeolites from a mixture of small organic alkylammonium salts and mesoscale cationic polymers.[33]

Figure 1 shows a schematic illustration of the new route for preparation of mesoporous zeolites. In the first step, silica gel is impregnated to incipient wetness with a concentrated solution of sucrose. During calcination in an inert gas (Ar),
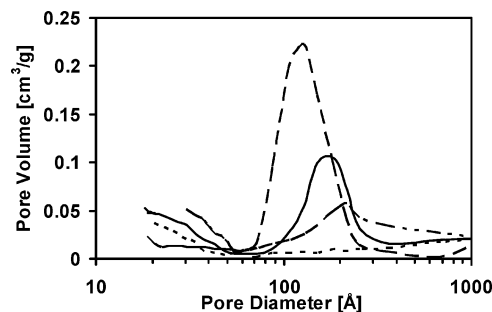
(20) Kustova, M. Yu.; Hasselriis, P.; Christensen, C. H. *Catal. Lett.* **2004**, *96*, 205.
(21) Christensen, C. H.; Schmidt, I.; Christensen, C. H. *Catal. Comm.* **2004**, *5*, 543.
(22) Christensen, C. H.; Schmidt, I.; Carlsson, A.; Johannsen, K.; Herbst, K. *J. Am. Chem. Soc.* **2005**, *127*, 8098.
(23) Schmidt, I.; Christensen, C. H.; Hasselriis, P.; Kustova, M. Yu.; Brorson, M.; Dahl, S.; Johannsen, K.; Christensen, C. H. *Stud. Surf. Sci. Catal.* **2005**, *158*, 1247.
(24) Kustova, M. Yu.; Rasmussen, S. B.; Kustov, A. L.; Christensen, C. H. *Appl. Catal., B* **2006**, *67*, 60.
(25) Schmidt, I.; Krogh, A.; Wienberg, K.; Carlsson, A.; Brorson, M.; Jacobsen, C. J. H. *Chem. Commun.* **2000**, 2157.
(26) Wei, X.; Smirniotis, P. G. *Microporous Mesoporous Mater.* **2005**, *89*, 170.
(27) Egeblad, K.; Kustova, M.; Klitgaard, S. K.; Zhu, K.; Christensen, C. H. *Micoporous Mesoporous Mater.* **2007**, *101*, 214.
(28) Liu, Y.; Pinnavaia, T. J. *J. Mater. Chem.* **2004**, *14*, 1099.
(29) Naydenov, V.; Tosheva, L.; Sterte, J. *Microporous Mesoporous Mater.* **2000**, *35*, 621.
(30) Tao, Y.; Kanoh, H.; Kaneko, K. *J. Phys. Chem. B* **2003**, *107*, 10974.
(31) Tao, Y.; Kanoh, H.; Kaneko, K. *Langmuir* **2005**, *21*, 504.
(32) Ivanova, I. I.; Kuznetsov, A. S.; Ponomareva, O. A.; Yuschenko, V. V.; Knyazeva, E. E. *Stud. Surf. Sci. Catal.* **2005**, *158*, 121.
(33) Xiao, F. S.; Wang, L.; Yin, C.; Lin, K.; Di, Y.; Li, J.; Xu, R.; Su, D. S.; Schlogl, R.; Yokoi, T.; Tatsumi, T. *Angew. Chem., Int. Ed.* **2006**, *45*, 3090.
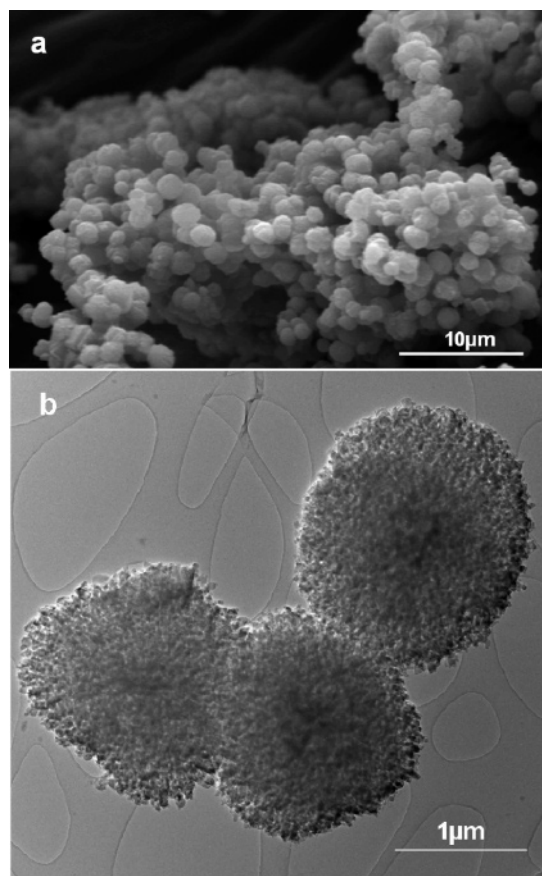
Figure 3. Representative (a) SEM and (b) TEM images of mesoporous ZSM-5 zeolite single crystals prepared by in situ carbon templating.

the auxiliary carbon particles are then formed by decomposition of sucrose inside the silica gel. After that, a zeolite synthesis gel is formed from the resulting carbon−silica composite by addition of the base and a suitable template. Upon complete crystallization, the carbon is removed by combustion and the mesoporous zeolite is formed.

The X-ray powder diffraction patterns for the mesoporous ZSM-5 and ZSM-11 zeolites are shown in Figures S1 and S2 of the Supporting Information. It is clearly seen that the samples exclusively contain highly crystalline MFI- and MEL-structured material, respectively.[34] The mesopore size distribution of the ZSM-5 zeolite after combustion of the carbon is shown in Figure 2 and the effect of changing the

(34) Database of zeolite structures: http://www.iza-structure.org/databases/.

carbon/silica ratio in the recipe is evident. Surface areas as well as micro- and mesopore volumes are summarized in Table S1 of the Supporting Information. Thus, it is clear that by introduction of more or less concentrated solutions of sucrose during impregnation of the silica, the mesopore volume can be tuned without altering the micropore volume.

Hg intrusion experiments gives essentially mesopore volumes identical to those obtained from nitrogen physisorption. This shows that the mesopores are actually accessible and distributed over the interior volume of the zeolite crystals. This is also supported by the representative images from scanning electron microscopy (SEM) and transmission electron microscopy (TEM) for the mesoporous ZSM-5 zeolite shown in Figure 3. From the SEM image (a), it can be seen that the sample is highly crystalline and that crystals of a quite uniform size are obtained. From the TEM image (b), it is easily possible to see the individual mesoporous zeolite crystals, which clearly features some brighter areas distributed all over. These brighter areas are the mesopores created by removal of the carbon introduced as sucrose. The vast majority of the crystals are mesoporous zeolite single crystals, but some less mesoporous zeolite crystals can sometimes also be formed. The average crystal size determined from SEM and TEM for the mesoporous zeolite crystals is about 1 μm, and the typical shape of MFI-type crystals is observed.

The mesoporous zeolite crystals are unique in the sense that they contain interconnected micropores and mesopores inside each individual single crystal. So far, the present method for the preparation of mesoporous zeolites is demonstrated as a new, very simple route to these hierarchical zeolites. The method applies in situ generation of the carbon template from sucrose impregnated onto silica gel, and therefore the resulting material is readily available at low cost. The method does not rely on the availability of special and expensive mesoporous carbons, only on the mesoporous silicas that are used widely and can be obtained easily by precipitation. However, the most important attribute of the present approach is that is allows careful design of the porosity. This is essential for catalytic applications, because this is the way that efficient mass transport can be tuned to maximize catalyst performance. With this simple method, it is possible that mesoporous zeolites could be so easily and inexpensively available that they will find use in industrial applications.

Supporting Information Available: Detailed synthesis procedures, X-ray diffraction, and pore analysis (PDF). This material is available free of charge via the Internet at http://pubs.acs.org.

CM071168N

Enhancing the Porosity of Mesoporous Carbon-Templated ZSM-5 by Desilication

Martin S. Holm,[a,b] Kresten Egeblad,[a] Peter N. R. Vennestrøm,[a] Christian G. Hartmann,[a] Marina Kustova,[b] and Claus H. Christensen*[b]

A tunable desilication protocol applied on a mesoporous ZSM-5 zeolite synthesized by carbon-templating is reported. The strategy enables a systematic manufacture of zeolite catalysts with moderate to very high mesoporosities. Coupling carbon-templating and desilication thus allow for more than a doubling of the original mesopore volume and mesopore surface area. The porosity effect arising from various treatment times and base amounts in the media has been thoroughly mapped. Initially, small mesopores are created, and as desilication strength increases the average mesopore size enhances. Crystallinity of the treated samples is retained, and electron microscopy indicates solely intracrystalline mesoporosity.

(© Wiley-VCH Verlag GmbH & Co. KGaA, 69451 Weinheim, Germany, 2008)

Introduction

Zeolites are crystalline microporous aluminosilicates that have found a multitude of industrial applications as, e.g. sorbents, ion-exchangers, and catalysts. The widespread application of zeolites in industry can be attributed to the inherent micropore system of molecular dimensions, which allows for shape-selective catalysis. Moreover, they are often thermally highly stable materials, which possess remarkably high surface areas. These properties make zeolites particularly useful for catalytic applications, and the use of zeolites as catalysts has indeed received significant attention.[1,2] However, molecular transport to the catalytically active micropore system in the bulk of the crystals may become a limiting factor for their activity in some catalytic applications.[3] Recently, several preparative strategies have been developed with the aim of producing zeolite materials that overcome this diffusion limitation.[4,5] The strategies pursued so far include increasing the width of the zeolite micropores,[6–9] decreasing the size of the zeolite crystals,[10–14] and the introduction of an auxiliary mesopore system in addition to the inherent micropore system.[15–18] The latter two classes of materials can be classified as hierarchical in terms of porosity because they have bi- or trimodal pore-size distributions, and the preparation of such materials by use of mesopore templates was reviewed very recently.[19] For the preparation of zeolites with intracrystalline hierarchical porosity, two main approaches appear to be the most promising,[20] namely carbon-templating[21–23] and desilication.[24–27]

In carbon-templating, porous zeolite crystals are produced by removal of auxiliary carbon particles encapsulated in the zeolite crystals during growth. In desilication, conventional purely microporous zeolite crystals are treated with dilute aqueous base to preferentially dissolve silica species from the zeolite crystals. Here, we show that the porosity of carbon-templated mesoporous zeolite crystals can be tuned, as well as increased by more than a factor of two, by subjecting the already mesoporous material to a desilication procedure. Coupling of these two procedures have in fact been attempted earlier, however, with limited success.[28] The process of desilication corresponds to a partial dissolution of the zeolite framework. Therefore, it is important either to use a limited amount of a base or to restrict the time during which the process is allowed to proceed.[29]

Results and Discussion

A mesoporous carbon-templated ZSM-5 zeolite was subjected to various desilication treatments as listed in Table 1.

Physico-chemical properties of the resulting materials from N_2 physisorption, XRD and NH_3-TPD measurements are included. First of all, it can be seen that the microporosity is preserved after desilication since the micropore volumes of the samples are not affected by the treatments. Moreover, it can be seen that the parent carbon-templated sample has a considerable mesopore volume of ca. 0.3 mL/g.

[a] Center for Sustainable and Green Chemistry, Department of Chemistry, Technical University of Denmark,
Building 206, 2800 Lyngby, Denmark
[b] Haldor Topsoe A/S,
Nymøllevej 55, 2800 Lyngby, Denmark
E-mail: chc@topsoe.dk
☐ Supporting information for this article is available on the WWW under http://www.eurjic.org or from the author.

Table 1. Textural data from N_2 adsorption/desorption experiments on the parent and desilicated samples.[a]

Sample	Base amount [mmol/g]	Time [min]	S_{BET} [m²/g]	S_{meso} [m²/g]	V_{meso} [mL/g]	V_{micro} [mL/g]	$D[101]$[b] [Å]	Acidity[c] [mmol/g]
Parent	–	–	408	117	0.30	0.11	677	0.164
1	3	30	408	162	0.37	0.11	595	0.180
2	5	30	422	195	0.47	0.10	513	0.206
3	7.5	30	478	222	0.63	0.11	494	0.235
4	10	30	478	232	0.72	0.10	460	0.272
5	15	30	503	234	0.75	0.11	386	0.293
6	8	5	295	142	0.33	0.06	–	–
7	8	10	466	241	0.64	0.10	–	–
8	8	15	443	210	0.66	0.10	–	–
9	8	20	456	208	0.70	0.11	–	–
10	8	30	450	201	0.73	0.11	–	–
11	8	70	445	181	0.65	0.11	–	–

[a] Samples 1–5 were desilicated in a 0.1 M solution and samples 6–11 in a 0.2 M solution. $V_{meso} = V_{ads,P/P0 = 0.99} - V_{micro}$. V_{micro} from t-plot. S_{meso} from BJH. Surface area of pores 17–3000 Å. [b] Scherrer equation. [c] NH_3-TPD. NH_3 desorbed at 175 °C for 2 h.

This porosity corresponds to a moderate mesopore surface area S_{meso} of 117 m²/g due to rather large mesopores centered around ca. 20–30 nm. The physisorption isotherms obtained from samples treated with different volumes of 0.1 M NaOH solutions for 30 min (samples 1–5) are shown in Figure 1(a). In Figure 1(a) it can be seen that the mesopore volume of the samples increases with increasing desilication strength. Moreover, closer inspection of Figure 1(a) reveals that a hysteresis loop starts to develop at a relative pressure of 0.45 at low treatment strengths (samples 1 and 2). This is attributed to the formation of new smaller mesopores, initially with a diameter below 10 nm as is evident from the BJH-derived pore-size distribution given in Figure 1(b).

The sizes of the created mesopores are in excellent agreement with previously published data on desilication of purely microporous ZSM-5 samples.[30,31] Interestingly, because the mesopores initially formed are smaller than the inherent mesopore system present, these results indicate that it is possible to create a hierarchical zeolite with a multi-level mesoporosity by coupling the carbon-templating and desilication protocols. As the desilication strength is increased, these smaller mesopores grow larger, as can be seen by the disappearance of the mesopores below 10 nm (samples 3 and 4) and simultaneous growth of pore volume attributed to pores around 15 nm. Thus, the observed increase in mesopore volumes apparent from Table 1 does not only originate from an increase in the pore sizes of already existing mesopores, but also from newly generated mesopores. The generation of mesopores can also be tuned by variation of the reaction time as evident from the physisorption data presented in Table 1 for samples 6–11. It can be seen, that the mesopore volume as well as the mesopore surface area of the parent mesoporous sample are doubled after only 10 min (sample 7). Moreover, it can be seen that further extending the desilication time only marginally increases the mesopore volume, and an extreme time has a detrimental effect on the mesopore surface area (sample 11). This is attributed to the pore size distribution extending significantly into the macropore region. Key sorp-
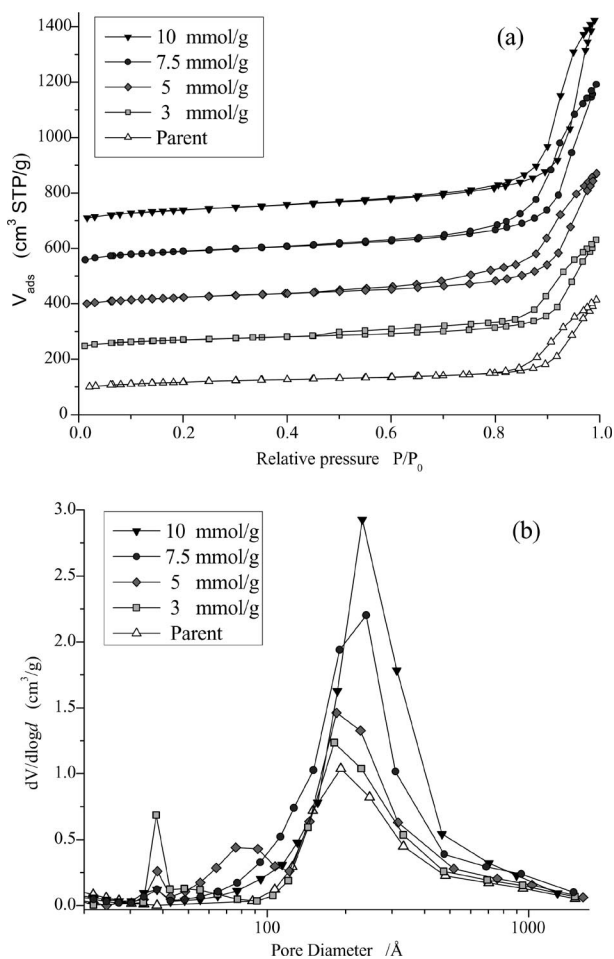

Figure 1. (a) N_2 adsorption/desorption isotherms of the parent along with samples 1–4. Isotherms of samples 1–4 are offset by 150 for illustrative reasons. (b) BJH-derived pore-size distributions.

tion isotherms and the respective BJH-derived mesopore diameters are given in the Supporting Information (Figure S1). Figure 2 shows the XRD patterns of the parent sample along with samples 1–5 illustrating the preserved crystallinity and phase purity of the treated samples. In ac-

cordance with results obtained after desilication of conventional zeolite samples, the intensity of the reflections gradually decrease as the desilication strength is increased.[32,33]
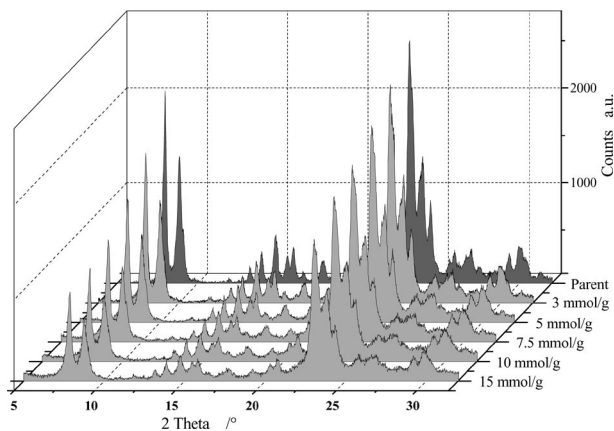

Figure 2. XRD diffractograms of parent sample and samples 1–5 desilicated for 30 min with increasing desilication strength.

The effective average crystal diameter calculated by the Scherrer equation reveal a gradual decrease in crystal diameter. The D[101] deflection was chosen for Table 1. Table S1 (Supporting Information) contains effective crystal sizes derived from other deflections. By analyzing the XRD results in relation to imaging obtained from SEM and TEM analysis, it appears unlikely that the desilicated crystals dismantle to produce interparticle mesoporosity. The observed decrease in the average crystal size could alternatively be explained by the formation of an increasing number of intracrystalline domains bordering a mesopore within the single crystal. From NH_3-TPD an acidity of 0.164 mmol/g was measured for the parent sample after desorption of NH_3 at 175 °C for 2 h. This acidity correlates to the anticipated Si/Al ratio of approximately 45 when compared to a calibration curve from ZSM-5 zeolites of known acidities, thus indicating complete aluminium incorporation from the gel during crystallization. Furthermore, it can be seen from Table 1 (samples 1–5) that the total acidity of the materials increase as a function of the desilication, as would be expected from the selective silicon extraction. Figure 3 presents the NH_3 desorption curves obtained after desorption of weakly bound NH_3 at 100 °C for 1 h and at 175 °C for 2 h. A continuing increase in total acidity and nearly a doubling for the most severely treated zeolites is apparent in both cases. In Figure 3(b) it can be seen that a significant contribution to the acidity orginates from a shoulder on the low-temperature side of the desorption maximum at ca. 365 °C. As the treatment strength increases, the shoulder intensifies, which is possibly due to partial (extra) framework aluminum species generated during the desilication.

Figure 4 gives representative SEM and TEM images of the parent and desilicated samples. SEM was used to verify the homogeneity of the parent material with respect to crystal size and porosity, and to visually monitor the effect of the desilication treatments. In Figure 4(a) a SEM image of the parent sample is shown. It can be seen that the crystals
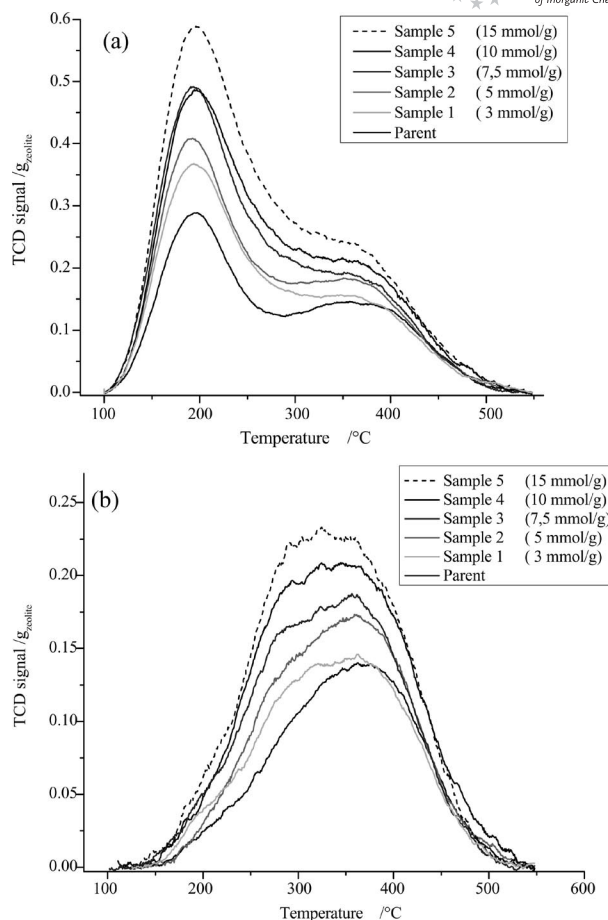

Figure 3. NH_3 desoprtion curves of parent sample and samples 1–5. Weakly bound NH_3 desorbed in He at (a) 100 °C for 1 h and (b) at 175 °C desorbing for 2 h.
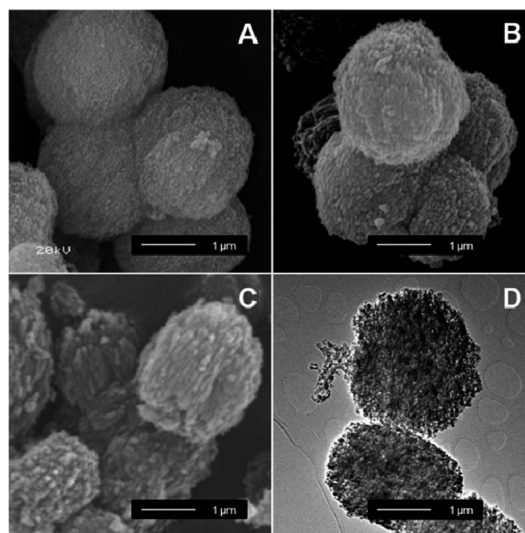

Figure 4. (a)–(c) SEM images of the parent sample, sample 7 (desilicated 10 min.) and sample 10 (desilicated 30 min), respectively. (d) TEM image of sample 10 (desilicated 30 min).

exhibit the well-known sponge-like morphology character-istic of mesoporous carbon-templated MFI zeolites.[34] Overview images of the parent sample confirmed that the crystals were similar in size (2–3 µm long) and that the vast majority of them exhibited this morphology. Figures 4(b) and (c) show SEM images of desilicated samples obtained after 10 min (sample 7) and 30 min (sample 10) treatment times, respectively. From these images, it is evident that de-silication leads to a gradual "roughening" of the crystals, which appear to be more and more rugged as the desil-ication time is increased. TEM analyses also revealed the sponge-like morphology of the crystals as evident from the highly contrasted image of the 30 min desilicated samples shown in Figure 4(d).

Conclusions

We have shown that the porosity of carbon-templated mesoporous ZSM-5 may be enhanced by a factor of at least two by desilication of such a sample in terms of mesopore surface area as well as mesopore volume. Two types of de-silication protocols were applied for tuning the porosity of the carbon-templated mesoporous sample: variation in the volume of hydroxide solution and variation in reaction time. Pore-size distribution plots revealed that at lower de-silication strengths both newly generated smaller mesopores (initally centered below 10 nm) as well as mesopores already present in the sample (centered around ca. 20–30 nm) con-tributed to the mesopore volume. With increased desil-ication strength, these smaller mesopores grew larger, eventually, after excessive desilication, into the macropore region. The method applied here could easily be extended to other zeolite structure types, and it therefore provides a useful and easy approach for systematically generating highly mesoporous zeolite samples.

Experimental Section

A mesoporous ZSM-5 sample was prepared by carbon-templating according to a modified literature procedure.[35] A nominal Si/Al ratio of 45 was used in the gel. Briefly, 2 g of carbon black pearls 2000 was impregnated with a fresh solution of aluminium isopro-poxide in tetrahydrofuran (0.084 g in 6 mL) and left to dry over-night. Then the carbonaceous material was impregnated with a mixture of tetrapropylammonium hydroxide (3.44 g, 40 wt.-%), aqueous sodium hydroxide (0.1 g in 0.5 g H_2O) and ethanol (3.03 g), and left to dry overnight. The material was impregnated with tetraethyl orthosilicate (3.87 g) and left to dry overnight before being crystallized at 180 °C for 5 d. The carbon matrix was re-moved by calcination at 550 °C in static air for 20 h reached at a ramp of ca. 2 °C/min. The proton form of the zeolites was obtained by threefold ion-exchange in a 1 M NH_4NO_3 solution and calci-nation at 550 °C in static air for 4 h. The sample was subjected to different desilication procedures by immersion of the zeolite sam-ples in aqueous sodium hydroxide solutions at 65 °C for various periods of time. After reaction, the desilicated samples were col-lected by filtration and washed thoroughly with water. Nitrogen physisorption measurements were conducted with a micromeretics ASAP 2020. Powder X-ray diffraction (XRD) patterns of the par-ent and desilicated samples were recorded with a Bruker AXS pow-der diffractometer. Scanning electron micrographs (SEM) were re-corded with a JEOL JSM 5900 equipped with an LaB_6 filament. Prior to measurements, the samples were sputter-coated with Au for 40 s by using a Polaron SC 7620. Transmission electron micro-scopy (TEM) images and selected area diffraction (SAD) were re-corded with a JEM 2000 FX with an accelerating voltage of 300 kV, as described previously.[36] NH$_3$-TPD measurements were per-formed with a Micromeritics Autochem II equipped with a TCD detector. Samples were transformed into proton form prior to NH$_3$-TPD analysis through a similar procedure as described above for the parent material. Dry weight of the samples was found after evacuation at 300 °C for 1 h. Weakly bound ammonia was de-sorbed prior to measurement at 100 °C in an He flow of 25 mL/min for 1 h or at 175 °C in an He flow of 50 mL/min for 2 h, respec-tively.

Supporting Information (see footnote on the first page of this arti-cle): N$_2$ physisorption isotherms and crystal-size measurements (calculated by use of the Scherrer equation from X-ray data).

Acknowledgments

[1] A. Corma, *Chem. Rev.* **1995**, *95*, 559.
[2] A. Corma, *Chem. Rev.* **1997**, *97*, 2373.
[3] M. Hartmann, *Angew. Chem. Int. Ed.* **2004**, *43*, 5880.
[4] Y. Tao, H. Kanoh, L. Abrams, K. Kaneko, *Chem. Rev.* **2006**, *106*, 896.
[5] J. C. Groen, C. H. Christensen, K. Egeblad, C. H. Christensen, J. Pérez-Ramírez, *Chem. Soc. Rev.* **2008**, accepted.
[6] M. E. Davis, C. Saldarriaga, C. Montes, J. Garces, C. Crowder, *Nature* **1988**, *331*, 698.
[7] C. C. Freyhard, M. Tsapatsis, R. F. Lobo, K. J. Balkus, *Nature* **1996**, *381*, 295.
[8] T. Wessels, C. Baerlocher, L. B. McCusker, E. J. Creyghton, *J. Am. Chem. Soc.* **1999**, *121*, 6242.
[9] A. Corma, M. Diaz-Cabanas, J. Martinez-Triguero, F. Rey, J. Rius, *Nature* **1992**, *418*, 514.
[10] L. Tosheva, V. P. Valtchev, *Chem. Mater.* **2005**, *17*, 2494.
[11] P. A. Jacobs, E. G. Derouane, J. Weitkamp, *J. Chem. Soc., Chem. Commun.* **1981**, 591.
[12] M. A. Camblor, A. Corma, S. Valencia, *Microporous Mesopo-rous Mater.* **1998**, *25*, 59.
[13] C. Madsen, C. J. H. Jacobsen, *Chem. Commun.* **1999**, 673.
[14] W.-C. Li, A.-H. Lu, R. Palkovits, W. Schmidt, B. Spliethoff, F. Schüth, *J. Am. Chem. Soc.* **2005**, *127*, 12595.
[15] C. J. H. Jacobsen, C. Madsen, J. Houzvicka, I. Schmidt, A. Carlsson, *J. Am. Chem. Soc.* **2000**, *122*, 7116.
[16] M. Ogura, S. H. Shinomiya, J. Tateno, Y. Nara, E. Kikuchi, M. Matsukata, *Chem. Lett.* **2000**, 882.
[17] F.-S. Xiao, L. Wang, C. Yin, K. Lin, Y. Di, J. Li, R. Xu, D. S. Su, R. Schlögl, T. Yokoi, T. Tatsumi, *Angew. Chem. Int. Ed.* **2006**, *45*, 3090.
[18] H. Wang, T. Pinnavaia, *Angew. Chem. Int. Ed.* **2006**, *45*, 7603.
[19] K. Egeblad, C. H. Christensen, M. Kustova, C. H. Christensen, *Chem. Mater.* **2008**, *20*, 946.
[20] K. Egeblad, C. H. Christensen, M. Kustova, C. H. Christensen, "Mesoporous Zeolite Crystals", in *Zeolites: From Model Mate-rials to Industrial Catalysts* (Eds.: J. Cejka, J. Perez-Pariente, W. J. Roth), Transworld Research Network, Kerala, India, **2008**, pp. 391–442.
[21] M. Y. Kustova, P. Hasselriis, C. H. Christensen, *Catal. Lett.* **2004**, *96*, 205.

[22] X. Wei, P. G. Smirniotis, *Microporous Mesoporous Mater.* **2005**, *89*, 170.

[23] Y. Tao, H. Kanoh, K. Kaneko, *J. Phys. Chem. B* **2003**, *107*, 10974.

[24] J. C. Groen, L. A. A. Peffer, J. A. Moulijn, J. Pérez-Ramírez, *Chem. Eur. J.* **2005**, *11*, 4983.

[25] J. C. Groen, J. A. Moulijn, J. Pérez-Ramírez, *J. Mater. Chem.* **2006**, *16*, 2121.

[26] M. Bjørgen, F. Joensen, M. S. Holm, U. Olsbye, K.-P. Lillerud, S. Svelle, *Appl. Catal. A* **2008**, *345*, 43.

[27] Y. Tao, H. Kanoh, K. Kaneko, *Adsorption* **2006**, *12*, 309.

[28] Y. H. Chou, C. S. Cundy, A. A. Garforth, V. L. Zholobenko, *Microporous Mesoporous Mater.* **2006**, *89*, 78.

[29] J. C. Groen, L. A. A. Peffer, J. A. Moulijn, J. Pèrez-Ramírez, *Colloids Surf., A* **2004**, *241*, 53.

[30] J. C. Groen, W. Zhu, S. Brouwer, S. J. Huynink, F. Kapteijn, J. A. Moulijn, J. Pérez-Ramírez, *J. Am. Chem. Soc.* **2007**, *129*, 355.

[31] M. Ogura, S. Shinomiya, J. Tateno, M. Nomura, E. Kikuchi, M. Matsukata, *Appl. Catal. A* **2001**, *219*, 33.

[32] Y. Song, X. Zhu, T. Song, Q. Wang, L. Xu, *Appl. Catal. A* **2006**, *302*, 69.

[33] J. S. Jung, J. W. Park, G. Seo, *Appl. Catal. A* **2005**, *288*, 149.

[34] K. Zhu, K. Egeblad, C. H. Christensen, *Eur. J. Inorg. Chem.* **2007**, 3955.

[35] M. Y. Kustova, A. L. Kustov, C. H. Christensen, *Stud. Surf. Sci. Catal.* **2005**, *158*, 255.

[36] K. Egeblad, M. Kustova, S. K. Klitgaard, K. Zhu, C. H. Christensen, *Microporous Mesoporous Mater.* **2007**, *101*, 214.

ELSEVIER

Mesoporous zeolite and zeotype single crystals synthesized in fluoride media

Kresten Egeblad, Marina Kustova, Søren Kegnæs Klitgaard, Kake Zhu,
Claus Hviid Christensen *

Center for Sustainable and Green Chemistry, Department of Chemistry, Building 207, Technical University of Denmark, DK-2800 Lyngby, Denmark

Abstract

We report the synthesis and characterization of a series of new mesoporous zeolite and zeotype materials made available by combining new and improved procedures for directly introducing carbon into reaction mixtures with the fluoride route for conventional zeolite synthesis. The mesoporous materials were all prepared by hydrothermal crystallization of gels adsorbed on carbon matrices which were subsequently removed by combustion. The procedures presented here resulted in mesoporous zeolite and zeotypes materials with MFI, MEL, BEA, AFI and CHA framework structures. All samples were characterized by XRPD, SEM, TEM and N_2 physisorption measurements. For the zeolite materials it was found that mesoporous MFI and MEL structured single crystals could indeed be crystallized from fluoride media using an improved carbon-templating approach. More importantly, it was found that mesoporous BEA-type single crystals could be crystallized from fluoride media by a newly developed procedure presented here. Thus, we here present the only known route to mesoporous BEA-type single crystals, since crystallization of this framework structure from basic media is known to give only nanosized crystals as opposed to mesoporous single crystals. For the zeotype materials it was found that highly crystalline mesoporous materials of AFI and CHA structure types could be synthesized using a newly developed procedure.
© 2006 Elsevier Inc. All rights reserved.

Keywords: Zeolite; Zeotype; Fluoride media; Mesopores; Carbon

1. Introduction

Zeolite-based molecular sieves represent one of the most important groups of inorganic materials with an extremely high importance in industrial applications as sorbents, ion-exchangers and catalysts [1]. In particular, the number of applications of zeolites as highly active, selective and stable catalysts in large-scale technologies steadily increases. They include oil refinery, petrochemistry, production of fine chemicals and environmental catalysis [2]. As well as zeolites new families of zeolite-like or zeolite-related materials known as zeotypes have been investigated [3]. Zeotype materials display great compositional diversity and frequently have frameworks unknown for zeolites [4].

In general, zeolites are prepared by hydrothermal crystallization from alkaline reaction mixtures [5], where OH^- acts as mineralizer. The fluoride ion is a unique mineralizer that has only recently been seriously examined for its use in zeolite and zeotype synthesis [3]. Flanigen and Patton were the first to employ fluoride-containing salts in the synthesis of silicalite-1 in 1978 [6]. The behavior of the fluoride ion is very similar to that of the hydroxide ion as a mineralizing agent and a complexing ion and it will also contribute to the formation of the molecular sieve structures. Contrary to the hydroxide mineralizer, the use of fluoride ions does not necessarily influence the pH of the gel. Thus, systems containing fluoride ions can still produce molecular sieve products even with gel pH below 5. In

---

* Corresponding author. Tel.: +45 4525 2402; fax: +45 4588 3136.
   E-mail address: chc@kemi.dtu.dk (C.H. Christensen).

the crystallization of molecular sieve phases, fluoride ions: act as agents solubilizing the framework-forming elements silicon and aluminum; slow down nucleation and growth rates, resulting in larger, more defect-free crystals; produce many all-silica phases because of the stability of the fluoro complexes of silicon; can impose a structure-directing role and contribute to the formation of previously unknown phases [3]. Syntheses of several zeolite types have been described in the literature [5–15], and different preparative strategies were also discussed in detail by Zones et al. [16]. However, the large-scale utilization of these microporous catalysts in the industry has so far not been explored to its full potential [17], because diffusion of reactants and products in the working catalyst often limits the overall performance of the catalyst. Several different preparative strategies have been attempted to surmount this problem [18], e.g. decreasing the zeolite crystal size [19–22], synthesizing materials with larger micropores (e.g. VPI-5 [23] and UDT-1 [24]), and the preparation of new mesoporous molecular sieves [25]. Significant attention has also been drawn to the generation of reasonably mesoporous zeolite single crystal materials by disintegrative post-synthetic treatments such as dealumination [26] and desilication [27,28]. Unfortunately, these kinds of approaches obviously impose certain restrictions on the zeolite composition, since they entail the selective removal of either aluminium or silicon ions from the zeolite framework. Mesopore generation by desilication, for instance, is highly dependant on the Si/Al ratio in order to be reasonably controlled [28], and dealumination necessarily leads to a less acidic material. Thus, these approaches have somewhat limited scope.

Recently, a new family of crystalline zeolitic materials was reported, the so-called mesoporous zeolite single crystals [29]. These new materials combine the advantages of both mesoporous molecular sieves and zeolites by featuring an additional intracrystalline mesopore system interconnected with the usual micropore system in each individual zeolite single crystal, resulting in a bimodal pore distribution. Additionally, these new materials are mechanically stable in the sense that they can easily be pelletized and crushed for use in catalytic applications [30]. Furthermore, it has been shown that the mesopore system of these hierarchical materials helps solving diffusion limitation problems by improving the mass transfer to and from the active sites [30–35]. These mesoporous zeolite single crystal materials may be prepared simply by crystallizing the zeolite around a carbon matrix that can eventually be removed by combustion. This synthesis scheme has so far resulted in mesoporous zeolite single crystals of MFI [29], MEL [36], MTW [37] and zeolite Y [38] framework structures, but other schemes have been presented as well, such as assembling zeolite seeds with organic structure directors present [39], by resin macrotemplating [40], by using carbon aerogels [38,41], by recrystallization [42], or by templating mesoporous zeolites from a mixture of small organic ammonium salts and mesoscale cationic polymers [43].

Here we show that a combination of the fluoride route with a new improved procedure for directly introducing carbon in the reaction mixture provides access to a wide variety of new mesoporous zeolite and zeotype materials. Thus, we present the syntheses of mesoporous MFI, MEL and BEA zeolite materials as well as mesoporous AFI and CHA zeotype materials prepared from synthesis gels containing fluoride ions.

2. Experimental

2.1. Physicochemical characterization

X-ray powder diffraction patterns (XRPD) were recorded using Cu-Kα radiation in the 2θ interval 5–50° using a Philips PW 1820/3711 powder diffractometer.

Nitrogen adsorption and desorption measurements were performed at liquid nitrogen temperature on a Micromeritics ASAP 2020. The samples were outgassed in vacuum at 200 °C prior to measurement. Total surface area was calculated according to the BET method. Meso- and micropore volumes were determined by the BJH and *t*-plot methods (desorption).

Scanning electron microscopy (SEM) was performed on a Philips XL20 FEG. The calcined zeolite samples were placed on a carbon film and Pt was evaporated onto the sample for approximately 20 min to achieve sufficient conductivity.

Transmission electron microscopy (TEM) was performed on a JEM 2000 FX with an accelerating voltage of 300 kV. Selected-area-diffraction (SAD) technique was used to obtain electron diffraction patterns from individual grains of powder. A few mg of the powdered samples was suspended in 2 ml ethanol, and the suspension was sonicated for 1 h. Then, the suspension was allowed to settle for 15 min, before a drop was taken and dispersed on a 300 mesh copper grid coated with holey carbon film.

2.2. Materials

For syntheses of the mesoporous zeolites and zeotypes, carbon black particles (BP-2000) having an average particle diameter of 12 nm (ASTM D-3249), obtained from Carbot Corporation, were used as carbon matrices. The carbon black was dried at 110 °C for 24 h prior to use. All other reagents were of reagent grade and used without further purifications: tetraethylorthosilicate (TEOS, 98 wt%, Aldrich), aluminum isopropoxide (Al(C_3H_7O)$_3$, 98 wt%, Aldrich), tetrapropylammonium hydroxide (TPAOH, 40 wt%, Fluka), tetrabutylammonium hydroxide (TBAOH, 40 wt%, Fluka), tetraethylammonium hydroxide (TEAOH, 35 wt%, Aldrich), triethylamine (TEA, 98 wt%, Fluka), piperidine (PIP, 99 wt%, Aldrich), ethanol (EtOH, 99 wt%, Aldrich), hydrofluoric acid (HF, 40 wt% or 48 wt%, Aldrich), aluminum nitrate nonahydrate (Al(NO_3)$_3 \cdot$9H$_2$O, 99.5 wt%, Merck), phosphoric acid

(H_3PO_4, 85 wt%, Merck), tetrahydrofuran (THF, 99 wt%, Aldrich) and deionized water.

2.3. General description for the syntheses of the mesoporous materials

The mesoporous zeolite materials were prepared according to the following general procedure. A mixture of TEOS and the appropriate structure-directing agent was mixed with a solution of aluminum nitrate in water. Then, 2 g of carbon was mixed with this solution, and the resulting mixture was left for 6 h before a concentrated aqueous solution of HF was added with stirring. The resulting gels were then introduced into stainless steel autoclaves and heated to a designated temperature for a designated period of time. Then, the autoclaves were cooled to room temperature, the products were recovered by filtration, washed with water and dried at 80 °C for 10 h. Finally, the organic template and carbon black material were removed by controlled combustion in air in a muffle furnace at 550 °C for 20 h expelling the CO_2 formed in this process via the micropores of the microporous materials.

The mesoporous zeotype materials were prepared according to the following general procedure. A solution of aluminum isopropoxide dissolved in THF was impregnated onto to 2 g of carbon. The carbonaceous materials were left to dry at room temperature and in air overnight, or at least for 6 h. Then, the dry carbon materials were impregnated with an aqueous solution of phosphoric acid, structure-directing agent and HF made by mixing the components in that order. The resulting gels were then hydrothermally crystallized in stainless steel autoclaves, and the products recovered as described above.

2.4. Synthesis of conventional and mesoporous MFI-type materials in fluoride media

The synthesis of conventional MFI-type crystals was based on the recipes from Camblor et al. [44] and Hazm et al. [13]. In a typical synthesis procedure, 3.47 g of TEOS (167 mmol) was mixed with 4.92 g of TEAOH (11.7 mmol) and stirred for about 10 min. Then, a clear solution of 0.075 g of aluminum nitrate (0.2 mmol) in 0.55 g water (197 mmol) was slowly added. This mixture was left with stirring for 6 h at room temperature in an open polyethylene vessel allowing the removal of ethanol formed during the hydrolysis of the TEOS. To the resulting solution, 0.585 g of 40 wt% HF (11.7 mmol) solution was finally added under stirring, which lead instantaneously to a thick gel. The composition of the resulting synthesis gel was 1 Al_2O_3:90 SiO_2:62 TEAOH:62 HF:773 H_2O. The resulting gel was introduced into a stainless steel autoclave, heated to 170 °C and kept there for three days. Afterwards, the product was recovered as described above.

The mesoporous ZSM-5 material was prepared according to the new improved procedure. In a typical synthesis procedure, 3.47 g of TEOS (167 mmol) was mixed with 4.92 g of TEAOH (11.7 mmol) and stirred for about 10 min. Then, a clear solution of 0.075 g of aluminum nitrate (0.2 mmol) in 0.55 g water (197 mmol) was slowly added. Then, 2 g of carbon was mixed with this solution. This mixture was left for 6 h at room temperature allowing the removal of ethanol formed during the hydrolysis of the TEOS. To the resulting carbon, 0.585 g of 40 wt% HF (11.7 mmol) solution was finally added with stirring. The composition of the synthesis gel was 1 Al_2O_3:90 SiO_2:62 TEAOH:62 HF:773 H_2O. The resulting gel was introduced into a stainless steel autoclave, heated to 170 °C and kept there for five days. Afterwards, the product was recovered as described above.

2.5. Synthesis of conventional and mesoporous MEL-type materials in fluoride media

The synthesis of conventional MEL-type crystals was based on the recipes from Camblor et al. [44] and Hazm et al. [13]. In a typical synthesis procedure, 3.47 g of TEOS (167 mmol) was mixed with 7.58 g of TBAOH (1.7 mmol) and stirred for about 10 min. Then, a clear solution of 0.075 g of aluminum nitrate (0.2 mmol) in 0.55 g water (197 mmol) was slowly added. This mixture was left with stirring for 6 h at room temperature in an open polyethylene vessel allowing the removal of ethanol formed during the hydrolysis of the TEOS. To the resulting solution, 0.585 g of 40 wt% HF (11.7 mmol) solution was finally added under stirring, which lead instantaneously to a thick gel. The composition of the resulting synthesis gel was 1 Al_2O_3:90 SiO_2:62 TBAOH:62 HF:773 H_2O. The resulting gel was introduced into a stainless steel autoclave, heated to 170 °C and kept there for three days. Afterwards, the product was recovered as described above.

The mesoporous ZSM-11 material was prepared according to the new improved procedure. In a typical synthesis procedure, 3.47 g of TEOS (167 mmol) was mixed with 7.58 g of TBAOH (11.7 mmol) and stirred for about 10 min. Then, a clear solution of 0.075 g of aluminum nitrate (0.2 mmol) in 0.55 g water (197 mmol) was slowly added. Then, 2 g of carbon was mixed with this solution. This mixture was left for 6 h at room temperature allowing the removal of ethanol formed during the hydrolysis of the TEOS. To the resulting carbon, 0.585 g of 40 wt% HF (11.7 mmol) solution was finally added with stirring. The composition of the synthesis gel was 1 Al_2O_3:90 SiO_2:62 TBAOH:62 HF:773 H_2O. The resulting gel was introduced into a stainless steel autoclave, heated to 170 °C and kept there for six days. Afterwards, the product was recovered as described above.

2.6. Synthesis of conventional and mesoporous BEA-type materials in fluoride media

The synthesis of conventional BEA-type crystals was based on the recipes from Camblor et al. [44] and Hazm et al. [13]. In a typical synthesis procedure, 3.47 g of TEOS

(167 mmol) was mixed with a mixture of 8.00 g of TEAOH (19 mmol) and 0.55 g water (197 mmol), and stirred for about 10 min. This mixture was left with stirring for 6 h at room temperature in an open polyethylene vessel allowing the removal of ethanol formed during the hydrolysis of the TEOS. To the resulting solution, 0.95 g of 40 wt% HF (19 mmol) solution was finally added under stirring, which lead instantaneously to a thick gel. The composition of the resulting synthesis gel was 1 Al_2O_3:90 SiO_2:100 TEAOH:100 HF:773 H_2O. The resulting gel was introduced into a stainless steel autoclave, heated to 140 °C and kept there for five days. Afterwards, the product was recovered as described above.

The mesoporous BEA-type material was prepared according to the new improved procedure. In a typical synthesis procedure, 3.47 g of TEOS (167 mmol) was mixed with a mixture of 8.00 g of TEAOH (19 mmol) and 0.55 g water (197 mmol), and stirred for about 10 min. Then, 2 g of carbon was mixed with this solution. This mixture was left for 6 h at room temperature allowing the removal of ethanol formed during the hydrolysis of the TEOS. To the resulting carbon, 0.95 g of 40 wt% HF (19 mmol) solution was finally added with stirring. The composition of the synthesis gel was 1 Al_2O_3:90 SiO_2:100 TEAOH:100 HF:773 H_2O. The resulting gel was introduced into a stainless steel autoclave, heated to 140 °C and kept there for five days. Afterwards, the product was recovered as described above.

2.7. Synthesis of conventional and mesoporous AFI-type materials in fluoride media

The syntheses of AFI-type materials were based on the procedure given by Cundy [4]. In a typical synthesis of con-

ventional AlPO-5 crystals, 1.5 g H_3PO_4 (13 mmol) was mixed with 1 ml H_2O and 1.62 g TEA (16 mmol) and the solution was cooled to 0 °C. To the cool solution, 2.04 g of aluminum isopropoxide (10 mmol) was added, and the mixture was left for 2 h before 0.27 g 48 wt% HF (6.5 mmol) was added. The mixture was stirred using a teflon spatula for 2 h before being transferred to a teflon-beaker which was placed in a teflon-lined stainless steel autoclave with an additional ca. 20 ml H_2O added outside the teflon-beaker. The final composition of the synthesis gel was 5 Al_2O_3:13 H_3PO_4:6.5 HF:16 TEA:76 H_2O. The autoclave was heated to 175 °C over 30 min and maintained at this temperature for two days. Afterwards, the product was recovered as described above.

The mesoporous AlPO-5 materials were synthesized using the following procedure. Typically, 2.04 g aluminum isopropoxide (10 mmol) was dissolved in 7 ml THF, and the solution was impregnated onto 2 g of carbon. The carbonaceous material was left to dry at room temperature and in air overnight, or at least for 6 h. Then, the dry carbon material was impregnated with an aqueous solution of phosphoric acid, triethylamine and hydrofluoric acid made by mixing the components in that order. Using this procedure, two mesoporous AlPO-5 samples were obtained, designated "AlPO-5 (s1)" and "AlPO-5 (s2)" corresponding to lower and higher amount of structure-directing agent in the gels, respectively. The final compositions of the synthesis gels were 5 Al_2O_3:13 H_3PO_4:6.5 HF:16 TEA:76 H_2O for AlPO-5 (s1) and 5 Al_2O_3:13 H_3PO_4:6.5 HF:25 TEA:76 H_2O for AlPO-5 (s2). The carbon materials were then transferred to teflon-beakers which were placed in teflon-lined autoclaves with ca. 20 ml water outside the beakers. The autoclaves were heated to 175 °C over 30 min and
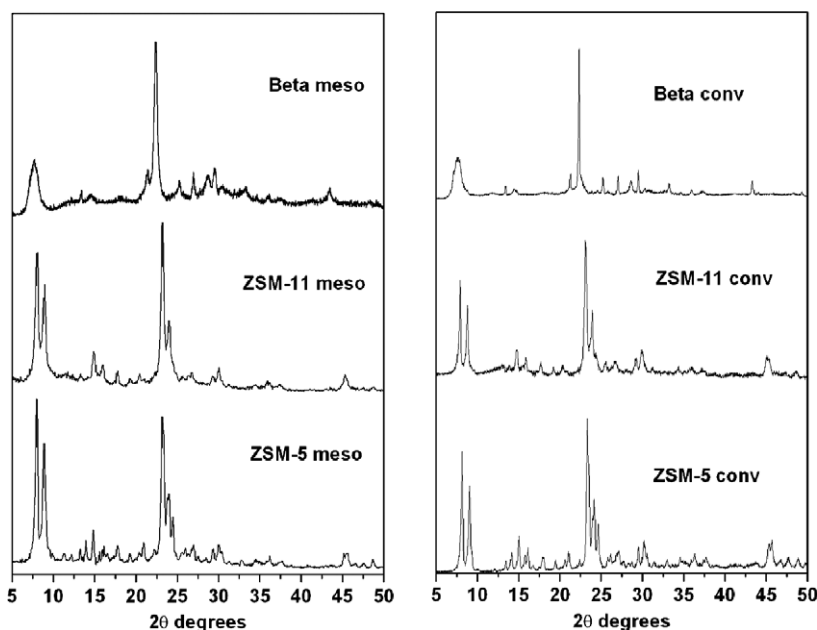

Fig. 1. XRPD patterns of ZSM-5, ZSM-11 and Beta zeolites synthesized in fluoride media. To the left is shown the XRPD patterns of the mesoporous samples, while to the right is shown the conventional samples.

maintained at this temperature for three days. Afterwards, the product was recovered as described above.

2.8. Synthesis of mesoporous and conventional CHA-type materials in fluoride media

The syntheses of the CHA-type materials were based on the procedures given by Tuel et al. [45]. In a typical synthesis of conventional AlPO-34 crystals, 2.04 g aluminum isopropoxide (10 mmol) was suspended in 8.7 g H_2O. To this mixture was added 1.15 g H_3PO_4 (10 mmol), 0.21 g 48 wt% HF (5 mmol) and 0.85 g piperidine (10 mmol). The resulting mixture was transferred to a teflon-beaker which was placed in a teflon-lined stainless steel autoclave with an additional ca. 20 ml H_2O added outside the teflon-beaker. The final gel composition was 5 Al_2O_3:10 H_3PO_4:5 HF:10 PIP:498 H_2O. The autoclave was heated to 190 °C over 30 min and maintained at this temperature for 4–5 days. Afterwards, the product was recovered as described above.

The mesoporous AlPO-34 materials were synthesized using following procedure. Typically, 2.04 g aluminum isopropoxide (10 mmol) was dissolved in 7 ml THF, and the solution was impregnated onto 2 g of carbon. The carbonaceous material was left to dry at room temperature in air overnight, or at least for 6 h. Then, the dry carbon material was impregnated with an aqueous solution of phosphoric acid, piperidine and hydrofluoric acid made by mixing the components in that order. The carbon materials were then transferred to teflon-beakers which were placed in teflon-lined autoclaves with ca. 20 ml water outside the beakers. The final gel composition was 5 Al_2O_3:10 H_3PO_4:5 HF:10 PIP:127 H_2O. The autoclaves were heated to

190 °C over 30 min and maintained at this temperature for 4–5 days. Afterwards, the product was recovered as described above.

3. Results

3.1. X-ray powder difraction

All XRPD patterns were obtained after synthesis and subsequent combustion of the organic template and the auxiliary carbon black material. XRPD patterns for the mesoporous ZSM-5, ZSM-11 and Beta zeolites are shown in Fig. 1, along with XRPD patterns of the conventional

Table 1
Nitrogen physisorption data of the samples after combustion of the organic template and the carbon matrix

Zeolite/ zeotype	Conventional/ mesoporous	V_{micro} (cm^3/g)[a]	V_{meso} (cm^3/g)[b]	BET area (m^2/g)[c]
ZSM-5	conv.	0.12	0.01	399
ZSM-5	meso.	0.11	0.31	346
ZSM-11	conv.	0.12	0.02	364
ZSM-11	meso.	0.10	0.29	342
BEA	conv.	0.20	0.03	499
BEA	meso.	0.18	0.36	507
AlPO-5	conv.	0.001	0.003	5
AlPO-5 (s1)	meso.	0.02	0.37	150
AlPO-5 (s2)	meso.	0.01	0.45	154
AlPO-34	conv.	0.26	0.007	563
AlPO-34	meso.	0.18	0.47	494

[a] Calculated by t-plot method.
[b] Calculated by BJH method (desorption).
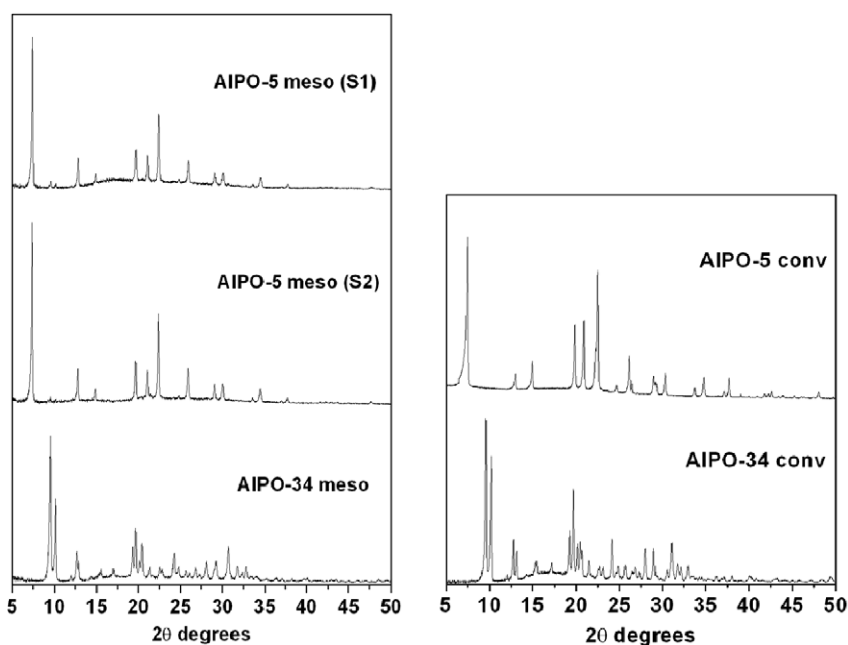[c] Calculated by BET method.

Fig. 2. XRPD patterns of AlPO-5 (s1), AlPO-5 (s2) and AlPO-34 zeotypes synthesized in fluoride media. To the left is shown the XRPD patterns of the mesoporous samples, while to the right is shown the conventional samples.

samples. XRPD patterns obtained from the mesoporous AlPO-5 (s1), AlPO-5 (s2) and AlPO-34 materials are shown in Fig. 2, along with XRPD patterns of conventional AlPO-5 and AlPO-34 samples.

3.2. Nitrogen physisorption

All physisorption data were acquired after combustion of the organic template and the carbon black material. In Table 1, the BET surface areas and micro- and mesopore volumes for all samples are summarized. The mesopore surfaces areas for all samples were in the range 40–60 m^2/g.
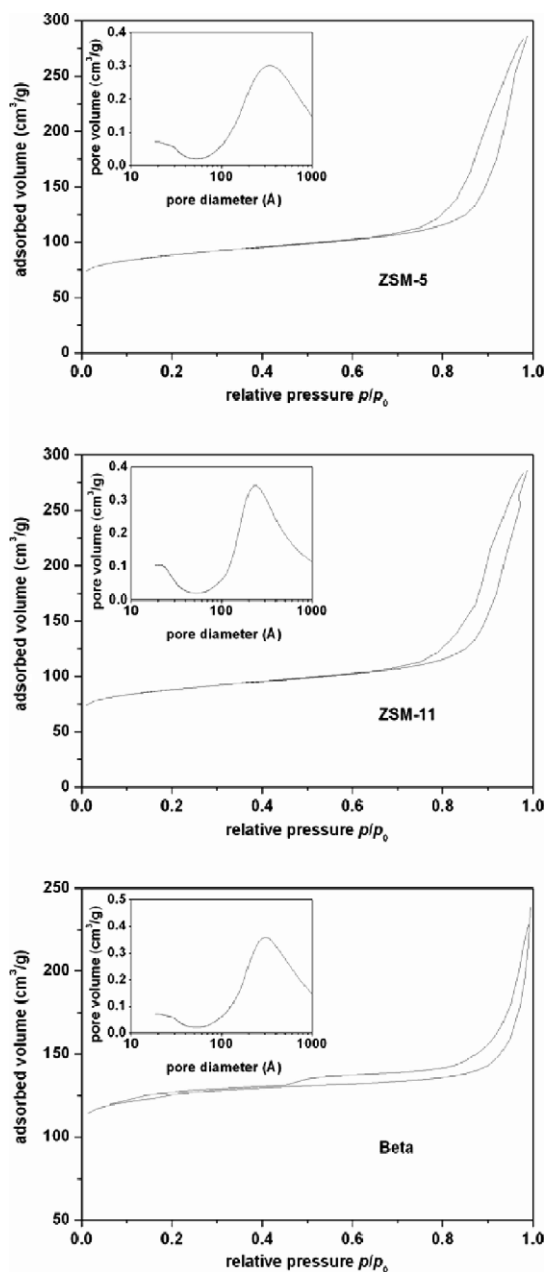
In Fig. 3, the nitrogen adsorption and desorption isotherms of the mesoporous ZSM-5, ZSM-11 and Beta zeolites are shown. Fig. 4 illustrates the nitrogen adsorption and desorption isotherms and pore size distribution for mesoporous AlPO-5 (s1), AlPO-5 (s2) and AlPO-34 zeotypes.

3.3. Scanning electron microscopy

The results of the scanning electron microscopic studies for conventional and mesoporous ZSM-5, ZSM-11, and Beta zeolites after combustion of the carbon are shown in Fig. 5. In Fig. 6, SEM images of conventional and

Fig. 3. Nitrogen adsorption and desorption isotherms of mesoporous ZSM-5, ZSM-11 and Beta zeolites synthesized in fluoride media. Inserts show pore size distribution of these materials.
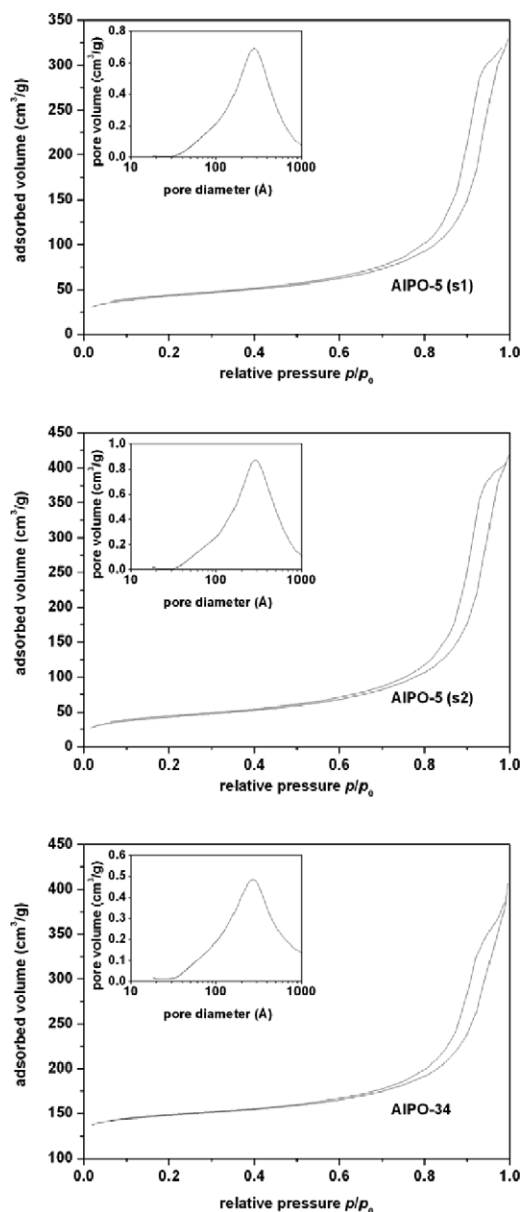

Fig. 4. Nitrogen adsorption and desorption isotherms of mesoporous AlPO-5 (s1), AlPO-5 (s2) and AlPO-34 zeotypes synthesized in fluoride media. Inserts show pore size distribution of these materials.
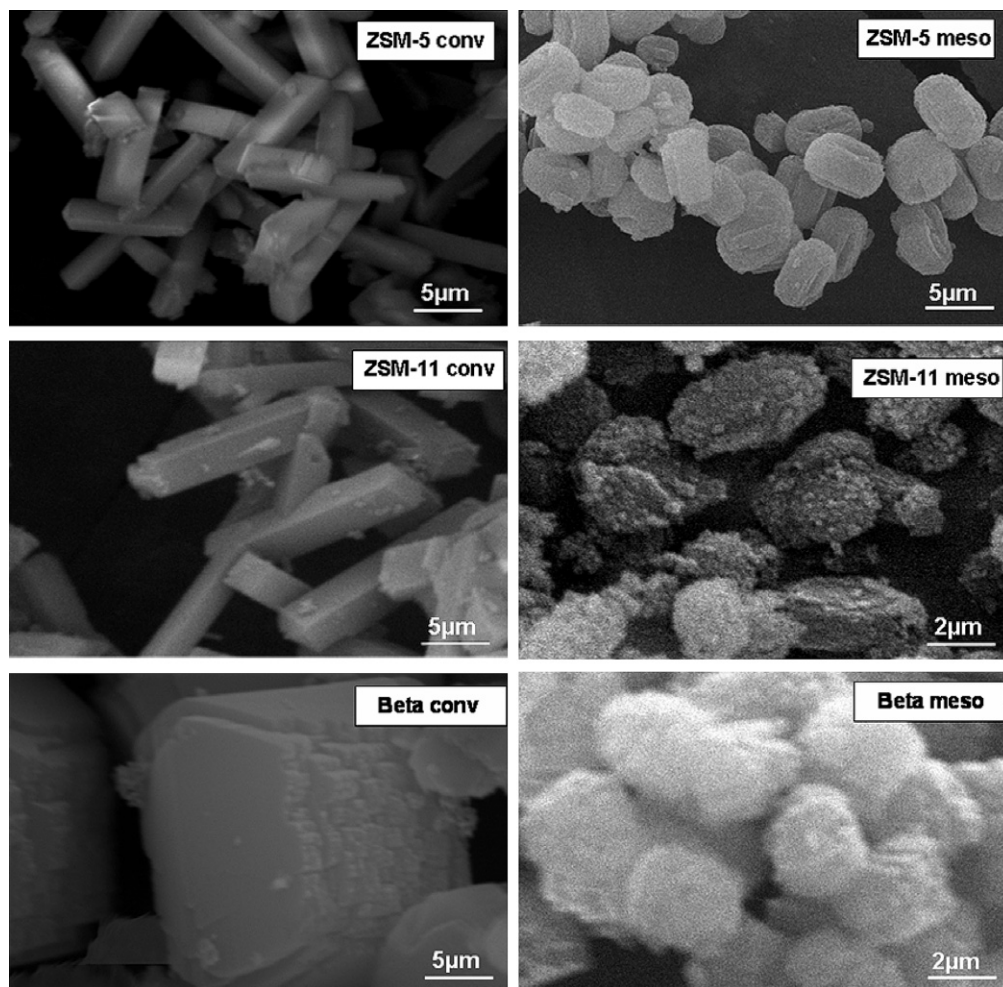
Fig. 5. SEM images of conventional ZSM-5 zeolite, mesoporous ZSM-5 zeolite, conventional ZSM-11 zeolite, mesoporous ZSM-11 zeolite, conventional zeolite Beta, and mesoporous zeolite Beta. All samples were synthesized in fluoride media.

mesoporous AlPO-5 (s1), AlPO-5, (s2) and AlPO-34 zeo-type samples are presented.

3.4. Transmission electron microscopy

The result of transmission electron microscopy for the mesoporous BEA-type zeolite after combustion of the carbon is shown in Fig. 7. Images of ZSM-5 and ZSM-11 were very to those previously published. Unfortunately, the zeo-type materials were too unstable in the electron beam to obtain TEM images of sufficient quality.

4. Discussion

4.1. X-ray powder diffraction

From Figs. 1 and 2, it is clearly seen that all zeolite and zeotype samples contain highly crystalline structured materials [46]. When comparing the mesoporous samples with the conventional samples, it is seen that there is a slight line-broadening in the peaks of the mesoporous samples.

From the XRPD patterns of the obtained AlPO-5 (s1) and AlPO-5 (s2) materials shown in Fig. 2 it is seen that both AlPO-5 samples contain highly crystalline AFI-structured materials. However, in the case of AlPO-5 (s1), there appears to be a slight amorphous background. Not surprisingly, it is seen that increasing the amount of template also increases the crystallinity of the ALPO-5 material. Thus, the AlPO-5 sample synthesized using a higher amount of template AlPO-5 (s2) contains no amormpous background. The XRPD pattern of the mesoporous AlPO-34 material shown in Fig. 2 is consistent with that of conventional CHA-type single crystals containing extra-framework water molecules [45]. The relatively sharp lines in the XRPD patterns are indicative of highly crystalline samples.

4.2. Nitrogen physisorption

According to the IUPAC classification of physisorption isotherms [47], all prepared mesoporous zeolite and zeo-type materials have Type IV isotherms. They contain a hysteresis loop at relative pressures higher than $p/p_0 = 0.4$, which is typical for mesoporous materials. From the pore
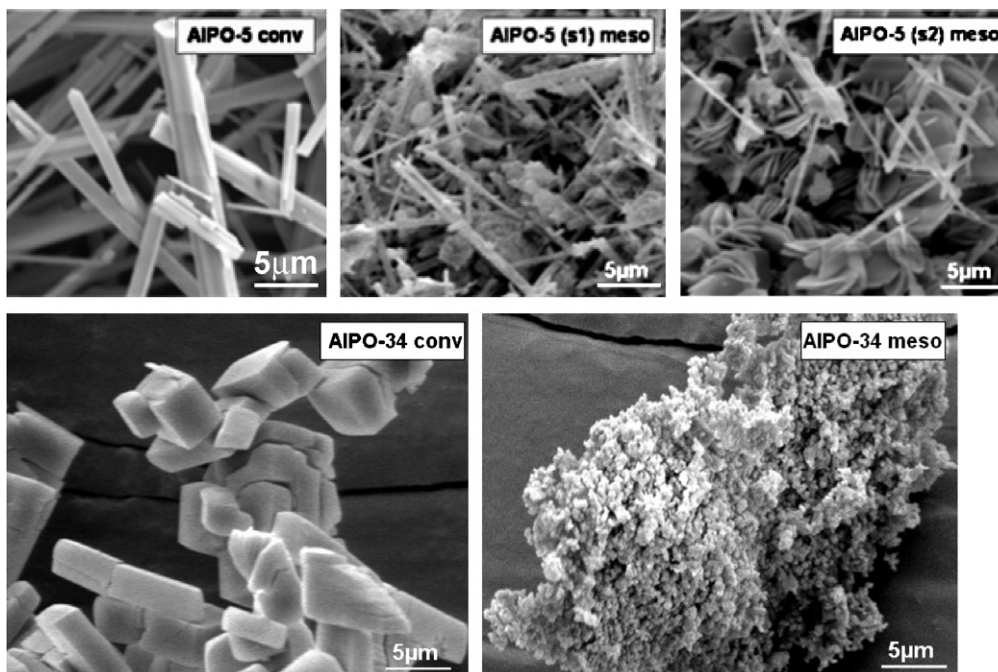
Fig. 6. SEM images of conventional AlPO-5 (s1) zeotype, mesoporous AlPO-5 (s1) zeotype, conventional AlPO-5 (s2) zeotype, mesoporous AlPO-5 (s2) zeotype, conventional AlPO-34 zeotype, and mesoporous AlPO-34 zeotype. All samples were synthesized in fluoride media.
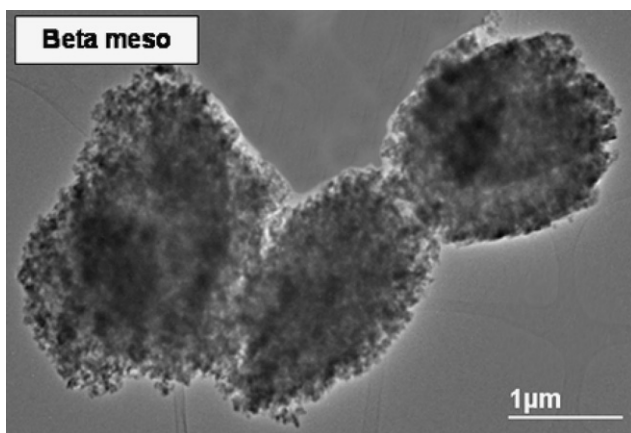

Fig. 7. TEM image of the mesoporous zeolite Beta.

size distributions of the synthesized ZSM-5, ZSM-11 and Beta zeolites shown in Fig. 3, it is clearly seen that all these materials have mesopores in the range of 250–300 Å. From the pore size distributions of the synthesized AlPO-5 and AlPO-34 zeotypes shown in Fig. 4, it is clearly seen that all materials have mesopores with an average size of about 300 Å. The very similar shape of the physisorption isotherms of all the prepared materials suggests that all the prepared materials feature the same kind of mesoporosity.

4.3. Scanning electron microscopy

All prepared zeolite samples appear to be highly crystalline. The average crystal size of the conventional zeolite crystals determined from SEM, are in all cases larger than that of the mesoporous zeolite crystals as shown in Fig. 5.

The typical coffin-shape of ZSM-5 and ZSM-11 crystals is observed for both conventional samples, and can also be seen for the mesoporous samples. The major difference between the conventional and mesoporous zeolite crystals is the presence of non-crystallographic intracrystalline mesopores resulting in the very high porosity and the relatively large average pore size of the mesoporous zeolite single crystals samples. The conventional zeolite Beta material has the typical rounded-cube shape. From the SEM image of the mesoporous zeolite Beta, it can be seen that the crystals have shapes typical for mesoporous single crystals. It was shown previously [48], that using the standard synthesis procedure in alkaline media it is possible to get only nanosized Beta material, and this was confirmed in the present study. Here, we show that use of fluoride ions allowed us to obtain mesoporous zeolite Beta single crystal materials.

The SEM studies of the conventional AlPO-5 sample shown in Fig. 6 reveals that this material consists of fairly long needled- or column-shaped crystals, typically with a crystal width in the range of 1–3 µm. For both of the mesoporous AlPO-5 samples the needle- or column-shaped crystal morphology is also observed, however, for these materials it seems that by increasing the amount of structure-directing agent in the gel, crystals with plate-like morphology appear in competition with the needle- or column-shaped crystals. This observation suggests that it is possible to crystallize mesoporous AlPO-5 materials with different crystal morphologies, and that varying the amount of structure-directing agent provides means for controlling the morphology of these mesoporous materials. Furthermore, the SEM analyses of both AlPO-5 (s1) and

AlPO-5 (s2) samples revealed that there were no nanosized crystals present in either of the samples. Thus, both these materials consist of mesoporous single crystals, even though the crystals do not clearly exhibit the sponge-like appearance common for the related zeolite materials. SEM analysis of the conventional AlPO-34 material reveals that this material consists of regularly shaped crystals with typical sizes in the range 2–10 μm, as shown in Fig. 6. In contrast to this, as is also illustrated in Fig. 6, the mesoporous AlPO-34 sample seems to consist of a sponge-like material or agglomerates of nanosized crystals, which might both explain the mesoporisity of the material. However, since the physisorption isotherms of the mesoporous AlPO-34 material is qualitatively identical to those of the zeolite materials, we propose that the mesoporisity of this materials does in fact result from mesopores generated within each individual crystal by removal of the auxilary carbon matrix and not from the individual crystals being of nanosize. Thus, all the prepared samples appear to be mesoporous single crystal materials.

4.4. Transmission electron microscopy

From the TEM image of the mesoporous BEA-type zeolite crystals, shown in Fig. 7, it is easy to see the individual mesoporous zeolite crystals, which are relatively large (around 2 μm in length) and with well-defined shape. Furthermore, the significant mesoporosity of the individual zeolite Beta crystals is clearly visible from the micrograph. The sponge-like appearance of the crystals is typical for this kind of mesoporous single crystal materials, and results from intracrystalline mesopores created by combustion of the carbon. In this work, the single crystal nature of the mesoporous BEA sample was confirmed by SAD, but previous works have shown that mesoporous crystals obtained in this way are generally mesoporous single crystals [49].

5. Conclusions

We have synthesized and characterized a number of new mesoporous zeolite and zeotype materials by extending the recently developed *carbon-templating strategy* to also incorporate *the fluoride route*. The procedure is extremely adaptable as shown by the synthesis of mesoporous zeolite as well as mesoporous zeotype materials. The procedure have not only afforded mesoporous ZSM-5 and ZSM-11 single crystals, which are possible to synthesize from basic media, but also mesoporous BEA-type single crystals, which so far may only be obtained by our new procedure combining carbon-templating with the fluoride route. Thus, this newly developed synthesis scheme opens up for synthesizing new mesoporous materials not available from basic crystallization gels. Also mesoporous AlPO-*n* zeotype materials of AFI and CHA framework structures could be synthesized using the combined carbon-templating fluoride route strategy. SEM analyses of the prepared mesoporous AlPO-5

(AFI) materials suggest that it is possible to synthesize this material in different crystal morphologies. The mesoporosity of the mesoporous AlPO-34 (CHA) material is not as easily recognized as for the other materials, but the strong resemblance of the shape of the physisorption isotherm of this sample with those of the mesoporous zeolite materials imply that this material also consists of mesoporous single crystals. Thus, the present investigation reveals that combining the fluoride route with carbon-templating provides access to a range of new materials by a highly versatile approach.

Acknowledgments

References

[1] A. Corma, Chem. Rev. 95 (1995) 559.
[2] R.A. Sheldon, R.S. Downing, Appl. Catal. A 189 (1999) 163.
[3] R. Szostak, Molecular Sieves-Principles of Synthesis and Identification, second ed., Blackie, London, 1998.
[4] C.S. Cundy, Stud. Surf. Sci. Catal. 157 (2005) 65.
[5] J.M. Chezeau, L. Delmotte, J.L. Guth, M. Soulard, Zeolites 9 (1989) 78.
[6] E.M. Flanigen, R.L. Patton, US 4 073 865 (1978).
[7] J.L. Guth, L. Delmotte, M. Soulard, N. Brunard, J.F. Joly, D. Espinat, Zeolites 12 (1992) 929.
[8] M. Soulard, S. Bilger, H. Kessler, J.L. Guth, Zeolites 7 (1987) 463.
[9] T. Blasco, M.A. Camblor, A. Corma, P. Esteve, A. Martinez, C. Prieto, S. Valencia, Chem. Commun. (1996) 2367.
[10] R. Mostowich, F. Testa, F. Crea, R. Aiello, A. Fonseca, J.B. Nagy, Zeolites 18 (1997) 308.
[11] M.A. Camblor, A. Corma, S. Valencia, J. Mater. Chem. 8 (1998) 2137.
[12] M.A. Camblor, L.A. Villaescusa, M.J. Diaz-Cabanas, Top. Catal. 9 (1999) 59.
[13] J.E. Hazm, P. Caullet, J.L. Paillaud, M. Soulard, L. Delmotte, Micropor. Mesopor. Mater. 43 (2001) 11.
[14] B. Louis, L. Kiwi-Minsker, Micropor. Mesopor. Mater. 74 (2004) 171.
[15] F. Schuth, W. Schmidt, Adv. Mater. 14 (2002) 629.
[16] S.I. Zones, S.J. Hwang, S. Elomari, I. Ogino, M.E. Davis, A.W. Burton, J. C. R. Chemie 8 (2005) 267.
[17] M. Hartmann, Angew. Chem. Int. Ed. 43 (2004) 5880.
[18] Y. Tao, H. Kanoh, L. Abrams, K. Kaneko, Chem. Rev. 106 (2006) 896.
[19] P.A. Jacobs, E.G. Derouane, J. Weitkamp, J. Chem. Soc. Chem. Commun. (1981) 591.
[20] M.A. Camblor, A. Corma, S. Valencia, Micropor. Mesopor. Mater. 25 (1998) 59.
[21] I. Schmidt, C. Madsen, C.J.H. Jacobsen, Micropor. Mesopor. Mater. 39 (2000) 393.
[22] L. Tosheva, V.P. Valtchev, Chem. Mater. 17 (2005) 2494.
[23] M.E. Davis, C. Saldarriaga, C. Montes, J. Garces, C. Crowder, Nature 331 (1988) 698.
[24] C.C. Freyhard, M. Tsapatsis, R.F. Lobo, K.J. Balkus, Nature 381 (1996) 295.
[25] C.T. Kresge, M.E. Leonowicz, W.J. Roth, J.C. Vartuli, J.S. Beck, Nature 359 (1992) 710.

[26] S. Donk, A.H. Janssen, J.H. Bitter, K.P. Jong, Cat. Rev. 45 (2003) 297.

[27] M. Ogura, S.H. Shinomiya, J. Tateno, Y. Nara, E. Kikuchi, M. Matsukata, Chem. Lett. (2000) 882.

[28] J.C. Groen, J.A. Moulijn, J. Pérez-Ramírez, J. Mater. Chem. 16 (2006) 2121.

[29] C.J.H. Jacobsen, C. Madsen, J. Houzvicka, I. Schmidt, A. Carlsson, J. Am. Chem. Soc. 122 (2000) 7116.

[30] I. Schmidt, C.H. Christensen, P. Hasselriis, M.Yu. Kustova, M. Brorson, S. Dahl, K. Johannsen, C.H. Christensen, Stud. Surf. Sci. Catal. 158 (2005) 1247.

[31] A. Corma, Chem. Rev. 97 (1997) 2373.

[32] C.H. Christensen, K. Johannsen, I. Schmidt, C.H. Christensen, J. Am. Chem. Soc. 125 (2003) 13370.

[33] C.H. Christensen, I. Schmidt, C.H. Christensen, Catal. Comm. 5 (2004) 543.

[34] C.H. Christensen, I. Schmidt, A. Carlsson, K. Johannsen, K. Herbst, J. Am. Chem. Soc. 127 (2005) 8098.

[35] M.Yu. Kustova, S.B. Rasmussen, A.L. Kustov, C.H. Christensen, Appl. Catal. B 67 (2006) 60.

[36] M.Yu. Kustova, P. Hasselriis, C.H. Christensen, Catal. Lett. 96 (2004) 205.

[37] X. Wei, P.G. Smirniotis, Micropor. Mesopor. Mater. 89 (2005) 170.

[38] Y. Tao, H. Kanoh, K. Kaneko, J. Phys. Chem. B 107 (2003) 10974.

[39] Y. Liu, T.J. Pinnavaia, J. Mater. Chem. 14 (2004) 1099.

[40] V. Naydenov, L. Tosheva, J. Sterte, Micropor. Mesopor. Mater. 35 (2000) 621.

[41] Y. Tao, H. Kanoh, K. Kaneko, Langmuir 21 (2005) 504.

[42] I.I. Ivanova, A.S. Kuznetsov, O.A. Ponomareva, V.V. Yuschenko, E.E. Knyazeva, Stud. Surf. Sci. Catal. 158 (2005) 121.

[43] F.S. Xiao, L. Wang, C. Yin, K. Lin, Y. Di, J. Li, R. Xu, D.S. Su, R. Schlogl, T. Yokoi, T. Tatsumi, Angew. Chem. Int. Ed. 45 (2006) 3090.

[44] M.A. Camblor, A. Corma, S. Valencia, Chem. Commun. (1996) 2365.

[45] A. Tuel, S. Caldarelli, A. Meden, L.B. McCusker, C. Baerlocher, A. Ristic, N. Rajic, G. Mali, V. Kaucic, J. Phys. Chem. B 104 (2000) 5697.

[46] Database of zeolite structures: <http://www.iza-structure.org/databases/>.

[47] C.N. Satterfield, Heterogeneous Catalysis in Industrial Practice, second ed., McGraw-Hill, New York, 1991.

[48] I. Schmidt, C. Madsen, C.J.H. Jacobsen, Inorg. Chem. 39 (2000) 2279.

[49] H. Janssen, I. Schmidt, C.J.H. Jacobsen, A.J. Koster, K.P. de Jong, Micropor. Mesopor. Mater. 65 (2003) 59.